

Master's thesis

Feasibility study on fiber reinforced polymer cylindrical truss bridges for heavy traffic

Mathis Chlosta
July 2012

Literature
study



Cover: Woven carbon fiber sheet typically used by the automotive industry. These sheets form the basis of high quality, high fiber content carbon fiber reinforced epoxy composites that serve as structural material in frame- or body-parts of state-of-the-art automobiles. [WEB: www.thetruthaboutcars.com]

MASTER'S THESIS LITERATURE STUDY

“FEASIBILITY STUDY ON FIBER REINFORCED POLYMER CYLINDRICAL TRUSS BRIDGES FOR HEAVY TRAFFIC”

“HAALBAARHEIDSSTUDIE NAAR CILINDRISCHE VAKWERKBRUGGEN VAN VEZELVERSTERKT
KUNSTSTOF VOOR ZWAAR VERKEER”

MATHIS CHLOSTA
JULY 2012

Department of Design & Construction
Faculty of Civil Engineering and Geosciences
Delft University of Technology
2628GN/2600GA Delft
The Netherlands
www.tudelft.nl

© Copyright 2012 Mathis Chlosta, Delft University of Technology, Delft, the Netherlands

All rights reserved. No part of this document may be reproduced for commercial purposes without written consent from the author. Permission is granted to reproduce for personal and educational use only with the use of proper citation. Commercial copying, hiring, lending and selling is prohibited without written consent from the author.

For inquiries regarding this literature study please contact the author via email: mchlosta@gmail.com

PREFACE

This document forms the basis of the MSc thesis 'Feasibility study on fiber reinforced polymer cylindrical truss bridges for heavy traffic'. It can be seen as an extensive appendix for this design study, which includes all necessary information on the subjects of fiber reinforced polymers as building material, fiber reinforced polymer bridge engineering, the fire safety of fiber reinforced polymers, cylindrical truss bridges and the use of finite element model- and analysis software packages for bridge engineering.

The research study very much relies on this literature study and it is therefore often referred to in the research study. Although the literature study was written primarily as backbone of the research and design study it can also be used as an isolated guideline for the design of fiber reinforced polymer bridges for heavy (road) traffic. Next to that it also gives a thorough overview on the fire safety of fiber reinforced polymers as structural material.

This literature study was carried out in cooperation with Delft University of Technology, Faculty of Civil Engineering & Geosciences, Department Design & Construction and the Dutch infrastructure authority Rijkswaterstaat, Dienst Infrastructuur, Kennisveld Materialen.

My gratitude goes to my graduation committee for providing me with all the information, help and support I needed. The graduation committee consisted of the following members:

Prof.ir. F.S.K. Bijlaard

Professor at Delft University of Technology, Faculty of Civil Engineering & Geosciences, Department of Design and Construction, Section Steel & Composite Structures

Dr. M.H. Kolstein

Associate Professor at Delft University of Technology, Faculty of Civil Engineering & Geosciences, Department of Design and Construction, Section Steel & Composite Structures

Dr.ir. M.A.N. Hendriks

Assistant Professor at Delft University of Technology, Faculty of Civil Engineering & Geosciences, Department of Design and Construction, Section Structural Mechanics

Dr.ir. A. de Boer

Senior Advisor/Specialist at Rijkswaterstaat, Dienst Infrastructuur, Directie Techniek en Infrastructuur

The Hague, July 2012

Mathis Chlost

Keywords: Fiber reinforced polymers, plastics, FRP, civil engineering, bridge engineering, structural engineering, structural design, bridge design, stiffness driven design, cylindrical truss, elliptical truss, tubular truss, spatial truss, truss topology optimization, grid size optimization, space efficiency, heavy traffic road bridge, truss topology, mechanical properties of FRP materials, fire safety, fire resistance, steel viaduct comparison, FEA, FEM, finite element modeling, finite element analysis, CFRP, carbon, epoxy

TABLE OF CONTENTS

1. INTRODUCTION.....	1
1.1 CHOICE OF MATERIAL	1
1.2 CHOICE OF SHAPE	4
1.3 RESEARCH OBJECTIVE	6
1.4 RESEARCH QUESTIONS	7
2. FIBER REINFORCED POLYMERS	9
2.1 FRP COMPOSITES MARKET	10
2.2 HISTORY OF FRP COMPOSITES IN GENERAL	13
2.2.1 Composites.....	13
2.2.2 Plastics	13
2.2.3 Fiber Reinforced Plastics.....	14
2.2.4 Fiber Reinforced Plastics in the building industry	15
2.3 HISTORY OF FRP COMPOSITES IN BRIDGE ENGINEERING	17
2.3.1 Miyun Bridge, China	17
2.3.2 Ulenbergstrasse Bridge, Germany	18
2.3.3 Aberfeldy Foot Bridge, Scotland	18
2.3.4 Plastic Bridge, Russel County, Kansas, USA	19
2.3.5 FRP bridges in the present	19
2.4 APPLICATIONS IN BRIDGES	20
2.4.1 All FRP	20
2.4.1.1 Pedestrian bridges.....	20
2.4.2 Hybrid FRP	20
2.4.2.1 FRP profiles	21
2.4.2.2 FRP bridge decks	21
2.4.2.3 Concrete-filled FRP tubes	21
2.4.2.4 FRP reinforcement.....	21
2.4.2.5 FRP tendons and cables.....	22
2.4.3 Replacement, repair and rehabilitation of bridge elements	22
2.4.3.1 Bridge deck repair and replacement.....	22
2.4.3.2 Flexural- and shear-strengthening.....	23
2.4.3.3 Column rehabilitation.....	23
2.4.3.4 External post-tensioning.....	23
2.5 MATERIALS	24
2.5.1 Reinforcements	25
2.5.1.1 Glass fibers	26
2.5.1.2 Carbon fibers	32
2.5.1.3 Aramid fibers	35
2.5.1.4 Natural fibers	38
2.5.1.5 Other reinforcements	41
2.5.2 Matrices	43
2.5.2.1 Metal matrices	43
2.5.2.2 Ceramic matrices	43
2.5.2.3 Carbon matrices	43
2.5.2.4 Polymer matrices	44
2.5.2.5 Thermoset resins	45
2.5.2.6 Thermoplastic resins	52
2.5.2.7 Biological resins	56
2.5.3 Additives	57
2.5.4 Production techniques	58
2.5.4.1 Pre-products	58
2.5.4.2 Open mold processes	62
2.5.4.3 Closed mold processes	65
2.5.4.4 Continuous processes	68
2.5.4.5 Comparison of all production techniques	70
2.6 MECHANICAL PROPERTIES.....	72
2.6.1 Properties of reinforcements, matrices and selected unidirectional composites	72
2.6.1.1 Reinforcement fibers	72
2.6.1.2 Matrix material	74
2.6.1.3 Unidirectional reinforced composites	74
2.6.2 Models for the estimation of the mechanical properties of composites	75
2.6.2.1 Mass and volume fractions for unidirectional reinforced composites	75
2.6.2.2 Law of mixtures model for unidirectional reinforced composites	75
2.6.2.3 Hashin-Shtrikman model for unidirectional reinforced composites	77

2.6.2.4 Halpin-Tsai model for unidirectional reinforced composites	78
2.6.2.5 Tsai-Hahn improvements of the Halpin-Tsai model.....	79
2.6.2.6 Empirical Puck model for unidirectional reinforced composites	80
2.6.3 Comparison of the different estimation models	81
2.6.4 Models for the estimation of the mechanical properties of dispersions	82
2.6.4.1 Kerner (1956)	82
2.6.4.2 Paul (1960)	83
2.6.4.3 Barentsen (1972)	83
2.6.5 Failure modes of unidirectional FRP	83
2.6.5.1 Longitudinal tension	84
2.6.5.2 Longitudinal Compression	84
2.6.5.3 Transverse tension and compression	85
2.6.5.4 Shear	85
2.6.6 Laminate theory	85
2.6.6.1 The classic (isotropic) plate theory	85
2.6.6.2 Laminate theory	87
2.6.6.3 Strength analysis of Laminates	91
2.6.6.4 Influence of the laminate build-up	91
2.6.7 Structural design of composites	93
2.6.7.1 Material factor	93
2.6.7.2 Conversion factor	94
2.6.7.3 Load factor	94
2.6.7.4 Strain criterion.....	94
2.6.7.5 Stress criterion	95
2.6.7.6 Combined stresses criterion	95
2.6.7.7 Buckling of line elements.....	95
2.6.8 Creep	96
2.6.9 Stress corrosion	97
2.6.10 Fatigue	97
2.6.10.1 Influence of matrix materials.....	98
2.6.10.2 Influence of reinforcement materials	98
2.6.10.3 Fatigue design according to CUR96	100
2.6.11 Joint Design	101
2.6.11.1 Bolted joints	102
2.6.11.2 Bonded joints	104
2.6.11.3 Combined joints	106
3. TRAFFIC BRIDGES	107
3.1 TYPES OF BRIDGES	107
3.1.1 Arch bridges	107
3.1.2 Suspension bridges	108
3.1.3 Cable stayed bridges	109
3.1.4 Girder bridges.....	110
3.1.5 Truss bridges	110
3.1.6 Background on the choice of bridge type for the fiber reinforced polymer bridge.....	111
3.2 FIBER REINFORCED POLYMER BRIDGE DECKS FOR FRP BRIDGES	111
3.2.1 Advantages of Fiber Reinforced Polymer Bridge Decks	111
3.2.2 Disadvantages of fiber reinforced bridge decks.....	112
3.2.3 Comparison of advantages and disadvantages	113
3.2.4 Types of fiber reinforced polymer bridge decks	113
3.3 LOADS ON TRAFFIC BRIDGES.....	118
3.3.1 Wind Loads.....	118
3.3.1.1 Wind pressure qp	118
3.3.1.2 Reference surface area A_{ref}	120
3.3.1.3 Force coefficient cf	120
3.3.1.4 Building coefficient $cscd$	121
3.3.2 Snow Loads.....	123
3.3.3 General load cases for traffic loads on road bridges	124
3.3.3.1 Load Model 1 (LM)	124
3.3.3.2 Load Model 2 (LM2)	125
3.3.3.3 Load Model 3 (LM3)	126
3.3.3.4 Load Model 4 (LM4)	126
3.3.3.5 Multi-component action.....	126
3.3.4 Fatigue loads on traffic bridges	126
3.3.4.1 Fatigue Load Model 1	127
3.3.4.2 Fatigue Load Model 2	127
3.3.4.3 Fatigue Load Model 3	127

3.3.4.4 Fatigue Load Model 4	127
3.3.4.5 Fatigue Load Model 5	128
3.3.5 Vibrations	128
3.3.5.1 Vibration of fiber reinforced polymers	128
3.3.5.2 Human induced vibrations.....	129
3.3.5.3 Vehicle induced vibrations	130
3.3.5.4 Wind induced vibrations.....	130
3.3.6 Serviceability limit state deflection limits	131
3.3.7 Other traffic loads on traffic bridges	132
3.3.7.1 Braking and acceleration forces.....	132
3.3.7.2 Vehicle on footways and cycle tracks	132
3.3.7.3 Collision forces	133
3.3.7.4 Load models for footways and cycle tracks	134
4. FIRE SAFETY	135
4.1 DEFINITION OF FIRE.....	135
4.1.1 <i>Fire curves</i>	137
4.2 FIRE SAFETY OF BRIDGES IN GENERAL.....	139
4.2.1 <i>Fundamentals</i>	139
4.2.2 <i>Specific bridge fire safety</i>	140
4.2.2.1 Methods of protecting bridges	141
4.2.2.2 Practical guidelines and codes.....	142
4.3 FIRE SAFETY OF FIBER REINFORCED POLYMERS.....	143
4.3.1 <i>Characteristic values describing the fire properties of a material</i>	144
4.3.1.1 Fire Reaction	144
4.3.1.2 Fire Resistance	145
4.3.2 <i>Thermal Decomposition of composites in fire</i>	146
4.3.3 <i>Fire Damage to composites</i>	147
4.3.3.1 Char formation	147
4.3.3.2 Delamination damage	148
4.3.3.3 Decomposition of thermosets under fire load.....	149
4.3.3.4 Decomposition of thermoplastics under fire load.....	150
4.3.3.5 Decomposition of fiber reinforcements under fire load	151
4.3.3.6 Fire Reaction properties of Fiber Reinforced Polymer Composites.....	152
4.3.3.7 Heat Release Rate	152
4.3.3.8 Time-to-ignition	153
4.3.3.9 Surface spread of flame	155
4.3.3.10 Limiting Oxygen Index	155
4.3.3.11 Smoke generation	156
4.3.3.12 Smoke toxicity	157
4.3.4 <i>Fire Resistance properties of FRP composites</i>	159
4.3.4.1 Back-face temperature build-up.....	159
4.3.5 <i>Mechanical properties of composites under fire load</i>	159
4.3.6 <i>Post-fire properties of compositeS</i>	163
4.3.6.1 Two-layer model for the post-fire mechanical properties prediction	164
4.3.7 <i>Improvement of fire properties of FRP compositeS</i>	165
4.3.7.1 Flame retardant fillerS	167
4.3.7.2 Flame retardant organic polymerS	171
4.3.7.3 Flame retardant inorganic polymers.....	174
4.3.7.4 Flame retardant fibers.....	175
4.3.7.5 Fire protective surface coatings.....	175
4.3.7.6 Flame retardant polymer nanocomposites.....	181
5. FEA/FEM OF FRP	185
5.1 SPECIAL FEATURES OF FRP IN FEA DESIGN	185
5.1.1 <i>Inhomogeneity</i>	185
5.1.2 <i>Anisotropicity</i>	185
5.1.3 <i>Laminate build-up</i>	185
5.1.4 <i>Connection detailing</i>	186
5.2 FEA/FEM SOFTWARE PACKAGES	186
5.2.1 <i>LUSAS</i>	186
5.2.2 <i>MSC – Nastran</i>	187
5.2.3 <i>ANSYS Structural</i>	187
5.2.4 <i>MIDAS Civil/TNO DIANA</i>	187

6. CASE STUDIES.....	189
6.1 CYLINDRICAL TRUSS BRIDGES AND SHELL BRIDGES.....	189
6.1.1 <i>Singapore Marina Bay Front Pedestrian Bridge</i>	189
6.1.2 <i>Singapore Henderson Waves Bridge</i>	191
6.1.3 <i>Lightrail Viaduct Beatrixkwartier The Hague</i>	192
6.1.4 <i>Peace Bridge Calgary</i>	193
6.1.5 <i>Greenside Place Linke Bridge</i>	194
6.1.6 <i>Design Papendorpe Brug, Utrecht, ABT</i>	195
6.1.7 <i>Roche-sur-Yon Pedestrian BridgE</i>	196
6.1.8 <i>Others</i>	197
6.1.8.1 <i>Luton Galaxy Link Bridge</i>	197
6.1.8.2 <i>T. Evans Wyckoff Memorial BridgE</i>	197
6.1.8.3 <i>Harthill FootbridgE</i>	198
6.1.8.4 <i>Webb BridgE</i>	198
6.2 ALL FRP BRIDGES	199
6.2.1 <i>Aberfeldy Footbridge</i>	199
6.2.2 <i>Lleida footbridge</i>	201
6.2.3 <i>Oosterwolde heavy traffic lift bridge</i>	203
6.2.4 <i>Harbourbridge Hartelhaven Rotterdam</i>	204
6.3 FIRE SAFETY IN BRIDGE ENGINEERING CASES.....	205
6.3.1 <i>Hafenstrassenunterfuehrung , Frankfurt am Main, Germany</i>	205
6.3.2 <i>Bridge Pavilion, EXPO2008 Zaragoza</i>	207
6.3.3 <i>Cable Stayed Bridge Fire Safety, Paper JOFPE 2009</i>	209
6.4 IsoTRUSS CFRP CYLINDRICAL TRUSS STRUCTURES	211
7. DURABILITY & SUSTAINABILITY	215
7.1 MOISTURE AND ALKALINE SOLUTION EFFECTS.....	215
7.2 THERMAL EFFECTS	216
7.3 UV-RADIATION	216
7.4 QUANTIFICATION OF ENVIRONMENTAL EFFECTS.....	217
7.5 SUSTAINABILITY.....	218
7.6 RECYCLING OF COMPOSITES	221
8. CODES AND GUIDELINES ON FRP	223
8.1 EUROCOMP DESIGN CODE AND HANDBOOK	223
8.1.1 <i>Eurocomp Design code</i>	223
8.1.2 <i>Eurocomp Handbook</i>	224
8.1.3 <i>Eurocomp Test reports</i>	224
8.2 CUR96 AND CUR2003-6.....	225
8.2.1 <i>CUR96 Recommendation</i>	225
8.2.2 <i>CUR2003-6 Background report</i>	225
8.3 FIBERLINE DESIGN MANUAL	226
9. COSTS OF FIBER REINFORCED POLYMER COMPOSITES	227
9.1 FRP BRIDGE COSTING EXAMPLES	227
9.1.1 <i>Cost comparison for different material Variants of the Fiberline Bridge, Kolding, DK</i>	228
9.1.2 <i>Design study of FRP alternative to the Millennium Bridge, London, UK</i>	228
9.2 COST OF POLYMER MATRICES.....	229
9.3 COST OF REINFORCEMENT FIBERS	230
9.4 COSTS OF FRP CONSTRUCTION ELEMENTS	231
9.4.1 <i>Cost of different bridge deck systems</i>	231
9.4.2 <i>Cost of selected FRP profiles</i>	232
9.4.3 <i>Cost estimates on fully assembled composites</i>	232

1. INTRODUCTION

Until now a normal traffic bridge would typically be constructed in concrete or steel. Some, mostly small-span bridges are made of timber. During the last decades a promising new material has slowly entered the civil engineering market: fiber reinforced polymer (FRP). This material's origin lies in the aerospace- and aviation industry, where it has been in use for many years already; mainly due to its very good strength-to-weight ratio. FRP deserves further investigation on application in the bridge industry.

During the last decade several smaller FRP pedestrian and cycling bridges have been constructed in the Netherlands, the rest of Western Europe and the USA. But there exist only very few FRP bridge which are suited for the heaviest traffic load classes. One bridge to call out is the Infracore all-FRP Bridge installed in Oosterwolde in the Netherlands on the 8th of July 2010. This bridge has a span of 12m.

So why a cylindrical truss bridge, and foremost, what exactly is a cylindrical truss bridge? The idea of cylindrical truss bridges is that the space above and next to the driving lanes is used for structural strength. One could say that it is essentially a tunnel tube placed as a bridge. The main advantage of these kinds of structure is the high possible span due to the large available construction height. Next to that, the space needed under the drive lane is very low; this can be very advantageous when using the bridge as a viaduct above other roads. Combined with the low weight of FRP this could lead to extremely efficient bridge structures.

Perhaps the single most disadvantageous characteristic of FRP is the unsatisfactory behavior under fire load. That is the reason why this property needs to be specially addressed in this introduction. In the past some research has been carried out on the application of FRP in the building- and bridge industry. It turned out that one of the biggest problems in using FRP is to achieve abundant fire resistance within the structure. An investigation has to be made on how this fire resistance can be improved in such a way that the needed fire safety can be guaranteed when applying FRP in bridge construction.

This literature review will investigate most of the knowledge on fiber reinforced polymers and its components and mechanics. Next to that the general needs of traffic bridges will be discussed as well as vibration, fatigue, durability, sustainability and costs of FRP in bridge engineering. Special attention will be given to the fire safety of fiber reinforced polymers, specifically when used in bridge engineering. Finally a review on the most applicable finite elements software packages will be given as well as some information on reference projects of fiber reinforced plastic bridges as well as tube type bridges.

1.1 CHOICE OF MATERIAL

The first question to ask when reading the cover of this report would be the choice of material. Why would a designer want to choose fiber reinforced polymers over traditional materials such as concrete, steel or a combination of both? On the other hand the question could also be asked the other way around. Why have fiber reinforced polymers been used so rarely in bridge engineering? Plastics are used in very large quantities in commodity applications, plastics are everywhere in everyday objects, so why not in bridges? First of all plastics are a much more complex material than the traditional building materials. Compared to steel and concrete where only dozens or maybe hundreds of different types exist, plastic has thousands of different formulations, which all have unique properties. Most of them are not suitable for engineering, due to their low strength and stiffness, but they were specially developed for their purpose, where strength and stiffness were only secondary parameters.

Around 1900 scientists and ingenuous individuals from the industry first thought of reinforcing plastic and thereby cleared the way for the use of plastics in engineering applications. By adding reinforcement to

plastic matrices, very significant improvement in mechanical properties could be made. Now, more than hundred years later engineering plastics slowly find their way in bridge engineering. It has to be said though that applications of fiber reinforced plastics are still limited to smaller parts made of reinforced plastics, such as parts of the bridge deck, girders, reinforcement bars, staying cables or handrails. Due to recent developments in the traffic bridge markets of Europe and the United states it became evident that reinforced plastics are very well suited as building material. In the last ten, maybe twenty years investigations have shown that many of the traffic bridges were already much deteriorated and structurally unsafe. Partly due to its low weight, reinforced plastic was found to be ideal as repairing material, mostly as strips, sheets or bars, glued to the super- and substructure of deteriorated bridges. Much research is still carried out in this matter and many of the deteriorated bridges still have to undergo reparation.

The application of fiber reinforced plastic in bridge repair gave more insight and knowledge on the properties of reinforced plastics. Combined with the development of high strength matrices and reinforcements with very good mechanical and resistance properties this is leading to a new understanding of fiber reinforced polymers as building material. Since this process is still going on, and very few contracting authorities dare to take the risk of building with new materials it is very appealing to investigate whether this fear has reasonable grounds.

In the past only a handful of all fiber reinforced plastic have been built, even less plastic bridges have been built that are suitable to take the loads of the heaviest common traffic. Fiber reinforced polymers have already shown their potential as high-tech, high-quality material in other industries such as the already mentioned aerospace industry and the military. Until now cost was often a factor that stopped high strength plastics from being used in large-scale applications such as bridge engineering. Developments in production technique have led to significant cost-reductions for reinforced plastics, which thus are more competitive now.

The structural- and building engineering industry is often seen as a somewhat conservative one, always holding on to known materials. Research, both practical and theoretical, is the only mechanism that can convince the builders of a new, efficient material that is perfectly suitable to replace "old" well-known building materials.

To sum up the abundant advantages that fiber reinforced polymers can offer, a list has been compiled of some of the greatest advantages of FRP. These reasons alone should be sufficient to think of FRP as a usable building material and investigate possibilities of an all FRP bridge. Of course FRP composites also have some disadvantages, such as the already described fire behavior issue. These and other disadvantages will be covered more in depth in the course of this research.

- Light weight
- High strength to weight ratio
- Corrosion- and weather resistance
- High directional strength (due to anisotropy)
- High flexibility to meet exact needs
- Dimensional stability (under alternating temperatures, moisture, stress etc.)
- Large, complex and prefabricated geometries possible
- High impact strength
- Low maintenance and high durability

These common advantages of fiber reinforced polymers as structural material can be extended by some more specific advantages of fiber reinforced polymers as structural material in bridge engineering:

Reduced mass

- Easier, faster and more economic installation, due to the less expensive machinery needed.

- Larger sections can be prefabricated and brought to the construction site, reducing not only transport costs, but also costly assembly time. Next to that prefabrication increases build quality due to the controlled environment.
- Reduction in size and cost of the bridge substructure, such as bearings, foundations, etc.
- Reduced energy consumption in transportation and production in comparison to steel and concrete.
- Reduction in size and energy consumption of the mechanical plant for opening/moving bridges.

Superior durability

- Resistant to atmospheric degradation, de-icing salts, spilled chemicals etc. due to tailor made composition of matrix and reinforcement.
- Reduction in maintenance requirements, through-life costs and disruption.
- Increased life span.

Ability to mold complex forms

- New aesthetic possibilities.
- Geometrically more efficient solutions.

Desirable electrical and thermal properties

- Can be electrically non-conductive, which may be advantageous near electrical installations.
- Can be thermally stable (especially when using carbon fiber), which may remove the need for expansion joints.

The list was partly derived from [A33, p2-3]

1.2 CHOICE OF SHAPE

Nowadays a typical highway bridge will be made of pre-stressed concrete girders in most of the cases. The most probable reason for this is likely to be the low cost and high efficiency of this structural system for spans of roughly 20-50m. Other spans call for different concepts, such as cable stayed bridges for long spans and truss bridges for medium spans. For longer spans steel is used very often, and steel truss bridges were introduced mid-19th century. In that time and the years after, industrial steel fabrication was still in early stage of development. Back then truss bridges typically had a rectangular cross section. Many examples can still be found through Europe, thousands of railway bridges of this type still exist. Earlier examples of steel truss bridges are the covered bridges, mainly found in North America, where the bridge was protected by a wooden cover and roof.



Fig. 1: Selection of modern truss bridges: (clockwise from top left): Webb Bridge, Melbourne, Australia; Peace Bridge, Calgary, Canada; Greenside Place Link Bridge, Edinburgh, Scotland; Light Rail Viaduct, The Hague, The Netherlands

Since then truss as structural system of heavy traffic bridge have somewhat fallen into oblivion, and more large cross section box girder bridges are built nowadays. However in the last 10-20 years interesting developments have been going on in the field of pedestrian bridges. Usually, due to the lower load conditions, developments of new structural shapes are much faster in pedestrian bridges than in heavy traffic bridges. More and more examples of modern truss pedestrian bridges can be found all over the world. The above picture shows a few recent examples of modern truss bridges.

Except for the last example, which is a railway bridge, all bridges are pedestrian bridges. The structural system is their common denominator; they all feature a cylindrical truss which wraps around the bridge deck. This shape is a new concept in the field of bridge engineering. It combines the high load bearing capacities of trusses with the slenderness of tube girders by transforming the traditional 2D truss bridge concept into a 3D cylindrical truss where the occurring forces are more evenly distributed between the members.

Next to the mechanical advantages of a cylindrical truss, it is also very slender and appealing, modern, innovative and futuristic, thus making it a perfect example of the cooperation of architect and engineer. Since this striking shape fits very well in modern architecture, and forms a real challenge for the engineer, it makes up a very interesting shape to study and analyze. Cylindrical trusses are very new in the bridge engineering industry and even newer in the heavy traffic bridge industry, which makes them an even more

interesting object to study. Very little research has been done on tubular trusses as load bearing system for heavy traffic bridges.

The given examples are all made of steel; by nature steel has a very high modulus of elasticity, thus making it very deformation resistant, even with smaller cross-sections. To achieve the same stiffness as steel elements, which is the product of modulus and the element's second moment of area, fiber reinforced plastic elements need a higher second moment of area, and thus larger element dimension. This is caused by the inherently lower modulus of elasticity which fiber reinforced polymers generally exhibit. The bridge examples can be seen as large diameter tubes, which make them a perfect shape for the application of fiber reinforced plastic as building material.

Also, Rijkswaterstaat expressed one of their future visions of so-called "traffic tubes". In this vision future highways will be placed inside large tubes or cylinders made of light weight structural materials such as fiber reinforced plastics. These tubes are both used as load bearing system and as containment for noise and emissions, enabling highways through urban, densely populated areas without any disturbance. Tubular trusses could very well be a suitable solution to the traffic tube vision. The voids between the structural members can be filled up, or the whole tube can be covered by impermeable, sound insulating layers.

Further reasons for the choice of a truss/girder bridge type over other bridge types will be discussed in [chapter 3.1], where the most commonly used bridge types are discussed.

1.3 RESEARCH OBJECTIVE

"Analysis on the feasibility of a cylindrical truss bridge design with a superstructure made up completely of fiber reinforced polymers. This bridge has to withstand heavy traffic loads and remain structurally safe under fire and heat loads. Both the composition of the reinforced plastic as well as the shape of the cylindrical truss and its members will be the main design parameters."

The main objective of this research is to analyze whether it is possible to make a feasible design of a fiber reinforced polymer tube type traffic bridge using the finite element method. In this design the fire safety will receive extra attention since it is one of the most unfavorable aspects of the application of FRP in the civil engineering industry. Whether a completely new design of a cylindrical truss will be made, or an existing cylindrical truss (steel) bridge will be used as a reference design is yet to be decided.

To make a logical, modern and efficient design a range of examples of tube type bridges and FRP bridges will be thoroughly analyzed. The actual state of the art on FRP application in the civil engineering industry will be investigated. The same holds for the current status of fire safety in bridge- and FRP engineering and the application of tubes, shells, lattice- and space-frame structures in bridge engineering.

The design of the FRP structure will be based on the material-specific properties of FRP. The design will also incorporate constructability of the bridge superstructure. The aim of the design is to keep the number of in-situ connections as low as possible. It is expected that a high percentage of the structure is prefabricated.

The structural behavior of the fiber reinforced tube type bridge will be compared to a corresponding design in steel. The aim is to show that FRP can compete with traditional steel structures. The consequences of the application of FRP for the foundation and the roadway will be shown. It still has to be decided how this steel-FRP comparison will be exactly set-up.

The stresses in the FRP and steel bridges will be analyzed and possible flaws will be resolved or redesigned. The FRP structure will be optimized in terms of material use and maximum occurring stresses. Optimization will also incorporate the lay-up, composition and material use of the FRP.

Vibrations, fatigue and long term problems such as durability and sustainability issues will be addressed, though they will not be the main point of interest during this research. The same holds for the costs of the designed structure.

1.4 RESEARCH QUESTIONS

The preceding chapter covers the research objective; from this objective the main research question can be directly derived:

"Can fiber reinforced polymer be used as stand-alone structural material to design a cylindrical truss bridge, which is able to withstand heavy traffic loads, while complying with known fire safety standards?"

Below a list of sub-questions can be found, which further describe the goals of this thesis. Most of the questions describe the goals of this literature study. Several questions will be resolved later on in the design stage of this research:

1. What are the structural characteristics of fiber reinforced polymers? What makes them (more) suitable for bridge construction (than other materials)?
2. What are the specific mechanical properties of fiber reinforced polymers? How can they be derived, described and calculated?
3. What are the required structural demands for road-traffic bridges?
4. What is the actual state-of-the-art on the application of FRP in (traffic) bridges? What makes the design of FRP bridges different from bridge design with materials such as concrete or steel?
5. What is the state-of-the-art on fire safety in bridge design? How much is obliged by codes and standards?
6. What is known about fire safety of fiber reinforced polymers. Are there any codes on fire safety of fiber reinforced polymers in civil engineering?
7. Which design tools can be used for computer aided design in FRP? Can regular FEM packages be used for anisotropic materials such as FRP? Which simplifications have to be made to make a feasible structural model?
8. How to design a cylindrical truss made of fiber reinforced polymers, regarding all given design loads, including fire loads?
9. How can the design be optimized, concerning maximum deflections and stresses and the material use?
10. How can the bridge be designed to meet the durability needs and a design-life of 100 years?

2. FIBER REINFORCED POLYMERS

Fiber reinforced polymers are a relatively new material that is very well suited to compete with traditional building materials such as steel, concrete and timber or masonry. FRP is composed of two main materials: the reinforcement and the polymer matrix which bonds the reinforcement into one monolithic whole. There are various material possibilities for the use of both parts. Next to that composites are also composed of fillers and additives.

The polymer matrix

The polymer is either of the thermoset or the thermoplastic type and based on resin products. The matrix is a continuous material which surrounds and supports the reinforcement by maintaining its relative position. Loose strands of e.g. glass fiber would not be structurally successful. Though the strength in FRP comes from the reinforcement, the polymer matrix delivers the form and ensures proper placement of the fibers. Next to that the resin also protects the reinforcement from outer influences such as weather, water, UV and so on.

All resin types function more or less in the same way. In their raw form they consist of loose molecular chains e.g. monomers which are dissolved in a substance. When the suitable curing agent, catalyst or accelerator is added to this substance, these chains begin to cluster and form a solid, three dimensional structure. The differences between the resins lie in their strength, curing, hardening and in the quality of the fiber-resin interface.

The reinforcement fibers

The other substantial part of FRP is the reinforcement fiber. There are a number of different types of reinforcement which differ foremost in their strength, their modulus and their elongation. All types of reinforcement can be implemented in the FRP in various weaves, filament or chopped strand mats, combination mats or roving.

The symbiosis

When the two parts are combined in the proper way, the curing agent will bond the fibers to the polymer and will form a structure. Performing this curing process in a controlled environment will dramatically increase the quality of the FRP product. Different manufacturing techniques are for example spray winding, centrifugal casting, vacuum bag or the autoclave.

2.1 FRP COMPOSITES MARKET

To give a short summary on the position of FRP composites as a material used in the industry this chapter was added. First of all a graphic is given on the total market volume of fiber reinforced polymers. It is clearly visible that since the 1970's the FRP market volume has almost quintupled. The total volume of FRP composites used is about 5.5 million tons. Compared to the annual steel worldwide steel use of 1.400 million tons, this is of course a small number. The difference with the annual concrete production is even bigger: In 2010 about 20.000 million tons of concrete were used in the industry. [B12, p3-4]

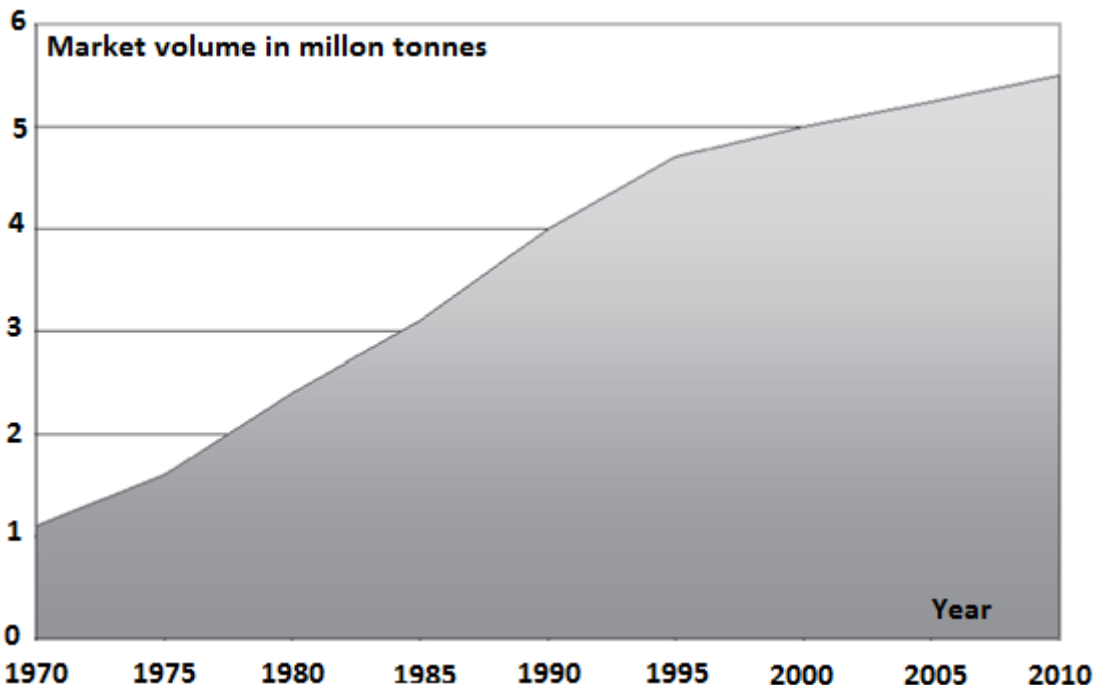


Fig. 2: Fiber reinforced polymer composites market volume from 1970 to 2010. [B12, p6]

Together the sub-markets below form more than 96% of the European FRP market volume. Thus they can be considered as a complete overview of the FRP market:

- Transport and traffic
- Electrics and electrical industry
- Mechanical engineering and machines
- Construction and Building industry
- Chemical industry, pipelines and containers
- Energy industry and offshore industry
- Sports and leisure

Of the submarkets above the “Building & Construction” market and the “Transport and traffic” market are the biggest. The latter includes the automotive industry, aviation industry, rail industry, shipping industry and the aerospace industry.

Examples for applications of FRP in the electrical industry are high voltage switches, cryostats and dry transformers. In the mechanical industry a variety of applications are available, think for example of FRP gears or CFRP leaf springs. Another high tech application of carbon reinforced polymers are rocket nozzles. The construction industry has already been covered before, bridge engineering will follow in the next chapter [chapter 2.3].

In the chemical industry a lot of different FRP encasements are used. Think of high pressure containers for gas or pipelines for corrosive substances. The renewable energy market poses great potential for FRP's, an example are blades or complete wind turbine assemblies. Examples for the use of FRP in the leisure industry have already been given before.

Below the submarkets are shown in a pie-chart. With both 33% Transport and Building & Construction clearly have the biggest market share. The other shares are significantly smaller. [B12, p4-6]

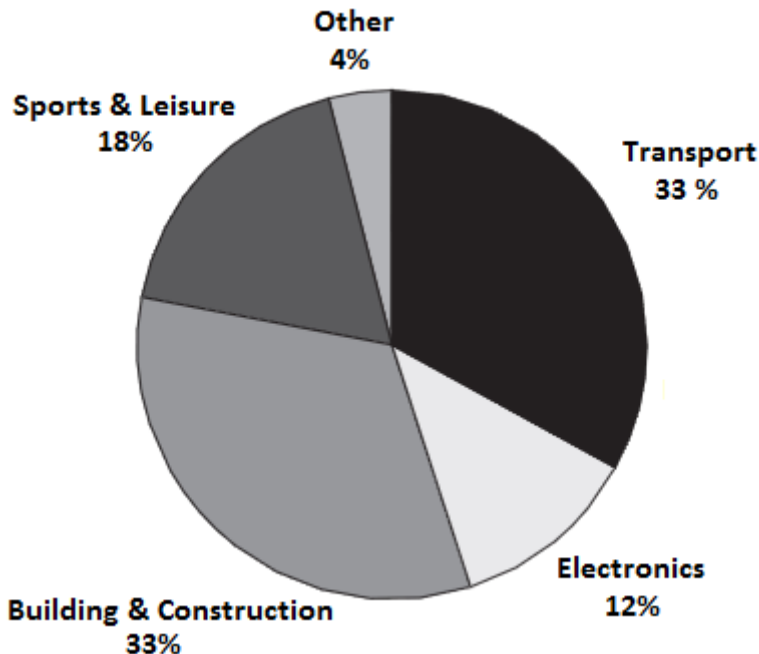


Fig. 3: Market shares in the fiber reinforced polymer composite market. (2002) [B12, p7]

Next some information on the market of different types of fiber reinforced polymers will be given. According to a 1997 study about 70% of all European FRPs are thermo hardening plastics; the remaining 30% are thermoplastic compounds. Generally a shift towards thermoplastic matrixes can be observed, a mere 2 years later, in 1999 their market share had already grown to 42%.

In the next graphic the spectrum of the most common FRP production methods can be studied. Two production methods clearly dominate the market: Open mold production methods are most used. Methods that are part of this group are for example hand-laminating or spray-up. The second most used production technique is the use of sheet- or bulk molding compound. These methods use premixed slurry of chopped strands and liquid resin which is injected into closed molds under pressure. More information on the different FRP production techniques will be given in a latter chapter [chapter 2.5.4].

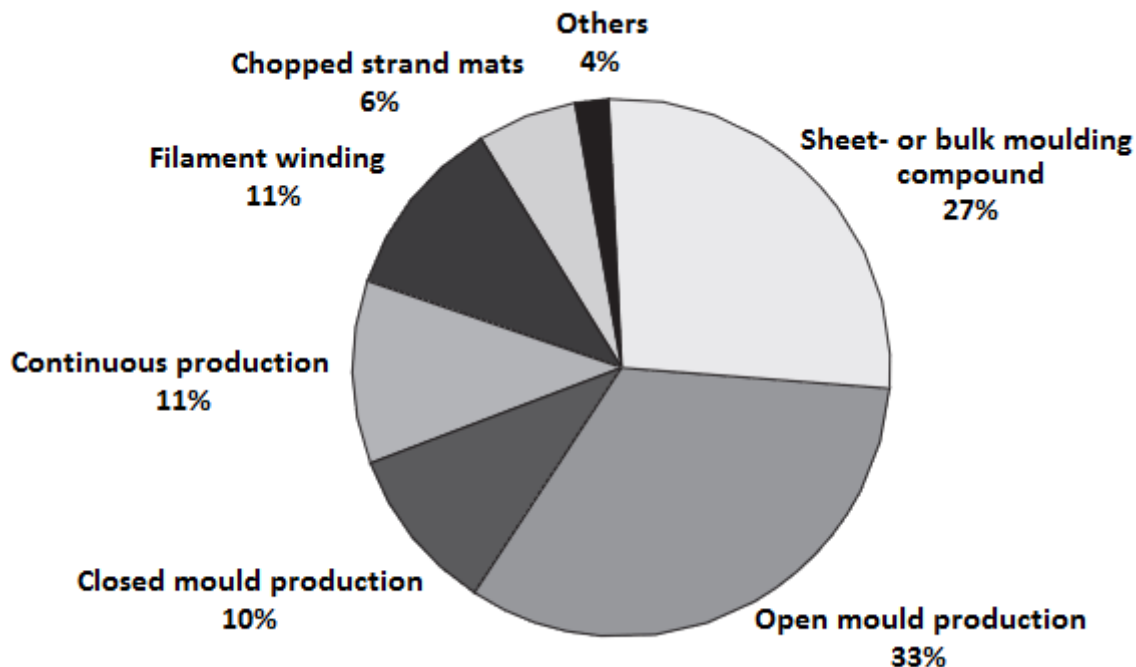


Fig. 4: Different production techniques for FRP composites and their market shares (2002) [B12, p10]

The most used reinforcement material is glass fiber. But due to the need for parts with higher strength and quality, a slight shift towards the much stronger carbon fibers could be observed during the last years. Other types of reinforcement have a smaller market share; natural fibers for example are only used for low-strength applications. The properties of different reinforcements will be covered in a later stage of this report [chapter 2.5.1; chapter 2.6.1.1].

As mentioned before FRP can consist of a great variety of matrix materials and reinforcement materials. Next to that other materials such as fillers and other additives can be added. This leads to a very large variety in material characteristics such as strength. The range of strength is about 50-2000 N/mm² and the range for stiffness is 10.000-400.000 N/mm². An example of a low-strength and -stiffness material is for example glass fiber chopped strand mat. On the other hand, one of the strongest FRP's are unidirectional carbon fiber reinforced prepgres with a fiber volume in excess of 60%.

Accordingly the difference in price for the different materials is also quite extreme: Anything is possible from about 2€/kg to prices in excess of 200€/kg. [B12, p7-8]

It is expected that due to the growth of production volume (see Fig. 8) the price for high strength composites such as carbon fiber reinforced polymers will drop, leading to an increase in the use for mass-production applications such as simple sections, beams or plates in the building industry.

To conclude, a short outlook on the areas of the world will be given where most research is done regarding FRP composites. A recent study by the "American Society of Civil Engineers" showed some interesting points on FRP in graduate education programs.

It seemed that European and Canadian universities offer the best education in FRP composites for construction subjects. But in general, the academic world has not yet implemented FRP to a sufficient extent. [P11, p6]

2.2 HISTORY OF FRP COMPOSITES IN GENERAL

In this chapter fiber reinforced composite history will be covered. First the history of composites as building material will be discussed followed by the history of modern plastics and finally of fiber reinforced plastics.

2.2.1 COMPOSITES

The advantageous combination of two different materials which act together as one solid composite substance has already been discovered several thousands of years ago. The first known composite material is the combination of straw and clay to construct building bricks. This combination of materials was first used by the ancient Egyptian, Chinese, and Israelite people several thousands of years ago. Nowadays this practice is still used by African tribes to counteract cracks in the silt bricks, and to enable a uniform drying process.



Fig. 5: One of the first known man-made composite construction materials: Straw-clay composite

Next to that is also known that the Egyptians were the first to use laminated timber construction techniques. The first recorded use is dated to 1500B.C. The Egyptians glued several thin layers of timber in series together to counteract the swell- and shrinking processes and to achieve a higher strength in all directions.

Another, totally different application can be found in ancient China and Japan. Blacksmiths mastered the art of composite sword-making very early. It is known that both peoples made composite sword blades, using both carbonated iron (steel) and traditional wrought iron.

2.2.2 PLASTICS

In contrast to the history of composites, the history of plastics is still very recent. The generally accepted start of the “plastic age” was in 1868 when John W. Hyatt developed the first real synthetic material in the USA. He produced a solid, stable nitrocellulose which is now well known as celluloid.

The next big step in the history of reinforced plastics was the invention of “Duroplast” or “Bakelite” in the 1910’s. The Belgian inventor Leo H. Baekeland was the first one to control a known reaction of phenol and formaldehyde to such an extent that fillers such as sawdust, paper or other fibrous materials could be added to produce the first real reinforced plastic. The name “Bakelite” was introduced shortly after the First World War in 1922.

Other developments in the field of Fiber Reinforced Plastics were “Formica”, “Celleron” and reinforced rubber. Formica was invented in 1913 by Daniel J. O’Connor; it was produced by pressing rolls of paper into a plate. Before pressing it the paper was soaked in resin. After hardening of the plate a solid sheet remained. Formica was primarily used as electric insulator.

Celleron is a material that was used in the 1930’s to produce non-metallic gears. It was a composite of cotton- or linen fibers and phenolic resin. The primary reason for the production of these new gears was noise reduction in automotive engines.

A few decades earlier, in 1850-1890 fiber reinforced rubber was developed. Driven by the transportation growing industry the need for air inflated rubber tires grew. In 1887 the Scott John B. Dunlop developed a new kind of fiber reinforced rubber air inflatable tires. He also built the first air inflated tire factory in that year. [B1, p3]

2.2.3 FIBER REINFORCED PLASTICS

The production and development of fiber reinforced plastics increased dramatically, also due to the Second World War, in the 1940's, when glass reinforced polyester radar domes (the so called "radomes") were introduced. One would think that a steel dome could fulfill the same structural goal, but steel shielded the radar radiation and therefore non-metallic alternatives had to be found. After that it didn't take long until the advantageous properties of this material were discovered in other fields of research. The first airplane (an American Vultee BT-15) with a hull made out of glass fiber reinforced plastic was built in 1944.

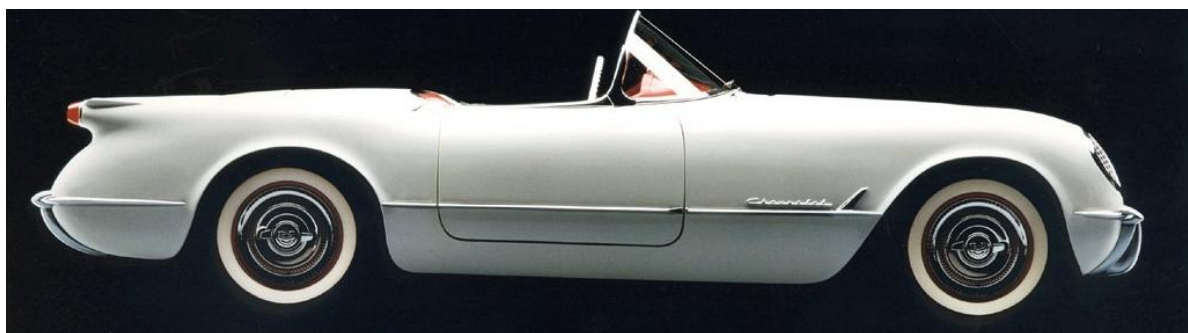


Fig. 6: The 1953 Chevrolet Corvette with an all GFRP body. [WEB, www.chevrolet.com]

After the 2nd World War fiber reinforced plastic started entering the civil market. The first memorable event was the production of the American Chevrolet Corvette in 1953. The body of this car was made of short multidirectional glass fibers in a polyester polymer matrix. It was produced using hand lay-up techniques and matched die moulding. [B16, p12]

After 1953 the production of Fiber Reinforced Plastics grew very steadily. A number of applications were found, from which many are still used in the same manner. Just to name a few applications for fiber reinforced plastics: ships, yachts, piping, storage tanks, electrical insulators, windmill sweeps and of course several other small scale applications such as: fishing rods, hockey sticks, tennis rackets, surfboards, kayaks. Other fields of application are the aviation industry, automotive industry or the aeronautic industry. Generally one can say that all of these applications need lightweight but also strong construction materials. This need probably led to the vast application of fiber reinforced plastics.

Nowadays mainly the high-tech industries such as the aerospace- or the aviation industry keep pushing the limits of FRP. An example is the brand new Airbus A380, in which a staggering 30% of the structural weight is made up of CFRP. The plan for the new Boeing 7E7 is an even higher percentage of 50%.



Fig. 7: The 70m long Visby ship of the Swedish Navy. [B12, p4] and the Airbus A380 with emphasis on the parts made of FRP. [B12, p5]

The military industry is maybe the biggest player in the FRP industry; the Swedish stealth boat "Visby" for example is commissioned by the Swedish Navy and is the largest all carbon reinforced polymer structure in the world. It has a length of 70m.[B12, p1]

2.2.4 FIBER REINFORCED PLASTICS IN THE BUILDING INDUSTRY

Next to the already mentioned application of glass reinforced plastics in radar domes during the Second World War, the application of FRP took a flight when a new method for the production of translucent corrugated sheets was introduced in the late 1950's in Germany. This method featured a continuous production process for glass reinforced polyester corrugated sheets which were then vastly used in the industrial building industry, e.g. for light strips in large scale roofing. [B11, p11]

Getting to know this new technology, between 1956 and 1970 about 70 types of all-FRP houses were designed and constructed. The most known house type is the American "Monsanto house" which was fabricated on a boat builder's yard and commissioned by the chemical company Monsanto in 1957. It was brought to "Disneyland California", where it would be an exposition item for a mere 10 years. After these first experiments with fiber reinforced polymers the chemical industry tried to push FRP materials towards mass use in the building industry. These companies were mainly interested in a fast increase of production volume and did not care for individual, architectural and creative needs. This could explain why FRP materials almost completely vanished from the building world by the end of the 1970's.[A08, p2-3]

Since the 1990's FRP's are used more and more in the building industry again. Several companies such as the Danish company Fiberline have played a major role in development of FRP parts. Nowadays, though a lot of different products are available and the building industry is slowly starting to acknowledge that reinforced polymers are a valuable alternative to traditional building materials.

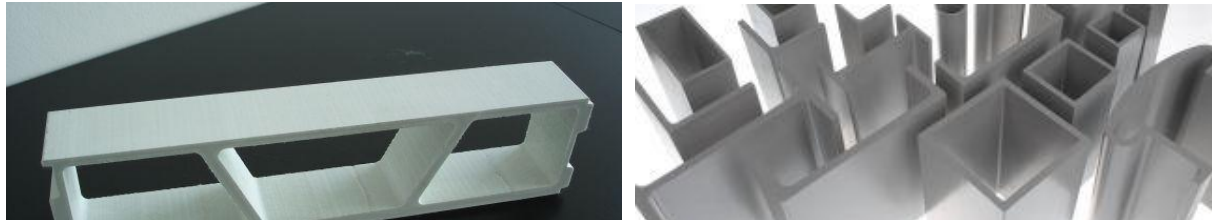


Fig. 8: Fiberline FBD300 Bridge deck profile for heavy loads and numerous examples of pultruded FRP profiles used in the building industry [WEB, www.fiberline.dk]

Below a short list can be found with some of the products which are available in FRP:

- Profiles (CHS, RHS, I-profiles, U-profiles, etc.)
- Planks and panels (sandwich panels, bridge decks, etc.)
- Façade- and window panels

An interesting project to call out is the "Eyecatcher Building", which was constructed for the Swiss Building Fair in 1999 in Basel, Switzerland. This building has 5 stories with a combined height of 15m. It was constructed using only FRP profiles. The bearing structure consist of a number of large GRFRP A-frames. The building was built by Fiberline in close cooperation with ETH Zürich. [P48, p10-11]



Fig. 9: The all-FRP Eyecatcher Building in Basel, Switzerland, 1998
[WEB, www.fiberline.dk]

Just to give an idea: Below two other FRP buildings are shown. Shape-wise anything is possible when using fiber reinforced polymer composites.

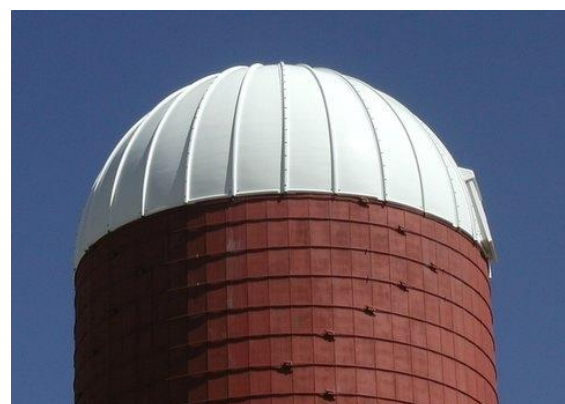


Fig. 10: Left: Non-metallic FRP building for EMC-measurements, built by Fiberline. Right: An FRP-dome acts as roof-structure for a traditional steel silo. [WEB, www.fiberline.dk]

2.3 HISTORY OF FRP COMPOSITES IN BRIDGE ENGINEERING

The history of fiber reinforced polymers in bridge engineering is still a very recent one. Until today FRP bridges make up only a minute part of all bridges. Most of the bridges are made of traditional construction materials such as timber and masonry, and foremost steel and concrete. The first experiments with FRP composite bridge were carried out in China in the late 1970's.

2.3.1 MIYUN BRIDGE, CHINA

The first FRP-deck bridge was the "Miyun Bridge" in China, constructed in 1982. This was a single span two-lane bridge suitable for a maximum load of 30t. It had a span length of 20.7m. This bridge was built-up of six quadratic sandwich girders, made of glass fiber – polyester composite. The deck was in-situ concrete. Exact dimensions can be found in the sketches below. One can clearly see the six quadratic FRP sections. [B15, p74-75]

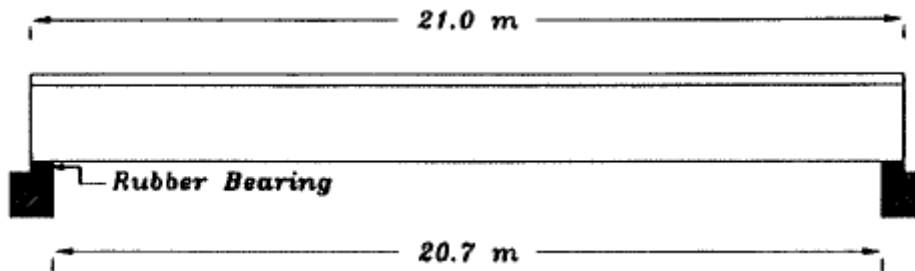


Fig. 11: Structural system of the Miyun bridge in China, 1982.[B15, p75]

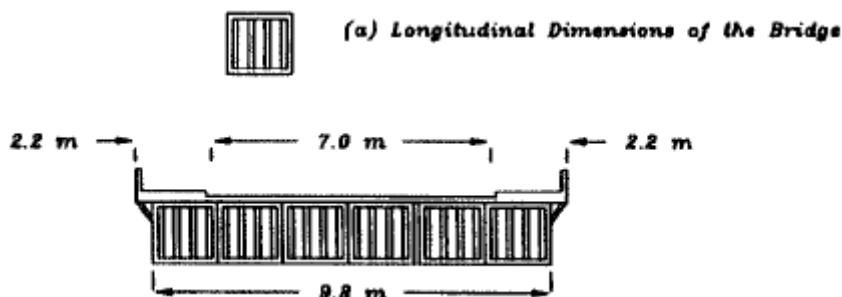


Fig. 12: Deck layout of the Miyun bridge in China, 1982.[B15, p75]

By the late 1980's and early 1990's, as the defense- and aerospace market somewhat waned, increased interest for FRP composites was generated in the civil engineering- and infrastructure markets. This increased demand as well as the development of new technologies, partly funded by Western governments, led to a significant drop in costs for manufacturing FRP composites.

Next to that it became evident that much of the post-war infrastructure in the developed world was in desperate need for thorough renovation. All of these developments led to a slightly higher acceptance of this new technology in the conservative (bridge) construction market. [P07, p1]

Most of the FRP used in bridge engineering today is applied in the form of sheets, strips as repairing or strengthening of existent bridge structures. Next to that some reinforcement bars for concrete structures have been made of FRP composites, substituting traditional reinforcement.

The use of bigger structural parts such as beams, decks, crossbeams, railings or even bridges made completely out of plastic composites is still very scarce. In a recent survey it was found that worldwide only 53 all-FRP bridges have been constructed. Most of which are pedestrian bridges, designed for small loads. [T07, p1, p62-67]

Although FRP composite products were first used in infrastructure bridge projects in Europe and Asia, the nation with the most research and experimental showcase projects would become the US starting in the 1990s. Below a selection of some other pioneering projects is shown. Next to the Chinese project already discussed before, this selection shows bridge projects in Germany, Scotland and the USA. [P4, p1-2]

2.3.2 ULENBERGSTRASSE BRIDGE, GERMANY

This bridge, constructed in 1986 at the Ulenbergstrasse in Duesseldorf, Germany was the first heavy load highway bridge using FRP pre-stressing tendons. The bridge is a normal girder-bridge with two spans of 21.3m and 25.6m. The bridge carries regular highway traffic and has a width of 15m. The concrete slab of the bridge was post-tensioned with 59 Polystal pre-stressing tendons, each made up of 19 glass reinforced polymer rods of nominal diameter 7.5mm. These tendons are block-anchored and carry a working load of 60kN. In total about 4 tons of glass fiber reinforcement was used for this bridge. This bridge also functions as a research bridge, being continuously monitored and periodically test loaded. [B21, p524]

2.3.3 ABERFELDY FOOT BRIDGE, SCOTLAND

This footbridge was constructed in 1992 in Aberfeldy in Scotland, crossing the local river Tay. The bridge was commissioned by a local golf club to connect two 9-hole golf courses. After a preliminary evaluation by the University of Dundee under Prof. Harvey it became evident that traditional materials would not be sufficient to meet all desired needs, such as light-weight and large span. As a result "Maunsell Structural Plastics" were appointed as lead structural engineers and it was decided to take on the challenge and build the first all-FRP footbridge in the world. Maunsell used their newly developed "Advanced Composites Component System" (ACCS), a system which uses prefabricated FRP panels joined by a combination of mechanical fasteners and bonded joints. [P22, p1-2]

In the picture below the structural system can be observed: the bridge is a cable-stayed bridge with two A-frame pylons carrying the load on the deck via a fan-shaped array of cables to the foundation. The span of the Aberfeldy footbridge is 63m, which is quite large for the application an all new technology such as FRP.

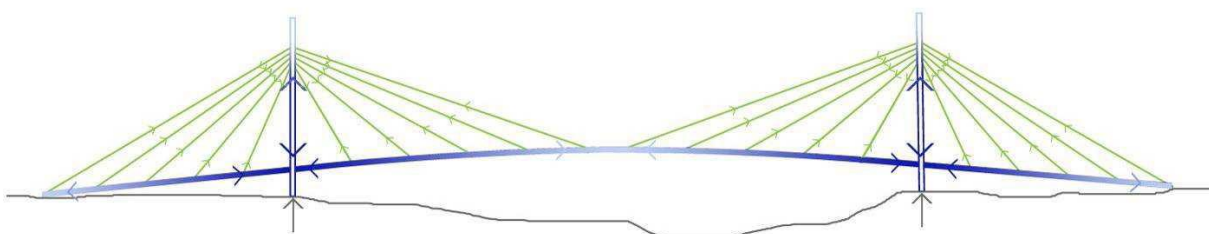


Fig. 13: The structural system of the Scottish Aberfeldy Footbridge (1992), the first all-FRP pedestrian bridge [P22, p3]

Nowadays this bridge is still used by the golf club. Due to the close involvement of the Dundee University, whose students also had a part in the design and construction of this bridge, it is still an object of constant survey and research. These researches show that, even with a minimum amount of service being

performed, the structural system of this bridge is still completely intact, except for some cosmetic problems. [P22, p10]

2.3.4 PLASTIC BRIDGE, RUSSEL COUNTY, KANSAS, USA

This bridge was the first bridge in North-America with an all-FRP vehicular bridge deck. It spans the “No Name Creek” in Russell County, Kansas. The plastic bridge, built in 1996 is a very small span bridge: It has a total length of only 7.3m and a very short span of only 6.4m. The width of this bridge is 8m, carrying two traffic lanes.

The bridge uses the “Kansas Structural Composites” Honeycomb Sandwich panel deck. It was primarily installed as demonstration project for the manufacturing company. Following this example, many more demonstration bridges were installed in the USA, leading to FRP becoming commercially viable. Currently over 50 FRP composite vehicle bridges have been installed throughout the USA. Below the FRP honeycomb deck system used by Kansas Structural Composites for this bridge can be seen.



Fig. 14: The Kansas Structural Composites honeycomb deck system [WEB: www.fhwa.dot.gov]

2.3.5 FRP BRIDGES IN THE PRESENT

The bridges discussed above show how FRP found its way into bridge engineering in the last 30 years. Currently composite fabricators and suppliers, along with a large number of researchers and institutions are actively developing and researching products for the civil infrastructure. All FRP applications in bridge are currently explored by numerous companies and institutions throughout the world.

The USA is currently leading the research and development of FRP composites for infrastructure bridge projects. The US Government and private institutions have funded many demonstration bridge projects that have been successfully constructed and monitored as part of on-going research. However there is still a lot to be learned about FRP composites in bridge engineering field.

Although FRP composites have been used for decades in multiple industries, the application of FRP composites has only recently been expanded to encompass the bridge engineering sector. FRP bridge engineering is still very small scale both in quantity of bridges, as in quantity of span length. [P4, p6-10]

2.4 APPLICATIONS IN BRIDGES

In this chapter the possibilities of using fiber reinforced polymers in bridge design will be discussed. Generally four types of application will be covered. First the application using most FRP in weight will be covered, the all-FRP bridge design. This will be followed by the hybrid FRP design using second most FRP in weight. The chapter will be concluded with replacement and repair of bridges by FRP materials.

2.4.1 ALL FRP

In order to be successful, advanced composite bridge system should be built up in a modular way and assembly should be rapid, simple and have reliable connections; the material should be durable. Any long construction- or maintenance period causes disruption to the traffic and is usually very expensive. Advanced FRP materials are durable and light-weight, consequently, they fulfill the above requirements, provided the initial design of the modular system is properly undertaken and the material is properly installed. [B21, p503]

The most used composite material is GFRP and although this material is strong in tension it has a low modulus of elasticity. If possible the stiffness should be increased by enhancing the shape of the FRP elements to give them an enhanced EI-value. Although significant advantages for construction can be derived from the lightweight and high strength-to-weight ratio of FRP materials, the durability and long-term performance issues still require further research. Also vibrations can pose problems due to the light weight and the accompanying low natural frequency. [B21, p503]

Currently, all FRP bridge systems tend to be more expensive than conventional bridge materials. However, the transportation and site procedures derived from the lighter weight material do financially compensate the greater cost of raw material. Furthermore, as the manufacturing processes become more sophisticated the cost will reduce. [B21, p503]

Of all described FRP applications in bridge engineering, all-FRP bridges are the most valuable for this research. Some examples have already been described [chapter 2.3.3] or will be described later in this report [chapter 6.2]. In total there are about 50-60 known all FRP bridges around the world (mid 2011). [T05, p62-67]

2.4.1.1 PEDESTRIAN BRIDGES

In contrast to the above described traffic bridges, FRP pedestrian bridges have been used in more occasions. FRP materials are frequently used in smaller scale pedestrian bridges, for example by the Dutch company 'Fibercore' [chapter 6.2.4], the Russian company ApATeCh in Moscow [T07, p55] or the Spanish built footbridge in Lleida [chapter 6.2.2].

FRP components used for pedestrian bridges are light weight, rapidly installed, environmentally friendly assembled and can be easily installed in remote areas. Sometimes FRP pedestrian bridges can even be installed by helicopter, as is the case with the Pontresina pedestrian bridge. [P19, p128][P32, p7]

2.4.2 HYBRID FRP

Hybrid FRP applications are all application in bridge engineering, where fiber reinforced polymers are used as a part of the load-bearing system. Throughout the years several methods have been developed to use FRP materials in bridge decks, as concrete reinforcement, in pre-stressing tendons or cable-stays, as column-confinement or just plain and simple as stock profile to form an alternative to normal steel profiles. In this section all of these methods will be described.

2.4.2.1 FRP PROFILES

Currently several manufactures of FRP profiles, mostly pultruded glass fiber reinforced polymer, exist. Two of the European top manufacturers being 'Fiberline' from Denmark and 'Topglass' from Italy. Both manufacturers offer a large number of different longitudinal profiles as well as plate elements. These sections can very well be used as substitute for normal steel or concrete elements. Especially their high corrosion resistance, light weight and high strength makes them very suitable for use in bridge engineering. [A48] [B25]

Note that when designing FRP flexural elements not only their strength is of great importance. Furthermore, FRP flexural elements are often deflection-limited, thus stiffness is the more important design parameter. Also, connections in FRP elements call for a special approach compared to steel. Often elements have to be adhesively joined, leading to much stiffer joints than when using mechanical fasteners only. [B22, p2.20-2.22] Typical FRP sections are I-profiles, L-profiles, U-profiles and RHS and CHS profiles. [B25, p1.2.13-1.2.22] FRP profiles can also be used for trusses, thereby improving the corrosion resistance significantly compared to steel trusses. [B22, p2.26]

2.4.2.2 FRP BRIDGE DECKS

It is reported that by 2003 worldwide over 90 commercially available pultruded FRP bridge deck systems have been used as a replacement for conventional highway bridge decks that are used for vehicular traffic. [B21, p506-507] Most commercially available decks consist of assemblies of adhesively bonded pultruded shapes. Continuous pultruded shapes are fabricated using well-established processes and assembled into modular panels. Typically construction of the deck is completed by installation of a wearing surface to protect the deck from mechanical damage. [P19, p127] The advantages of FRP bridge decks are high durability, corrosion resistance, fatigue resistance, high strength, rapid installation, low life-cycle costs, light weight and high quality manufacturing processes under controlled environments. [B21, p507]

The expected life-span of a conventional highway bridge deck currently lies at about 15 years in Europe. Often repair or replacement is then required, thereby drastically increasing the maintenance cost. If installed separately from the main bearing system, modular FRP bridge decks can improve cost-effectiveness of repair and maintenance measures. They provide a low-weight, corrosion-resistance and rapid installation with minimum traffic disruption. To give an idea, typical GFRP bridge decks weigh about 20% of conventional concrete decks and in the case of typical highway bridges can be erected in two days, while guaranteeing a service life 2x to 3x times greater than concrete decks. [B21, p506-507]

2.4.2.3 CONCRETE-FILLED FRP TUBES

Concrete-filled FRP tubes provide an effective alternative to conventional reinforced concrete piles. The composite piles consist of a filament wound GFRP outer shell which acts as a stay-in-place formwork and non-corrosive reinforcement for a concrete core. The FRP shell also protects the concrete core from exposure to harsh environmental conditions and provides confinement for the concrete thereby increasing the strength and ductility of the pile. [P19, p126-127]

2.4.2.4 FRP REINFORCEMENT

The first FRP reinforced concrete materials were developed in the 1960s. Several decades later one-dimensional CFRP and GFRP bars are widely commercially fabricated and used as reinforcement for concrete structures. Due to their excellent corrosion resistance and their enhanced erection- and handling speeds, FRP reinforcing bars have been extensively used for a number of concrete structures including bridges, highway pavements, maglev rails and structures housing magnetic resonance imaging equipment. FRP materials are also fabricated as two-dimensional grids, in a similar fashion of conventional steel welded wire fabric, which were used as reinforcement for a concrete bridge deck. [P19, p123] [P36, p3]

Shear stirrups represent another application of FRP in bridges since these particular reinforcements are the most susceptible to deterioration due to corrosion. Typically a minimum concrete cover is provided for shear reinforcements. Moisture ingress into cracked cover concrete can cause corrosion of the stirrups and spalling of the cover concrete. [P19, p123]

2.4.2.5 FRP TENDONS AND CABLES

The high-strength characteristic of one-dimensional FRP products has been effectively used for pre-stressing concrete bridge girders. Several different types of CFRP and AFRP rods and tendons are used in pre-stressing applications. Note that due to their anisotropy FRP cables and tendons are always placed parallel and never in twisted arrangements. The German bridge Ulenbergstrasse in Düsseldorf, also discussed in [chapter 2.4], which was constructed in 1986, was the first vehicular bridge in the world to use composite pre-stressing tendons [P19, p125]

The main advantages of FRP materials in applications as tendons or cables are their excellent tensile strength, their non-corrosiveness; they are non-magnetic and are lightweight. Furthermore, they also have a better fatigue resistance than steel cables. The low weight of FRP cables causes a reduced sag in the cable stays. Of the three main FRP materials, GFRP, AFRP and CFRP, carbon fiber reinforced polymer and aramid fiber reinforced polymers offer the best properties for use in cables and tendons due to their low weight, and lower susceptibility to stress-corrosion (creep rupture). Note that FRP cables are still more costly than normal steel elements and also require different, more complex anchoring systems compared to steel, due to their low transverse strength. Despite these drawbacks, the use of FRP cables and tendons has substantially grown over the last years and is expected to keep growing over the next years. [B21, p514] [B22, p2.2-2.3]

2.4.3 REPLACEMENT, REPAIR AND REHABILITATION OF BRIDGE ELEMENTS

While composites are often used for new bridge structures, another very practical, effective and promising use of FRP materials has emerged in the last decades: the repair, strengthening, rehabilitation and replacement of parts of existing bridge structures, both steel and reinforced/pre-stressed concrete. Many different options do exist for these means, mostly using adhesively bonded FRP sheets. In this chapter most of the existing methods will be described. [B21, 510]

2.4.3.1 BRIDGE DECK REPAIR AND REPLACEMENT

Many studies prove that by externally bonding FRP plates or sheets excellent retrofitting mechanisms to increase deck strength as well as stiffness of aging or deteriorated structures are created. [P91] [T13] The advantages of this retrofitting method include reduced labor costs, minimum shutdown time/cost and traffic disruption, and minimal maintenance requirements. In all known cases an increase in strength and stiffness was observed. Furthermore, it was also found that the benefits of such a retrofitting system do not deteriorate over time. [P91, p5]

In a TU Delft laboratory experiment, research and finite element validation it was proven that previously fatigue damaged steel plates of, in the Netherlands very common, orthotropic steel bridge decks can be substantially strengthened by adhesively bonded GFRP laminates. The observable stresses in the steel plate under the GFRP composite reduced by a factor of 6, thereby also positively influencing the left-over fatigue life of the bridge deck. [T13, p161-162]

2.4.3.2 FLEXURAL- AND SHEAR-STRENGTHENING

Externally bonded FRP sheets and pre-cured laminates are commonly used for flexural- and shear-strengthening of concrete bridge structures. The scheme below shows the principle of shear- and flexural strengthening. FRP sheets are typically used for structures with severe surface irregularities or geometric discontinuities, since the dry fibers can be easily shaped to match the surface and placed using epoxy adhesive. Pre-cured laminates are used when higher levels of strengthening are required; usually they are bonded by thermoset adhesives. [P19, p131]

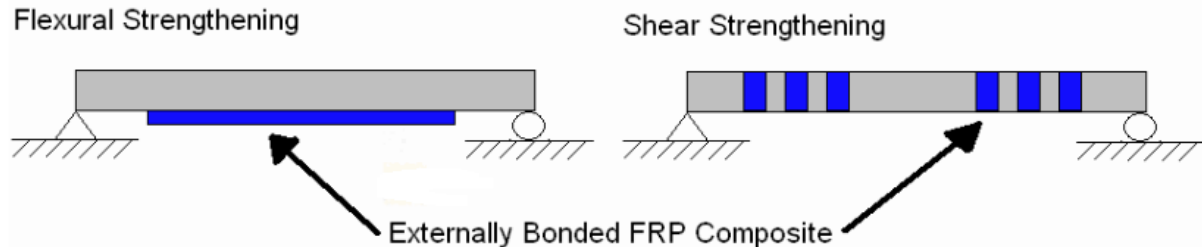


Fig. 15: Principle of shear and flexural strengthening using FRP bonded sheets. [P15, p4]

Both strengthening methods are considered to be 'bond-critical', as they rely on the bond between the FRP and the concrete or steel to transfer stresses. [P15, p4] Another method of strengthening structures is the insertion of near-surface mounted rods, strips or bars. In this procedure FRP composite elements are embedded in narrow adhesive-filled grooves that have been cut into the (concrete) elements. This method can also be applied in timber bridge girders.[P19, p131]

Flexural- and shear strengthening methods do not only exist for concrete elements. The successes in concrete applications led to the development of FRP strengthening methods for steel and cast-iron bridges. Several examples are known where the capacity of old bridges was increased by placing CFRP sheets in a wet lay-up process.[P19, p134] Note that due to high stiffness of steel, only high modulus fiber reinforced polymers can be used, else the reinforcement would only be utilized after the steel in its vicinity had yielded. [B21, p518-519]

2.4.3.3 COLUMN REHABILITATION

Wrapping concrete columns with FRP sheets is currently a common technique used for the rehabilitation of concrete columns. The wraps provide confinement for the concrete, thereby increasing the axial compressive strength and ductility of the column. [P19, p133]

It has been found that FRP sheet confinement of columns is only effective for round columns, because only in that case a truly homogenous confinement of the column is possible. Confinement triggers two main effects: firstly, an increase of the confined peak stress and secondly an increase of the post-peak ductility and ultimate strength of the concrete column. [B21, p519]

FRP confined concrete columns are also often used in areas prone to frequent earthquakes, such as Japan. The FRP sheet confinement enhances the seismic resistance of bridge piers and structural columns. Next to that, the closed FRP sheets also prevent ingress of moisture and thereby improves the durability of the column. [P19, p133]

2.4.3.4 EXTERNAL POST-TENSIONING

Similar to the FRP tendons used to pre-stress newly built concrete girders, it is also possible to strengthen existing concrete girders by applying stress through external FRP post-tension tendons. Especially CFRP and AFRP tendons are very suitable for the use as external pre-stressing tendons due to their high corrosion resistance, excellent fatigue resistance compared to steel and generally high durability. [B21, p515]

A research by the University of Miami illustrated the possibilities of post-tensioning existing structures with external CFRP tendons. In this research two demonstration projects were successfully finished, having developed practical methods to use CFRP post-tensioning to limit deflections and increase the load-bearing capacity of an existing concrete girder. [P92, p7]

2.5 MATERIALS

As stated in the introduction of this chapter on fiber reinforced polymers, as the name composite suggests, this material consists not only of one material such as steel for example. FRP composites consist of two main ingredients: the matrix, usually some kind of (liquid) plastic. This matrix is combined with a strong fibrous material such as for example carbon. Together, these two materials form a solid, inhomogeneous and anisotropic building material called fiber reinforced polymer.

Next to the fibers and the matrix, FRPs consist of additives which control the reaction between matrix and fiber and ensure that the material surface is resistant to various kinds of influences, such as corrosive, wet or fire-hazardous environments.

The fibers in FRPs work similar to muscle- or wood-fibers. They reinforce their embedding substance and provide it with improved mechanical properties. In this respect the interaction between fibers and polymer matrix is very important. The fibers perform extremely well under tension, but particularly bad, when under pressure or flexure.

In contrast, unreinforced plastics or polymers can be used to form usable structural components but are very brittle (in the case of thermo hardeners) or too flexible (in the case of thermoplastics).

Only after combination of the fiber and plastic, and a strong bond between the two, high performance structural parts like airplane parts, car parts or highly stressed sporting goods such as canoes or tennis rackets become possible. [B11, p17]

In the following all possible materials and combinations will be discussed in-depth. All properties and consequences of the use of a certain material will be covered.



Fig. 16: High performance 3D braided CFRP rocket nozzle [B19, p6] and the interface between short glass fibers and resin matrix under the electron microscope [B11, p125]

2.5.1 REINFORCEMENTS

Fibers in reinforced plastics are primarily used to reinforce the resin by transferring the stress under an applied load from the weaker resin matrix to the much stronger fiber. Plastics provide valuable and versatile materials for the use as matrices, but other materials, such as metals, ceramics, and cements, can also be used as matrices for fibrous reinforcement composites.

For an efficient reinforced plastic under stress, the elongation of the fiber must be less, and its stiffness modulus higher than that of the matrix. Stress transfer along the fiber-matrix interface can be improved by use of binders, or special coupling agents. The diameter of the fiber also plays an important part in maximizing stress transfer. Smaller diameters give a greater surface area of fiber per unit weight, to aid stress transfer in a given reinforcement context. [B16, p25-28]

The most common fibers nowadays are glass fibers, carbon fibers, aramid fibers and natural fibers. Next to that nylon- and polyester fibers are also used. All of these fibers have a low density and give the plastic that is reinforced a higher strength and stiffness. The low fiber density is one of the main reasons for the excellent strength/stiffness to weight ratio.

One can yield the highest performance when the used fibers are of near-to-infinite length and when they are inserted unidirectional and isotropic. The more anisotropic the fibers are inserted, and the shorter the fibers get, the lower the mechanical properties. But even fibers with only 1mm length can still reinforce thermoplastics when inserted through for example injection molding.

This large array of possibilities regarding length, direction and type of fiber brings just another great advantage of FRP composites. The composite can be completely tailor made following the specific mechanical needs for any project. This leads to a far better efficiency of material use, than for example when using steel or concrete.

All fibers behave quasi-elastic until breaking, whereby carbon fibers are much stiffer and lighter than glass fibers. This is part of the reason that for many high performance applications in the transport industry carbon is preferred over glass. [B11, p17-18]

In this chapter all of the above mentioned reinforcement types will be covered.

- Glass fibers
- Carbon fibers
- Aramid fibers
- Natural fibers
- Other fibers

2.5.1.1 GLASS FIBERS

The idea to use fine glass fibers in weaving processes to produce textile glass was developed by the French physicist Ferchault de Réaumur in the late 18th century. However industrial production of continuous glass fibers only started in 1935 in Newark, Ohio, USA when the company Owens & Canning developed a production method suitable for industrial production. Production in Europe started only 3 years later in Germany. The first industry that used glass fibers was the electrical industry, hence the common name the glass fiber type "E-glass". Since this the 1930's glass fiber production has undergone a constant evolution of better products and more efficient production.

Glass fibers are the most widely used reinforcements; over 90% of all FRPs are made of glass fiber. The oldest and still most popular form is E-glass or electrical grade glass. Other types of glass fibers are A-glass or alkali glass, C-glass or chemical resistant glass, and the high strength R-glass and S-glass. Under laboratory circumstances glass fibers can resist tensile stresses of about 7000 N/mm², whereas commercial glass fibers reach 2800 to 4800 N/mm². [B16, p28]

Nowadays glass fibers are produced by a process called "direct melt system". In this system the crude materials needed for glass production, such as limestone, siliciumdioxide, aluminumdioxide, kaolin, quartz and others are grinded and checked for pureness.

Afterwards they are inserted in a giant melting bath, where they are heated up to about 1600°C. The crude materials are inserted in a continuous process. After reaching the desired temperature the molten glass is fed directly to platinum-rhodium nozzles or bushings with a diameter of about 1-2mm. This bushing is electrically heated and has about 100-1000 drawing points.

The molten glass is drawn through the bushings into continuous filaments at a speed of about 50 m/s. The individual filaments are now coated with size and other additives as emulsion before being brought together in strands with a diameter of about 5-24 µm.

The filaments are now spun into strands or basic fibers with a linear weight of 2.5-4800 tex, or weight (in gram) per kilometer. These strands can then be used to produce various products such as roving, continuous filament mats, chopped strand mat. The scheme below shows the production process as well as most of the final glass fiber products. [B11, p123-124]

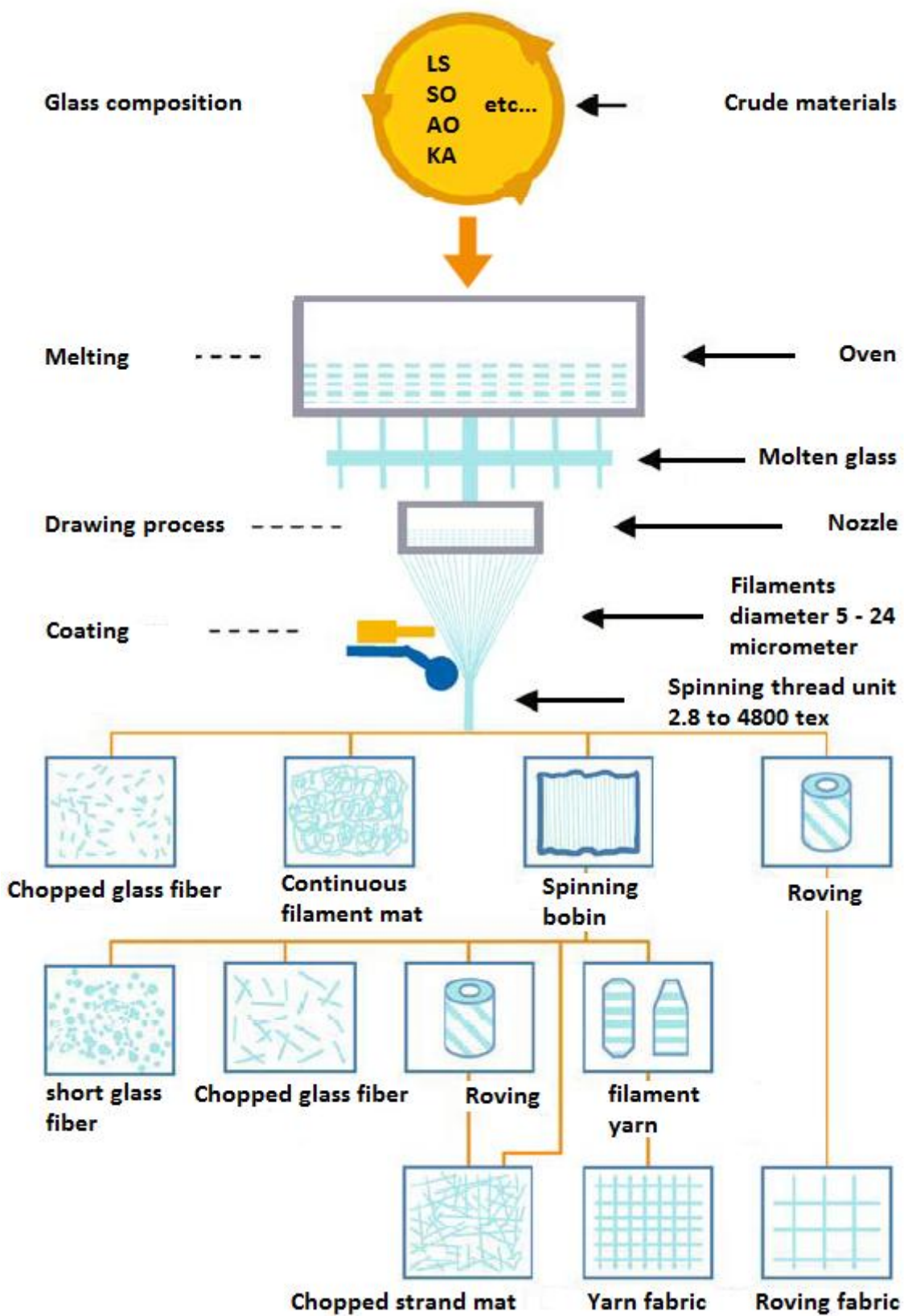


Fig. 17: The production process of glass fibers and the final products [B11, p124]

In the following several tables will be presented to show some of the characteristics of the different glass fiber grades. The first table shows the chemical composition of the different glass fiber grades. The chemical composition is given here solely as an overview and introduction.

Component	E-Glass	R-Glass	A-Glass	C-Glass	EC-Glass
SiO ₂	52,4	60,0	72,5	63,6	58
Al ₂ O ₃ and FeO ₃	14,4	25,0	1,5	4,0	12,4
CaO and MgO	21,8	20,0	12,5	16,6	23
B ₂ O ₃	10,6			6,7	
Na ₂ O and K ₂ O	0,8		13,5	9,1	

Table 1: Chemical composition of different grades of E-, R-, A-, C-, and EC-glass fibers [B11, p1123][B15, p114]

In the table below a comparison between various glass-fiber types can be seen. It is clearly visible that the high strength R-Glass offers the best performance. It has both the highest tensile modulus as well as the highest tensile strength. The most used grade, the E-Glass performs second best. It is also obvious that the fracture-strain for all glass types is quite low. Steel can typically take strains in excess of 10% before fracturing. A conclusion to be made here is, that glass fibers have a bad ductile performance compared to steel. They behave very brittle.

Type	E-Glass	R-Glass	A-Glass	C-Glass	EC-Glass
Density	2,6	2,53	2,68	2,52	2,72
Tensile strength [N/mm ²]					
- Filament (not coated)	3.400	4.400	3.000	2.400	3.445
- Roving (coated)	2.400	3.600			
Tensile modulus[N/mm ²]	73.000	86.000	73.000	70.000	73.000
Fracture strain [%]	4,8	4,8	4,4	4,8	4,8
Softening point[°C]	846	985	773	750	882

Table 2: Comparison between E-, R-, A-, C-, and EC-glass fibers [B11, p132]

As mentioned before there are a number of different products that are made of glass fiber filaments. To show the difference between these products and their mechanical properties the following table was made. The properties of the woven cloth, chopped strand mat and continuous roving are compared. The last material is the heaviest and has the highest fiber content; it therefore has the best mechanical properties. The tensile modulus is 3-10x times higher than that of the other materials. The same holds for the flexural modulus and strength, being 2-8x times higher than that of the other material.

Next to that it is interesting to see that the differences between the manufactured and raw glass fiber material is quite noticeable. Whereas the raw material has a tensile modulus of 73.000 N/mm² (in the case of E-glass), the chopped strand mat has a tensile modulus that is 10x times lower, although it has a fiber content of about 30%. Among others, this leads to the conclusion that next to fiber content also the direction of the fibers is of great significance for the mechanical properties of the glass fiber product.

Type	Unit	Woven Cloth	Chopped Strand Mat	Continuous roving
Glass content	%	55	30	70
Specific gravity		1,7	1,4	1,9
Tensile strength	N/mm ²	300	100	800
Compressive strength	N/mm ²	250	150	350
Flexural strength	N/mm ²	400	150	1.000
Flexural modulus	N/mm ²	15.000	7.000	40.000
Impact strength	kJ/m ²	150	75	250
Coefficient of linear thermal expansion	x 10 ⁻⁶ /°C	12	30	10
Thermal conductivity	W/mK	0,28	0,2	0,29

Table 3: Mechanical properties of three different GFRP products [B16, p49]

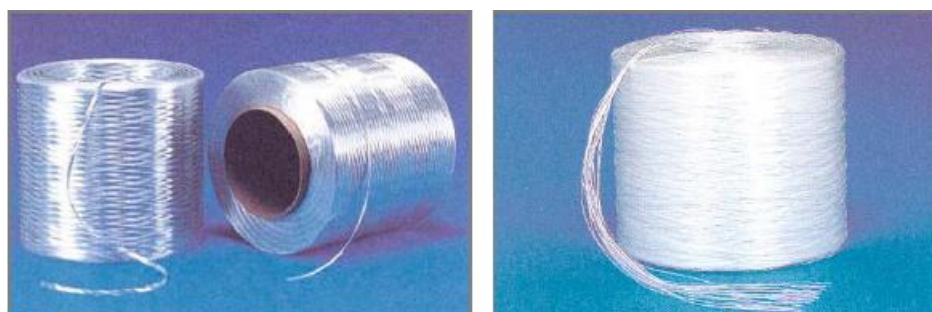
The last table shows that the different glass fiber applications can have completely different mechanical properties; it is therefore advisable to give an overview on the available GF-products. Below the following products are explained

- Continuous filament roving
- Chopped strand mats
- Continuous filament mats
- Woven glass fabrics

Continuous filament rovings

Rovings are specified by the type of glass (e.g. E-glass), the filament diameter (e.g. 10µm) and the weight per kilometer (e.g. 1200 tex). Two types of rovings exist, direct rovings and assembled rovings. Direct rovings are composed of parallel filaments and assembled rovings are spun. This leads to a more loose packing in the case of the assembled rovings. Direct rovings are used for Pultrusion, Extruding, continuous filament winding and weaving, whereas assembled roving are mostly used for continuous filament mats, chopped strand applications and spray ups. One could say that the direct rovings are more suitable for high strength applications, due to their more dense packing, parallel packing, thus more integer strands. Also direct rovings are smoother and have less problems with fraying strands.

Rovings are subassemblies; they are delivered in spools, which are post processed to final products such as for example continuously wound pipelines or pultruded profiles. [B11, p127]

**Fig. 18: Spool of E-glass fiber direct rovings (left) and assembled rovings (right) [B11, p127]**

Chopped strand mats

Chopped strand mats (CSM) are an application of rovings. The rovings are cut to a specified length, e.g. 50mm and are randomly spread on a conveyor belt. To obtain a satisfactory bond between the loose fibers the fibers are sprinkled with polyvinyl- or acetate binders. Typical percentages for binders are 3-6% in volume. After the binder has cured, the fibers have formed a continuous and coherent mat. CSMs weigh about 225-900g/m², with 300 g/m² or 450 g/m² being the most common weights. Besides weight per square meter, strand fineness, strand length and type of binding agent are important parameters for the qualification of chopped strand mats.

CSMs are typically used for processes like hand lay-up, hot pressing or continuous plate production. Below a picture can be found of a typical manufacturer supplied chopped strand mat. [B11, p128]



Fig. 19: Typical glass fiber chopped strand mat [B11, p129]

Continuous filament mats

Continuous filament mats (CFM) are produced in a similar way as the CSMs. The produced rovings fall on a conveyor belt, where they form multiple layers. Next a binding agent is added and the mats are compacted to form a sturdier solid. After that the mats are rolled on a spool. Specification of CFMs happens in the same way as with CSM, with one added parameter: the mesh type.

CFMs are typically used for pultrusion, continuous production methods, the fabrication of preforms and hot pressing. As shown in the picture below, CFMs look quite similar to CSM.[B11, p128]



Fig. 20: Typical glass fiber continuous filament mat [B11, p129]

Woven glass fabrics

Woven glass fabrics (WGF) are mostly 2-dimensional cloths that are machine-woven. WGF can be divided in two classes: Those prepared from rovings, and those from yarn. Weaving untwisted E-glass rovings into fabric produces the woven roving fabric. Yarn based fabrics are woven from continuous filament glass fibers, which have been twisted with 20-40 turns/meter. Together with the use of size this enables the weaving of very uniform cloth.

Just like traditional cotton cloths, WGF exist in several different weaves, such as for example: plain weave, twill weave, satin weave and unidirectional weave. The satin weave has the best mechanical properties in all directions, whereas the unidirectional weave has the best properties in the weaving direction.

Generally WGF have far better mechanical properties than CSMs or CFMs, that is also the reason why they are mostly used in applications where higher mechanical performance is needed. WGFs are supplied in weights from a few hundred to 1200 g/m². If needed, combinations of CSM/CFM/WGF are also possible. [B22, p3.6-3.7]

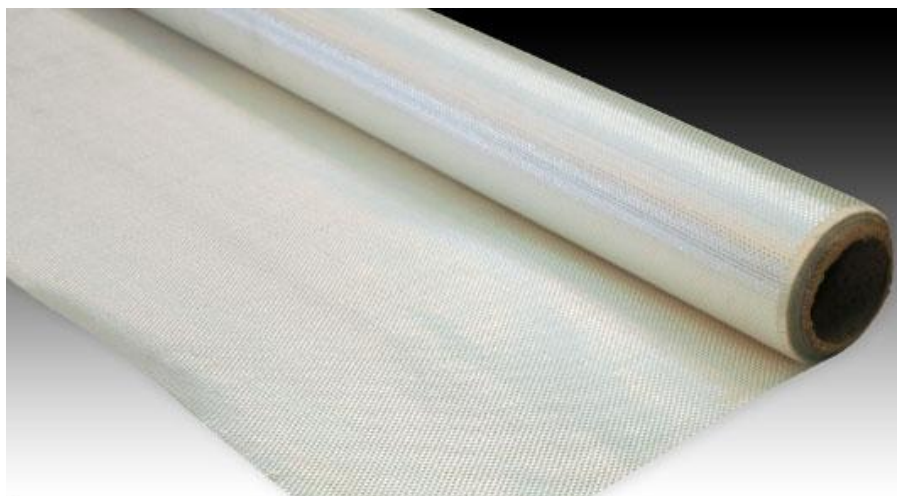


Fig. 21: Woven glass fabric as supplied by the manufacturer. [B11, p130]

Glass fiber cuttings

Next to the above mentioned products, this is another glass fiber product that is available from manufacturers. Glass fiber cuttings are used to randomly reinforce pourable molding compounds or polymer granulates. Characteristic properties are filament diameter, type- and amount of size, fiber fineness and fiber length. [B11, p130]



Fig. 22: Glass fiber cuttings [B11, p130]

2.5.1.2 CARBON FIBERS

Carbon fibers (CF) started off in a completely different way than glass fibers, the first patents on the application of carbon fibers date already from 1878 and 1879/1892. In those years Joseph W. Swan and Thomas A. Edison invented a method to produce carbon fiber glow wires for light bulbs. In these methods the carbon fibers were produced using natural fibers. A mere 50-60 years later production methods using polyacrylonitrile(PAN) as source material or precursor were introduced by "Union Carbide" and "DuPont" in the 1940s and 1950s. It took another 30 years until industrial, commercial production of carbon fibers started in Japan in 1976 and was introduced in Europe only a few years later.[B11, p139-140]

The first industrial applications were found in the end of the 1960s, when carbon fiber reinforced epoxy resins were first used in the aerospace industry, the military and the aviation industry. At the end of 1980s, when CF became somewhat cheaper and prices dropped under the 100 €/kg boundary it was more and more used for leisure applications such as golf clubs, tennis rackets and racing bikes. Since then expectations regarding light weight and high performance structural parts have continuously grown. The world market has doubled in the period 1998-2010 and worldwide annual production capacity exceeds 30.000 tons per year (in 2010). [P45, p1]

Carbon fiber production

The production is more complex and energy intensive than the production of glass fibers. Generally two methods for the production of carbon fibers exist. The difference between these processes lies in the precursors used. The scheme below shows the two production processes.

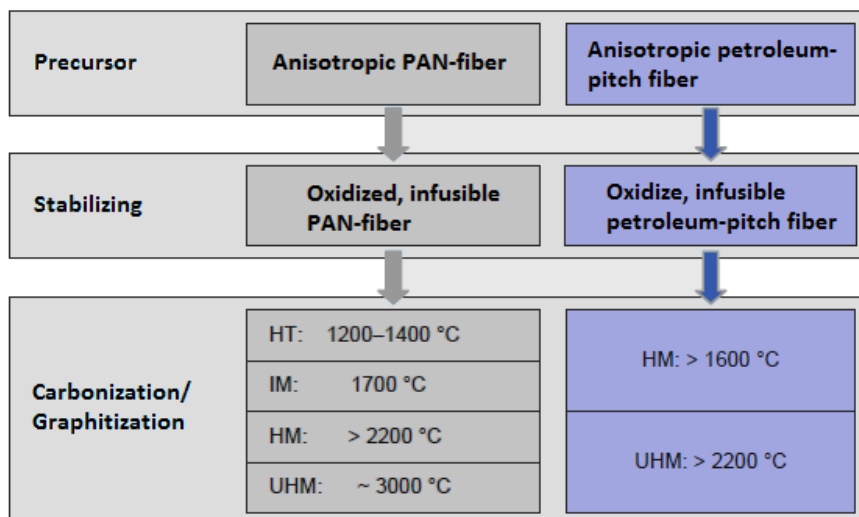


Fig. 23: The two carbon fiber production processes with two different precursors.[B11, p140]

The production process on the left hand, which uses polyacrylonitrile or PAN as a precursor, is by far the most common production process for carbon fibers. The thermoplastic PAN reacts in an oxidizing milieu in the stabilizing phase. In this phase so called ladder polymer chains develop. These chains form long pyridine rings chains through cyclisation. The obtained fiber is infusible, this is a prerequisite for the following carbonization. In this process the pyridine chains congregate to molecular ribbons and form three-dimensional graphite like structures.

As shown in the scheme, depending on the final curing temperature, which can vary from 1.200 °C to more than 3000 °C, different classes of carbon fibers are formed. These are: High tenacity (HT) fibers, intermediate modulus (IM) fibers, high modulus (HM) fibers and ultra-high modulus (UHM) fibers. The following figure shows that these different fiber classes exhibit large differences in mechanical properties. It is interesting to see that the highest tensile strength of carbon fiber is 6.500 N/mm², whereas the highest glass fiber tensile strength was 4.400 N/mm², in the case of R-grade glass fibers. The difference in tensile modulus is even greater: 675.000 N/mm², in the case of carbon UHM carbon fibers compared to only 86.000 N/mm² for R-grade glass fibers. It therefore becomes evident that carbon fibers are much stronger,

with the tensile strength being 1,5x times higher, and stiffer, with the tensile modulus being almost 8x times higher. [B11, p140]

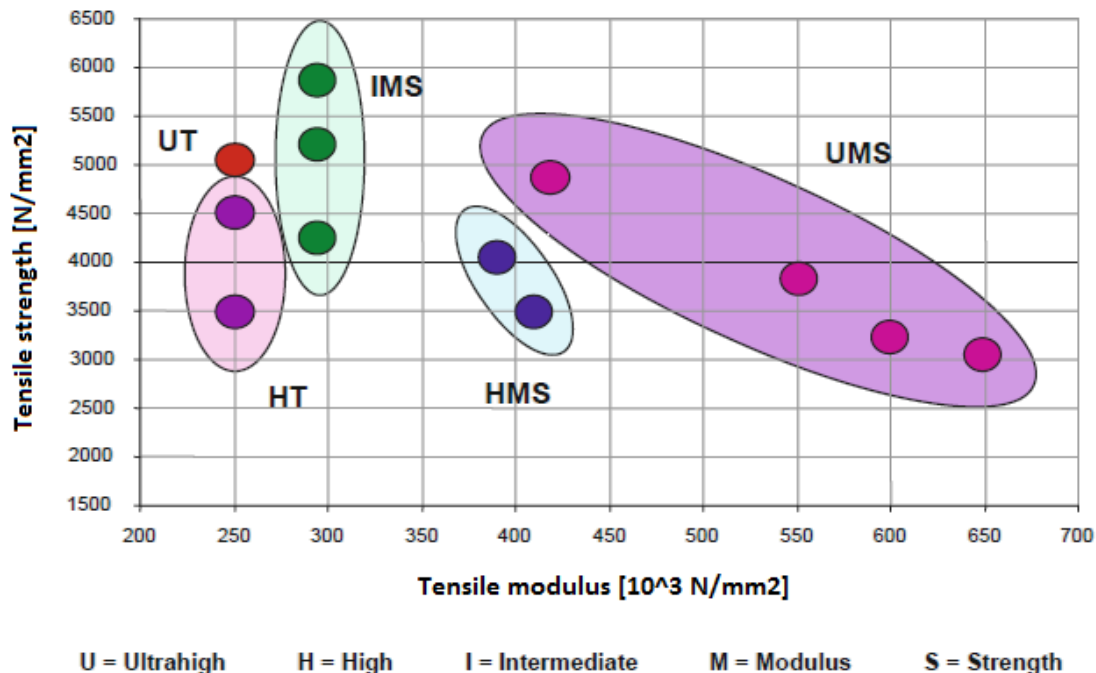


Fig. 24: Tensile strength and tensile modulus of different carbon fiber grades. [B11, p141]

Back to the other production process, the right hand process, it uses petroleum-pitch (PP) as precursor. These types of carbon fiber have a higher E-modulus and lower tensile strength than PAN-carbon fibers. During the production process the petroleum pitch is heated until condensation. This leads to the buildup of poly aromatics that are aligned in the fiber direction. At a temperature of about 400°C fluid crystalline substance emerges. This substance is transformed into oriented fibers, using a spinning process. Likewise the PAN-process these fibers are now oxidized to make them infusible. Then they are carbonized and graphitized to produce a carbon fiber. [B11, p141]

A problem of both PAN-carbon fibers as well as PP-carbon fibers is the fact that due to the nature of the carbon atoms and the high temperatures used during production, the surface of the fibers become exceptionally smooth and aligned. This leads to low resin-bonding strength. As an example, the following experiment was carried out: Two identical epoxy resin specimens were reinforced with uncoated and untreated carbon fibers, one with HT-fibers (cured at 1200 °C) and one with HM-fibers (cured at >2200 °C). The short term bending strength of the HT-specimens was about 60 N/mm², whereas the strength of the HM-specimen was only 25 N/mm². [B11, p142] This emphasizes the need for suitable surface treatments for carbon fibers to improve the matrix-fiber bond.

Surface treatment

Generally three types of surface treatment can be distinguished:

- Wet oxidation
- Thermic oxidation
- Anodic oxidation

Oxidation enhances the wettability of fiber and matrix. Next to that it can also enable a chemical bond between the reactive molecules of fiber and matrix. In most cases oxidation even physically alters the surface of the carbon fibers. Wet oxidation uses several oxidation agents, such as for example nitric acid. The processes used most in the industry are the thermic- and anodic oxidation

During anodic oxidation the fiber is channeled through an electrolyte bath and switched as anode. As electrolyte diluted acids, bases or saline solutions are used. Thermic oxidation is performed in gaseous environments of oxygen/nitrogen mixtures or carbon dioxide at temperatures of 400°C -1100°C. The thermic oxidation omits the need for washing processes.[B11, p141-143]

Carbon fiber characteristics

Carbon fibers are very versatile, because of their extremely high strength to weight- and stiffness to weight ratio. Next to that they are chemically inert, electrically conductive, thermic stable, infusible, biocompatible and permeable for Roentgen rays.

Carbon fiber stiffness or modulus of elasticity can range from that of glass to three times that of steel. The most widely used types have a modulus of 200.000-400.000 N/mm². The table below shows some characteristics of different types of carbon fiber tows. A tow is an untwisted bundle of continuous filaments. The table is only a short, representative overview of the available tows, since there are many more types available.

Type	T300	T1000G	M40J	M60J	M40
Density [g/cm3]	1,76	1,8	1,77	1,94	1,81
Number of filaments per tow	1.000-12.000	12.000	6.000-12.000	3.000-6.000	1.000-12.000
Tensile strength [N/mm ²]	3500	6370	4410	3820	2740
Tensile modulus[N/mm ²]	230.000	294.000	377.000	588.000	392.000
Elongation [%]	1,5	2,2	1,2	0,7	0,7
Mass per unit length [tex]	66-800	485	225-450	100-200	61-278

Table 4: Mechanical properties of different types of carbon fiber tows. [B16, p70]

Carbon fibers can be directly processed as final product or processed as pre-product. Final products can for example be directly woven tubes or pultruded sections. Pre-products are short-length fibers, twisted and non-twisted yarns, continuous filaments or the earlier mentioned tows. Because carbon fiber final products are extremely varying in mechanical properties it is difficult to compare them with each other. Next to that more than 500 different types of products are available. In the following table a carbon fiber/epoxy sheet molding compound (SMC) is compared to two woven CF/epoxy fabrics, both at the end of the scale: One being the highest grade woven fabric available, one being one of lowest grade fabrics available. To give an overview an example high grade carbon/epoxy composite is added.[B16, p73] [B11, p144]

Type	Unit	55%CF SMC	Lowest grade CF Epoxy fabric	Highest grade CF Epoxy fabric	Carbon epoxy
Carbon fiber content	%	55	n.a.	n.a.	67
Density	g/cm ³	1,45	1,15	1,8	n.a.
Tensile strength ultimate	N/mm ²	289	50	2.100	1.362
Modulus of elasticity	N/mm ²	55.100	6.600	520.000	140.000
Flexural yield strength	N/mm ²	613	110	1.600	1.383
Flexural modulus	N/mm ²	34.500	6.410	125.000	122.000
Compressive yield strength	N/mm ²	275	50	1.720	1.084
Compressive modulus	N/mm ²	31.700	8.200	140.000	136.000
Shear strength	N/mm ²	65,5	0,8	120	87,4

Table 5: Comparison between three types of carbon fiber/epoxy products [www.matweb.com] [B16, p78]

To conclude this chapter some pictures of carbon fibers are given:



Fig. 25: FEA-designed carbon fiber reinforced epoxy curved beam [WEB, www.element6composites.com]



Fig. 26: Pultruded CF- reinforced sections [WEB, www.element6composites.com]

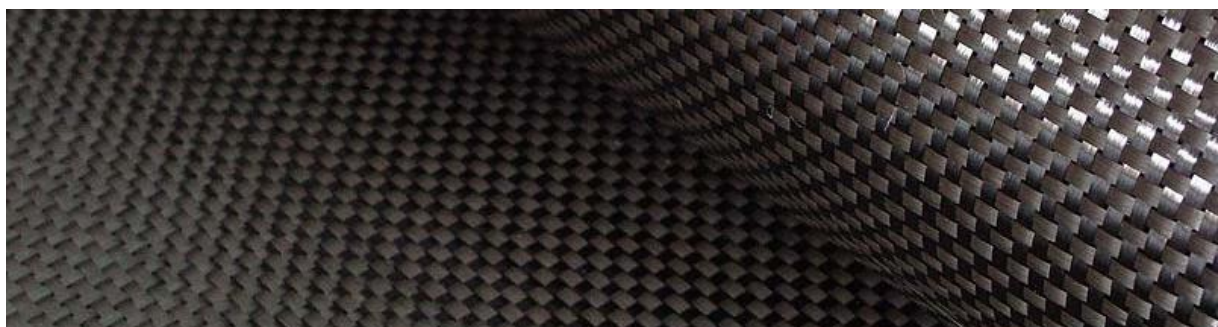


Fig. 27: Woven carbon fiber fabric without polymer matrix [WEB, www.element6composites.com]

2.5.1.3 ARAMID FIBERS

Aramid fibers, often also called nylon fibers, were developed in the 1960s and 1970s, when the chemical industry wanted to develop an alternative for steel reinforcements in rubber tires. One of the first developing companies was the famous company "DuPont". They developed a para-aramid fiber in the 1970s called Kevlar®, which still is a very well-known product. First only developed for the tire industry, it quickly became evident that aramid was also very well suited for use in the ballistics industry and as a surrogate for asbestos.

Aramid fiber production

Aramid fibers are part of the group of Poly-para-phenylen-terephthalamide fibers (or PPTA-fibers). To produce this polymer the two monomers Para-phenylenediamin (PPD) and Terephthaloyldichloride (TDC) are put in a suitable solvent to let them condensate in a poly-condensation process and form PPTA. Because PPTA is very insoluble, strong acid such as 100% sulfuric-acid have to be used to spin a wire from the PPTA/sulfuric-acid solution. This thick 20/80-ratio solution is heated before being put through under pressure through the spinning nozzles. After being put through the nozzle, the fine filaments still have to coagulate in a water/sulfuric-acid solution. After coagulation the filaments are spun into yarn. The yarn still has to be washed, neutralized and dried in several steps before it can be wound on a coil. After that the fibers are coated. In contrast to carbon fibers this coating is not applied for a better bond in the matrix, but foremost for better handling in the following production steps. The aramid yarn can now be further processed into pulp, short fibers or into woven fabric and others. Aramid fibers in aramid yarn are typically not twisted or tangled and have a distinct bright golden yellow color. [B11, p133-139][B16, p68-71]

Because aramid fibers and –yarns are mostly used as impregnated, fabrics and tows, such as ropes, sowing fabrics, sails, bulletproof vests, yarns, spun yarns, prepges and many more their mechanical porperties are given in the specific standards for these kind of products. In the table below a comparison between three types of aramid fibers is given, two products without impregnation, and one with impregnation.

Type	Unit	Aramid fiber - standard modulus	Aramid fiber - high modulus	Twaron 2200 1610dtex, twisted	Twaron 2200 1610dtex impregnated
Density	g/cm ³	1,44	1,45	1,45	1,45
Tensile strength	N/mm ²	3000	3000	3100	3750
Tensile modulus	N/mm ²	72.000	105.000	105.000	124.000
Fracture strain [%]	%	4,0	2,7	2,7	2,8

Table 6: Mechanical properties of four types of aramid fibers [B16, p135]

Aramid fiber characteristics

Aramid fibers have excellent properties such as a high tensile modulus, high tensile strength, low weight, high impact resistance, high resistance to abrasion, good creep rupture characteristics and mechanical & chemical resistance over a wide temperature range. Next to that aramid also has a negative thermal coefficient, low heat- and electrical conductivity and infusibility. Another property of aramid that has to be pointed out, because it differs from other reinforcements is the high elongation before fracture. Nowadays aramid is often used when a high strength and low weight together with a high impact resistance is needed. Common applications are bullet proof vests, air freight containers, cooling vehicles, ship hulls and in more recent times also structural strengthening of civil structures. Bridges under collision load are best reinforced with aramid fibers laminates due to its very high tenacity. A disadvantage of aramid fibers is the low compression strength; it only is equivalent to normal glass fibers. The compressive modulus of aramid is of the same order of its tensile modulus, but the fracture strain is only about 0,5%. This will cause a much earlier fracture, in case of compressive stresses.

The aramid fiber market was as big as about 37.000t in 2002. But yearly growth rates are estimated to be about 10%. A reason for this could be the possibility to use aramid as hybrid reinforcement, for example in combination with glass fibers. It has to be pointed out that only a mere 2% of the yearly production of aramid is used as fiber reinforced polymers, the rest is used as fabric or roping. Aramid fibers are compatible with any kind of matrix polymer, although thermoplastic matrixes host aramid about 20% more efficient. Due to their higher ductility they are more compatible to aramid with its high elongation. In the table below two aramid reinforced epoxy composites are compared, one high modulus unidirectional composite, and one high modulus woven composite: [B11, p133-139][B16, p68-71]

Type	Unit	Aramid fiber - high modulus - UD	Aramid fiber - high modulus - woven
Density	g/cm ³	1,31	1,27
Tensile strength	N/mm ²	1400	560
Tensile modulus	N/mm ²	76.000	30.000

Table 7:Comparison between two aramid fiber reinforced epoxy composites [B16, p137]

Typically aramid fibers have a fiber count of about 1,7dtex and a diameter of 12µm. New developments aim for varying fiber sizes, both large fiber count for some industrial purposes, as well as extremely small fiber counts for some ballistic applications. Next to that the industry works on methods to greatly increase the surface area of short length aramid fibers to bond them even better in various matrixes. An increase of 0,1 m²/g to 7-9 m²/g has already been achieved through a compounding process. This vast increase has significantly improved the composite properties, particularly the abrasion resistance and higher strength and stiffness. In the past handling of aramid fibers was always slightly more difficult compared to other fibers, due to the specific material properties such as high tenacity. Recently special techniques for aramid fibers have been developed, resulting in an equal machinability as for other reinforcements.

In the following a few aramid fiber applications will be shown. Among FRP composite reinforcement materials, aramid fibers are the most uncommon in civil engineering applications. In the first picture application as staying cable under tension is shown. Other possible civil applications would be repair or strengthening of bridge substructures through gluing of aramid reinforced textiles. Mostly aramid fibers with high modulus are used in this field. [B11, p133-139][B16, p68-71]

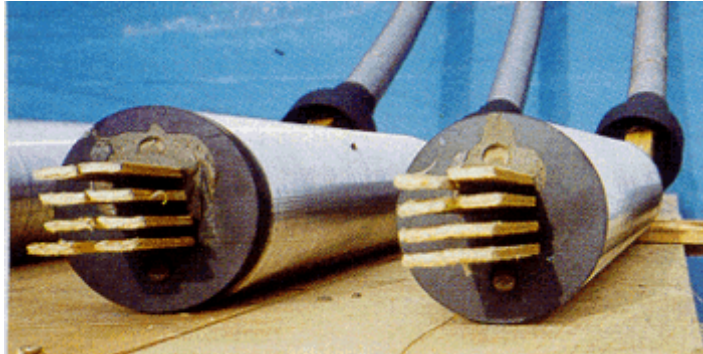


Fig. 28: Rectangular aramid fiber reinforcement for bridge staying cables [WEB, www.teijinaramid.com]

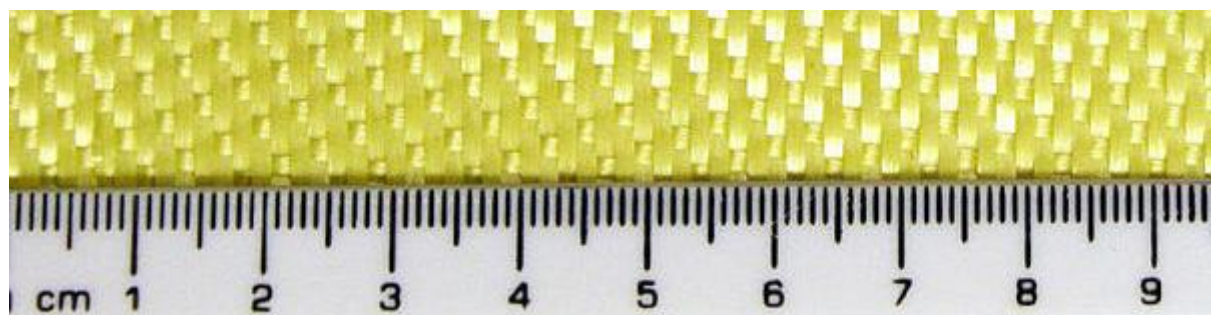


Fig. 29: Aramid fiber woven cloth without polymer matrix [WEB, www.teijinaramid.com]

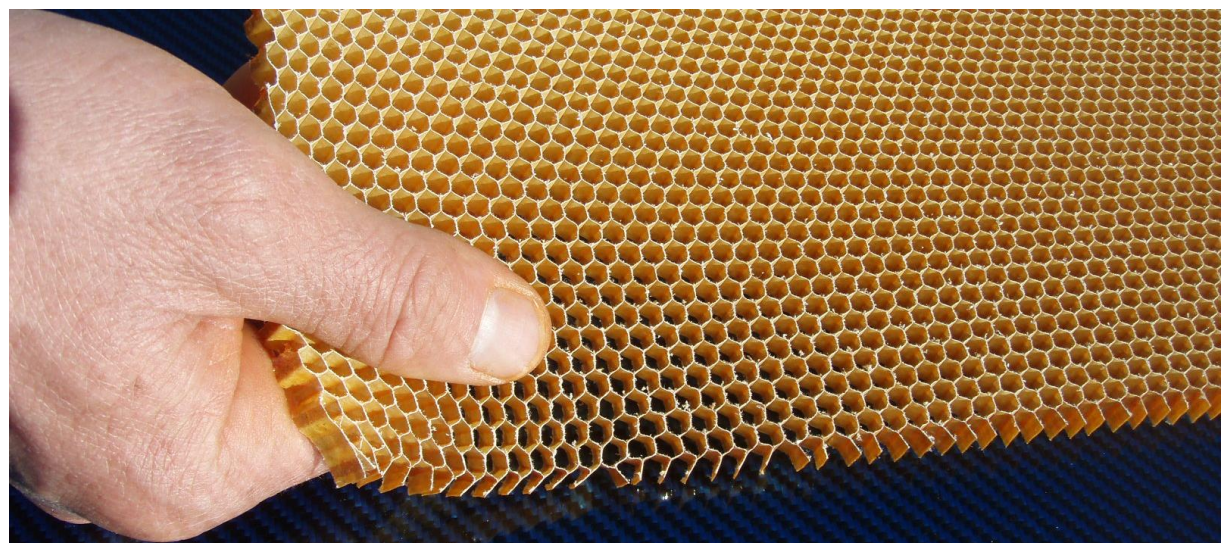


Fig. 30: Aramid fiber honeycomb cloth used for sandwich construction. [WEB, www.fibermaxcomposites.com]

2.5.1.4 NATURAL FIBERS

Natural fibers are derived from organic materials, vegetable matter and other natural materials. Natural fibers are the oldest known reinforcement. First used thousands of years ago, modern applications as plastic reinforcement have been introduced in 1941, when Henry Ford proposed a vehicle with a body made of hemp-fiber/resin composite. Natural fibers kept being used in the automotive industry, particularly wood- and cotton fibers were used up to the 1980s. The famous East German Trabant had a body made partly of natural fiber composite. Since then natural composites have been constantly improved, resulting in high tech materials that are still often used in the automotive industry, for example in car-door interior trims and in lorry driver cabins. [P44, p5]

Natural fibers share some of the advantages that glass, aramid and carbon have. Natural fibers also have a good strength to weight ratio and a low density. Next to that natural fibers have some advantages over other fibers. First of all natural fibers have a much smaller CO₂ footprint than for example glass fiber. Studies performed in 1997 by DaimlerChrysler show that production of natural composite liner costs about 80% less energy than glass fiber liner. The low dependency of natural fibers results in a unique prize stability compared to other synthetic fibers. [B11, p147] Another advantage of natural fibers is the obvious excellent biodegradability especially when the fibers are combined with biological matrices. Natural fibers also exhibit a better damage tolerability in reinforced polymers.

While natural fibers have some great advantages, as mentioned, they also show some rather big disadvantages: They are hydrophilic and tend to absorb water, which degrades the fibers; they are not as temperature stable as the other fibers. Due to their natural origin the fibers also show a quite extreme variation in quality and thus also in mechanical properties. The natural origin also causes the natural fibers to be susceptible to fungal and insect attacks. The moist/hydrophilic nature of the fibers also causes them to be very incompatible with hydrophobic matrices, because the polymers will not adhere well to the fiber surface. It has to be said though, that various chemical treatments for natural fibers exist, which can improve the mechanical properties significantly.[B16, p59-60]

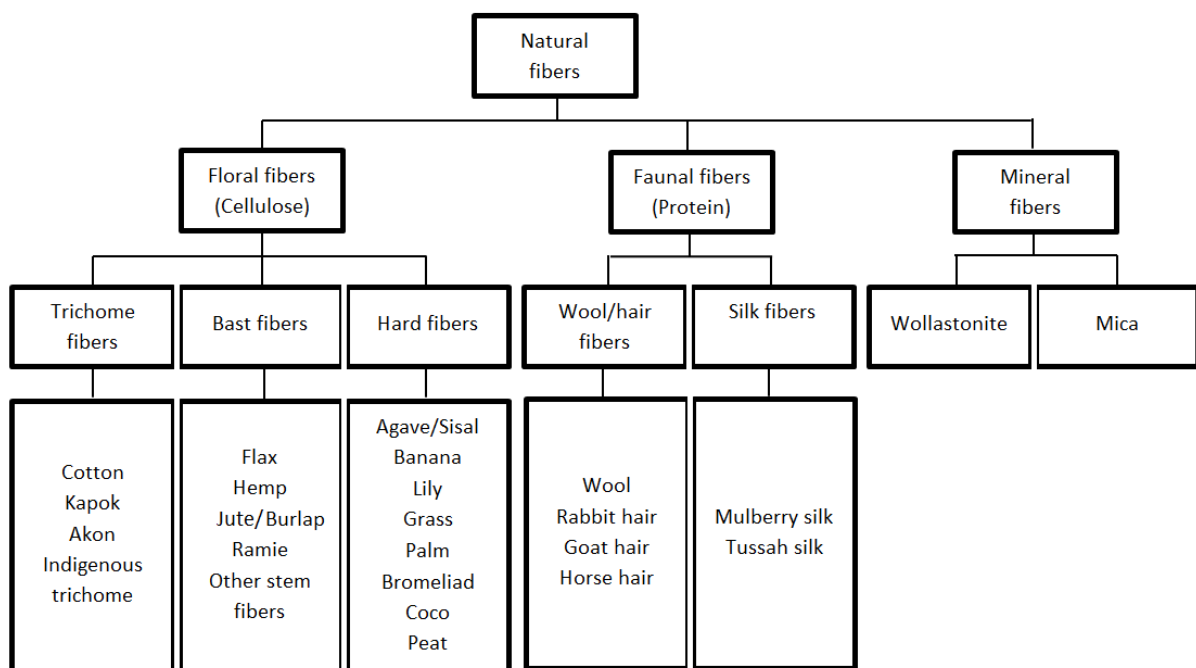


Table 8: Overview of most natural fibers available, divided in subgroups by origin.

The table above shows the natural fibers used today, the fibers can be subdivided into three large groups: The floral fibers or fibers which are vegetable, based on plants and are mostly made of cellulose. Then the faunal fibers or fibers based on animal products such as wool, hair or silk. The last group of fibers are the mineral fibers, which are comprised of ground rocks as well as natural, refined, or synthetic minerals. These groups are then again divided into several other groups. Natural fibers are just as diverse and varied as

nature itself. The reason for this lies in the fact that the main building materials of natural products are composites, combinations of fibers and matrices.

Floral fibers are divided into:

- Trichome fibers: This is the official expression for any kind of plant hair. Examples for trichome fibers are the well-known cotton fibers and some other less known plants such as Kapok and Akon.
- Baste fibers: baste fibers are long stretched cellular bundles found in the stems of some plants. In plants they bring structural stability and suppleness/malleability. They are often reinforced by the chemical lignin. Examples are the very common Flax and Hemp fibers as well as Ramie.
- Hard fibers: These fibers are found in leaves, leaf sheaths, fruits and crops of specific plants. Typically they are much harder than baste fibers. Examples are the very well-known Sisal fiber, which is derived from Agave leafs and palm-, peat-, banana-, coco fibers and various others. [B11, p148]

Faunal fibers are divided in silk fibers and wool/hair fibers. Several types of animal fibers are used, as well as several silk types. Since faunal fibers are only used for the production of weavings, cloths, yarn etc. and are never used as reinforcement of plastics or polymers they will not be covered in detail.

Mineral fibers are subdivided in two groups, which represent only a part of the available mineral fibers. Mineral are often used as filler in reinforced composites and not so much as fiber reinforcement. Wollastonite fibers have been used as filler in injection molded polyurethane resins which can resist up to 190°C. These resins have seen some applications in automotive construction. Mica is a generic name to describe a group of complex hydrous potassium aluminate silicate materials that share a unique laminar crystalline structure. Mica is used in the form of very thin high aspect ratio particles that are tough and flexible. Mica fibers are used as reinforcement mostly for thermoplastics; they improve the tensile- and flexural strength as well as the flexural modulus. Next to that Mica fibers also reduce creep and shrinkage, eliminate warp and increase heat distortion temperatures.

Below a table with various reinforcements in 40wt% polypropylene matrix is given. It is interesting to see that the tensile strength of the 100% polypropylene specimen is not affected or is negatively affected by the mineral reinforcements/fillers. The real advantage of the mineral fibers are the improved flexural modulus, heat distortion temperature and shrinkage values, as stated before.

Type	Unit	100% polypropylene	Mica HiMod	Silica	Wollastonite
Tensile strength	N/mm ²	31,58	30,58	21,30	25,44
Flexural modulus	N/mm ²	1654,74	7653,18	2620,01	5102,12
Shrinkage	%	2,30	0,80	1,50	0,60
Heat distortion temperature	°C	65,56	114,44	67,78	87,78

Table 9: Strength, stiffness, shrinkage and heat distortion temperature comparison of various mineral reinforcements [B16, p64]

Because the number of natural fiber types is so large only a handful of them will be covered, this will be Sisal, Flax, Hemp, Jute and Ramie. All of these fibers are used in the fiber reinforced polymer industry. Below a small comparative table is shown. Generally the median strength values of natural fibers are about a quarter of the glass fiber values, the median stiffness value, or modulus is only one fifth of that of glass fiber. Looking at the table it becomes clear though, that Ramie and Abaca behave quite different and are much stiffer (about 3x times) and stronger (about 2-3x times) than the other fibers. Since these fibers are only industrially known for a few years, this could offer some potential for higher grade natural fiber reinforced polymer composites.[B11, p149]

Type of fiber	Unit	Sisal	Flax	Hemp	Jute	Cotton	Ramie	Abaca
Density	g/cm ³	1,3	1,46	1,5	1,42	1,51	1,54	1,44
Tensile strength	N/mm ²	428	874	827	571	618	1.250	1.100
Modulus of elasticity	N/mm ²	4.575	14.583	12.984	17.339	11.844	35.953	n.a.

Table 10: Comparative table of natural, floral fibers used in the reinforced plastics industry [B11, p149]

Sisal fiber

This white fiber is produced from the leaves of the agave plant. This plant is mostly found in Central America, the West Indies and some parts of Africa. Sisal has been in use as cordage, tow, binder twine and reinforced plastic since at least 1950. Sisal can be used as low cost filler, when chopped. It is mostly used in bulk (dough) molding compounds and typically more with phenolic matrices than with thermosetting polyester or epoxy resins.

Flax fiber

Flax fiber is reported to withstand almost similar tensile forces as Ramie and can out-perform glass fiber on a weight-for-weight basis. Bio-composites of flax fibers have properties comparable with glass fiber bases thermoplastic (LLDPE/HDPE) composites. Furthermore flax is used particularly in the automotive industry, for example in polypropylene thermoplastic matrices in an extrusion/compression molding technique developed by Daimler Chrysler.[P49, p133] [B16, p60]

Hemp fiber

Hemp fibers are often used by stakeholders in the automotive industry to improve clean production. It is obtained from the Cannabis Sativa plant. Ford uses it for example to replace the glass fiber chopped strand mats used in the roof sheeting of the high roof model of the Ford transit. In this case it is molded by resin transfer molding. The main gains of the use are the lower weight and cost of the hemp fibers.

Jute fiber

Jute fiber is one of the most important natural fibers. Production takes place in tropical and subtropical countries such as India, Bangladesh, Vietnam and Thailand. Applications in reinforced plastics such as thermosetting resins like unsaturated polyester or vinyl ester resins have been intensively studied. Application in thermoplastics is not advised due to the low adhesive capacities of the fiber/matrix bond. Jute fiber is very popular both as reinforcement but also as filler. High performance unidirectional-oriented tensile strength can reach values up to 600 N/mm² and an elastic modulus of 20.000 N/mm².

When the high water absorption and the poor interfacial adhesion problems can be eliminated, jute fiber reinforced plastics could replace timber or even glass fiber reinforced plastics. This could be done by using chemical treatments like silane coupling agents, polyisocyanate, vinyl monomer linkages or compatibilizers. A promising method is to treat the fiber with a phenolic resin based on cardanol formaldehyde. Jute fibers treated with this resin can bear comparison with glass fiber reinforced plastics.[B16, p61-62]

Ramie fiber

Ramie fiber is a high strength natural fiber that can compete with glass fibers. It is derived from the 2,5m high Chinese relative of the common stinging nettle. Various organizations, such as for example DaimlerChrysler study this fiber as replacement for glass fiber, in for instance interior fittings of some Airbus planes. Ramie fiber was only introduced lately as reinforcement fiber because processing it was very difficult.

Below a table is given to compare two typically used industrial compression molding products that use natural fiber. These two materials are used in the automotive industry for their low cost and good environmental performance, such as low energy consumption in production. Notice the comparably low strength and stiffness values in comparison to glass, aramid and carbon fibers.

Type	Unit	Johnson Natural fiber EP	Johnson EcoCor
Fiber content	%	65	50
Fiber type	n.a.	Flax/Hemp (1:1)	Bast fiber
Matrix type	n.a.	Epoxy (TS)	PP (TP)
Density	g/cm ³	0,80-0,85	0,86-0,90
Flexural strength	N/mm ²	50-70	45-55
Flexural modulus	N/mm ²	4.000-5.000	2.300-2.700
Tensile strength	N/mm ²	40-50	25-30

Table 11: Comparison between natural fiber reinforced plastic products used in the automotive industry [P44, p23]

2.5.1.5 OTHER REINFORCEMENTS

Next to the already discussed fibers a number of different other fibers do exist. These fibers will only be covered briefly:

Polyester fibers

Thermoplastic polyester can be processed into low density, high tenacity fibers with a good impact resistance but a low modulus. It is used where low cost, light weight, and high impact and abrasion resistance is needed. Polyester fibers are mostly used in surface tissue for laminates or as fiber mats, in sheet molding compounds or resin transfer moldings. Due to its high impact and abrasion resistance and its low weight (about 50% of glass fiber) polyester filament is mostly used as outer or exterior layer, toughening layer, as surfacing veil, thin core or core bedding. [B16, p55-56]

Polyethylene fibers

Very low density fibers can be produced from ultra-high molecular weight polyethylene (UHMWPE). Fibers of this kind offer one the highest strength-to-weight ratios available. UHMWPE is made of aligned polymer chains with a high failure strain and good impact resistance. A big disadvantage of these fibers is the low modulus and the high costs of surface treatment of the fiber to use it in a matrix polymer. These disadvantages are the reason that PE fibers are very rarely used in reinforced plastics.

Some data on UHMWPE fibers: This material has as an extremely low specific gravity of 0,97 (compared to aramid 1,44) and is 35% stronger than aramid. Also, it has a high energy/fracture ratio, making it very suitable for ballistic application. PE fibers have an impact energy absorption that is about 20x times higher than that of glass, aramid or graphite. PE has a low melting point of 147°C. Possible applications for composites are boat hulls, radomes and structural components. [B16, p56-57]

Hybrid fibers

Hybrid fibers are a combination of different types of reinforcement in the same matrix polymer. The main goal of using hybrids is cost reduction, since there exist extreme differences in reinforcement pricing. For example: Aramid reinforced resin composite is about 8x times as costly as E-glass reinforced resin composite. The most common application of hybrids is the combination of expensive, high strength reinforcements with glass reinforcement. Design of a hybrid reinforced composite is reserved to specialist with sufficient financial funds. One high tech application is a boron/graphite prepreg, composed of small diameter graphite fibers between boron fibers, leading to fiber content of about 80%. This prepreg offers mechanical characteristics that are unseen with any material. Its flexural stiffness is about twice as high as that of carbon and 40% higher than boron. It is needless to say that its price also exceeds other reinforcements by a multiple. [B16, p57]

Ceramic fibers

Ceramic fibers possess unique abrasion- and corrosion resistance and have high temperature stability. They consist of roughly 50wt% alumina and 50wt% silica. Although glass fibers are also ceramic fibers, they are generally not categorized so, because of their differing properties and their large field of application. [B16, p58]

Silicon Carbide fibers

This relatively heavy fiber with a specific density of about 2,7 was developed for the reinforcement of metal- and ceramic matrixes used in very advanced aerospace- and military applications. They were introduced as a surrogate because of the high price of boron and its fast degradation of mechanical properties at temperatures above 540°C. [B16, p58]

Whisker fibers

Whiskers are metallic and non-metallic single crystals with sizes in the micrometer range. They have ultra-high strength and modulus, a very high melting point, high resistance to oxidation, low weight due to their near perfect crystalline structures with a minimum of defects. They have an excellent resistance to fracture which is unprecedented in other reinforcements. Due to their complex production and extremely high prices, whiskers have only been applied in small quantities in specialty applications, such as in the aerospace industry. Whiskers can be used in various matrices, such as plastics, ceramics or metals. The picture clearly shows how high the strength values of whiskers really are. [B16, p58-59]

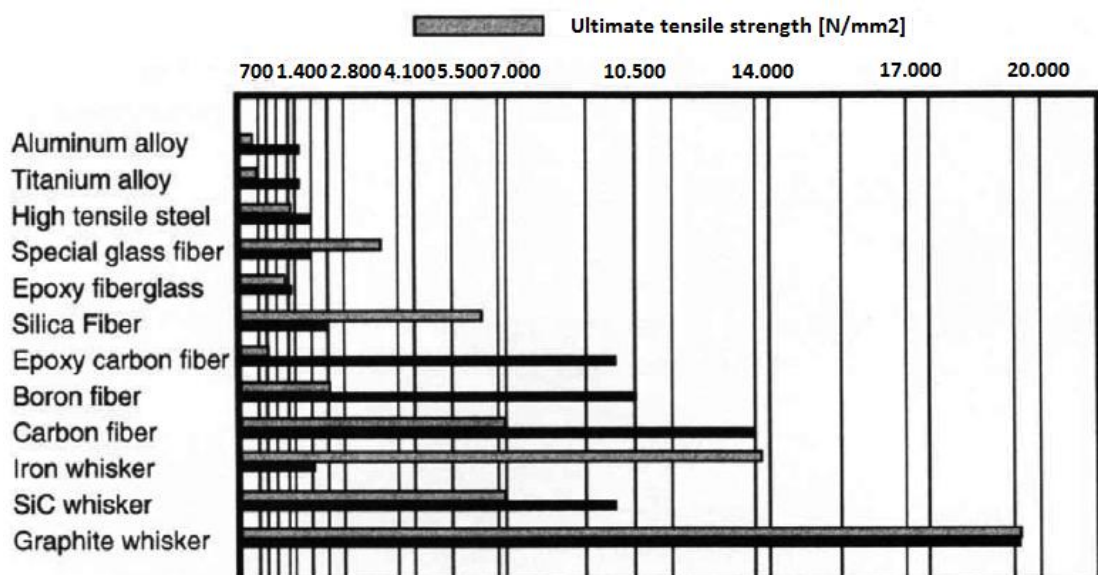


Fig. 31: Comparison of ultimate tensile strength of various materials [B16, p59]

Boron fibers

Boron fibers were the first high strength, high modulus fibers to be produced. The research started already in the 1950s. The production process is very costly, as it involves chemical vapor deposition from a gaseous mixture of hydrogen, boron trichloride on a heated tungsten substrate of 12,5 µm. The resulting boron fibers are 100-200 µm in diameter. They have a uniform elastic modulus of 400.000 N/mm² and tensile strength of 3.650 N/mm². Usually these high performance fibers are used in combination with an expensive high performance epoxy matrix. As with all other high cost reinforcements these fibers are mainly used in the aerospace industry and the military. [B16, p77]

Graphite fibers

Graphite fibers are made just like carbon fibers and have equally high properties. Graphite is a relatively soft, black material. The difference with carbon fibers is the even higher curing temperature of up to 9750°C. This leads to a high modulus of elasticity, a higher stiffness and a higher ratio of elemental carbon in the fiber (more than 99%). Graphite fibers are not only resistant to creep and fatigue, have a good wear

resistance, and a good vibration damping, thermal stability and long term resistance to corrosion. They are also stronger than steel, lighter than aluminum and stiffer than titanium. Due to high temperatures needed during production graphite fibers are even more expensive than the already expensive carbon fibers. [B16, p75-77]

2.5.2 MATRICES

Fibers are of little use unless they are bonded together to make up a structural element that can carry loads. The binder material is normally called a matrix (plural: matrices). Matrices have manifold purposes: First of all the matrix has to support the embedded fibers, it also has to protect the fibers from outside influences, and last, the matrix has to transfer stresses from one fiber to another, being especially important when several fibers are broken.

Typically the mechanical properties of matrices are lower than that of the fiber: They have a lower density, a lower stiffness and a lower strength. However the combination of both can have advantages of both parts, being of low density and having excellent mechanical properties. Matrix materials can be polymers, metals, ceramics or carbon. The temperature resistance and cost of the material increase in the order of the list. The three last matrix materials will only be covered very briefly, since they are not used in the civil engineering industry. The main application of these high-tech matrices is the aerospace industry and military. [B03,p5]

2.5.2.1 METAL MATRICES

The most important metals used as a matrix are aluminum, titanium, magnesium and copper alloys. The matrices can be reinforced with several types of (high tech) fibers, whiskers, wires or particulates. To name a few examples: boron fibers, graphite fibers, alumina fibers, silicon carbide whiskers, titanium carbide particulates, niobium titanium wires. It becomes evident that the reinforcements as well as the matrices are mostly exotic elements. Metal composites tend to have extremely high stiffness and strength as well as excellent temperature stability. Due to their exoticness they are only used in advanced and costly applications such as the aerospace industry or as electronic substrate. [WEB, www.substech.com]

2.5.2.2 CERAMIC MATRICES

Ceramic matrices are generally also reinforced with ceramic fibers/whiskers/particulates. The correct name is therefore Ceramic Fiber Reinforced Ceramic (CFRC). They can also be reinforced by carbon fibers, whereby they can also be considered ceramic. The reasons for the development of CFRCs are mainly the mechanical shortcomings of normal ceramics; they fracture easily, the crack resistance or toughness is very low. Reinforcing fibers drastically increase crack resistance, elongation to fracture, dynamical load capability, and thermal resistance. Mostly carbon-, silicon carbide- or alumina fibers are used to reinforce a matrix of the same material. Just like metal matrices, CFRC are only used in very special cases like: heat shield systems for space vehicles, components of high-temperature gas-turbines, high performance brake discs etc. [WEB, www.substech.com]

2.5.2.3 CARBON MATRICES

Carbon matrices are usually reinforced with highly ordered graphite fibers. Graphite fiber reinforced carbon (GFRC) is stiffer, stronger and lighter than steel or other metals. Partly due to their high production temperature of sometimes up to 10.000°C they have excellent thermal properties, being dimensionally stable and having constant mechanical properties at temperatures over 2.000°C. Elastic moduli of 3D-reinforced GFRCs have values of 15.000-20.000N/mm², unidirectional reinforced GFRCs have moduli of 150.000-200.000N/mm². Next off they have properties like low weight, high abrasion resistance, non-brittle failure and high corrosion resistance. Drawbacks of GFRCs are the fast oxidation, bringing a need for expensive coatings and the complex production, which leads to high material costs, limiting application to the aerospace industry and military. [WEB, www.substech.com]

2.5.2.4 POLYMER MATRICES

The rest of this chapter will be about this type of matrix, since it is by far the most used material to act as matrix in fiber reinforced composites. Polymers (poly=many and mer=molecule) is the chemical name that is used to describe large molecules, that are composed of repeating structural units, which are connected by covalent chemical bonds. Generally three types of polymers exist; linear polymers, branched polymers and cross-linked polymers. See the picture below for a short schematic representation.

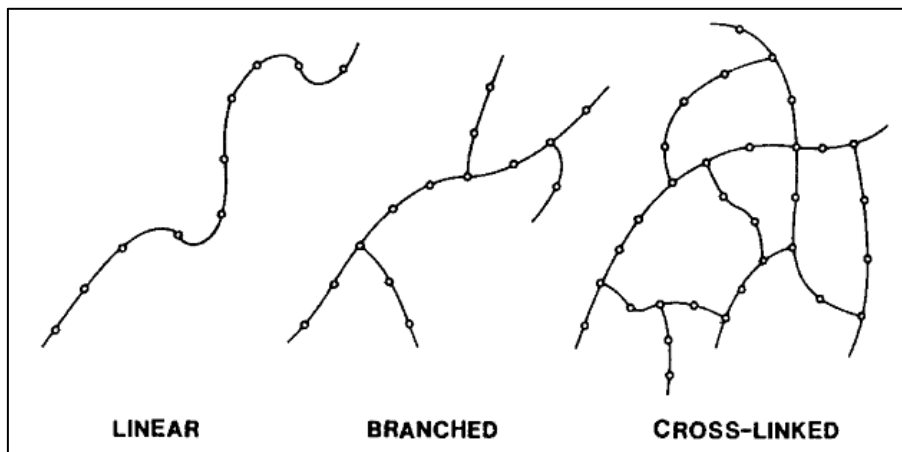


Fig. 32: The three polymer groups, defined by their chemical build-up [B03, p5]

A linear polymer is merely a chain of mers, a branched polymer consists of a primary chain of mers with other chains that are attached in three dimensions, very much like a tree. Cross-linked polymers have large number of 3D highly interconnected chains. What could be expected is actually true: the linear polymer is the least strong and stiff of the three and the cross-linked polymer is the strongest and stiffest.

The classification of structural polymers is somewhat linked to the above mentioned classification. Firstly there are rubbers: they are cross-linked polymers that have a semi-crystalline structure at well below room temperature but act as the rubbers we know at room temperature and above.

Secondly there are the thermoplastics; they are branched polymer chains that generally do not cross-link at all. Thus, they can be repeatedly softened and hardened by heating and cooling. Typical thermoplastics are nylon, polyethylene and polysulfone.

The third group of the structural polymers is the thermosets. They are composed of polymers that are chemically reacted until almost all the molecules are irreversibly cross-linked in a 3D-network. Examples for this kind of polymers are epoxies, phenolics and polyimides. [B03, p5]

Another classification of plastics or polymers is the division of all plastics in commodity plastics (CP) and engineering plastics (EP). Commodities such as polyethylenes (PE), polyvinyl chlorides (PVC), polypropylenes (PP) or polystyrenes (PS) account for over 67% of worldwide plastic production. EPs generally meet higher requirements such as heat resistance, impact strength, chemical resistance and higher strength and stiffness. Examples are polycarbonates (PC), nylon and acetyls. Most of the thermoset plastics and the reinforced thermoplastics are of the engineering type. Polymers are called plastics when fillers, additives or reinforcement are added. By far the most polymers available are plastics. Although over 35.000 types of plastic do exist only about 20 are popularly used. [B16, p110]

To give a small explanation on why pure polymers are used very seldom, the table below can be used: In this table NEAT plastic (Noting Else Added To plastic) is compared with two variations on the material. The first material is the same plastic reinforced with glass fiber reinforcement and the second is plastic with the added filler talc.

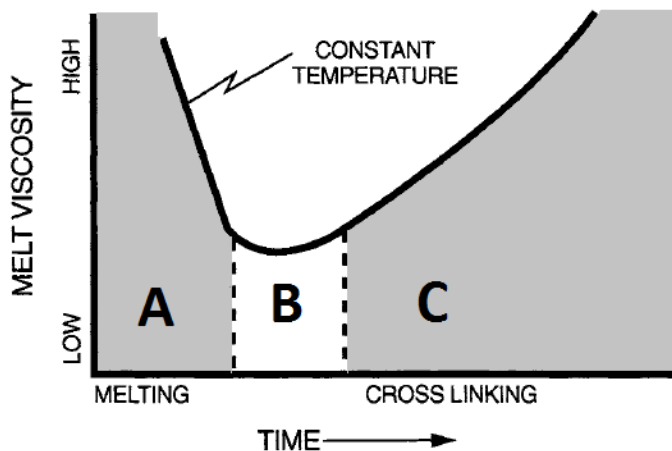
Type	Unit	NEAT polypropylene plastic	Glass reinforced plastic	fiber PP-plastic	Talc added PP-plastic
Reinforcement	wt%	n.a.	40		n.a.
Filler	wt%	n.a.	n.a.		40
Flexural modulus	N/mm ²	1.240	7.600		3.970

Table 12: Comparison between virgin plastic, reinforced plastic and a plastic with added filler. [B16, p110]

Backed by the above table it can be concluded that the general performance of any used plastic is very much governed by the added fillers, additives and reinforcements. In the following the large groups of engineering plastics will be covered: thermosets and thermoplastics. Generally thermosets are more common in the fiber reinforced plastic markets. Nonetheless some important applications of thermoplastics do also exist. To conclude the polymer matrices chapter, some information on biological/natural resins and plastics will be given.

2.5.2.5 THERMOSET RESINS

Thermosets (TS) are heated to process them. At higher temperatures they solidify and become infusible and insoluble. Once cured the plastic cannot be re-softened with heat. Thermoset plastics undergo a cross-linking chemical reaction of its molecules by the action of heat and usually pressure, oxidation radiation and other means. In most of the cases this means that the thermoset can only cure when curing agents, catalysts or hardeners are added in the reaction process. Due to the achieved tightly cross-structure TSs resist high temperatures, have higher strength and stiffness and provide greater thermal stability than thermoplastics. TSs are usually used in their liquid state.

Fig. 33: The A-B-C curing stages of thermoset plastics [WEB, www.substech.com]

The above picture shows the different stages of curing of thermoset plastic. In the A-phase the plastic is completely uncured with no to almost no cross-linking taking place. During the A-phase the melt viscosity rapidly drops to reach its lowest point in the following B-phase, where the cross-linking process starts. The B-phase is called partially cured. Some TS molding compounds and prepgs are delivered in this state, the reaction can be stopped at this point with some thermoset types. The C-phase is the fully cured phase, during this phase the cross-links find their final position, which leads to a drastic increase in melt viscosity. Melt viscosity provides a means of measuring flow of a melted material which can be used to evaluate the consistency of materials.

TSs thus offer high thermal stability, good rigidity and hardness and resistance to creep. Because the curing process of TSs is irreversible, the material can only be recycled into fine particles which can be used as low-cost filler for other plastic assemblies.

As already mentioned, thermosets have little use as pure resin, but require addition of other chemicals to make them processable. For reinforced plastics the compounds usually comprise a resin system with curing agents, catalysts, hardeners, inhibitors and plasticizers. Also appropriate fillers and reinforcement have to be added. The resin, acting as binder, dictates the dimensional stability, heat, chemical resistance and basic flammability. The reinforcement primarily dictates the strength and stiffness of the composite.

Once compounded for processing, meaning with all agents added, the TS has a pot life that is also called working life. It is usually in the range of 10 minutes to 2 hours. Some special fillers can improve mechanical properties or dimensional stability but most of the control specific properties such as UV-stability, electrical conductivity, or, more important, flame resistance and retardancy. [B16, p133-134]

Thermosets offer a wide range of matrix materials for reinforcement by fibers, flakes, beads, or particulate materials such as talc and mica. The most common reinforcement by fiber is glass fiber. In the following the 7 most common thermosetting matrices will be discussed. The thermoset resins to be discussed are:

- Epoxy resin
- Phenolic resin
- Polyester resin
- Polyimide and polyamide-imide
- Polyurethane resin
- Silicone resin
- Vinyl ester resin

These resins are not single resins, but all represent a group of resins which are of the same type. The reason for this lies in the great number of ingredients that form the parameters of thermoset resin. So many different ingredients have been used, that is almost impossible to list them all here. As a start-off, the thermoset resin descriptions are given in the table below, which briefly compares the resin groups.

Resin type	Characteristics	Limitations
Epoxy	Excellent composite properties Very good chemical resistance Good thermal properties Very good electrical properties Low shrinkage on curing Can be B-staged (as prepreg)	Long cure cycles Best properties obtained only with cure at elevated temperature Skin sensitizer
Phenolic	Very good thermal properties Very good fire properties (self-extinguishing) Can be B-staged Good electrical properties	Color limitation Alkali resistance Contact with foodstuffs
Polyester	Wide choice of resins - easy use Cure at room temperature and elevated temperature Very good composite properties Good chemical properties Good electrical properties	Emission of styrene Shrinkage on curing Flammability Cannot be B-staged
Polyimide and polyamide-imide	Excellent thermal properties Good composite properties Good electrical properties Good fire properties	Restricted choice of color Arc resistance Acid and alkali resistance
Polyurethane	Good composite properties Very good chemical resistance Very high toughness (impact) Good abrasion resistance	Nature of isocyanine curing agents Color Anhydrous curing Cannot be B-staged
Silicone	Very good thermal properties Excellent chemical resistance Very good electrical properties Resistant to hydrolysis and oxidation Good fire properties (self-extinguishing) Non toxic	Lack of adhesion Long cure cycles Can only be cured at elevated temperatures
Vinyl ester	Good fatigue resistance Excellent composite properties Very good chemical resistance Good toughness	Emission of styrene Shrinkage on curing Flammability No B-stage

Table 13: Comparison between the 7 most common thermoset resin types [B16, p135]

Epoxy resins

Epoxy resins are linear polymers produced by condensing epichlorhydrin with bisphenol-A. Other formulations are glycidyl esters, glycidil ethers of novolac resins and brominated resin. In contrast to thermoset polyester and vinyl esters they do not contain any volatile monomer components. Different resins are produced by variation of the component-ratios.

Because epoxies are usually high in viscosity they have to be heated to a temperature of 50°C - 100°C to be workable. They can also be dissolved in an inert solvent to reduce viscosity. Curing agents, such as catalysts, hardeners and accelerators are used, acting by catalytic action or directly reacting with the resin.

Generally epoxies provide the highest performance of all thermosets. They are characterized by very high strength in compression, tension and flexure. Also they exhibit a very low shrinkage, very good adhesion values, very good electrical properties and chemical resistance and low moisture absorption. Next to that they offer excellent resistance to corrosion, high strength-to-weight ratio, and dimensional stability. With suitable additives they can exhibit excellent resistance to heat, going up to 290°C, and electrical insulation performance. Epoxies can be formulated to cure at room temperature or with the aid of heat. Normally heat curing yields epoxies with maximum performance. A slight drawback of epoxies is the longer curing time than other thermosets.

After the thermoset polyester resins epoxies are the most widely used thermosets in reinforced plastics, complementing them at the higher ends of performance. Due to the very good properties of epoxy resins, they are often used with high performance reinforcements, such as carbon fiber or high fiber contents of glass fiber. They are mostly used in filament winding, contact molding and lay-up. Because of their high corrosion resistance, they are also used as surface-coating layer for other materials or plastics. The epoxies chemical resistance, toughness, flexibility and adhesion is unmatched by most other plastics.[B16, p136-137]

Phenolic resins

Phenolic resins are produced by reacting phenol with formaldehyde. They are formulated with one- or two-stage curing systems. They have been in use since 1907, making them the first commercially available synthetic material. Then, they were particularly interesting to many industries due to their low cost.

Phenolics are characterized by low creep, excellent dimensional stability, good water and chemical resistance and good weather ability. The point where phenolics really outrun other thermosets is the heat- and fire behavior though. Without additives they are almost infusible, have no auto-propagation of flames, very low emission of smoke and toxic fumes, low heat release and no release of flammable vapor. They have heat resistance up to 150°C, without additives. Phenolics of course have some draw backs, because they are brittle, they have to be combined with additives, such as siloxane, to improve their impact performance. Next to that they have lower mechanical properties than most other thermosets.

Because of their limited properties they are mostly used in special applications where fire- and heat-resistance is needed. Where better mechanical properties are needed other plastics are used. Production processes most used with phenolics are compression transfer and injection molding. During curing they behave slightly more critical than other plastics, they have a time to temperature to viscosity behavior that has to be monitored.[B16, p137-139]

(Thermoset) polyester resins

Polyesters are a very large group of plastics, spanning both thermoplastic and thermoset polymers. Thermoset polyesters are also called unsaturated polyesters, which distinguishes them from thermoplastic or saturated polyesters. Thermoset polyesters are the most widely used thermoset matrices for reinforced plastics. The term thermoset polyester covers a very large chemical family, which is usually manufactured by reacting dihydric alcohols (glycols) and dibasic organic acid. By elimination of water between the acids and glycols, ester linkages are formed, producing long chain molecules. These molecules are usually dissolved in a reactive organic solvent. Polyesters are usually classified by the types of dihydric alcohols, dibasic organic acids and solvents used. The sum of these three components will greatly influence the polymer chain length and –structure, and thus the properties of the polyester resin.

Polyesters therefore have a widely varying range of properties. Usually though, they offer a good balance of mechanical, electrical and chemical-resistance properties at relatively low cost. Furthermore they also have good dimensional stability and are easy-to-handle. Drawbacks are the styrene emission during the cross-linking process and the high shrinkage.

To make the polyester workable, the polymer is usually dissolved in styrene or a monomer containing unsaturated vinyl. Together with heat and a chemically activated free radical initiation the polyester forms a 3D network at about 170°C - 200°C. In this stage the polyester can be kept unhardened for about 6 months. After application of the initiator, they are then cured at room temperature, under heat of about 60°C - 90°C or by UV- or visible light. The possibility of cold-curing polyester from its liquid to its solid form is one of the main reasons for its wide-spread use in large structures. Because cold-curing takes about 1-2 weeks at room temperature, accelerators are often used. Additives, fillers and pigments are often used to increase viscosity, reduce volatilization, add strength, counteract shrinkage and add color and UV-absorbers.

Polyesters are mostly used in reinforced plastics, with glass fiber as reinforcement. As mentioned before many types of thermosetting polyesters exist. Properties like heat resistance, resistance to hydrolysis, impact strength, flexibility, light refraction, electrical properties, flammability and strength can be tailored by specific chemical constituents. The following types of resin are typical thermoset polyester resins. Their names clearly state their specific goals:

- Standard
- Chemical-resistant/corrosion-resistant
- Flame retardants
- Gel-coats

Current developments include the application of solvents that drastically reduce the styrene and acetone emission during production. These are very harmful for the health of the workers involved and have successfully been reduced by many manufacturers. Because the developed solvents are quite expensive, systems have been created to recover used solvents, recycle them and reuse them. [B16, p139-148]

The table below gives a short overview on the mechanical performance of different types of glass reinforcement in a thermoset polyester matrix.

Type	Unit	No reinf.	Chopped roving	Roving fabric	Bidirect. fabric	Unidirec. fabric	Unidirec. roving
Typical glass content	%	n.a.	30	50	65	65	75
Density	g/cm ³	1,2	1,4	1,65	1,75	1,75	2
Tensile strength	N/mm ²	85	100	270	460	680	1.150
Tensile modulus	N/mm ²	4.200	7.700	16.000	22.000	34.000	42.000
Flexural strength	N/mm ²	120	180	300	600	900	1.300
Flexural modulus	N/mm ²	4000	7000	15000	21000	32000	40000

Table 14: Mechanical performance of different glass fiber reinforcements in a polyester thermoset matrix

Polyimide resins

Polyimides are available in thermoset and thermoplastic versions. They are known as the most heat- and fire-resistant plastics available. If the choice of plastic fell on polyimide, usually reinforced plastics are made of the thermoset version. Polyimides are difficult to process by conventional means. Techniques range from powder metallurgy to special injection, transfer, compression and extrusion systems. The most commercially interesting form of polyimides are special powder that are formed in reaction vessels. They can be used for extrusion, injection and compression molding, and preparation of prepgres through powder-coating.

Polyimides have heat resistances up to 540°C for short periods and very good stability at elevated temperatures. However they have to be molded at 300°C and post-cured at 400°C. Also, they have good impact resistance, tensile strength and –modulus, dimensional stability and resistance to combustion. Due to their complicated fabrication and curing, they are mostly used in costly applications such as critical engineering parts in the aerospace, automotive and electrical industry, subjected to high heat, and corrosive environments. Typical values for tensile strength are 165 N/mm² and for the tensile modulus 2.860 N/mm². [B16, p151-152]

Polyurethane resins

These resins are based on the reaction of di-isocyanates with polyols (polyesters or polyethers) which are hydroxyl-terminated. They must be cured under anhydrous conditions and the reaction can be very fast. For processing the two components, isocyanates and polyol are brought together in mixing/dispensing head, from which they are injected into a closed mold. Resin injection mold techniques can also be applied. [B16, p152-153]

Polyurethanes have high impact strength and toughness and an excellent resistance to abrasion. Next to that they are mainly used as adhesive, which shows that they have excellent reinforcement bonding properties. Finally they also exhibit very good resistance to chemicals.

In reinforced plastics polyurethanes are mainly used for resin injection molding, where, together with the mixing of the polyurethane compound, chopped reinforcement and fillers etc. are added into the dispersion head. Formulation for sheet molding compounds and filament winding is also possible with polyurethanes. Due to their high impact resistance, polyurethanes are often used for external panels in the automotive industry.

Silicone resins

Opposed to other plastics that are based on carbon, silicone resins are based on silicon. These resins are semi-organic and consist of chains of alternate silicone- and oxygen atoms. They are cross-linked by heating with a catalyst like cobalt naphtenate, zinc octoate or triethanolamine. Mostly, rigid silicones, as needed for reinforced plastics can be formulated on polysiloxane resins, giving high thermal stability of over 250°C.

Silicone matrices are known for their excellent long-term heat-resistance, low water absorption, very good electrical properties and good weather ability. [B16, p153-154]

Vinyl ester resins

Just like the polyester thermoset polyesters, these matrices are also unsaturated. Vinyl ester resins are cured by peroxide catalyzed addition polymerization of vinyl groups and anhydride crosslinking of hydroxyl groups at room- or elevated temperatures. Similar to polyesters different kinds of vinyl esters exist, categorized according to their chemical complements. Bisphenol-A cured vinyl esters are characterized by chemical resistance, epoxy novolac cured vinyl esters by the used solvent, the heat-resistance and the used flame retardant.

In general, vinyl ester resins are tough, stiff and flexible in a wide range. They provide exceptional high strength properties in corrosive and chemical environments, compared to thermoset polyesters for example. Vinyl ester resins combine the best features of polyester and epoxy resins. Their strength is almost as high as epoxy strength, but they are less expensive and easier to handle. Next to that they are also heat-and chemical resistant, possess good impact- and fatigue resistance, have low permeability to water and good electrical and thermal insulation properties.

To work with vinyl esters at room temperature, their viscosity has to be lowered dissolving the ester in a solvent like styrene. The reaction has to be boosted by using peroxide catalysts and cobalt accelerators. To achieve maximum temperature resistance, high-temperature post-cure is necessary at temperatures of 70°C - 120°C. For this hot-cure different systems of chemicals, such as benzoyl peroxide or tertiary-butyl peroxybenzoates have to be used.

Vinyl esters are very well compatible to glass, graphite, carbon and aramid fibers. The most common applications are chemical-resistant equipment, tanks and pipes and structural and automotive parts. Vinyl ester can also be used for bulk- and sheet molding compounds. Popular processes regarding vinyl ester reinforced plastic production are pultrusion, laminating, transfer molding and filament winding. As with thermoset polyester resins the vinyl ester is diluted with 30-50% styrene to make it workable. The toxic properties of styrene led to the development of low styrene emission resins. Examples are special bisphenol-A epoxy vinyl esters and high performance novolac epoxy vinyl esters that are only about 10% more costly than normal vinyl ester resins. Below a small table is given, comparing normal and low styrene emission vinyl ester resins. Low styrene emission vinyl ester resins have no mechanical disadvantages over standard vinyl esters. [B16, p148-151]

Type	Unit	Standard resin	Low styrene emission resin
Tensile strength	N/mm ²	115	124
Tensile modulus	N/mm ²	8.600	8.700
Flexural strength	N/mm ²	172	193
Flexural modulus	N/mm ²	7800	7800

Table 15: Comparison between LSE vinyl ester and standard vinyl ester. [B16, p150]

Other thermoset resins

Next to the thermoset resins that have already been discussed, there are a number of other resins that have been developed for special applications. Below a very brief list of these resins is given:

Alkyd resins

These resins are mainly used for high heat and electrical applications.

Allyl resins

Allyl resins are often used in fiber reinforced plastics. Usually they are compression- or transfer molded. They have high heat- and moisture resistance and are mainly used when high and long-term environmental resistances are needed.

Bismaleimide resins

These resins have similar properties as epoxy resins, but with better heat resistance (up to 230°C). In reinforced plastics they are mainly used for military aircrafts and aerospace applications.

Furane resins

Furane resins offer the best chemical resistance of all thermoset plastics. However they require highly acidic catalysts, which make application complicated.

Melamine resins

These resins offer high hardness, good pigmentation potential and good electrical properties. They are rarely used as structural reinforced plastic.

Polyetheramide resins

This is a high-performance resin which has tensile modulus and –strength which is about 50% higher than that of epoxy resins and has five times the toughness. The resin has very good adhesion to carbon- and glass fibers. Tests have shown that Polyetheramides surpasses normal epoxy resins in almost every mechanical property by about 50%. The shear strength under hot-wet conditions is reported to be even 80% higher. Flammability, smoke release and volatility are low and the material is very easy to process, due to its low viscosity.

PETI-5 resin

This is another high-performance resin developed by NASA. It has excellent fatigue-resistance and is fully functional at constant high temperatures (it was tested for 60.000 hours at a constant temperature of 180°C). Its toughness is about 30x times higher than that of standard epoxy. A drawback is the post curing need for a temperature of 370°C and a high pressure autoclave.

PMR-15 resin

This resin is a high-tech version of the polyimide resin, being able to withstand constant working temperatures of 320°C. It was developed by NASA and is only used in jet engines.

Hybrid resins

These resins are composed of two different polymer components such as for example vinyl ester resin and polyurethane resin. These resins have properties that outrun those of their components. The given example has a tensile strength of 80 N/mm² and a flexural strength of 150 N/mm².[B16, p154-157]

2.5.2.6 THERMOPLASTIC RESINS

In contrast to thermoset resins, thermoplastic resins become solid during cooling. They can be repeatedly heated and cooled with mostly minor property losses. The behavior can be compared to the behavior of an ice cube: it melts when heated and it turns back into the original solid shape when cooled. To minimize degradation and decomposition the thermoplastic must be tightly controlled during the heating process. The table below shows the most common thermoplastics, divided in two groups by their molecular structures: Crystalline thermoplastics and amorphous thermoplastics.

Crystalline	Amorphous
<i>Acetal</i>	<i>Polycarbonate</i>
Best property balance Stiffest unreinforced thermoplastic Low friction	Good impact resistance Transparent Good electrical properties
<i>Polyaramide (Nylon)</i>	<i>Modified PPO</i>
High melting point High elongation Toughest thermoplastic Absorbs moisture	Hydrolytical stability Good impact resistance Good electrical properties
<i>Polyester (glass-reinforced)</i>	
Polyester (glass-reinforced) High stiffness Lowest creep Excellent electrical properties	

Table 16: Crystalline and Amorphous thermoplastic overview [B16, p113]

Crystalline plastics

Crystalline plastics have a highly ordered molecular structure, resulting in a sudden liquefaction at given point of applied heat and not in a gradual softening with increasing heat. The liquefaction temperature lies between 115°C for low-density polyethylenes and 330°C for polytetrafluoroethylenes. The mechanical properties of crystalline plastics are greatly influenced by their melt-flow behavior. They shrink anisotropically in the melt-flow direction, shrinking less in the direction of the flow. Generally the chemical resistance is very high. Reinforcements can drastically improve heat distortion temperature and strength and stiffness levels. Examples of crystalline thermoplastics are polyethylene, polypropylene, polyphenylene sulphide, polyetheretherketone, polythalamide, and thermoplastic polyimide.

Amorphous plastics

Amorphous plastics are plastics which do not have a crystalline structure. The molecules form no pattern but act more like an unordered cluster of molecular chains. This random structure is the main reason for their gradual melting behavior. Without additives, amorphous plastics are often brittle when solid. They shrink uniformly in flow direction and transverse to it, leading to lower mold shrinkages and warping than crystalline plastics. Amorphous plastics rapidly lose strength above liquefaction temperature (glass transition temperature). Examples for these plastics are polystyrene, polymethyl methacrylate, and some higher performance plastics, such as polyethersulphone, polyarylsulphone and polyetherimide.

Liquid crystal polymers

Next to that there exists another group of thermoplastics: the liquid crystal polymers. These exhibit self-reinforcing properties during processing due to their internal reinforcing molecular structure. Being part of the group of polyesters, they possess densely packed fibrous polymer chains, leading to high strength and stiffness, and making them high performance plastics. They have a low melt-viscosity, and are more easily processed. Also, they have the lowest warp and shrinkage of all thermoplastics. Other advantages of liquid crystal polymers are high strength-to-weight ratio, excellent weathering- and radiation-resistance, good dimensional stability, low thermal expansion, excellent flame resistance and high fracture-toughness.

Thermoplastics can be reinforced by fibers, flakes, beads or particulates. The greatest advantage of thermoplastics in reinforced plastics is that they are very easy molded in mass-production. Thermoset plastics are much more difficult to process in this aspect. Modern fiber- and compounding technology permits high fiber contents and long length fibers in injection molding, compression molding, stamping, pultrusion and tape layering or winding. As it was the case with thermoset resins, glass is still the most used reinforcement.[B16, p113-117]

Acetal resins

These resins have similar properties and a similar appearance as polyamide resins and are often used in hybrid applications. Due to their low coefficient of surface friction, resistance to fatigue and abrasion, resistance to chemicals and heat, excellent creep life and high strength and stiffness they are often used for mechanical products such as gears, cranks, cams etc. Use in civil engineering applications is limited.

Polyamide (nylon) resins

Nylon resins are most often used in reinforced thermoplastic composites due to their low-cost and ease in compounding. Nylon is very tough, has an excellent chemical resistance. These resins have a relatively high moisture absorption, which can lead to less dimensional stability. Many different kinds of reinforcements and additives can be applied with polyamide resins, leading to a great array of possible properties. Generally polyamides can compete with engineering resins such as polyphenylene sulphide when reinforced with glass or carbon.

Polyarylate resins

Polyarylates are aromatic polyesters that have a similar structure to that of polycarbonate. The properties are also comparable: they are very tough, easy to process, have a high heat distortion temperature and a good resistance to weathering. Related to these resins are the polyester carbonates which are often used for safety equipment, electrical hardware, transportation and automotive components and in the construction industry.

Polycarbonate resins

These are among the strongest thermoplastics. They have a range of advantageous properties: they have a good overall heat- and flame-resistance, excellent electrical properties, good toughness and a good dimensional stability. They are very well compatible with glass reinforcements, although additives have to be added to counteract brittle behavior of the matrix.

(Thermoplastic) polyester resins

This term covers a large group of resins such as polybutylene terephthalate and polyethylene terphthalate. Often they are also called saturated polyesters (see the chapter on thermoset polyesters). Generally they have similar properties as polyamide resins, except that the polyester have a lower moisture absorption and thus a higher dimensional stability. Due to the high speed of crystallization thermoplastic polyester are very well suited for mass-production techniques with fast molding cycles, even at low temperatures (65°C – 85°C). Among the thermoplastic resins only polybutylene terphthalate (PBT) has the potential to be used in fiber reinforced plastics, a sample with 50% glass fiber content has shown a stiffness of about 19.000 N/mm². However, reinforcement of PBT has shown problems such as rough, uncontrollable surfaces, which make application on a large scale problematic.

Polyethylene (PE) resins

Many different formulations, such as high density polyethylene or low density polyethylene exist for this resin. It is mostly applied as film for packaging etc. and as material for sewage piping. Application as matrix for reinforced plastics is very rare, although it could be suitable as neutral carrier for specialty additives and pigments.

Polypropylene (PP) resins

After nylon this is the most used thermoplastic in reinforced plastic composites. The reason for this lies particularly in the low cost. Polypropylene compounds reinforced with glass fiber are used relatively often, although special coupling agents are needed for a good bond between fiber and matrix. An advantage of these resins is the relatively good recyclability. [B16, p117-133]

Polystyrene (PS) resins

This resin is almost exclusively used in its unreinforced form. Many different variations exist, being all cut to fit special needs. Although it is technically possible to reinforce this plastic with glass fibers, little commercial interest has been raised. Some special styrene maleic anhydrides resins have been developed which can be reinforced with glass mats, yielding equal results as polypropylene thermoplastics.

Polyvinyl chloride(PVC) resins

This plastic is very well known and often called “poor man’s engineering plastic”. It possesses exceptional flexibility in formulation and processing producing flexible to rigid plastics. Some applications of polyvinyl chlorides in reinforced plastics have already been developed, such as heavy-duty fabrics or conveyor belting. It has not yet been used in civil engineering applications.

Polyetherimide resins

This is an amorphous high performance thermoplastic. It possesses a high temperature resistance, rigidity and impact strength. Good long-term creep performance makes it an alternative to metals in some structural applications. It can be reinforced with glass fiber or carbon fiber.

Polyimide resins

As stated in the thermoset plastic section, this material also exists in a thermoset version. The properties of the thermoplastic polyimide resins are very well comparable to thermoset polyimide, although most applications in reinforced plastics feature the thermoset version of this resin. [B16, p117-133]

Polyketone resins

These resins are among the highest performing engineering thermoplastics. They provide excellent thermal resistance up to 245°C and good mechanical, chemical and electrical properties. They are self-extinguishing and have a low smoke-emission. Despite of their high costs they are often used together with high-performance reinforcing fibers to form a high-quality composite. These resins are mostly used for thermoplastic prepreg materials, using mats, fabrics and continuous fibers.

Polyphenylene resins

This group of resins consists of polyphenylene ether, polyphenylene oxide and polyphenylene sulphide. They have been one of the most successful groups in the medium/higher range of cost and performance. Generally they provide good heat stability and particularly good flammability properties. The first group has the best mechanical properties at temperatures up to 120°C. The last group has best impact resistance, being also very resistant to fatigue and creep. Both groups are available as molding compounds and as extruded sheets reinforced with glass or carbon.

Polysulphone resins

These resins have been developed with high heat stability in mind. They can cope with continuous temperatures of 180°C and more. Next to that they have a very good oxidative resistance and a high mechanical strength. Mostly they are used for electrical- and medical equipment as well as for example in aircraft interiors. Use in civil engineering is limited to none. [B16, p117-133]

To conclude this part on thermoplastic resin a general outline is given. Although some applications were given in the latter; thermoplastic resins are only used in reinforced plastics for specialty applications. Most of the thermoplastics are used in commodity plastic and not in engineering plastic. One reason for this lies in the fact that they have to be molded in high temperatures to keep them viscous. Thermoplastic resins can best be used as filled systems for non-structural, low-temperature applications.[B22, p3.19]

Because there are some, admittedly rare applications of fiber reinforced thermoplastic resins available. a comparative table on high performance thermoplastic resins is given. The upper table shows the properties of the unreinforced resins. The lower table shows the properties of the resins, reinforced with 30% short glass fibers.

Resins not reinforced				
Type	Unit	Polyether sulphone	Polyether imide	Poly-phenylene sulphide
Melting point	°C	n.a.	340	277
Heat distortion temp.	°C	205	200	n.a.
Continuous use temp.	°C	180	170	220
Tensile strength	N/mm ²	85	105	75
Flexural modulus	N/mm ²	2.600	3.000	4.200
Resins reinforced with 30% short glass fibers				
Type	Unit	Polyether sulphone	Polyether imide	Poly-phenylene sulphide
Melting point	°C	n.a.	340	277
Heat distortion temp.	°C	215	210	260
Continuous use temp.	°C	180	180	180
Tensile strength	N/mm ²	160	160	135
Flexural modulus	N/mm ²	10.000	10.000	11.000

Table 17: Comparison of three high-performance thermoplastics, with and without reinforcement. [B16, p133]

2.5.2.7 BIOLOGICAL RESINS

Biological resins or polymers are plastics with renewable components. Naturally synthesized polymers such as proteins, cellulose or starches have to be chemically altered to use them as thermoplastics. Processes using natural fermentation synthesis do also exist. Generally biological resins are not used as engineering- or reinforced plastic. The reason for this lies mainly in the industry applications that were developed in the last decades. Biopolymers are still mostly used in film form, acting as packing material. More reasons are the high fracture strain and the bad rheological behavior that these polymers exhibit. Biopolymers are almost exclusively used as commodity plastics. Below the three only biopolymers are described which could act as matrix in reinforced plastic. Though they would offer the advantage of biological degradability, when they would be combined with reinforcements and additives, recycling would still be complicated and costly. [B11, p103-105]

Cellulose thermoplastic resins

These resins are based on esters and cellulose and are only 50% biological. The main application areas are injection molding and extrusion. Cellulose based thermoplastic resins have tensile strength values from 19-45 N/mm² and an elastic modulus of 900-1.900 N/mm². They are not very humidity-resistant and can take short term temperatures up to about 100°C.

Polylactic acid thermoplastic resins

These biopolymers exhibit comparable properties as the thermoplastic polystyrenes. The only drawback is the low temperature resistance of about 60°C. An advantage of these resins is the low cost. General mechanical properties are a tensile strength up to 55-60 N/mm² and an elastic modulus of 3.500-4.000 N/mm².

Polyhydroxybutyrate-valerate thermoplastic resins

This biopolymer is naturally occurring, produced by bacteria which synthesize glucose to hydroxybutyrate which is then assembled into long polymer chains. It has similar properties to polypropylene and polyethylene but is very hard to produce artificially on an industrial scale. Another drawback compared to polypropylene is the high brittleness of the plastic. Polyhydroxybutyrate-valerate thermoplastic resins exhibit tensile strength and elastic moduli of 15-25 N/mm² and 900-2.000 N/mm² respectively. They can withstand temperatures up to 120°C. [B11, p105-109]

To compare the above biological resins a small table was made. Next to already described biological resins, a biological epoxy was added, which is produced by epoxidizing plant oils.

Type	Unit	Cellulose TP	Polylactic acid TP	Polyhydroxylbutyrate-valerate TP	Biological Epoxy
Tensile strength	N/mm ²	19-44	55-60	15-27	n.a.
Tensile modulus	N/mm ²	900-1.850	3.500-4.000	900-2.700	1.700-3.000
Flexural modulus	N/mm ²	n.a.	3.700	1.700-3.500	n.a.
Temperature range	°C	-50-103	n.a.	-30-120	n.a.

Table 18: Comparison between various biological resins [B11, p105-111]

2.5.3 ADDITIVES

Additives are generally applied in reinforced plastics to improve properties such as mechanical strength, elastic modulus, chemical- and thermic resistance. Next to that they can also improve electrical- and impact properties, and improve bonding behavior between matrix and fiber. Another use to be pointed out is the improvement of workability during the production process and surface finish due to the application of additives. Finally, additives exist which act as flame-retardants, plasticizers, heat- or light stabilizers etc.

Next to the already given properties, fillers are also used often to reduce costs of the matrix. Not every filler is compatible with every matrix resin, so care must be taken when deciding which materials to use. Fillers are mostly applied as particulates, beads or platelets. Examples of fillers are alumina, calcium carbonate, carbon black, clay, cotton flock, glass bubbles, graphite, mica, quartz or talc and many others. Choice of filler depends largely upon the requirements of the end item, type of material in the reinforced plastic and the method of fabrication.

Next to the given property improvements due to the addition of fillers there are also a large number of additives that are used to improve the curing process. Examples are catalysts, cross-linking enhancers, plasticizers, flexibilizers, toughening agents, reinforcing agents, bond enhancers, flow promoters, stabilizers. Due to the large number of available additives a classification according to their use is given:

Additives that assist processing

Processing stabilizers, processing aids and flow promoters, internal and external lubricants, thixotropic agents that control the viscosity properties at different temperatures

Additives that modify the bulk mechanical properties

Plasticizers, flexibilizers, reinforcing agents, toughening agents, strengtheners, shrinkage reducers, breathers

Additives that reduce formulation costs

Diluents, extenders, particle fillers

Additives that modify the surface properties

Antistatic agents, slip additives, anti-wear additives, anti-block additives, adhesion promoters

Additives that modify the optical properties

Pigments and dyes, nucleating agents

Additives that act anti-aging

Anti-oxidants, UV-stabilizers, fungicides

Flame retardants

All agents that improve heat/fire behavior. Examples are antimony oxide and alumina trihydrates, which can greatly improve flame retardancy and reduce smoke emissions in specific resin systems

Application of a specific additive to improve the desired property of the reinforced plastic can lead to deterioration of other properties. During the design of reinforced plastic the needs of the product need to be specified, according to which appropriate additives can be determined. [B22, p3.24] [B16, p158-170][B11, p173-222]

2.5.4 PRODUCTION TECHNIQUES

In this chapter different production techniques of fiber reinforced plastics will be discussed. The chapter will start with an introduction on the available pre-products which are used to make reinforced plastic structural material. In the following the three main groups of assembly methods will be discussed: Open mold processes, closed mold processes and continuous processes. The general order of production is as follows:

- Mixing resin and activator
- Dispensing resin into mold
- Impregnating reinforcement with resin
- Positioning reinforcement
- Curing

2.5.4.1 PRE-PRODUCTS

Below the most used pre-production techniques are shown. Next to the discussed techniques, several others do exist, but since they are specialty applications which are not very common they will not be shown.

Woven fabric

Woven fabric is very often used in reinforced plastics. With this technique higher strength- and stiffness values are achieved than with randomly orientated fiber fabrics; yet still yielding lower strength and stiffness values than unidirectional reinforced plastic. Several different 2D weaves exist. Some of those are pictured in the scheme below:

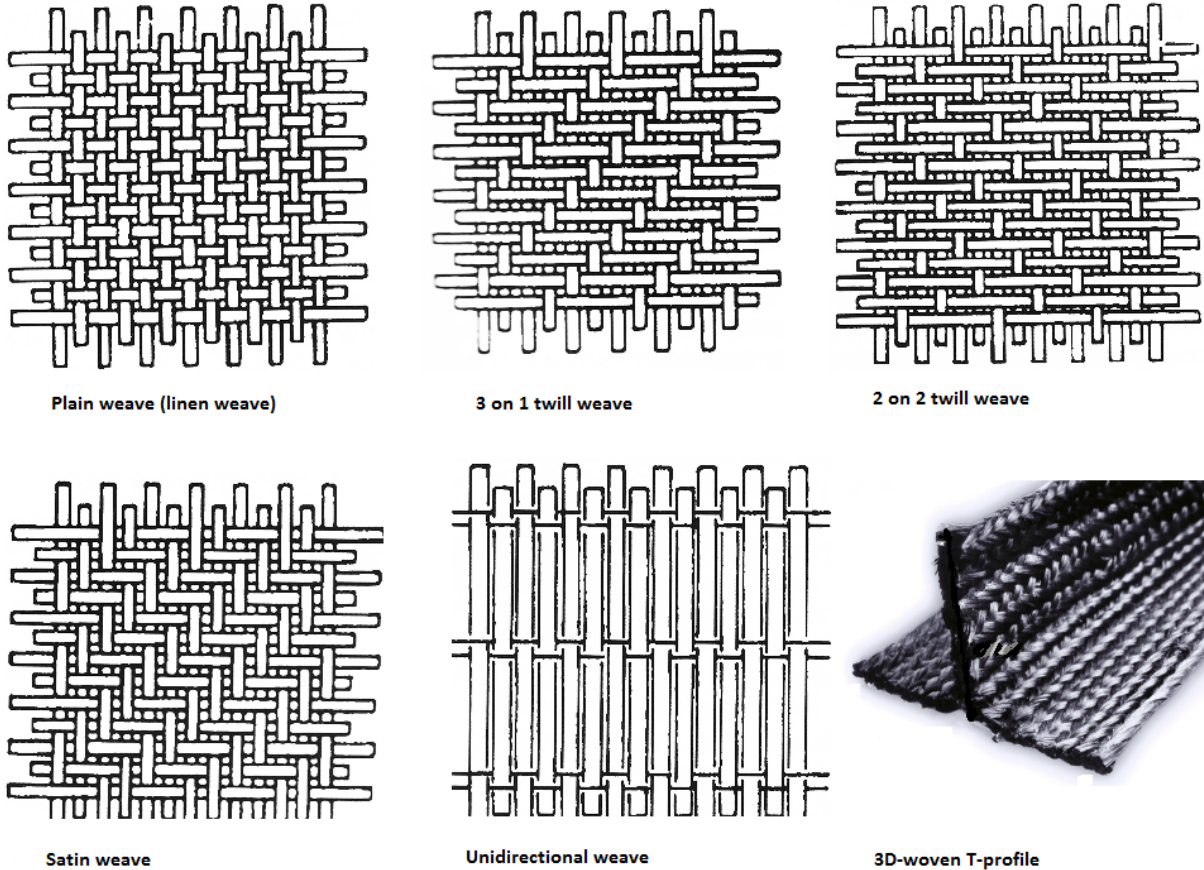


Fig. 34: Several weave types for reinforcement of plastic composites [B22, p3.6-3.7][B11, p226]

Care has to be taken when using woven fabrics in further production processes. The yarn can float and shift during impregnating, which has to be avoided, since it reduces uniformity of mechanical properties. Weave mechanical properties are about 10% to 40% lower due to the curvature of the yarn than that of unidirectional reinforced plastic. Woven fabrics with minimized yarn curvature are thus the strongest woven fabrics. Woven fabrics have multi-directional fiber, which make mechanical properties better than transverse-to-fiber properties in unidirectional reinforced plastics. Woven fabrics can also be multi-layered or have a specific thickness provided by spacer fabric. Fabrics can be stitched or welded to produce more complex shapes.

Next to the standard 2D woven fabric, recent developments have led to more advanced 3D woven profiles such as the T-profiles, shown in the above picture. More and more companies offer complex 3D woven shapes, which are produced using CAD software and programmable complex machinery. [B11, p223-227]

Randomly orientated continuous fiber fabric

Randomly orientated fiber fabric, also known as continuous filament mat is often used for lower strength applications in fiber reinforced plastics. The filaments or yarns can have varying diameters and orientations in three dimensions. The filaments are usually bonded by chemical coatings and application of heat and pressure. The picture below shows the fiber layout of such fabric.



Fig. 35: Randomly orientated continuous filament fabric [WEB]

Prepregs

The term prepreg is a short form of the correct description pre-impregnated materials, denoting a predefined ratio of continuous fiber and uncured matrix material. They are used mostly for unidirectional reinforcement with thermosetting resins, and for woven fabric reinforcements with thermoplastic matrices. To stop the matrix from premature solidification solvents are added, after which the assembled prepreg is dried. Another method is the application of a thin matrix film onto the rovings. Due to exactly known fiber directions and the specified and uniform fiber/matrix ratio, and the high fiber contents prepgs reach high mechanical properties. Next to that prepgs also lead to a cleaner final production, since no additional resin application is needed. They are often used for thin-walled shell type structures due to their thinness.

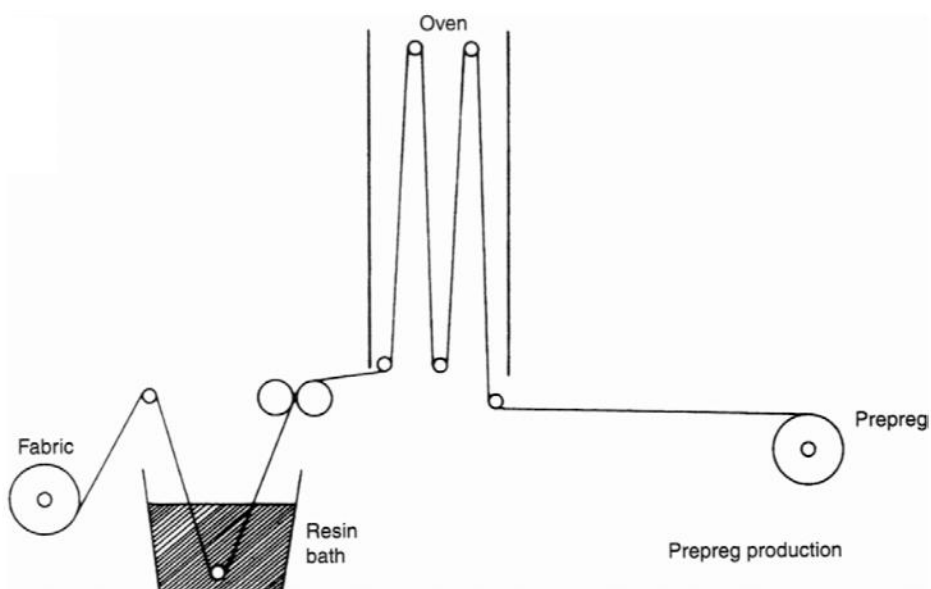


Fig. 36: Basic production process of prepregs. [B16, p220]

Prepreg materials can be used for various production techniques, leading to high quality, high fiber content products. Normally prepgres are cured at temperatures of about 120°C -180°C, but for large scale products, such as boat hulls up to 30m resins with curing temperatures as low as 75°C are also possible. [B16, p216-221]

Sheet molding compounds

Sheet molding compounds are a special form of prepgres, they are ready to mold materials that are usually composed with thermosetting resins. They are usually made by mixing and metering the compound, feeding in the reinforcement, wetting out the fibers, rolling up the sheet and allowing the material to mature. After that the sheets can be charged into a mold such as a matched-die- or compression-mold.

Sheet molding compounds can reach greater thicknesses than traditional prepgres (3mm compared to 0,1-0,4mm). Fiber contents are mostly between 25% and 50%. In order improve workability and prevent pressing out of the resin, the polymer is always thickened with viscosity agents. The compound is a complete mix of thickener, resin, fillers, additives and reinforcement by continuous fiber mat which is finished as continuous mat and cut into sheets for molding. Next to standard sheet molding compounds many special compounds exist which can reach fiber contents of for example 80% in the case of XMC (or cross-wound molding compound). Sheet molding compound can also be used for large structural applications, such as boat hulls.

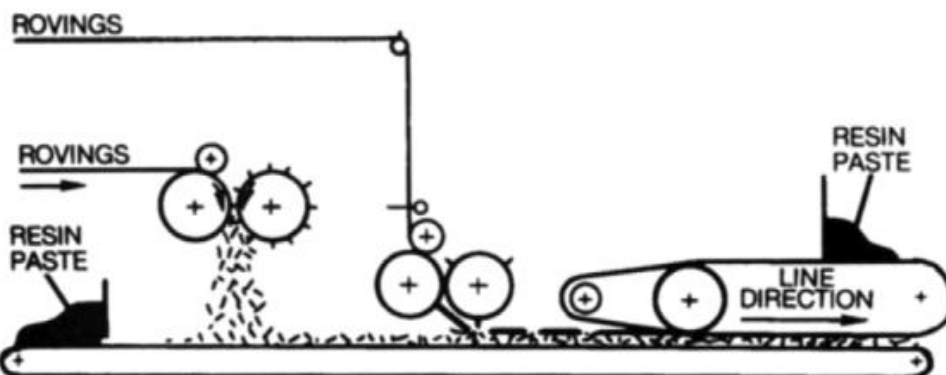


Fig. 37: Basic sheet molding compound production using rovings and chopped fibers [B16, p224]

Sheet molding compounds are widely used as standard material for low- and high-pressure molding of medium to large products, offering lots of potential for mass production manufacturing with superior finish and excellent mechanical properties. The above picture shows sheet molding compound production using both chopped fibers and fiber rovings. [B16, p221-228]

Bulk molding compounds

This method is similar to the sheet molding compound method, as it uses about the same mixtures. In contrast to the latter it is also used with thermoplastic resins. Those resins are more easily molded in mass production quantities. With bulk molding compound typically only short fibers are used, glass being most common. Bulk molding compound has a thick consistency and is normally extruded in a thick rope-like form, which is then processes furthers. Because they have a higher filler content and a lower fiber content than sheet molding compounds, bulk molding compounds exhibit lower strength and stiffness values. Typical fiber contents are 15%-25%.

Bulk molding compound is manufactured by feeding the paste premix, consisting of resin, additives, fillers and viscosity agents into a Z-blade mixer, where glass fiber is added and mixed in until an equal distribution is achieved. The resulting dough is then extruded. As with sheet molding compound many compound variations exist. With some of the variations, bulk molding compounds can reach thicknesses of 50mm. The picture below shows the basic production process. [B16, p238-243]

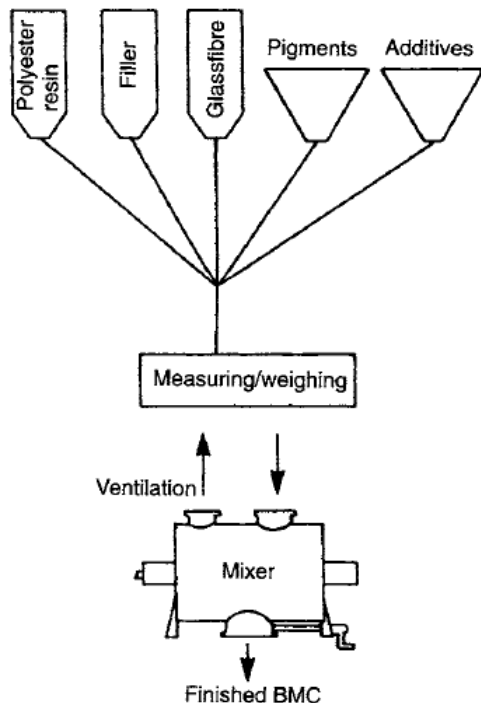


Fig. 38: Bulk molding compound production [B16, p241]

Nonwovens (or tissues, veils)

Non-wovens were already briefly covered in the glass fiber chapter, this chapter is intended to give some more information on them. Nonwovens are surface shapes that are composed of continuous- or cut fibers. The fibers are bonded either mechanically, chemically or thermic. The weight of nonwovens is typically $15\text{-}70\text{g/m}^2$. The low weight and high drapability makes them exceptionally suitable for improvement of reinforced plastic component surfaces. Due to the low fiber content, they cannot be used as high-strength structural material.

Mechanical bonding

The fibers are consolidated mechanically either by special felt needles or by high pressure water jets. Both processes entangle the fibers to form the tissue. Mechanical bonding can both produce nonwovens with high density and low drapability or nonwovens with lower density and high drapability. A big advantage of mechanically bonded nonwovens is the absence of other substances than the fiber.

Chemical bonding

In this process the fibers are bonded by a chemical, often called the binder. The binder is applied either by spray-up, sweeping or saturation. Mostly chemical bonding is used for low density, loose nonwovens. Because additional substances are now present in the nonwovens, the properties of these substances can be used advantageously for the final product. Chemically bonded nonwovens are often used as surface layer in reinforced plastics. Properties are for example added fire-resistance, electrical conductivity or added surface-smoothness. Properties of the surface are dependent on the chemical and filament type used. Specially coated graphite fibers for example are used for fire resistance. They foam up and reach up to 9x times their original volume and act as heat/flame barrier.[B11, p367]

Heat bonding

For heat bonding thermoplastic fibers with a low melting temperature are mixed with the main fibers. During heating the thermoplastic fibers melt and act as glue, and thus connect the matrix fibers. Two methods for heating exist: Firstly the hot air application, which produces low density, loose nonwovens. Secondly heated rollers are used which consolidate the matrix while heating it. This method produces more densely packed nonwovens, which are often used for smooth surfaces of pipes and tanks. [B11, p165-173]

2.5.4.2 OPEN MOLD PROCESSES

In this chapter the different production techniques using an open mold will be discussed. Open mold production techniques are among the oldest and simplest fiber reinforced plastic production processes. Usually no heat or additional pressure is used to cure the produced elements. This makes open mold processes easy to apply, but also causes low production rates, due to long curing times.

Hand lamination

The hand lamination process is the oldest fabrication process. It is labor intensive and messy, but still often used due to its flexibility and low outlay in molds and equipment. As depicted below the process consists of manual layup of reinforcement in a mold, and manual application of resin and consolidation of the reinforcement with a roller. Usually multiple layers of reinforcement and resin are applied. Advantages of hand lamination are the low capital outlay, no limits in size and high flexibility. Disadvantages are the operator dependency, labor-intensity, low production rate, only one molded face and the poor weight and thickness control. [B22, p4.2-4.3]

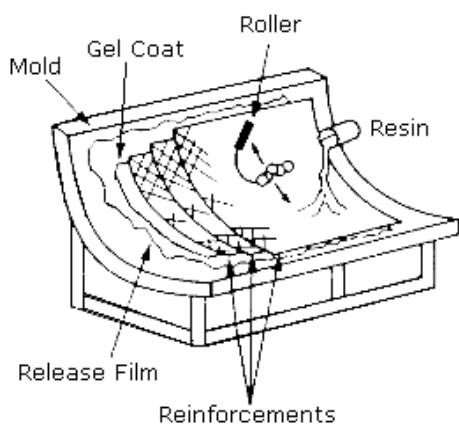


Fig. 39: Hand lamination production process [WEB, www.osha.gov]

Automated tape lamination

Automated tape lamination is a modern production technique overcoming the operator problem of the hand lamination. It uses a robot to apply prepreg reinforcement tapes in a defined way. The picture below shows the production process.

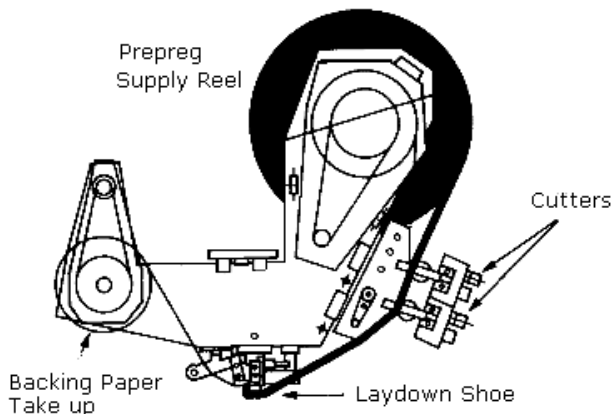


Fig. 40: Automated tape lamination production process [WEB, www.osha.gov]

Saturation

Saturation is a very similar process to hand lamination, the main difference is that the resin is not applied by simply pouring it in the mold by hand, but that the mixed resin is applied with an air-driven spray-gun. Resin and catalyst are mixed in the gun. Due to the spraying process only low viscosity resins can be used. With

saturation resin control is better than with hand lamination, but fiber content and thickness control are still in the hands of the operator. [B22, p4.3-4.4]

Spray up

In the spray-up production process chopped fibers and mixed resin are applied to the mold simultaneously. Continuous rovings are fed into the spray-gun, where a chopper prepares the fibers for application. Consolidation of the reinforcements still takes place by hand. Advantages of the spray up process are the high production rates, the low cost and the large possible sizes. Disadvantages are the poor detailing ability, the lack of control of fiber distribution and thickness, the dependancy on the operator's skills and the absence of directional reinforcements. [B22, p4.4-4.5]

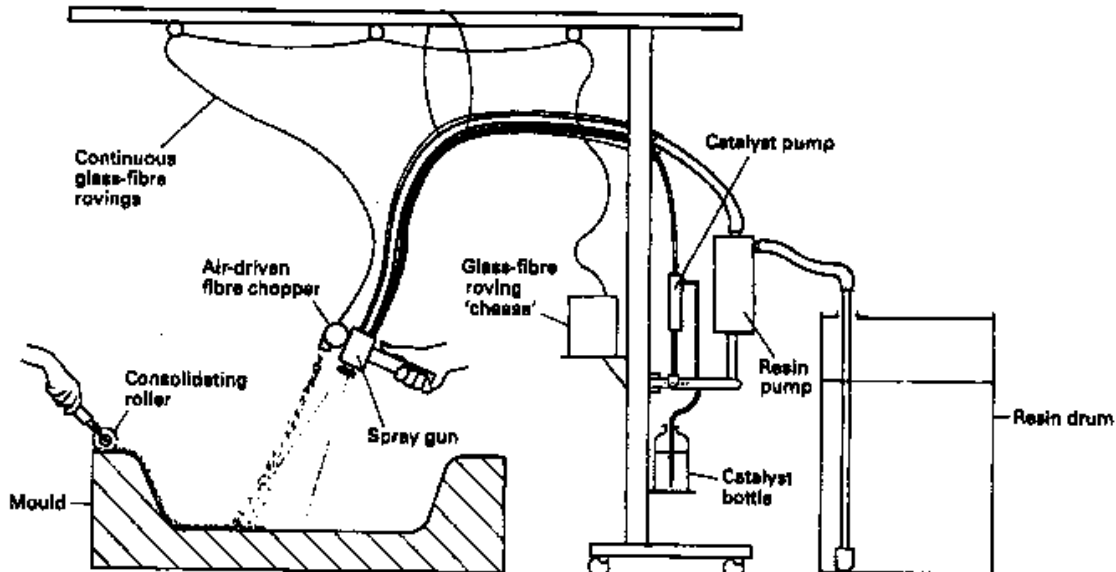


Fig. 41: Spray up production process [B22, p4.4]

Auto spray up

To overcome one of the biggest disadvantages of the spray up process, the auto spray up uses a controllable robot to control the gun orientation, speed and spray properties. This process is used for mass production of simple shapes. Due to the application of ever advancing robot techniques, more and more complex shapes become possible with this process. However, one of the greatest disadvantages remains: The lack of possibility to apply directional reinforcement. [B22, p4.5]

Filament winding

Filament winding is the method of choice to produce pressure vessels and other hollow shapes such as pipes, circular sections, gas bottles and tanks. The component is molded on a form, giving a molded surface on the inside. It is then mounted on a rotating shaft, where it is spun with rovings, which have been fed through a resin bath before. Through the alteration of the speed of the mold and roving feeder fiber orientation and thickness can be very well controlled. By varying the tension on the roving the fiber content and consolidation can also be controlled very well. Next to stated advantages, the high production rate and the excellent mechanical properties are advantages too. Due to the nature of the process the range of shapes is very limited and the possibilities of practical winding patterns are limited. The scheme below explains the production process. [B22, p4.5-4.7]

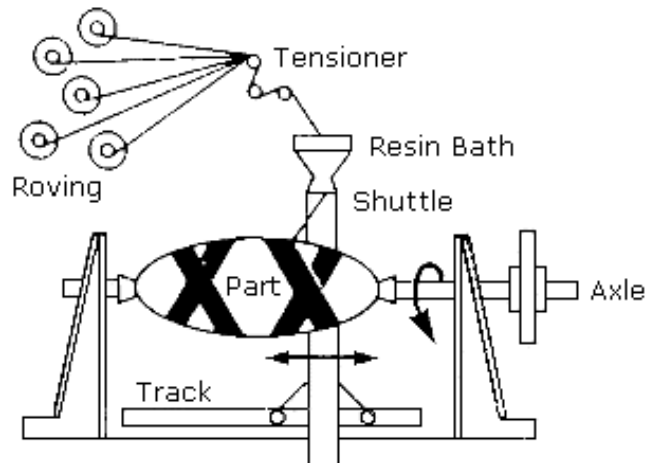


Fig. 42: Filament winding production process [WEB, www.osha.gov]

Spray winding

Spray winding combines the auto spray up process with the filament winding process. The combination of the two processes leads to alternating layers of spray up layers with high fiber content wound layers. Spray wound components achieve greater wall thickness more easily and cost-effective. A drawback is the lower strength of spray wound components compared to completely filament wound components. [B22, p4.7]

Centrifugal casting

Centrifugal casting is also used to produce hollow components, but the molded surface is on the outside. Resin and reinforcements are placed in a hollow mold, which is rotated at high speeds. The centrifugal acceleration forces the components against the mold surface, expelling air and consolidating the laminate. The higher density of the reinforcements pushes them more to the outside, leaving a more resin-rich inside. Both chopped fibers as well as directional reinforcements can be used. See the picture below for a sketch of the process. Advantages are the high production range, good fiber content and thickness control, good consolidation and the smooth resin-rich inner surface. Disadvantages are the form-limitation to cylinders and the non-molded inner surface. [B22, p4.7-4.9]

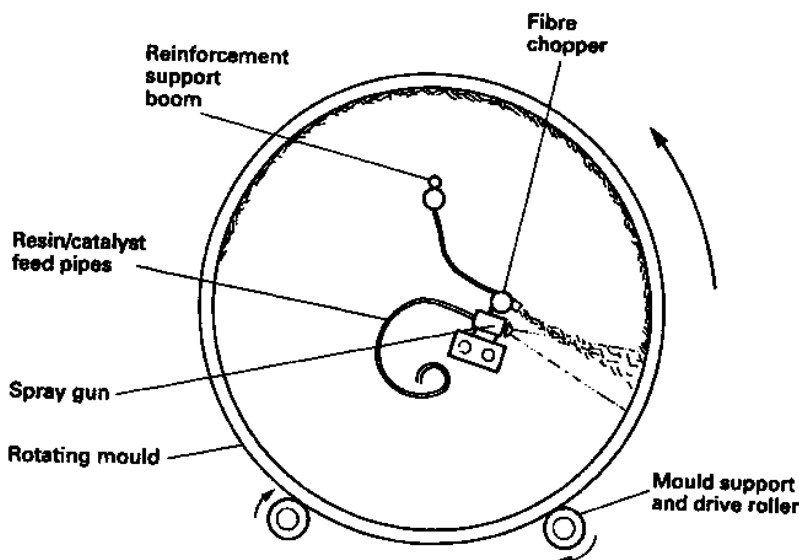


Fig. 43: Centrifugal casting production process [B22, p4.8]

2.5.4.3 CLOSED MOLD PROCESSES

Closed mold processes generally lead to higher production rates due to a shorter curing time than open mold processes. Typically they are more costly due to the needed processing temperature and -pressure. In the following the different available processes will be described.

Vacuum bag

This is the simplest form of closed mold processes. Reinforcement and mixed resin are applied by hand in a open mold, after which an airtight film is laid over the laminate, which is then attached to a vacuum hose. Through the extraction of air, the consolidation of the reinforcement takes place. Sometimes additional consolidation by manual rolling is needed. Advantages of vacuum bag production process are the large components possible and the well-suited-ness for producing sandwich panels. Disadvantages are the labor insensitivity, low productivity and only one accurate surface. The picture below shows the process. [B22, p4.10]

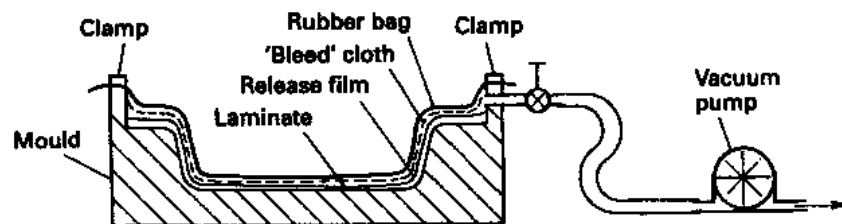


Fig. 44: Vacuum bag production process [B22, p4.10]

Pressure bag

The pressure bag process is similar to the vacuum bag process, but in contrast to this process it uses over-pressure and not under-pressure. This leads to higher possible consolidation pressures (up to 3,5bar), thus a better consolidation and a higher fiber content. Also, the pressure bag can be filled with hot steam to increase the curing temperature and to reduce the curing time. A disadvantage of the pressure bag is the need for a more robust mold to withstand the occurring pressures. Pressure bag production is mostly used for high quality components and uses prepgres as base material. The picture below explains the principle. [B22, p4.11]

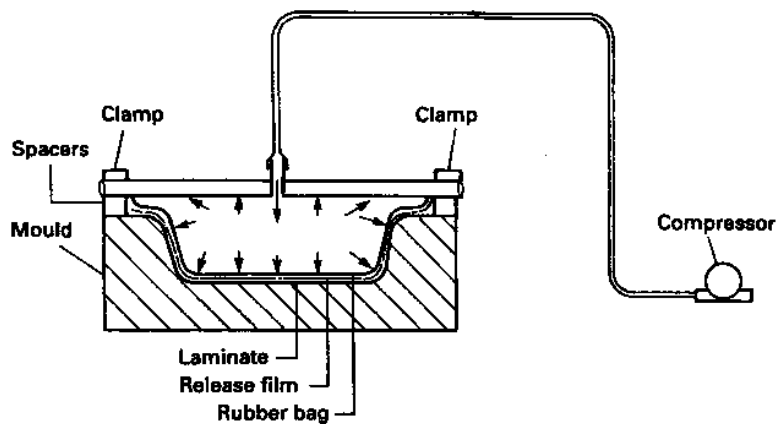


Fig. 45: Pressure bag production process [B22, p4.11]

Autoclave

The autoclave combines the pressure-bag- and the vacuum-bag-processes. Among all production processes it produces components of the highest quality. Nowadays only prepgres materials are used in autoclave production. During the process, a vacuum bag assembly (as described earlier) is loaded into a pressurized oven, called the autoclave. The oven is then closed, and vacuum, pressure and heat are simultaneously

applied on the laminate. Advantages of the autoclave production are the very high component quality, high fiber content, low void content and the controlled cure. Disadvantages are the very high cost and the lack of production speed. The scheme below illustrates the process. [B22, p4.12-4.13]

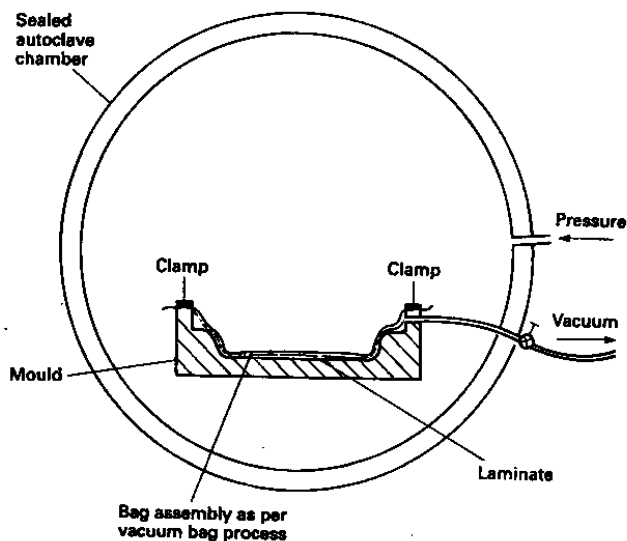


Fig. 46: Autoclave production process [B22, p4.12]

Matched mold

This is the simplest form of match mold processes. Male and female molds are pushed together with simple mechanical clamps or presses. The two molds are a loose fit, so that excess resin is pushed out. The reinforcement, both directional and chopped fibers, is laid on the hollow mold and impregnated by hand laminating. Matched molds produce components with accurate dimensions and a good finish quality on both surfaces. [B22, p4.13]

Cold press

Cold press processes function similarly to matched molds. The difference lies in the mechanism exerting pressure. In cold presses this is a controlled hydraulic press, which also distributes the resin over the reinforcement, purging air from it at the same time. The reinforcement pack is assembled dry and placed on the hollow mold. Advantages of cold pressing are the good surface on both sides, good production rate and accurate dimensions. Disadvantages are the size-limitation by press size and the low fiber content. The picture below shows the cold press process. [B22, p4.14-4.15]

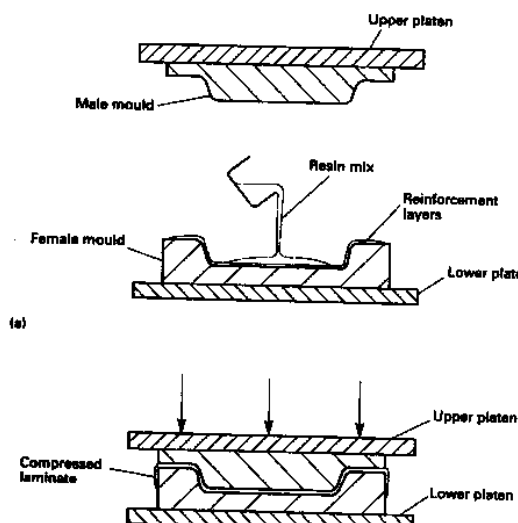


Fig. 47: Cold press production process [B22, p4.14]

Hot press

The hot press production process uses sheet- and bulk molding compounds as well as prepreg/low-viscosity resin combinations. Normally the press is heated to about 140°C, which leads to the need for metal molds. Due to the high temperature curing time is dramatically reduced, thereby drastically increasing the production rate compared to the cold press. Other advantages are fine detail and close tolerance and the low cost. Disadvantages are the limitation in mechanical properties due to the molding compounds and material flow, which causes property variability. The picture below shows a similar process as with the cold press, except for the addition of heat. [B22, p4.16-4.17]

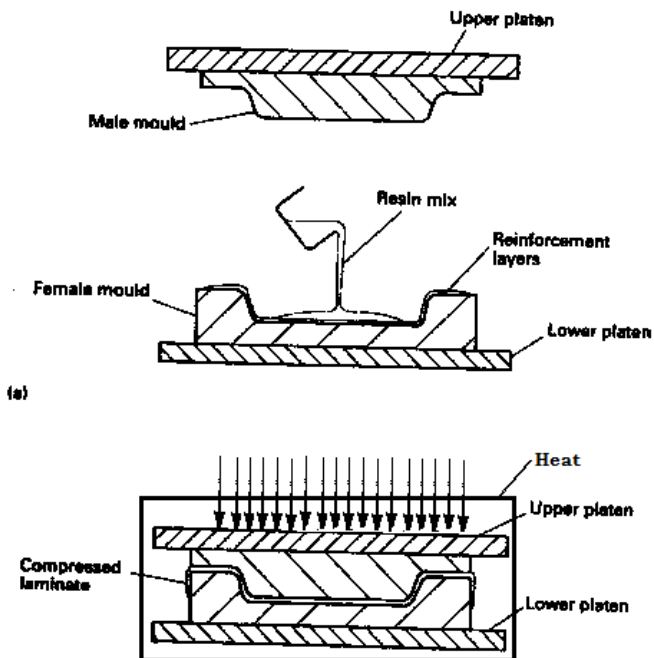


Fig. 48: Hot press production process [B22, p4.16-4.17]

Resin injection molding (resin transfer molding)

Resin injection molding functions similar to cold pressing: the reinforcement is put in the mold, then the molds are closed and clamped together. After closing, pre mixed resin is injected in the molds. Injection takes place under pressures up to 2bar, leading to the need for robust molds. Resin injected components are limited to random reinforcement and low fiber content, but more complex shapes than with cold pressing can be achieved. Other advantages are the good surface on two sides, accurate dimensions, the wide range of part geometry and the reasonable production rate. Disadvantages are the low fiber content and the high tooling costs. The picture below illustrates the process. [B22, p4.18-4.19]

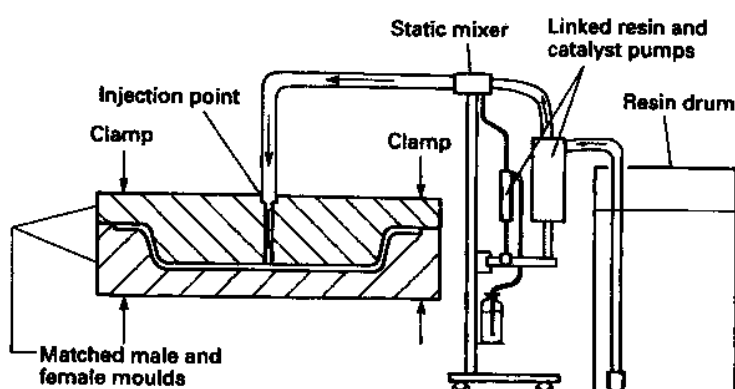


Fig. 49: Resin injected molding production process [B22, p4.18]

Vacuum-assisted resin injection molding

This is the advanced version of resin injection molding, leading to higher fiber contents, larger moldings and the freedom to use high strength reinforcements. The major difference is the application of a flexible glass reinforced plastic upper mold which enables free resin transfer, and is then pulled in its intended shape by the application of a vacuum, which also consolidates the reinforcement and removes air. The vacuum also clamps the molds tightly. Advantages are the high fiber content, large size, low cost and the full range of reinforcements. Disadvantages are the difficulty in production and the higher cost than cold pressing. [B22, p4.19-4.20]

Injection molding

Injection molding uses a completely preassembled dough of mostly thermoplastic resin with all additives and random reinforcements. This dough is inserted into the closed mold by a feeding screw. Advantages of injection molding are the very high production rate, close tolerances and complex shapes. Disadvantages are the limited mechanical properties, due to the random reinforcement and the size limit. The picture below illustrates the process. [B22, p4.21-4.22]

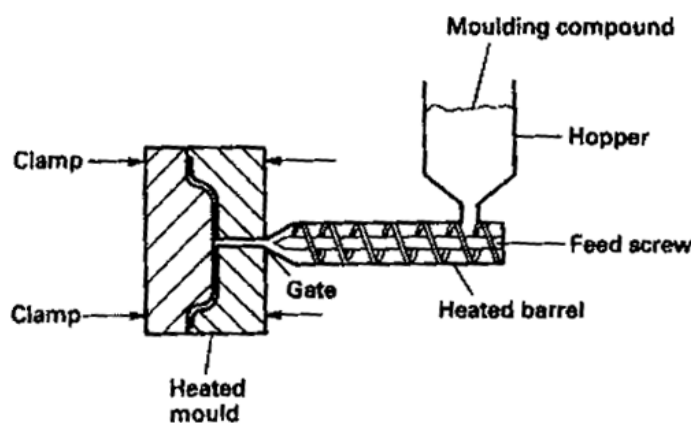


Fig. 50: Injection molding production process [B22, p4.21]

2.5.4.4 CONTINUOUS PROCESSES

Continuous processes are typically automated to some degree and are used to produce larger numbers of identical parts relatively quickly. These processes are typified by pumping of the resin mixture into the mold, followed by closed curing.

Continuous laminating

In this process resin and reinforcement are combined and contained between two layers of film which carry the laminate over a conveyor to the oven and to final cutting. Usually continuous laminating is used for flat sheets or corrugated profiles. The reinforcements are fed through a resin bath for impregnation, then through rollers which produce their final shape. After this the continuous sheet is put through an oven and cut to size. Advantages of this process are the very high production rate, low cost, consistency and good mechanical properties. The main disadvantage is the obvious shape limitation. See the sketch below for a process overview. [B22, p4.23-4.24]

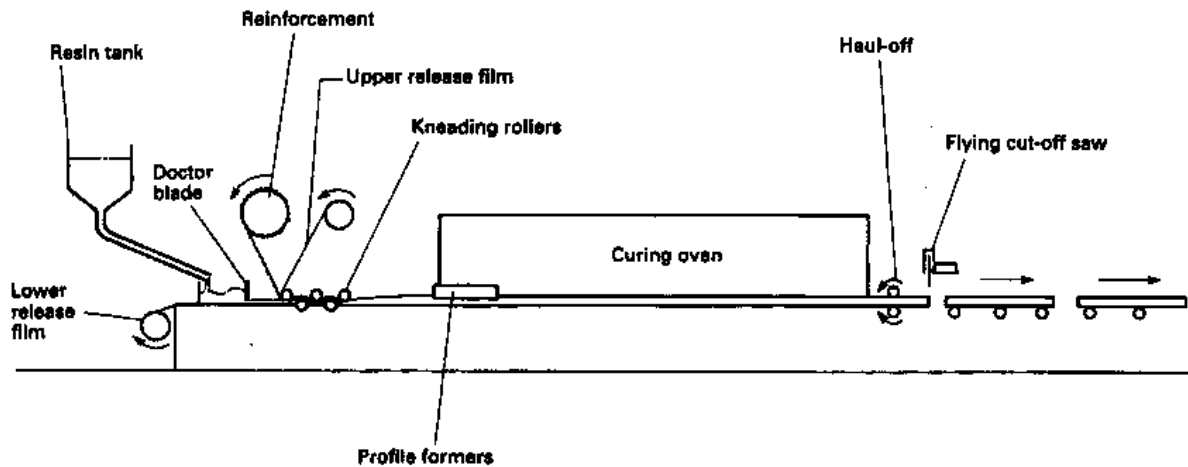


Fig. 51: Continuous lamination production process [B22, p4.23]

Pultrusion

The pultrusion process is very often used for the production of high strength reinforced plastic profiles. In this process, the reinforcement is pulled through a resin bath and then through a heated die, which forms it to the final profile shape. It then emerges fully cured from the die and can be directly cut to length. Sometimes resin is injected directly into the die. Due to the constant tension in the reinforcement it has an excellent longitudinal alignment and hence very high and consistent mechanical properties. Pultrusion can also produce complex profiles with intricate details, or multiple cells. Advantages of the pultrusion process are the excellent mechanical properties, the high production rate, close tolerances and the high consistency. Disadvantages are the shape limitation (longitudinal profiles) and the limited transverse properties. See the picture below for a sketch of the pultrusion process. [B22, p4.25-4.26]

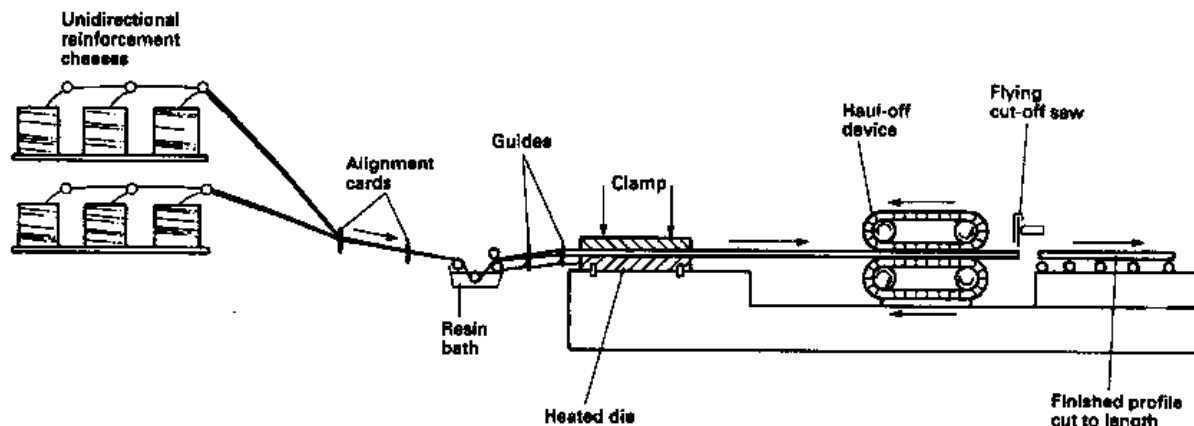


Fig. 52: Pultrusion production process [B22, p4.25]

Continuous filament winding

This production method produces filament wound tube continuously. Several moving winding heads rotate around the cylindrical form, where the component is assembled. The mandrel is composed of steel bands which form the cylindrical form. After a certain length the steel bands collapse and reform at the beginning to the cylindrical form. Just like normal filament winding, this process produces components of excellent mechanical properties at a high production rate and good consistency. The disadvantage of this process is the shape limitation: cylinders only, and the winding orientation limitation: spiral windings only. [B22, p4.27]

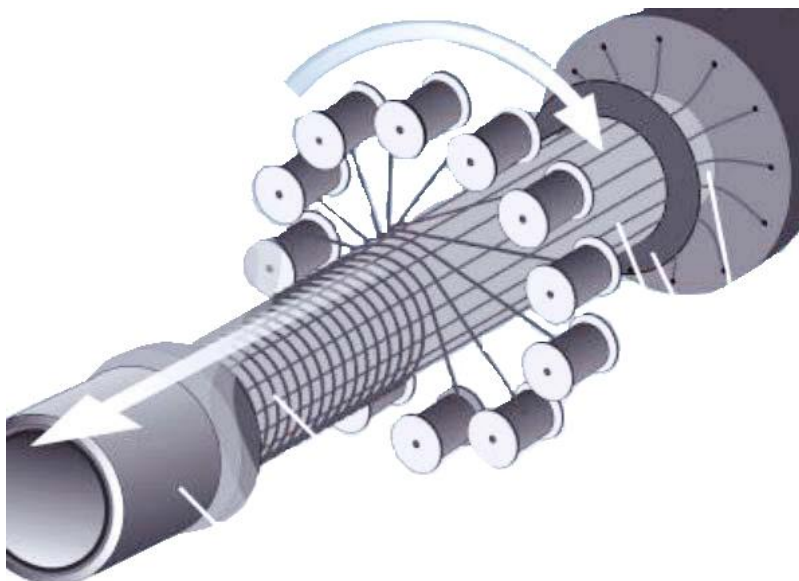


Fig. 53: Continuous filament winding production process [B11, p358]

2.5.4.5 COMPARISON OF ALL PRODUCTION TECHNIQUES

In the following table the different production techniques are compared according to performances and properties like fiber volume, size range, processing pressure, processing temperature, detail tolerance and relative production cost. Due to the large array of components that are produced using these techniques it is not possible to point out the “best” production technique. Many of the processes have been developed specifically for one product.

To give a little guidance on preferable production techniques, cells which represent the best value for the specific property of that column are hatched green. The best fiber contents for example are achieved with (continuous) filament winding, autoclave and pultrusion. The production methods with the best detail tolerance are the matched mold, cold press and hot press processes.

The data in the table has been derived from [B22, p4.3-4.27]

Type	Fiber volume [%]	Size range [m ²]	Processing pressure [bar]	Processing temperature [°C]	Detail tolerance [mm]	Relative production cost [-]
------	------------------	------------------------------	---------------------------	-----------------------------	-----------------------	------------------------------

Open mold processes						
Hand lamination	13-50	0,25-2000	ambient	ambient	1,0-5,0	High
Automated tape lamination	20-60	0,25-500	ambient	ambient	0,2-1,0	Moderate/High
Saturation	13-50	0,25-2000	ambient	ambient	1,0-5,0	Moderate/High
Spray up	13-21	2,00-100	ambient	ambient	1,0-3,0	Low
Auto-spray up	13-22	2,00-100	ambient	ambient	2,0-3,0	Very Low
Filament winding	55-70	0,1-100	ambient	ambient	1,0-2,0	Moderate/Low
Spray winding	40-60	0,1-100	ambient	ambient	2,0-3,0	Very low
Centrifugal casting	20-60	0,5-100	ambient	40-60	1,0-3,0	Moderate/Low

Closed mold processes						
Vacuum bag	15-60	0,5-200	ambient	ambient	1,0-3,0	Very High
Pressure bag	20-70	0,5-200	1-3,5	20-70	1,0-3,0	Very High
Autoclave	35-70	0,25-5,0	1-10,0	20-140	0,5-1,0	Very High
Matched mold	15-25	0,25-5,0	1-2,0	20-50	0,25-1,0	Low
Cold press	15-25	0,25-5,0	2,0-5,0	20-50	0,25-1,0	Low
Hot press	12-40	0,1-2,5	50-150	130-150	0,2-1,0	Very low
Resin injection molding	10-15	0,25-5,0	1-2,0	20-50	1,0-2,0	Moderate
Vacuum-assisted resin injection molding	15-35	1,0-3,0	1-2,0	15-30	2,0-5,0	Moderate/High
Injection molding	5-10	0,01-1,0	750-1500	140	0,1-0,5	Very Low

Continuous processes						
Continuous laminating	10-25	Up to 2m width	ambient	100-150	1,0	Very low
Pultrusion	30-65	Up to 1m width	varies	130-150	0,2-0,5	Low
Continuous filament winding	55-70	Up to 2m diam.	ambient	ambient	1,0-2,0	Low

Table 19: Comparison between different fiber reinforced polymer production systems.

2.6 MECHANICAL PROPERTIES

In the structural engineering industry often designs are made and materialized using homogenous, isotropic materials such as for example steel. Homogenous means that the properties of the material are independent of the exact location in the material, the properties are thus the same in every point of the material. Isotropic means that the properties are independent of the direction in the material. [B01, p1]

Natural composites such as wood, bone and plant fibers are heterogeneous and anisotropic. They have a certain growing direction in which the properties differ greatly from the perpendicular direction. Man-made composites are inspired by this natural material and thus have the same characteristics as their natural counterparts.

Fiber reinforced polymer composites are not only anisotropic in their strength- and stiffness-behavior; they can also have other anisotropic properties such as swelling behavior, temperature expansion, heat transfer, electrical conductivity and others.

In the following the behavior on macro-scale of the composites will be assumed to be anisotropic, homogeneous and linear elastic. This assumption is quite accurate and is most-often used in literature. [B01, p6].

To make estimates of the direction-dependent stiffness properties of fiber reinforced polymer composites based on the composition and properties of the components, models that accurately describe the properties of the single components are needed. In this chapter some of the most often used models will be described. [B01, pV]

2.6.1 PROPERTIES OF REINFORCEMENTS, MATRICES AND SELECTED UNIDIRECTIONAL COMPOSITES

In this chapter the most important mechanical properties of the components of a composite as well as of some example composites will be given. Common reinforcements and matrix material will be covered. Note that the tabulated data was derived from literature and should act mainly as indication. For composites it is impossible to derive a completely accurate datasheet as it is possible for steel. Despite this fact the tables give a good overview of the properties.

2.6.1.1 REINFORCEMENT FIBERS

In the following graph and table some important mechanical properties of different types of glass fibers, carbon fibers and aramid fibers are given. The graph below shows the stress-strain relationship of these materials compared to that of steel. [B01, p19-23]

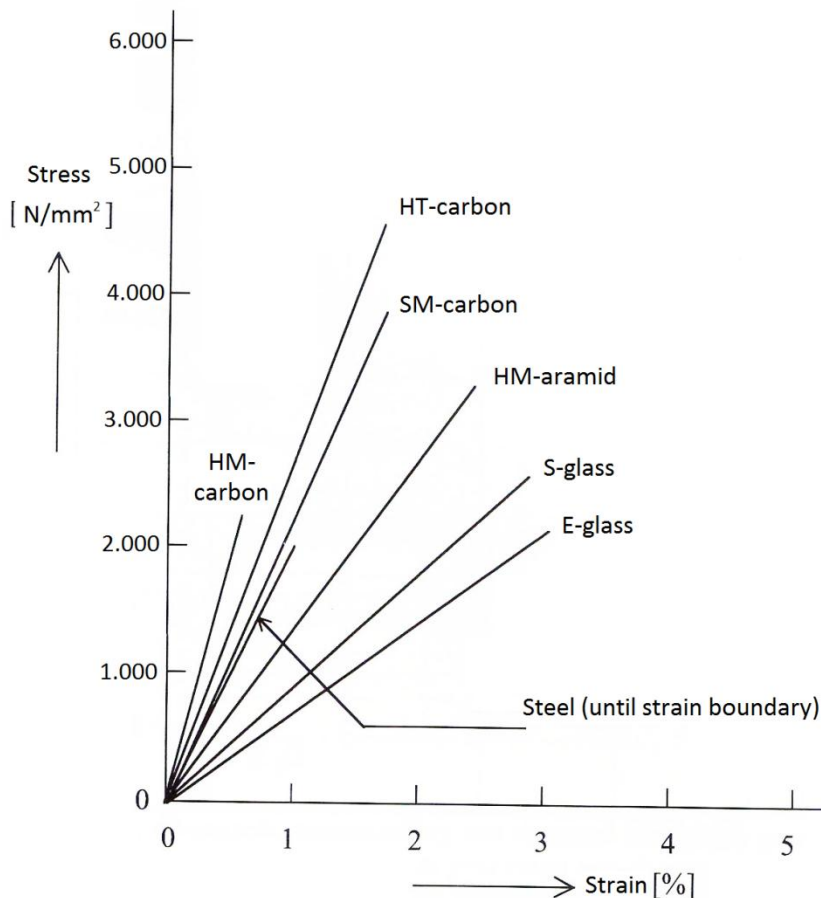


Fig. 54: Stress-strain relationships of different fiber reinforcement materials [B01, p22]

In the table E-glass stands for electrical-grade glass fiber, S-glass stands for strength-grade glass fiber. SM-carbon stands for standard modulus carbon fiber, HT-carbon stands for high tenacity carbon fiber, HM-carbon stands for high modulus carbon fiber. HM-aramid also stands for high modulus aramid fiber.

Property	Symbol	Unit	E-glass	S-glass	SM-carbon	HT-carbon	HM-carbon	HM-aramid
Density	ρ_f	kg/m³	2.540	2.490	1.800	1.800	1.850	1.450
Modulus of elasticity	E_f	10^3 N/mm^2	70	85	220-240	250-300	360-420	130
Poisson's ratio	ν_f	-	0,22	0,26	0,26	0,26	0,28	0,30
Tensile strength	s_f	10^3 N/mm^2	1,7-2,7	2,0-3,0	3,5-4,5	4,4-5,0	2,0-3,0	3,0-3,5
Rupture strain	e_f	%	2,4-3,7	2,3-3,5	1,5-1,9	1,5-1,8	0,5-0,7	2,3-2,6
Long. Lin.Therm. Exp.Coeff.	α_{fL}	$10^{-6}/\text{K}$	5,00	-	1,00	0,00	-0,50	-3,00
Trnsv. Lin.Therm.Exp.Coeff.	α_{fT}	$10^{-6}/\text{K}$	-	-	-	-	-	60,00

Table 20: Mechanical properties of different reinforcement fiber materials [B01, p21]

2.6.1.2 MATRIX MATERIAL

In the table below the mechanical properties of two common types of thermoset resins are displayed. The first resin type is an unsaturated polyester resin. The second type is an epoxy resin. In the table three different formulations of this resin are treated. The epoxy resins differ in curing temperature. [B01, p23]

Property	Symbol	Unit	Unsaturated Polyester Resin	Epoxy Resin	Epoxy Resin	Epoxy Resin
Curing temperature	T _c	°C	-	20	80+140	120+160
Density	ρ _m	kg/m ³	1.150-1.250	1.150-2.000	1.150-2.000	1.200-1.300
Modulus of elasticity	E _m	10 ³ N/mm ²	2,4-4,6	3,5	3,5	3,5
Poisson's ratio	v _m	-	0,35	0,35	0,35	0,35
Tensile strength	s _{tm}	N/mm ²	40-85	50-70	60-80	80-90
Compressive strength	s _{cm}	N/mm ²	140-150	90,0	130,0	120,0
Rupture strain	e _m	%	1,2-4,5	2,0-4,0	3,0-5,0	4,0-5,0
Lin. Therm. Exp. Coeff.	α _m	10 ⁻⁶ /K	80-150	90,0	60,0	65,0

Table 21: Mechanical properties of different thermoset matrices [B01, p23]

2.6.1.3 UNIDIRECTIONAL REINFORCED COMPOSITES

In the table below mechanical properties of different unidirectional reinforced composites are given. To be able to compare the composites they all have the same fiber content of 60%. Next to that they all feature the same matrix material, namely epoxy resin.

Property	Symbol	Unit	E-glass	SM-carbon	HT-carbon	HM-aramid
Density	ρ	kg/m ³	2.000	1.550	1.550	1.350
Long. modulus of elasticity	E _L	10 ³ N/mm ²	40	130	150	75
Flexural modulus	E _B	10 ³ N/mm ²	35	125	130	70
Transv. Modulus of elasticity	E _T	10 ³ N/mm ²	10,0	9,0	10,0	5,5
Long. Transv. Shear Modulus	G _{LT}	10 ³ N/mm ²	4,5	6,0	6,0	2,5
Long. Transv. Poisson's Ratio	v _{LT}	-	0,27	0,30	0,30	0,32
Long. Tensile strength	s _{lt}	N/mm ²	800	1.550	1.700	1.400
Long. Compressive strength	s _{lc}	N/mm ²	500	1.250	1.500	270
Bending strength	s _b	N/mm ³	850	1.600	1.750	625
Transv. Tensile strength	s _{tt}	N/mm ²	30	70	55	30
Transv. Compressive strength	s _{tc}	N/mm ²	140	200	250	55
Long. Transv. shear strength	s _{lt}	N/mm ²	65	90	80	35
Interlaminar shear strength	ILSS	N/mm ²	40	100	125	60
Long. Lin.Therm. Exp.Coeff.	α _{fl}	10 ⁻⁶ /K	7	1,5	0,5	-2
Trnsv. Lin.Therm. Exp.Coeff.	α _{ft}	10 ⁻⁶ /K	20	25	30	60

Table 22: Mechanical properties of different composites based on epoxy resin with a fiber content of 60% [B01, p23]

2.6.2 MODELS FOR THE ESTIMATION OF THE MECHANICAL PROPERTIES OF COMPOSITES

In this chapter some of the most common models for the estimation of the different mechanical stiffness of unidirectional reinforced composite will be given and compared. The start of this chapter will be made using simple models that only use volume fractions to predict the mechanical properties. Later some more complex models will be described.

2.6.2.1 MASS AND VOLUME FRACTIONS FOR UNIDIRECTIONAL REINFORCED COMPOSITES

The composition of a general FRP material can be defined by either the weight fractions or the volume fraction of the components. In this chapter the general case of only the reinforcement and the matrix is considered. If the densities of the components are denoted by ρ_m for the matrix and ρ_f for the fiber, the density of the composite is given in terms of volume fractions V_m and V_f by the following equation. In the case of more than two components present in the composite, the expressions below can be readily extended to cover more components. [B01, p4-5][B07, p167]

$$\rho = V_m \rho_m + V_f \rho_f \quad (2.1)$$

The formula above is called the “rule of mixture”. Alternatively, using weight fractions, W_m and W_f :

$$\frac{1}{\rho} = \frac{W_m}{\rho_m} + \frac{W_f}{\rho_f} \quad (2.2)$$

Of course, volume fractions can be expressed in terms of weight fractions by:

$$V_m = \frac{\frac{W_m}{\rho_m}}{\frac{W_m}{\rho_m} + \frac{W_f}{\rho_f}} = \frac{\rho_f}{m_m \rho_f + m_f \rho_m} m_m \quad (2.3)$$

$$V_f = \frac{\frac{W_f}{\rho_f}}{\frac{W_m}{\rho_m} + \frac{W_f}{\rho_f}} = \frac{\rho_m}{m_m \rho_f + m_f \rho_m} m_f \quad (2.4)$$

And vice versa

$$W_m = \frac{V_m \rho_m}{V_m \rho_m + V_f \rho_f} = \frac{\rho_m}{\rho} V_m \quad (2.5)$$

$$W_f = \frac{V_f \rho_f}{V_m \rho_m + V_f \rho_f} = \frac{\rho_f}{\rho} V_f \quad (2.6)$$

2.6.2.2 LAW OF MIXTURES MODEL FOR UNIDIRECTIONAL REINFORCED COMPOSITES

The preceding values for the volume fractions of the components can be used to make estimations on the longitudinal and transverse Young's modulus, Poisson's ratio and shear modulus of the corresponding composite. The procedures to make these calculations are given below. Note, that this method is a simple

method of estimation and provides somewhat inaccurate values for the mechanical properties of composites. However, due to its simplicity and ease of application it is still very often used in composite engineering and manufacturing.

Modulus of elasticity

First the longitudinal stiffness of unidirectional reinforced composite will be derived, on the assumption of the ‘law of mixtures’. An example for a unidirectional reinforced composite is a pultruded section. The expression for the longitudinal modulus of elasticity E_L is as follows: [B01, p9]

$$E_L = \frac{\sigma_L}{\varepsilon_L} = \frac{V_f \sigma_f + V_m \sigma_m}{\varepsilon_L} = \frac{V_f \sigma_f}{\varepsilon_f} + \frac{V_m \sigma_m}{\varepsilon_m} = V_m E_m + V_f E_f \quad (2.7)$$

To give an idea of the parts that reinforcement fibers and matrix play in the overall longitudinal stiffness of the composite: The modulus of elasticity of glass fibers is generally about 20x times higher than that of an arbitrary thermoset resin matrix. For carbon fibers and aramid fibers behave even stiffer. [B01, p9]

Using the same model of the simple ‘law of mixtures’ the transversal modulus of elasticity E_T can be calculated using the following derivation: [B01, p10]

$$\frac{1}{E_T} = \frac{\varepsilon_T}{\sigma_T} = \frac{V_f \varepsilon_f + V_m \varepsilon_m}{\sigma_T} = \frac{V_f \varepsilon_f}{\sigma_f} + \frac{V_m \varepsilon_m}{\sigma_m} = \frac{V_m}{E_m} + \frac{V_f}{E_f} \quad (2.8)$$

or alternatively

$$E_T = \left(\frac{V_m}{E_m} + \frac{V_f}{E_f} \right)^{-1}$$

Both expressions voor E_L and E_T are simple ‘law of mixtures’ expressions that have been derived assuming a uniform stress and strain distribution throughout the composite. In reality the stress and strain will differ greatly between fiber reinforcement and matrix, due to the discrepancy in modulus of elasticity. Therefore equations 2.7 and 2.8 can only be used to approximate the upper and lower bounds of the composite modulus. [B07, p168]

Unidirectional fiber composites, such as the mentioned pultruded sections usually correspond closely to equation 2.7, although it may be necessary to apply a correction factor for fiber undulation (deviation of the fiber straightness) and finite fiber length. Although equation 2.8 is often used to calculate the transverse modulus it significantly underestimates this quantity. Its accuracy van be greatly improved by making allowance for the constraining effects of the fibers by replacing E_m with its equivalent ‘plane strain’ value $E_m(1 - \nu_m^2)$ thereby altering equation 2.8 as follows: [B07, p168]

$$E_T = \left(\frac{V_m}{E_m(1 - \nu_m^2)} + \frac{V_f}{E_f} \right)^{-1} \quad (2.8a)$$

ν_m = Poisson’s ratio of the matrix material

Poisson’s ratio

Using the simple ‘law of mixtures’ the principal, or longitudinal Poisson’s ratio ν_{LT} of an unidirectional reinforced composite can be calculated by the following formula: [B01, p12][B07, p168]

$$\nu_{LT} = \nu_f V_f + \nu_m V_m \quad (2.9)$$

The non-principal or transverse Poisson's ratio ν_T can be calculated using the ratio of the transverse and longitudinal modulus of elasticity: [B07, p168]

$$\nu_T = \frac{E_T \nu_L}{E_L} \quad (2.10)$$

Shear modulus

Knowing the Poisson's ratio and elastic modulus of a unidirectional reinforced composite the shear moduli G_L and G_T can be calculated using the following expressions: [B01, p5]

$$G_L = \frac{E_L}{2(1 + \nu_L)} \quad (2.11)$$

$$G_T = \frac{E_T}{2(1 + \nu_T)} \quad (2.12)$$

2.6.2.3 HASHIN-SHTRIKMAN MODEL FOR UNIDIRECTIONAL REINFORCED COMPOSITES

This model is the first advanced model to be described, it only uses the variation principle and it describes the mechanical properties by comparing two solids of the same volume and with the same boundary conditions. One of the solids is homogeneous and anisotropic, the other heterogeneous and isotropic. The formulae below describe the upper and lower boundaries for the following mechanical properties of unidirectional reinforced statistically homogeneous composites: the compression modulus k^* , the longitudinal stiffness E_L^* , the longitudinal-transverse Poisson's ratio ν_{LT}^* , the two shear moduli G_{LT}^* and G_{TT}^* and the transverse stiffness E_T^* . According to the inventors of it, the Hashin-Shtrikman model is the most accurate model, when only using the volume fractions as input. [B01, p85-87]

if $k_f > k_m$ and $G_f > G_m$:

$$k_m + \frac{V_f}{\frac{1}{k_f - k_m} + \frac{V_m}{k_m + G_m}} \leq k^* \leq k_f + \frac{V_f}{\frac{1}{k_f - k_m} + \frac{V_m}{k_m + G_m}} \quad (2.13)$$

$$\frac{4V_f V_m (\nu_f - \nu_m)^2}{\frac{V_m}{k_f} + \frac{V_f}{k_m} + \frac{1}{G_m}} \leq E_L^* \leq \frac{4V_f V_m (\nu_f - \nu_m)^2}{\frac{V_m}{k_f} + \frac{V_f}{k_m} + \frac{1}{G_f}} \quad (2.14)$$

$$\frac{V_f V_m (\nu_f - \nu_m) \left(\frac{1}{k_f} - \frac{1}{k_m} \right)}{\frac{V_m}{k_f} + \frac{V_f}{k_m} + \frac{1}{G_f}} \leq \nu_{LT}^* \leq \frac{V_f V_m (\nu_f - \nu_m) \left(\frac{1}{k_f} - \frac{1}{k_m} \right)}{\frac{V_m}{k_f} + \frac{V_f}{k_m} + \frac{1}{G_m}} \quad (2.15)$$

only if $\frac{\nu_f - \nu_m}{k_f - k_m} < 0$, else opposite

$$G_m + \frac{V_f}{\frac{1}{G_f - G_m} + \frac{V_m}{2G_m}} \leq G_{LT}^* \leq G_f + \frac{V_m}{\frac{1}{G_m - G_f} + \frac{V_f}{2G_f}} \quad (2.16)$$

$$G_m + \frac{V_f}{\frac{1}{G_f - G_m} + \frac{V_m(k_m + 2G_m)}{2G_m(k_m + G_m)}} \leq G_{TT}^* \leq G_f + \frac{V_m}{\frac{1}{G_m - G_f} + \frac{V_f(k_f + 2G_f)}{2G_f(k_f + G_f)}} \quad (2.17)$$

$$\left[\frac{1}{4G_{TT}^{(-)}} + \frac{1}{4k^{(-)}} + \frac{(v_{LT}^{(+)})^2}{4E_L^{(-)}} \right]^{-1} \leq E_T^* \leq \left[\frac{1}{4G_{TT}^{(+)}} + \frac{1}{4k^{(+)}} + \frac{(v_{LT}^{(-)})^2}{4E_L^{(+)}} \right]^{-1} \quad (2.18)$$

2.6.2.4 HALPIN-TSAI MODEL FOR UNIDIRECTIONAL REINFORCED COMPOSITES

The Halpin-Tsai equations are the single most used relationships for the prediction of the mechanical properties of unidirectional reinforced composites. The reason for their wide acceptance lies presumably in the ease of application of the formulae. The formulae have been derived in the late 1960's, using earlier model attempts by Hill (1964) and Tsai (1964). The Halpin-Tsai model is of semi-empirical nature and mostly based on an extensive curve-fitting study. The curve-fitting was also done for test samples with other reinforcements than solely continuous circular cross-section fibers. Amongst the samples were short fibers and continuous fibers with an elliptical cross-section. [B01, p92] [B07, p169]

The first formula below is the most general Halpin-Tsai equation which can be used to predict the following mechanical properties: the moduli of elasticity, the shear moduli and the Poisson's ratio. In the formula the P denotes the property to be calculated. HS stands for the Halpin-Tsai function which has the following variables: P_f, P_m are the base mechanical properties of the fiber and the matrix, respectively. V_f and V_m are the fiber- and matrix volume fractions. η_P is a component which is dependent on the ratio of stress distribution between the components. [B01, p92-93]

$$P = HS(P_f, P_m, V_f, \xi_P) = P_m \frac{1 + \xi_P \eta_P V_f}{1 - \eta_P V_f} \quad (2.19)$$

$$\text{where } \eta_P = \frac{P_f + P_m}{P_f + \xi_P P_m}$$

$$\text{such that } P = P_m \frac{P_f + \xi_P (V_f P_f + V_m P_m)}{V_m P_f + V_f P_m + \xi_P P_m} \quad (2.20)$$

The formula above can be used for all stiffness parameters: The longitudinal stiffness E_L^* of the composite, the transverse stiffness E_T^* , the longitudinal-transverse Poisson's ratio v_{LT}^* and the two shear moduli G_{LT}^* and G_{TT}^* . The most often used form of the Halpin-Tsai equations, which assumes that the components behave isotropic, the fibers are continuous and have a circular cross-section. [B01, p93]

$$E_L^* = V_f E_f + V_m E_m \quad (2.21)$$

$$v_{LT}^* = v_f V_f + v_m V_m \quad (2.22)$$

$$E_T^* = E_m \frac{E_f + 2(V_f E_f + V_m E_m)}{V_m E_f + V_f E_m + 2E_m} \quad (2.23)$$

$$G_{LT}^* = G_m \frac{G_f + V_f G_f + V_m G_m}{V_m G_f + V_f G_m + G_m} \quad (2.24)$$

$$G_{TT}^* = G_m \frac{(3 - 4v_m)G_f + V_f G_f + V_m G_m}{(3 - 4v_m)(V_m G_f + V_f G_m) + G_m} \quad (2.25)$$

The factor ξ_p , which was used in the formulae above, is the contingency-factor, which is dependent on the mechanical property that is to be calculated, the fiber length and diameter and cross-section shape. Some of its values are denoted in the table below. [B01, p92-93]

Case	ξ_p
Perfectly aligned continuous fibers Young's modulus E_L , parallel to fibers	$\xi_L=\infty$
Imperfectly aligned (or wavy) continuous fibers Young's modulus E_L , parallel to fibers	$\xi_L < \infty$ (often in the range of 100-1000 adjusted to allow for lack of perfect fiber alignment)
Aligned discontinuous fibers Length L and diameter D Young's modulus E_L , parallel to fibers	$\xi_L=2L/D$
Aligned continuous or discontinuous fibers Young's modulus E_T , perpendicular to fibers	$\xi_T=2$
Aligned continuous or discontinuous fibers Shear modulus G_{LT} , shear parallel to fibers or Shear modulus G_{TT} , shear perpendicular to fibers	$\xi_T=1$
All fiber types, Principal Poisson's ratio, v_{LT}	$\xi_T=1/(3-4 v_M)$ for isotropic matrices

Table 23: Values for the contingency factor ξ_p [B07, p170] [B01, p92]

2.6.2.5 TSAI-HAHN IMPROVEMENTS OF THE HALPIN-TSAI MODEL

After the Halpin-Tsai formulae had been introduced, Tsai and Hahn tried to further improve these formulae. They concentrated on the case of circular cross-section reinforcements and thereby derived some adapted mass- and volume-fractions formulae. The Tsai-Hahn models are furthermore based on the assumption of an isotropic matrix and transverse isotropic fibers, which is the case for glass, carbon and aramid fibers. [B01, p93]

Below the general formula for arbitrary properties can be found [formula 2.26] as well as the corresponding worked out formulae for the longitudinal stiffness E_L^* of the composite, the transverse stiffness E_T^* , the longitudinal-transverse Poisson's ratio v_{LT}^* and the inverses of the two shear moduli G_{LT}^* and G_{TT}^* . Next to that an expression for the effective transversal compression modulus k^* is given. Note that if the shear modulus of the matrix is negligibly small compared to the longitudinal transverse shear modulus of the fiber ($G_m \ll G_{LT,f}$), which is often the case, the expressions simplify even more. [B07, p93-94]

$$P = \frac{V_f}{V_f + \eta V_m} P_f + \frac{\eta V_m}{V_f + \eta V_m} P_m \quad (2.26)$$

$$E_L^* = \frac{V_f}{V_f + \eta V_m} E_{L,f} + \frac{\eta V_m}{V_f + \eta V_m} E_m \quad (2.27)$$

$$\eta = 1$$

$$v_{LT}^* = \frac{V_f}{V_f + \eta V_m} v_{LT,f} + \frac{\eta V_m}{V_f + \eta V_m} v_m \quad (2.28)$$

$$\eta = 1$$

$$\frac{1}{G_{LT}^*} = \frac{V_f}{V_f + \eta V_m} \frac{1}{G_{LT;f}} + \frac{\eta V_m}{V_f + \eta V_m} \frac{1}{G_m} \quad (2.29)$$

$$\eta_{LT} = \frac{1}{2} \left(1 + \frac{G_m}{G_{LT;f}} \right) \text{ or if } G_m \ll G_{LT;f}: \eta_{LT} \cong \frac{1}{2}$$

$$\frac{1}{k^*} = \frac{V_f}{V_f + \eta V_m} \frac{1}{k_f} + \frac{\eta V_m}{V_f + \eta V_m} \frac{1}{k_m} \quad (2.30)$$

$$\eta_k = \frac{1}{2(1 - \nu_m)} \left(1 + \frac{G_m}{k_f} \right) \text{ or if } G_m \ll G_{LT;f}: \eta_k \cong \frac{1}{2(1 - \nu_m)}$$

$$\frac{1}{G_{TT}^*} = \frac{V_f}{V_f + \eta V_m} \frac{1}{G_{TT;f}} + \frac{\eta V_m}{V_f + \eta V_m} \frac{1}{G_m} \quad (2.31)$$

$$\eta_{TT} = \frac{1}{4(1 - \nu_m)} \left(3 - 4\nu_m + \frac{G_m}{G_{TT;f}} \right) \text{ or if } G_m \ll G_{LT;f}: \eta_{TT} \cong \frac{3 - 4\nu_m}{4(1 - \nu_m)}$$

$$\frac{1}{E_T^*} = \frac{1}{4G_{TT}^*} + \frac{1}{4k^*} + \frac{(\nu_{LT}^*)^2}{E_L^*} \quad (2.32)$$

2.6.2.6 EMPIRICAL PUCK MODEL FOR UNIDIRECTIONAL REINFORCED COMPOSITES

In 1969 Puck used a vast array of test results to obtain a new set of empirical formulae for the transverse Young's modulus E_T^* and the shear modulus G_{LT}^* of glass fiber reinforced composites via curve-fitting. For the longitudinal Young's modulus E_L^* and the longitudinal transverse Poisson's ratio ν_{LT}^* he used the normal law-of mixtures approach, described before. Afterwards several other researchers used the Puck formulation to derive similar expressions for carbon fiber reinforced composites. [B01, p96]

The general expression of Puck is as described below. In this formula P is the property to be calculated, limited to E_T^* or G_{LT}^* in the case of these formulae. Furthermore P_m and P_f are the corresponding properties of the components given by $\frac{E_m}{1-\nu_m^2}$ and E_f for E_T^* ; and G_m and G_f for G_{LT}^* . [B01, p96]

$$P = P_m \frac{1 + \alpha V_f^\beta}{\gamma V_f \frac{P_m}{P_f} + V_m^\delta} \quad (2.33)$$

$$E_T^* = \left(\frac{E_m}{1 - \nu_m^2} \right) \frac{1 + \alpha V_f^\beta}{\gamma V_f \left(\frac{E_m}{1 - \nu_m^2} \right) / E_f + V_m^\delta} \quad (2.34)$$

$$G_{LT}^* = G_m \frac{1 + \alpha V_f^\beta}{\gamma V_f \frac{G_m}{G_f} + V_m^\delta} \quad (2.35)$$

with $\alpha, \beta, \gamma, \delta = \text{empirical parameters}$

The empirical parameters $\alpha, \beta, \gamma, \delta$ are given for three different groups of researchers: Puck (1969) and Förster & Knappe (1971) concentrated on glass fiber reinforced polymer composites. Schneider, Menges & Peulen (1981) investigated carbon fiber reinforced polymer composites.

Test data	Parameter	E_T	G_{LT}
Puck (1969) GFRP	α	0,85	0,6
	β	2	0,5
	γ	1	1
	δ	1,25	1,25
Förster & Knappe (1971) GFRP	α	0	0,4
	β	-	0,5
	γ	1	1
	δ	1,45	1,45
Schneider (et al.) (1981) CFRP	α	1	0,25
	β	3	0,5
	γ	6	1,25
	δ	0,75	1,25

Table 24: Empirical values for the Puck model parameters $\alpha, \beta, \gamma, \delta$ [B01, p96]

2.6.3 COMPARISON OF THE DIFFERENT ESTIMATION MODELS

In literature [B01], the models that were described above have been compared for an epoxy glass fiber composite with given stiffness values and Poisson ratios for the fiber and for different fiber volume fractions. [B01, p98-99]

Longitudinal modulus of elasticity

The first observation that was made after calculation with all formulae, was that for the longitudinal modulus, E_L , the results for all formulae were very similar. That led to the generally accepted hypothesis that for E_L the general law of mixtures approach (equation 2.7) has sufficient accuracy. Also the Hashin-Shtrikman boundaries (equation 2.14) turned out to lie very close to another, as well as very close to, if not the same as, the law of mixtures. However it is advised to introduce a reductive misalignment factor to the longitudinal modulus values, because practice often yields slightly lower stiffness values than the calculated stiffness. [B01, p98]

Transverse modulus of elasticity

The Hashin-Shtrikman boundaries (equation 2.18) vary much more for the transverse modulus of elasticity E_T . Compared to the other models, such as the Halpin –Tsai approach (equation 2.23) and the Puck approach (equation 2.34) the upper Hashin-Shtrikman boundary yields too high values for E_T . The Puck and Halpin-Tsai approach as well as the Hashin-Shtrikman lower boundary lie within a 10-15% deviation of another. Of the three models, the last gives the safest, yet sufficiently exact estimation of the transverse stiffness; this is also the same value that the Tsai-Hahn model predicts (equation 2.32). The normal law of mixtures approach for the transverse modulus (equations 2.8 and 2.8a) yields values that are too conservative. [B01, p98, p100]

Longitudinal shear modulus

The longitudinal shear modulus G_{LT} is estimated best by the lower Hashin-Shtrikman boundary (equation 2.16) as well as the Halpin-Tsai equation (equation 2.24) and the Tsai-Hahn approach (equation 2.29). All three approaches give the same values for G_{LT} . The Hashin-Shtrikman upper boundary gives too high stiffness estimations, the Puck estimation (equation 2.35) gives values close to the other models, yet yields values, that are still too high. The law of mixtures approach (equation 2.11) again gives an estimate that is too conservative. [B01, p100]

Transverse shear modulus

As it was the case with the longitudinal shear modulus, the transverse shear modulus G_{TT} is best approached by the lower Hashin-Shtrikman boundary (equation 2.17). The Halpin-Tsai equation (equation 2.25) and the Tsai-Hahn approach (equation 2.31) give the same values for G_{TT} . The upper Hasin-Shtrikman boundary (equation 2.17) estimates a transverse shear stiffness, which is too high. The law of mixtures (equation 2.12) yields far too conservative values for G_{TT} . [B01, p100]

Longitudinal-transverse Poisson ratio

The last material property that was investigated was the longitudinal-transverse Poisson ratio ν_{LT} . It turned out that the normal law of mixtures (equation 2.9) yielded similar results as the Hashin-Shtrikman approach (equation 2.15) although the values that the law of mixtures approach yielded were marginally larger. Therefore the law of mixtures approach is often used for calculation of ν_{LT} . [B01, p100]

Conclusion

The above considerations on the different mechanical properties of FRP composites showed that of all the described models the Hashin-Shrikman lower boundary is most accurate and safe in all cases. In some of the properties other models yield the same values as the Hashin-Shrrikman, but yet are more inaccurate in other properties. The law of mixtures approach is very often used in many studies, but only yields accurate results for the longitudinal modulus of elasticity and the longitudinal-transverse Poisson ratio, where the Hashin-Shrikman approach yields similar or the same results.

Furthermore it is reported that in the case of other fiber reinforced composites than the described epoxy glass fiber composite, the results of the models are similar, thus the above models can be readily used for all fiber reinforced composites. [B01, p100]

2.6.4 MODELS FOR THE ESTIMATION OF THE MECHANICAL PROPERTIES OF DISPERSIONS

Because composites are often not only reinforced with fibers but also altered by additives and fillers, it is important to know what the influence of dispersed particles in a polymer matrix is. In this chapter several models to predict the bulk modulus K^* , the shear modulus G^* , the Poisson's ratio ν^* and the Young's modulus E^* are presented. For the Young's modulus two expressions by Paul (1960) and Barentsen (1972) exist, which both give boundaries for the modulus. [B01, p96-97]

2.6.4.1 KERNER (1956)

$$P = P_m \frac{1 + \zeta \xi V_d}{1 + \xi V_d} \quad (2.36)$$

$$\text{with } \zeta = \frac{P_d - P_m}{P_d + \zeta P_m}$$

$$K^* = K_d \frac{1 + \zeta \xi V_d}{1 + \xi V_d} \quad (2.37)$$

with $\xi = \frac{K_d - K_m}{K_d + \left(\frac{4G_m}{3K_m} = \frac{2(1 - 2\nu_m)}{1 + \nu_m} \right) K_m}$

$$G^* = G_d \frac{1 + \zeta \xi V_d}{1 + \xi V_d} \quad (2.38)$$

with $\xi = \frac{G_d - G_m}{G_d + \left(\frac{7 - 5\nu_m}{8 - 10\nu_m} \right) K_m}$

2.6.4.2 PAUL (1960)

$$E^* \geq \left(\frac{V_d}{E_d} + \frac{V_m}{E_m} \right)^{-1} \quad (2.39)$$

$$E^* \leq \frac{1 - \nu_d - 4\nu_d \nu + 2\nu^2}{1 - \nu_d - 2\nu_d^2} \nu_d E_d + \frac{1 - \nu_m - 4\nu_m \nu + 2\nu^2}{1 - \nu_m - 2\nu_m^2} \nu_m E_m \quad (2.40)$$

$$\text{with } \nu = \nu^* = \frac{(1 - \nu_m - 2\nu_m^2) \nu_d V_d E_d + (1 - \nu_d - 2\nu_d^2) \nu_m V_m E_m}{(1 - \nu_m - 2\nu_m^2) V_d E_d + (1 - \nu_d - 2\nu_d^2) V_m E_m} \quad (2.41)$$

2.6.4.3 BARENTSEN (1972)

$$E^* = \frac{E_I^* + E_{II}^*}{2} \quad (2.42)$$

$$E_I^* = E_m + \frac{\lambda^2 E_d (1 - \lambda^2) E_m}{\lambda^2 (1 - \lambda) E_d + (1 - \lambda^2 + \lambda^3) E_d}$$

$$\text{with } \lambda^3 = V_d \quad (2.43)$$

$$E_{II}^* = E_m \left(1 - \lambda^2 + \frac{\lambda^2 E_d}{(1 - \lambda) E_d + \lambda E_d} \right)$$

$$\text{with } \lambda^3 = V_d$$

2.6.5 FAILURE MODES OF UNIDIRECTIONAL FRP

In this chapter the most common failure types of unidirectional fiber reinforced polymer composites will be discussed. Although this chapter will describe the micromechanical processes during failure,

micromechanical theories on the calculation of fracture characteristics, such as the “shear-lag theory for a single short fiber” [B01, p151-155] and the “slip theory for a single short fiber” [B01, p155-158] will not be covered, they are beyond the scope of this report.

2.6.5.1 LONGITUDINAL TENSION

In longitudinal tension the matrix and the fiber undergo an equal extensional strain. Because the Poisson ratio of the polymer matrix is usually bigger than that of the fiber, the matrix will constrict around the fibers, inducing a transverse pressure on them. Because in practice the matrix always has a larger failure strain than the fibers, the fiber will fail before the matrix. [B01, p161]

After the first fiber has failed, and the loading is sustained at the same level, the two fiber parts, which are now stress-neutral at the ends, have to be ‘charged’ to an equal strain level as present in the surrounding matrix material. This process takes place by an added shear stress in the bonding layer between the fiber and the matrix. The fibers adjacent to the broken fiber have to take up this shear stress through the matrix and the bonding layers. This results in a reduced tension strength in a small zone around the failed fiber, leading to an increased strain in this zone, thus inducing an added load in the material around the failure zone. [B01, p161]

When the tension load is sustained after the first fiber failure, the increased strain in the composite will cause other fibers to fail as well, not necessarily in close proximity to the failure zone. When a critical number of fibers have failed in a small area, the failures will accumulate, thus causing large failure cracks. The failure has a chain-reaction character. [B01, p161]

A reduced fiber volume will increase the added load on the adjacent fibers of a failure zone. The probability of a failure accumulation in close proximity to the initial failure zone will therefore significantly grow. The failure cracks occur brittle and will be large and straight, in transverse direction to the fibers. Higher fiber volume contents will cause more, much smaller cracks at various places in the composite, failure of the composite will arise, when the small cracks start forming one bigger connected array of cracks, causing a stepped crack pattern due to slipped-out fibers. If the fiber volume content is even higher the small transverse cracks can lie even further apart, during complete failure they will be connected through long, longitudinal cracks, the matrix will shear off the fibers along these cracks. [B01, p162]

2.6.5.2 LONGITUDINAL COMPRESSION

In longitudinal compression unidirectional reinforced composites will usually fail before the maximum compression strength of the fibers has been reached. The individual fiber can be considered as slender columns that will fail by buckling, although they are continuously supported by the adjacent matrix. When micro-buckling occurs in a particular fiber the matrix surrounding it will deform, inducing a transverse force on the adjacent fibers. This causes the adjacent fibers to buckle as well, in phase with the first buckled fiber, thus leading to shear stresses in the matrix and debonding and/or shear failure. [B01, p162]

However, in longitudinal compression it is also possible that debonding has occurred in an earlier stage, because, due to the higher Poisson ratio, the matrix undergoes more radial expansion, inducing an extra tensile force on the bond region between fiber and matrix. Shear failure is also possible in longitudinal compression, the composite will fail in a 45° angle to the stressed direction because the maximum shear strength of the fibers and/or matrices is reached. The last possible failure mechanism in longitudinal compression is failure of the fiber, because they are stressed beyond the compressive strength limit. Aramid fiber are for example known to defibrillate under compression. [B01, p162]

The failure behavior of unidirectional FRP composites is very hard to predict, even experimental testing can lead to confusing results, because the boundary conditions, experiment set-up and dimensions of the test specimen can very much influence the failure mode. [B01, p162]

2.6.5.3 TRANSVERSE TENSION AND COMPRESSION

The dominating property in transverse tension of unidirectional FRP composites is the fact that the fibers are much stiffer than the matrix. Under transverse load the strain in the matrix links between the fibers is therefore much higher than in the fibers themselves. The composite will now fail due to tension failure in the matrix and/or debonding. The crack direction is transverse to the stress direction. Higher fiber volume contents or stiffer fibers increase the strain level in the matrix links and thereby reduce the transverse tension strength. The presence of voids has a similar effect, causing stress concentrations near the voids, which are amplified by the high strains in the matrix. [B01, p163]

The increased strain level in the matrix levels has little influence on the strength of the composite in transverse compression. The dominant failure mode in this case is shear failure of the matrix in a 45° angle to the stressed direction, in which the shear stress is the biggest. Sometimes this mode is accompanied by debonding of the fiber matrix interface. [B01, p163]

2.6.5.4 SHEAR

In longitudinal-transverse shear the dominant failure mode is shear failure of the matrix, sometimes also shear failure of the interface layer of fiber and matrix. In that case, cracks parallel to the fibers are formed. Usually shear failure is initiated at weak spots in the bonding layer or at voids, that is also why the transverse tension strength is positively correlated to the longitudinal-transverse shear strength. [B01, p163-164]

2.6.6 LAMINATE THEORY

In many applications fiber reinforced polymers are applied in laminates, thus a sequence of stacked plate elements with a constant thickness, called lamellas, which are glued to each other in the 'laminating process'. The lamellas are considered to be adhered to each other such that they cannot shift. It is also assumed that the lamellas of a laminate behave like a plate, according to the "classic plate theory" [B01, p165-169]. In this chapter the basis of the classic plate theory will be described to introduce the "lamine theory", which is essential for the strength and stiffness calculation of fiber reinforced polymer composite laminates.

2.6.6.1 THE CLASSIC (ISOTROPIC) PLATE THEORY

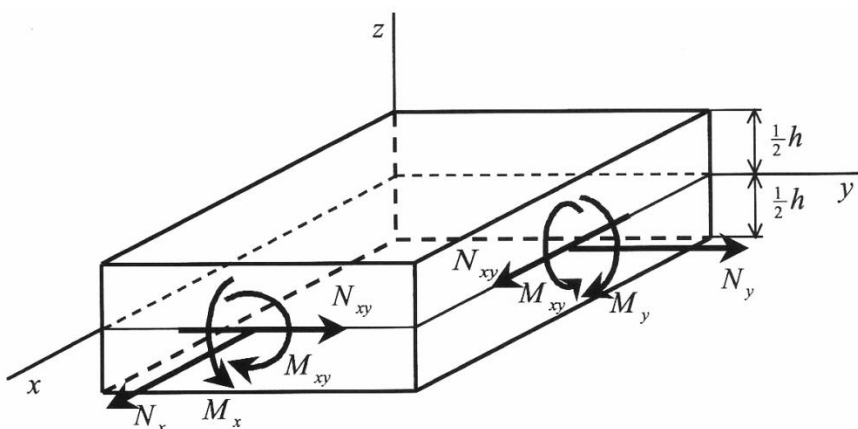


Fig. 55: Plate element with forces acting on it [B01, p168]

The most important prerequisites of the classic plate theory will be given in this chapter. The theory is valid for thin plates, in which there is assumed to be no normal force in the normal direction to the plate (in z-direction). The graphic above shows a plate element with all forces acting on it. [B01, p168]

The values for the normal forces N_x, N_y, N_{xy} in x, y en x-y direction can be calculated according to the following formulae [B01, p168]:

$$N_x = \int_{-\frac{1}{2}h}^{\frac{1}{2}h} \sigma_x dz; \quad N_y = \int_{-\frac{1}{2}h}^{\frac{1}{2}h} \sigma_y dz; \quad N_{xy} = \int_{-\frac{1}{2}h}^{\frac{1}{2}h} \tau_{xy} dz \quad (2.44)$$

The values for the moments M_x, M_y, M_{xy} in x, y en x-y direction can be calculated according to the following formulae [B01, p168]:

$$M_x = \int_{-\frac{1}{2}h}^{\frac{1}{2}h} \sigma_x z dz; \quad M_y = \int_{-\frac{1}{2}h}^{\frac{1}{2}h} \sigma_y z dz; \quad M_{xy} = \int_{-\frac{1}{2}h}^{\frac{1}{2}h} \tau_{xy} z dz \quad (2.45)$$

These formulae can be put in vector notation, which yields the following two formulae for the normal forces and the moments: [B01, p169]

$$\{\mathbf{N}\} = \begin{Bmatrix} N_x \\ N_y \\ N_{xy} \end{Bmatrix} = \int_{-\frac{1}{2}h}^{\frac{1}{2}h} \begin{Bmatrix} \sigma_x \\ \sigma_y \\ \tau_{xy} \end{Bmatrix} dz = \int_{-\frac{1}{2}h}^{\frac{1}{2}h} \{\sigma\} dz \quad (2.46)$$

$$\{\mathbf{M}\} = \begin{Bmatrix} M_x \\ M_y \\ M_{xy} \end{Bmatrix} = \int_{-\frac{1}{2}h}^{\frac{1}{2}h} \begin{Bmatrix} \sigma_x \\ \sigma_y \\ \tau_{xy} \end{Bmatrix} z dz = \int_{-\frac{1}{2}h}^{\frac{1}{2}h} \{\sigma\} z dz$$

Since the plate is assumed to be isotropic and subject to Hooke's Law in matrix notation the above formulae can be joined to correlate the planar stresses to the strains following [B01, p169]:

$$\begin{Bmatrix} \sigma_x \\ \sigma_y \\ \tau_{xy} \end{Bmatrix} = \begin{bmatrix} Q_{11} & Q_{12} & 0 \\ Q_{12} & Q_{11} & 0 \\ 0 & 0 & Q_{66} \end{bmatrix} \begin{Bmatrix} \varepsilon_x \\ \varepsilon_y \\ \gamma_{xy} \end{Bmatrix} \text{ or } \{\mathbf{N}\} = [\mathbf{Q}] [\boldsymbol{\varepsilon}] \quad (2.47)$$

$$\text{with } Q_{11} = \frac{E}{1 - \nu^2}; \quad Q_{12} = \nu Q_{11}; \quad Q_{66} = \frac{E}{2(1 + \nu)}$$

In this formula, $Q_{11}; Q_{12}; Q_{66}$ are called the "plate stiffness values", with which linear elastic formulae for the normal forces, moments and the plate deformation can be obtained. $\{\varepsilon^0\}$ is the deformation vector and $\{\kappa^0\}$ is the curvature vector. Note the factor $\frac{1}{12}h^3$ describing the difference between the moment and normal force. [B01, p169]:

$$\{\mathbf{N}\} = [\mathbf{Q}] \int_{-\frac{1}{2}h}^{\frac{1}{2}h} [\boldsymbol{\varepsilon}] dz = [\mathbf{Q}] \int_{-\frac{1}{2}h}^{\frac{1}{2}h} [\{\varepsilon^0\} + \{\kappa^0\}z] dz = h[\mathbf{Q}]\{\varepsilon^0\} \quad (2.48)$$

$$\{\mathbf{M}\} = [\mathbf{Q}] \int_{-\frac{1}{2}h}^{\frac{1}{2}h} [\boldsymbol{\varepsilon}] z dz = [\mathbf{Q}] \int_{-\frac{1}{2}h}^{\frac{1}{2}h} [\{\varepsilon^0\}z + \{\kappa^0\}z^2] dz = \frac{1}{12}h^3[\mathbf{Q}]\{\kappa^0\}$$

2.6.6.2 LAMINATE THEORY

After the plate theory has been described, it can be extended to cover laminates also. As described before, laminates are built up of lamellas which are assumed to carry planar stress only; because it is assumed that no shifting between the lamellas is possible, the laminate will deform as a whole.

Description of laminates with identical unidirectional lamellas

To properly describe the build-up of laminates with identical lamellas a code was introduced. The number denotes the orientation of the fibers, the first subscript denotes the number of lamellas with the same fiber direction, and the subscript "S" denotes the symmetry of the laminate. [B01, p171-172]:

$$[0|0|30|-30| - 30|30|90|90|30|-30| - 30|30|0|0] \quad (2.49)$$

$$\text{equal to } [0_2|30|-30_2|30|90_2|30| - 30_2|30|0_2]$$

$$\text{equal to } [0_2|30|-30_2|30|90_2]_s$$

Hooke's Law for single anisotropic lamellas

In the graphic below a typical laminate with 4 lamellas is shown. All lamellas are composed of identical unidirectional FRP, wherein the 2 inner layers are parallel to each other, and in a 90° angle to the outer 2 layers. The laminate is bent in the longitudinal direction (case I). [B01, p170]

The bending strain is positive at the top side, linearly becoming negative at the bottom side over the height of the laminate. Due to symmetry, it is equal to 0 at the mid-plane. Because the lamellas are assumed to be individually homogenous and anisotropic, the bending stress inside the lamellas will also behave linear. However, at the lamella interface they will be discontinuous, jumping in steps because of the difference in modulus of elasticity between the inner and outer layers. These jumps are the reason why the following derivations will be based on the deformations. [B01, p170]

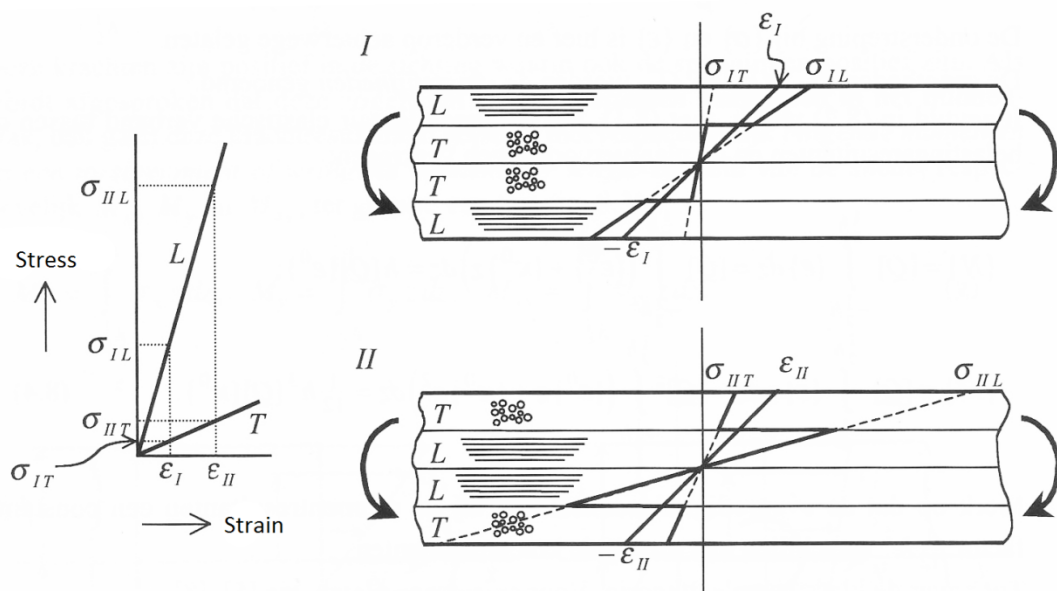


Fig. 56: Bending stress and strain diagram for a laminate of four identical unidirectional lamellas [B01, p170]

For every lamella k a set of axes is introduced: $(x'_1, x'_2, x_3)_k$ being parallel to the (x, y, z) set of axes of the laminate. The $(x'_1, x'_2)_k$ plane lies in the $(x_1, x_2)_k$ plane and the axis are rotated by an angle ϑ_k . This angle is called the orientation angle ϑ_k and is defined positively counter clock-wise. [B01, p171]

In its own set of axes Hooke's Law for each lamella k can be taken from the formula below. It is in matrix form and links the stresses to the strains through the stiffness matrix of the lamella. [B01, p171]

$$\begin{bmatrix} \sigma_1 \\ \sigma_2 \\ \sigma_6 \end{bmatrix}_k = \begin{bmatrix} Q_{11} & Q_{12} & Q_{16} \\ & Q_{22} & Q_{26} \\ & & Q_{66} \end{bmatrix}_k \begin{bmatrix} \varepsilon_1 \\ \varepsilon_2 \\ \varepsilon_6 \end{bmatrix}_k \text{ or } [\sigma]_k = [Q]_k [\varepsilon]_k \quad (2.50)$$

Hooke's Law in transformed form for lamella k

$$\begin{bmatrix} \sigma'_1 \\ \sigma'_2 \\ \sigma'_6 \end{bmatrix}_k = \begin{bmatrix} Q'_{11} & Q'_{12} & Q'_{16} \\ Q'_{22} & Q'_{26} \\ Q'_{66} \end{bmatrix}_k \begin{bmatrix} \varepsilon'_1 \\ \varepsilon'_2 \\ \varepsilon'_6 \end{bmatrix}_k \text{ or } [\sigma']_k = [Q']_k [\varepsilon']_k \quad (2.51)$$

Transformation formulae

To transform the stiffness values Q_x of the non-rotated set of axes to the rotated stiffness values Q'_x the following transformation formulae can be used using the orientation angle ϑ_k : [B01, p173]

$$Q'_{11} = Q_{11}\cos^4\vartheta + Q_{22}\sin^4\vartheta + 2(Q_{12} + 2Q_{66})\sin^2\vartheta\cos^2\vartheta - 4Q_{16}\sin\vartheta\cos^3\vartheta - 4Q_{26}\sin^3\vartheta\cos\vartheta \quad (2.52)$$

$$Q'_{22} = Q_{11}\sin^4\vartheta + Q_{22}\cos^4\vartheta + 2(Q_{12} + 2Q_{66})\sin^2\vartheta\cos^2\vartheta + 4Q_{16}\sin^3\vartheta\cos\vartheta + 4Q_{26}\sin\vartheta\cos^3\vartheta$$

$$Q'_{12} = (Q_{11} + Q_{22} - 4Q_{66})\sin^2\vartheta\cos^2\vartheta + Q_{12}(\sin^4\vartheta + \cos^4\vartheta) - 2(Q_{16} - Q_{26})\sin\vartheta\cos\vartheta(\sin^2\vartheta - \cos^2\vartheta)$$

$$Q'_{66} = (Q_{11} + Q_{22} - 2Q_{12} - 2Q_{66})\sin^2\vartheta\cos^2\vartheta + Q_{66}(\sin^4\vartheta + \cos^4\vartheta) - 2(Q_{16} - Q_{26})\sin\vartheta\cos\vartheta(\sin^2\vartheta - \cos^2\vartheta)$$

$$Q'_{16} = (Q_{11} - Q_{12} - 2Q_{66})\sin\vartheta\cos^3\vartheta - (Q_{22} - Q_{12} - 2Q_{66})\sin^3\vartheta\cos\vartheta + Q_{16}\cos^2\vartheta(3\sin^2\vartheta - \cos^2\vartheta) + Q_{26}\sin^2\vartheta(\sin^2\vartheta - 3\cos^2\vartheta)$$

$$Q'_{26} = (Q_{11} - Q_{12} - 2Q_{66})\sin^3\vartheta\cos\vartheta - (Q_{22} - Q_{12} - 2Q_{66})\sin\vartheta\cos^3\vartheta + Q_{16}\sin^2\vartheta(\sin^2\vartheta - 3\cos^2\vartheta) + Q_{26}\cos^2\vartheta(3\sin^2\vartheta - \cos^2\vartheta)$$

Transformation formulae for orthotropic lamellas

If the lamella are orthotropic, the axes are normally chosen along the main material directions of the particular lamella, then the following condition holds: [B01, p173]

$$(Q_{16})_k = (Q_{26})_k = 0 \quad (2.53)$$

Then [formula 2.50] becomes:

$$\begin{bmatrix} \sigma_1 \\ \sigma_2 \\ \sigma_6 \end{bmatrix}_k = \begin{bmatrix} Q_{11} & Q_{12} & 0 \\ Q_{22} & Q_{26} & 0 \\ & & Q_{66} \end{bmatrix}_k \begin{bmatrix} \varepsilon_1 \\ \varepsilon_2 \\ \varepsilon_6 \end{bmatrix}_k \text{ or } [\sigma]_k = [Q]_k [\varepsilon]_k \quad (2.54)$$

And the transformation formulae for orthotropic lamellas become somewhat simpler and less work-intensive: [B01, p173]

$$\begin{aligned}
Q'_{11} &= Q_{11}\cos^4\vartheta + Q_{22}\sin^4\vartheta + 2(Q_{12} + 2Q_{66})\sin^2\vartheta\cos^2\vartheta \quad (2.55) \\
Q'_{22} &= Q_{11}\sin^4\vartheta + Q_{22}\cos^4\vartheta + 2(Q_{12} + 2Q_{66})\sin^2\vartheta\cos^2\vartheta \\
Q'_{12} &= (Q_{11} + Q_{22} - 4Q_{66})\sin^2\vartheta\cos^2\vartheta + Q_{12}(\sin^4\vartheta + \cos^4\vartheta) \\
Q'_{66} &= (Q_{11} + Q_{22} - 2Q_{12} - 2Q_{66})\sin^2\vartheta\cos^2\vartheta + Q_{66}(\sin^4\vartheta + \cos^4\vartheta) \\
Q'_{16} &= (Q_{11} - Q_{12} - 2Q_{66})\sin\vartheta\cos^3\vartheta - (Q_{22} - Q_{12} - 2Q_{66})\sin^3\vartheta\cos\vartheta \\
Q'_{26} &= (Q_{11} - Q_{12} - 2Q_{66})\sin^3\vartheta\cos\vartheta - (Q_{22} - Q_{12} - 2Q_{66})\sin\vartheta\cos^3\vartheta
\end{aligned}$$

Coupling forces and deformation

The z-coordinates of lamella k are z_{k-1} and z_k , for which $z_{k-1} < z_k$. For the laminate height h the boundaries of the laminate are $z_0 = \frac{1}{2}h$ and $z_n = \frac{1}{2}h$. The strain at a distance z of the mid plane of the laminate are, for lamella k defined by: [B01, p174]

$$\{\varepsilon'\}_k = \{\varepsilon^0\} + z\{\kappa^0\} \text{ with } z_{k-1} \leq z \leq z_k \quad (2.56)$$

The stress for the same lamella k is then defined by the following formula: [B01, p174]

$$\{\sigma'\}_k = [Q']_k \{\varepsilon^0\} + z[Q']_k \{\kappa^0\} \text{ with } z_{k-1} \leq z \leq z_k \quad (2.57)$$

If this formula is combined with [formula 2.46], keeping in mind that because of the stress-jumps at the lamella interfaces it is not possible to integrate over the whole height of the laminate in one go, but a summation of the separate lamella integrations has to be made, the following formulae for the laminate are derived: [B01, p174]

$$\begin{aligned}
\{N\} &= \begin{Bmatrix} N_x \\ N_y \\ N_{xy} \end{Bmatrix} = \sum_{k=1}^n \int_{z_{k-1}}^{z_k} \begin{Bmatrix} \sigma'_1 \\ \sigma'_2 \\ \sigma'_6 \end{Bmatrix}_k dz = \sum_{k=1}^n \int_{z_{k-1}}^{z_k} \{\sigma'\}_k dz \quad (2.58) \\
\{M\} &= \begin{Bmatrix} M_x \\ M_y \\ M_{xy} \end{Bmatrix} = \sum_{k=1}^n \int_{z_{k-1}}^{z_k} \begin{Bmatrix} \sigma'_1 \\ \sigma'_2 \\ \sigma'_6 \end{Bmatrix}_k zdz = \sum_{k=1}^n \int_{z_{k-1}}^{z_k} \{\sigma'\}_k zdz
\end{aligned}$$

The term $\{\sigma'\}_k$ can be substituted in these formulae, using [formula 2.57]:

$$\begin{aligned}
\{N\} &= \left[\sum_{k=1}^n [Q']_k (z_k - z_{k-1}) \right] \{\varepsilon^0\} + \left[\sum_{k=1}^n [Q']_k (z_k^2 - z_{k-1}^2) \right] \{\kappa^0\} \quad (2.59) \\
\{M\} &= \left[\frac{1}{2} \sum_{k=1}^n [Q']_k (z_k^2 - z_{k-1}^2) \right] \{\varepsilon^0\} + \left[\frac{1}{3} \sum_{k=1}^n [Q']_k (z_k^3 - z_{k-1}^3) \right] \{\kappa^0\}
\end{aligned}$$

Components of stiffness and coupling

Now, three components are introduced, the component of the in-plane modulus A_{ij} , the component of the coupling stiffness B_{ij} and the bending stiffness component D_{ij} . A_{ij} determines the in-plane stiffness of the laminate for tension, compression and shear. B_{ij} couples the in-plane loads $\{N\}$ with the out-of-plane

deformations $\{\kappa^0\}$ and the moments $\{M\}$ with the in-plane deformations $\{\varepsilon^0\}$. D_{ij} determines the bending- and torsional stiffness of the laminate. The three components are: [B01, p174]

$$A_{ij} = \sum_{k=1}^n (Q'_{ij})_k (z_k - z_{k-1}) \text{ with } i,j = 1,2,6 \quad (2.60)$$

$$B_{ij} = \frac{1}{2} \sum_{k=1}^n (Q'_{ij})_k (z_k^2 - z_{k-1}^2) \text{ with } i,j = 1,2,6$$

$$D_{ij} = \frac{1}{3} \sum_{k=1}^n (Q'_{ij})_k (z_k^3 - z_{k-1}^3) \text{ with } i,j = 1,2,6$$

Laminate stiffness matrix

These components can be written in matrix-form to link the in-plane and out-of-plane forces with the deformations: [B01, p175]

$$\begin{Bmatrix} \{N\} \\ \{M\} \end{Bmatrix} = \begin{bmatrix} [A] & [B] \\ [B] & [D] \end{bmatrix} \begin{Bmatrix} \{\varepsilon^0\} \\ \{\kappa^0\} \end{Bmatrix} \quad (2.61)$$

In an expanded view, a 6x6 matrix can be yielded. Since the parts $[A]$, $[B]$, $[D]$ of the laminate stiffness matrix are all symmetric, the 6x6 stiffness matrix of the laminate is also symmetric. [B01, p175]

$$\begin{Bmatrix} N_x \\ N_y \\ N_{xy} \\ M_x \\ M_y \\ M_{xy} \end{Bmatrix} = \begin{bmatrix} A_{11} & A_{12} & A_{16} & B_{11} & B_{12} & B_{16} \\ & A_{22} & A_{26} & & B_{22} & B_{26} \\ & & A_{66} & & & B_{66} \\ & & & D_{11} & D_{12} & D_{16} \\ & & & & D_{22} & D_{26} \\ & & & & & D_{66} \end{bmatrix} \begin{Bmatrix} \varepsilon_x^0 \\ \varepsilon_y^0 \\ \gamma_{xy}^0 \\ \kappa_x^0 \\ \kappa_y^0 \\ \kappa_{xy}^0 \end{Bmatrix} \quad (2.62)$$

In-plane-, coupling- and flexural compliance

Often it is necessary to calculate the deformations of a laminate due to given forces and moments. Therefore the matrix in [formula 2.62] needs to be inverted, thereby yielding a direct expression for the deformations out-of-plane $\{\kappa^0\}$ and the in-plane deformations $\{\varepsilon^0\}$: [B01, p176]

$$\begin{Bmatrix} \{\varepsilon^0\} \\ \{\kappa^0\} \end{Bmatrix} = \begin{bmatrix} [a] & [b] \\ [b]^T & [d] \end{bmatrix} \begin{Bmatrix} \{N\} \\ \{M\} \end{Bmatrix} \quad (2.63)$$

In this formula $[a]$ is the component of in-plane compliance, $[b]$ is the coupling compliance and $[d]$ is the flexural compliance given by: [B01,p178]

$$[a] = ([A] - [B][D]^{-1}[B])^{-1} \quad (2.64)$$

$$[b] = ([B] - [D][B]^{-1}[A])^{-1} = -[a][B][D]^{-1}$$

$$[d] = ([D] - [B][A]^{-1}[B])^{-1}$$

In the formula below it is shown how the stresses in the direction of the laminate set of axes can be calculated from the stresses in the k -th lamella and its local set of axes. The formula below is also valid for

the strains $\{\varepsilon_1, \varepsilon_2, \varepsilon_6\}$, in that case the values for the stresses has to be substituted by the strain values. [B01, p178, p185]

$$\begin{bmatrix} \sigma_1 \\ \sigma_2 \\ \sigma_6 \end{bmatrix}_k = \begin{bmatrix} \cos^2\vartheta & \sin^2\vartheta & 2\sin\vartheta\cos\vartheta \\ \sin^2\vartheta & \cos^2\vartheta & -2\sin\vartheta\cos\vartheta \\ -\sin\vartheta\cos\vartheta & \sin\vartheta\cos\vartheta & -\cos^2\vartheta - \sin^2\vartheta \end{bmatrix}_k \begin{bmatrix} \sigma'_1 \\ \sigma'_2 \\ \sigma'_6 \end{bmatrix}_k \quad (2.54)$$

2.6.6.3 STRENGTH ANALYSIS OF LAMINATES

For the strength-analysis the stresses and strains of every individual lamella have to be calculated for a given stress on the laminate. For every lamella these values have to be compared to the applicable ultimate strength- or stiffness criterion. Because the whole laminate theory is linear, it is sufficient to apply an unity-load and to check with what factor the unity-load has to be multiplied to reach the ultimate strength- or stiffness criterion per lamella. The smallest factor then determines the so-called 'first-ply-failure' load which is the load at which the first lamella of laminate fails. This load differs for every load type. [B01, p181]

Some laminates can withstand higher loads even after first-ply-failure. The application area of the composite laminate determines whether stressing beyond the first-ply-failure load is allowable or not. An added difficulty when additional stressing after first-ply-failure is allowed, is that to which degree the already failed lamellas can take up any load. A safe estimate is to re-calculate the capacity of the laminate with the strength of the failed lamella set to zero, finding the next lowest unity-load factor at which the strength of the corresponding lamella. [B01, p181]

2.6.6.4 INFLUENCE OF THE LAMINATE BUILD-UP

It is important to realize that the coupling matrix $[B]$ couples the in-plane loads with out-of-plane deformation and the out-of-plane loads with in-plane deformations. This element of the laminate stiffness matrix [formula 2.61] makes the behavior of composites very complex, as shown in the graphic below, were a laminate consisting of two unidirectional lamellas laminated in an 90° angle $[0|90]$ is subjected to a normal forces. Due to the stiffness difference between the transversely loaded lamella and the longitudinally loaded lamella a bending moment is induced in the laminate, deforming it out of plane. [B01, p190]

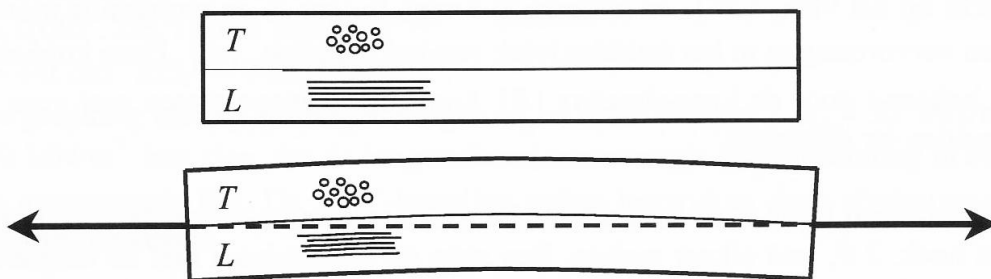


Fig. 57: Influence of the coupling behavior on asymmetric laminates [B01, p191]

It turns out that if the laminate is built up symmetrically, the coupling matrix becomes zero, and the behavior of the laminate is significantly less complex. If the coupling matrix $[B]$ becomes zero the following parts also become zero: [B01, p190]

$$[B] = 0 \rightarrow [a] = [A]^{-1}; [b] = 0; [d] = [D]^{-1} \quad (2.65)$$

If a laminate is built up totally symmetric no bending is induced in the case of normal stress. Next to that, in the case of thermal expansion or creep no torsion or bending is induced next to the planar stresses. This is a major advantage and it is therefore very advisable to design symmetric laminates only. [B01, p190]

To conclude this chapter two graphs are given on the influence of the fiber direction in the lamellas of a laminate on the strength and stiffness behavior of a laminate:

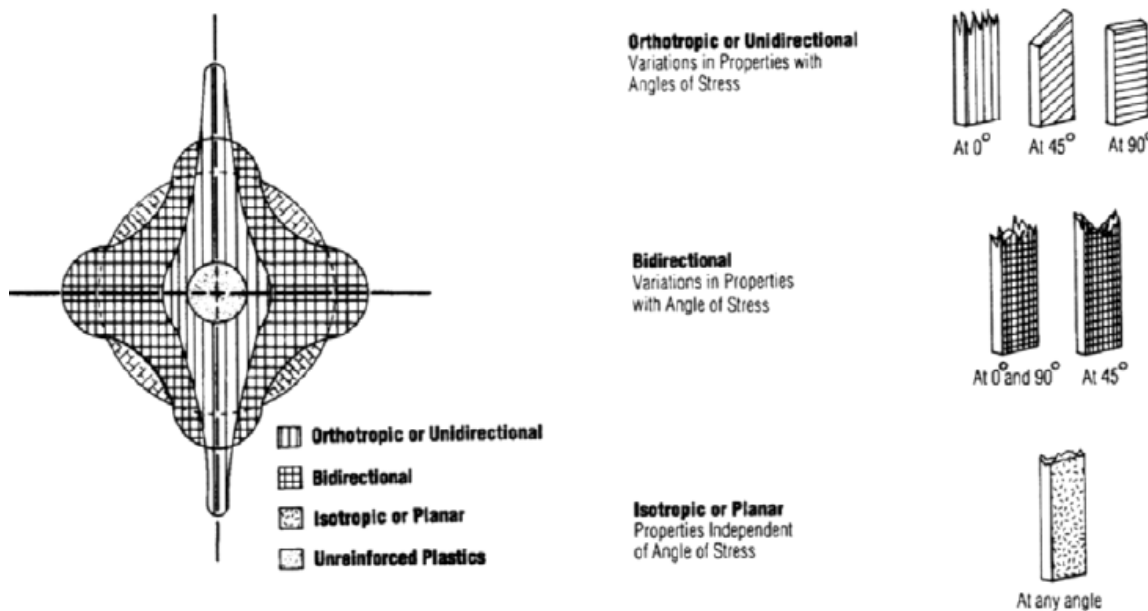


Fig. 58: Influence of the fiber direction on the strength and stiffness of laminates (1 of 2) [B16, p645]

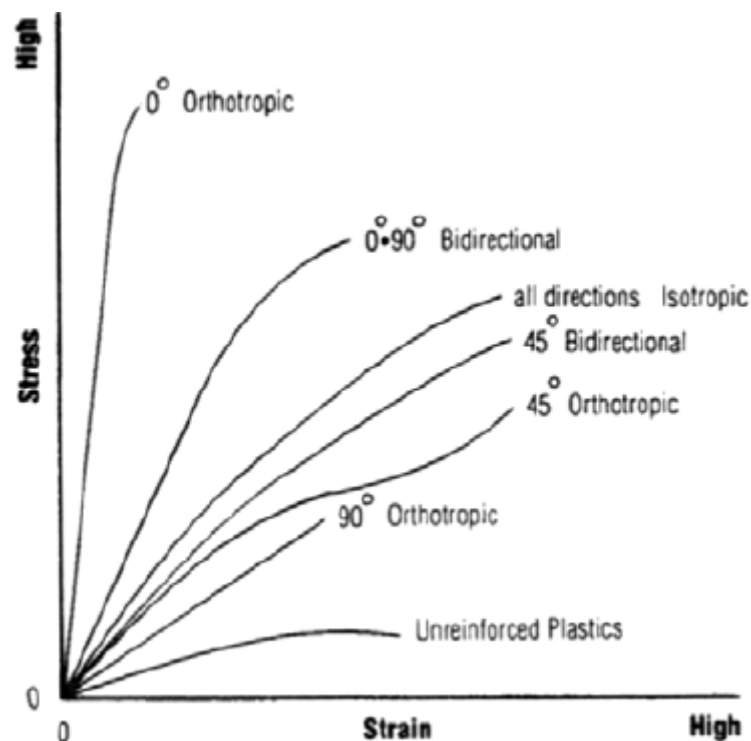


Fig. 59: Influence of the fiber direction on the strength and stiffness of laminates (2 of 2) [B16, p645]

2.6.7 STRUCTURAL DESIGN OF COMPOSITES

In this chapter the European Eurocomp Design Code [B14] as well as the Dutch CUR96 recommendation [CUR96] and the European Eurocode [NEN-EN1990] will be used to derive important rules on the structural design of fiber reinforced polymers structures. Note, that both the Eurocomp Design Code as well as the CUR96 recommendation were intended for GFRP composites only. In this chapter it is assumed that the same approaches can also be used for CFRP and AFRP materials.

First some information on the general safety philosophy of FRP composites will be given. Afterwards advice will follow on the limitation of the stress and strain, combined stresses and buckling of FRP line elements.

The general safety philosophy of the CUR96 recommendation on FRP structural design is very similar to the Eurocode safety standards. The following general formula holds for all design calculations on fiber reinforced polymers: [CUR96, p10]

$$S\gamma_f \leq R / (\gamma_m \gamma_c) \quad (2.66)$$

γ_f = load factor

γ_m = material factor

γ_c = conversion factor

In the above formula S denotes the effects of the imposed design loads, whereas R denotes the characteristic strength of the structure. The factors have to be calculated or taken from the appropriate parts of the CUR96 recommendation as described below.

2.6.7.1 MATERIAL FACTOR

The material factor has to be derived from the following formula: [CUR96, p11]

$$\gamma_m = \gamma_{m,1} \gamma_{m,2} \quad (2.67)$$

Wherein $\gamma_{m,1} = 1,35$, which is the partial material factor, taking into account the uncertainties in deriving the correct material properties. $\gamma_{m,2}$ is the partial material factor, which takes into account the uncertainties in the production method. $\gamma_{m,2}$ can be derived from the following table: [CUR96, table 1, p12]

Method of manufacture	Partial material factor	
	Fully post-cured laminate	Not fully post-cured laminate
Fiber spray-up	1,60	1,90
Hand lay-up	1,40	1,70
VA-RTM or RTM (vacuum injection)	1,20	1,40
Continuous filament winding	1,10	1,30
Prepeg lay-up	1,10	1,30
Pultrusion	1,10	1,30

Table 25: Values of the partial material factor for different FRP production techniques [CUR96, table 1, p12]

Note that for stability checks, such as described in [chapter 2.6.8.4], the product of γ_m and γ_f has to be at least $\gamma_m \gamma_f \geq 2,5$. [CUR96, p28]. For strength calculations the minimum value for the material factor is $\gamma_m \geq 1,5$. [CUR96, p12]

2.6.7.2 CONVERSION FACTOR

The conversion factor for FRP composites has to be calculated according to the following formula: [CUR96, p12]

$$\gamma_c = \gamma_{ct}\gamma_{cv}\gamma_{ck}\gamma_{cf} \quad (2.68)$$

Wherein γ_{ct} is the conversion factor for temperature effects, $\gamma_{ct} = 1,1$. γ_{cv} is the conversion factor for humidity effects being $\gamma_{cv} = 1,0$ for structures in continuously dry environments, $\gamma_{cv} = 1,1$ for structures in variable humidity conditions (applicable for normal traffic bridges) and $\gamma_{cv} = 1,3$ for continuously wet environments. The conversion factor for fatigue effects γ_{cf} is equal to $\gamma_{cf} = 1,1$. The conversion factor for creep, γ_{ck} , is covered in [chapter 2.6.8]. The table below shows which conversion factors need to be used for which specific verification. Note that applying all conversion factor always yields a safe, conservative result. [CUR96, table 2, p13]

Type of walking	Ultimate limit state			Serviceability limit state		
	Strength	Stability	Fatigue	Stiffness	Vibration	First crack
Conversion factor for temperature	x	x	x	x	x	x
Conversion factor for humidity	x	x	x	x	x	x
Conversion factor for creep	x	x	-	x	-	x
Conversion factor for fatigue	-	x	-	x	x	x

Table 26: Application of different conversion factors for different applications [CUR96, table 2, p13]

2.6.7.3 LOAD FACTOR

The load factor for FRP composites is the same as for structures made of other materials. It has to be calculated according to the following guideline, derived from Eurocode 0, Basis of structural Design [NEN-EN 1990:2002, table A1.2(B), p59]

For the ultimate limit state:

$$\text{permanent action } \gamma_{f,p} = 1,35 \quad (2.69)$$

$$(\text{leading}) \text{ variable action } \gamma_{f,v} = 1,50$$

For the serviceability limit state:

$$\text{permanent action } \gamma_{f,p} = 1,00 \quad (2.70)$$

$$(\text{leading}) \text{ variable action } \gamma_{f,v} = 1,00$$

Wherein γ_{ct} is the conversion factor for temperature effects

2.6.7.4 STRAIN CRITERION

The CUR96 recommendation gives an universal strain criterion, which limits the strain to 1,2% for every direction in the composite. This criterion was derived using the 'first ply failure criterion' which states that when the first ply of a laminate composite reaches the maximum strain of 1,2%, the whole laminate has reached its maximum strain level. The strain has to be calculated following: [CUR96, p31]

$$\frac{\varepsilon_{i,j,S}}{\varepsilon_{i,j,R}} \leq \frac{1}{\gamma_f \gamma_m \gamma_c} \quad (2.71)$$

In this formula $\varepsilon_{i,j,S}$ is the strain imposed by the load conditions in direction i and with load type j (tension, compression, shear). $\varepsilon_{i,j,R}$ is the maximum allowable strain which is set to 1,2% by the CUR96 recommendation. Calculation has to be done for each ply individually, except if the strain is constant for the laminate cross section.

2.6.7.5 STRESS CRITERION

Similar to the strain criterion, the CUR96 recommendation also gives a stress criterion which limits the maximum stress in the laminate according to the following formula: [CUR96, p32]

$$\frac{\sigma_{i,j,S}}{\sigma_{i,j,R}} \leq \frac{1}{\gamma_f \gamma_m \gamma_c} \quad (2.72)$$

In this formula $\sigma_{i,j,S}$ is the stress imposed by the load conditions in direction i and with load type j (tension, compression or shear). $\sigma_{i,j,R}$ is the maximum allowable stress .

2.6.7.6 COMBINED STRESSES CRITERION

Since stresses in one direction often have combined effects, the CUR96 recommendation also gives rules to combine tension-, compression- and shear stresses in multiple directions: [CUR96, p32]

$$\text{tension: } \left(\frac{\sigma_{1,t,S}}{\sigma_{1,t,R}} \right)^2 - \left(\frac{\sigma_{1,t,S} \sigma_{2,t,S}}{\sigma_{1,t,R}^2} \right)^2 + \left(\frac{\sigma_{2,t,S}}{\sigma_{2,t,R}} \right)^2 + \left(\frac{\tau_{12,S}}{\tau_{12,R}} \right)^2 \leq \left(\frac{1}{\gamma_f \gamma_m \gamma_c} \right)^2 \quad (2.73)$$

$$\text{compr.: } \left(\frac{\sigma_{1,c,S}}{\sigma_{1,c,R}} \right)^2 - \left(\frac{\sigma_{1,c,S} \sigma_{2,c,S}}{\sigma_{1,c,R}^2} \right)^2 + \left(\frac{\sigma_{2,c,S}}{\sigma_{2,c,R}} \right)^2 + \left(\frac{\tau_{12,S}}{\tau_{12,R}} \right)^2 \leq \left(\frac{1}{\gamma_f \gamma_m \gamma_c} \right)^2 \quad (2.74)$$

All stresses are given in the 1,2,12 direction. Combined stresses have to be checked for each ply individually. If stresses in other directions arise, they have to be transformed using the appropriate formulae, with ψ being the angle to the 1,2,12 directions. [CUR06, p32]:

$$\sigma_{1,j,S} = (\cos^2 \psi) \sigma'_{1,j,S} \quad (2.75)$$

$$\sigma_{2,j,S} = (\sin^2 \psi) \sigma'_{2,j,S}$$

$$\tau_{12,S} = (\sin \psi \cos \psi) \tau'_{12,S}$$

2.6.7.7 BUCKLING OF LINE ELEMENTS

Girders and columns under compression have to be checked for buckling stability. According to CUR96, the buckling load P_b of a girder or column (line element) can be calculated according to: [CUR96, p30]

$$P_b = k \pi^2 \frac{\sum E_i I_i}{L^2} \quad (2.76)$$

Wherein the factor k is a factor which takes into account the support conditions of the line element: $k = 1,0$ for two hinged supports, $k = 2,046$ for one hinged support and one clamped support, $k = 4,0$ for

two clamped supports and $k = 0,25$ for one clamped support and one free unsupported end. [CUR96, table 18, p30]

2.6.8 CREEP

Creep is the time dependent deformation of a material under a constant load. The creep modulus can be defined from the additional strain exhibited by a material after a given elapsed time. The creep modulus is the apparent stiffness as determined by the total deformation to the time defined. For design it is convenient to describe the process of creep in a material by an effective reduction in modulus with time. [B14, p101]

Since most fibers exhibit near-to-zero creep, in composites creep is largely dominated by the matrix behavior, that is influenced by a large number of matrix factors, among which are resin type, volume fraction of fibers, interfacial bonding, form of the reinforcement, orientation of the fibers,. Next to that the following environmental factors also influence the creep behavior: temperature, loading regime, aggressive chemicals, and moisture content. [B14, p101-102]

Composites reinforced with unidirectional stiff fibers and stressed in the fiber direction can be highly creep resistant as the fiber attracts a high proportion of the load in line with its stiffness relative to the polymer matrix. Bi-directional woven composite laminates do not perform as well as unidirectional materials, the presence of crimp (bends) in the fibers gives rise to local stress concentrations in the polymer, which may cause cracking. In critical applications non-woven continuous fiber reinforcements are preferred. [B14, p252-253]

Generally said, the greater the degree of cross-linking in the resin, the higher the volume fraction of reinforcement, the stronger the bond between fiber and matrix or the greater the margin between the working environment and the onset of the resin temperature susceptibility, the smaller the creep and the higher the creep modulus after a given time. Also, higher applied loads lead to higher stresses and thus to a higher creep rate. [B14, p102]

Resistance to creep is dependent on the alignment of fibers to match the external loading and minimize stresses in the matrix. When subjected to tensile stresses, carbon composites resist long term creep very well. In off axis situations creep rates will be higher and in compression the contribution by the matrix to local fiber stability is critical and lower allowable stresses are required. Although aramid fibers have high inherent tensile strength, particularly in unidirectional construction, in composites they tend to have creep rates very much higher than similar glass or carbon composites.[B14, p253-254]

The 'Eurocomp design code' [B14, p101-104] as well as the 'ICE Manual of Bridge Engineering' [B21, p499] advise to perform creep tests on every composite material to derive its long term mechanical behavior. Next to that both give no analytical methods to calculate creep behavior.

The Dutch recommendation on FRP structural design, CUR96, recommends taking the creep behavior into account by applying a special creep conversion factor γ_{CK} . This factor can only be used for creep behavior in the longitudinal direction of a ply. In the case of creep in other directions, the CUR96 procedure must be used, taking into account the different ply-directions. [CUR96, p13-14]

$$\gamma_{CK} = t^n \quad (2.77)$$

where t = load duration in hours

$$n = 0,01 \text{ for UD - ply}$$

$$n = 0,04 \text{ for woven - ply}$$

$$n = 0,1 \text{ for mat-ply}$$

2.6.9 STRESS CORROSION

Glass fiber composites are susceptible to a phenomenon known as stress corrosion where a laminate under stress in an acidic or basic environment can fail catastrophically at very low stresses if the environment can gain access to the fibers by diffusion or, more likely, a crack. Under normal circumstances the aggressive medium is isolated from the reinforcement fiber by the matrix resin. However, if for some reason there is a crack present in the laminate, then the medium can gain access to the fiber, which is attacked and loses its strength. The fiber has now lost its ability to act as a crack stopper. If the composite is under stress, then the fiber fails and the crack can proceed, thus allowing the process to repeat until the laminate fails. [B14, p258].

The stress corrosion phenomenon is time-, stress-level-, environment-, matrix- and fiber-related. Failure is deemed to be premature since the FRP fails at a stress level below its ultimate capacity. Carbon fibers are relatively unaffected by stress corrosion at stress levels up to 80% of ultimate limit state strength (or even 95% in tension [B21, p515]). Just as glass fibers, aramid fibers are also susceptible to stress corrosion. The quality of the resin has a significant effect on time to failure and the sustainable stress levels. In general, carbon fiber epoxy composite is least vulnerable to stress corrosion, followed by aramid vinyl ester composite. Of the three examples, glass fiber polyester is most vulnerable to stress corrosion. [T13, p25-26]

To prevent stress corrosion in GFRP composites it is advised to limit the permanent allowable stress to about 20% [B21, p515] to 30% [B25, p0.0.14] of the ultimate limit state strength of the glass fiber reinforced composite.

2.6.10 FATIGUE

Fatigue is the degradation of the mechanical properties of a material due to alternating stresses over time. An alternating stress significantly smaller than the ultimate static strength of the material can lead to cracks, crack propagation and eventually even fracture. This makes fatigue an important factor to take into account. [B01, p241-250] The graph below shows the fatigue life process, at a certain time the cyclic stress σ_c becomes larger than the residual strength σ_R , which then leads to failure.

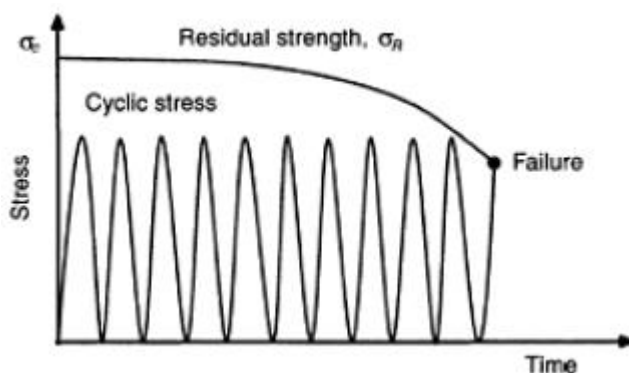


Fig. 60: Schematized fatigue process [B17, p4]

It is generally known, that compared to steel, fiber reinforced polymers exhibit a much better fatigue behavior. The reason for this lies in the different nature of the materials: In steel structures, usually welded or bolted connection details are decisive for the fatigue life. In such connections significant imperfections exist, which cause high local stress concentrations. The notch sensitivity of the metal, which is dependent on the steel quality and the median stress level, determines the rate of crack growth, and thus the residual fatigue life of the metal. [B01, p241][CUR2003-6, p76]

In fiber reinforced polymers the fatigue strength is dependent on the static strength of the composite and on the median stress level present. Notch sensitivity does not play a large role because of the inhomogeneous nature of the material. In contrast to metals, fiber reinforced polymer composites are already full of small micro-scale imperfections in the material before loading. Examples are delamination, broken filaments, matrix cracks, bonding failure between matrix and fiber and small voids. The propagation and growth of these small imperfections does occur during alternating loading, but happens in a much slower way than in metals. The reason for this is that the matrix has a dampening influence; the individual fibers act as crack-propagation-stopper and for example in laminates, cracks only propagate within single plies. [B01, p241]

Summarizing the above it can be stated that FRP composites have a linear-elastic stress-strain behavior up to failure and generally have lower residual stresses than steel structures. Therefore, fatigue is driven primarily by the peak stress in cycle, since it determines the maximum concentrated stress at a micro-imperfection. This in turn determines the incremental damage per cycle. The damage usually has the form of resin-cracking, although other failure modes do also occur. [B17, p756]

2.6.10.1 INFLUENCE OF MATRIX MATERIALS

The graphs below show results of some of the first fatigue tests performed on glass fiber reinforced composites by Boller in the 1950s and 1960s. The graph compares the fatigue life of phenolic resin, polyester resin, epoxy resin and silicone resin for increasing stress amplitudes. For low stress cycles (up to about 10^5 cycles) phenolic resins can withstand higher stress amplitudes. But for the more interesting, and in bridge engineering more common, higher cycles ($> 10^7$ cycles) epoxy resins show higher residual strength levels. [B17, p11-12]

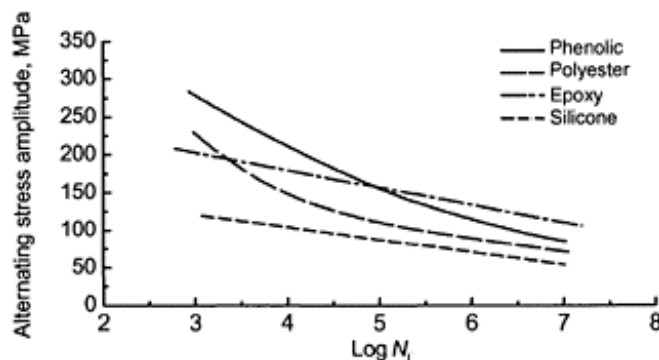


Fig. 61: Left: Fatigue life for increasing stress amplitude for different GFR composites. [B17, p11]

It was found that high fiber contents of 65%-70% give best fatigue performances. This strengthens the general belief that fatigue failure and material degradation is mostly caused by matrix damages such as debonding and cracking. The fatigue response of more rigid matrix material with a high resistance to matrix-cracking combined with glass fiber reinforcement will generally be better than that of weak, easily cracking matrix. Also, an easily cracking matrix, will also take up water more easily in a humid environment, causing more matrix degradation and worsening the fatigue life. Thus moisture resistant resins such as the thermoplastic PEEK are considered to have an outstanding fatigue resistance. Especially PEEK reinforced with carbon fiber (in itself insensitive to moisture) have excellent fatigue properties. Carbon fiber reinforced composites are less dependent on the resin properties. [B17, p23]

2.6.10.2 INFLUENCE OF REINFORCEMENT MATERIALS

In this chapter the influence of the reinforcement material will be covered. In the following glass fibers, carbon fibers and aramid (Kevlar) fibers will be shortly discussed. In general fibers such as glass and carbon fibers do not show the characteristic weakness of metals under fatigue loading. If the composite carries the load primarily by fiber tensile strength and large elastic or viscoelastic deformations are prevented by the composite, which is clearly the case in unidirectional reinforced high fiber content composites, then high modulus fibers, such as carbon exhibit very good fatigue resistance. If carbon fibers act as woven

reinforcement, their fatigue performance is slightly decreased, due to the waviness of the fibers in the load carrying direction. Still, of the three discussed reinforcements, CFRP generally has the best fatigue life. [B17, p22-23]

Below two graphs are shown, which compare three cross-plyed composites, which are identical, apart from the reinforcement type. They are all typical composites with a reinforcement content of 65%. CFRP stands for carbon fiber reinforced polymers, GRP for glass reinforced polymers, and KFRP for Kevlar (aramid) reinforced polymers. The left picture shows the behavior of the composites under random loading, causing compression loads. It can be seen that compression and shear stresses are more damaging to aramid composites than to glass and carbon composites. Normally, in the mode tested in the left graph, matrix cracking and delamination would dominate the composite fatigue behavior. This is demonstrated by the CFRP and FRP results in the graph. However the aramid fiber behave different, due to the intrafibrillar weakness. This weakness can be observed in the picture shown below [Fig. 56]. [B17, p28]

The right graph shows the same composites under repeated tensile loading. This time the vertical axis denotes the strain level. The intrafibrillar weakness of the KFRP fibers is visible after about 5×10^3 cycles, where the slope of the curve increases for the KFRP composite. After about 10^7 cycles, all curves seem to be leveling out at approximately the same strain level. Also, it is clearly visible that CFRP has a much higher modulus than KFRP and especially GRP, which behaves least stiff. [B17, p16]

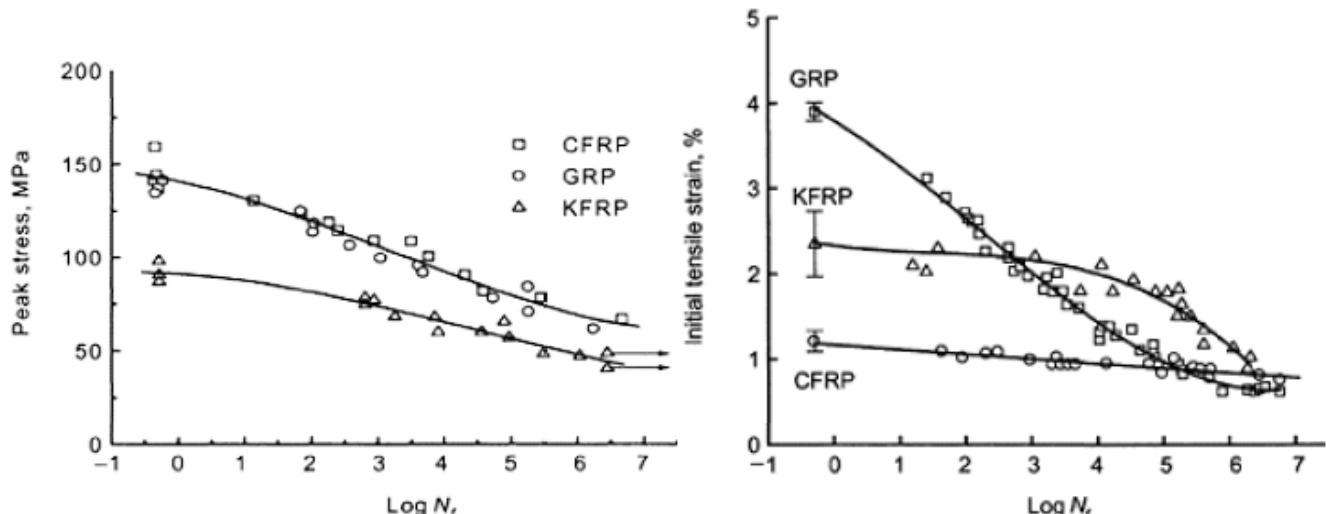


Fig. 62: Left: Stress-Log life curves for 65% carbon-, glass- and aramid-reinforced epoxy composites tested at 45° to the main fiber directions [B17, p27] Right: Strain-Log life curves for the same cross-plyed composites. [B17, p16]

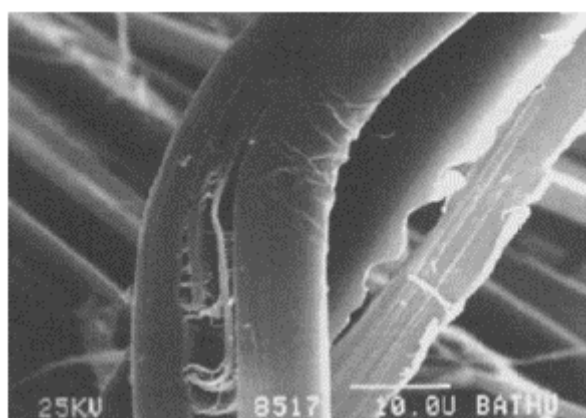


Fig. 63: Splitting and kinking damage in Kevlar-49 fibers after fatigue cycling [B17, p29]

2.6.10.3 FATIGUE DESIGN ACCORDING TO CUR96

In the Dutch preliminary fiber reinforced polymer design code CUR96 a straight-forward method is given to estimate the fatigue life of any given glass fiber reinforced polymer composite structure. Note that although this code is only valid for glass reinforcements, the general method could well be used for other reinforcement materials. In this chapter a general design method will be described.

First the factor R needs to be calculated, this factor describes the proportion of minimum stress σ_{min} (compression) and the maximum stress σ_{max} (tension). The factor thus describes the mean stress level in the composite. If the R factor is $R = -1$, than the minimum stress (compression) is exactly of the same magnitude as the maximum stress (tension). In literature this is called pure alternating current. [CUR2003-6, p77-78]

$$R = \frac{\sigma_{min}}{\sigma_{max}} \quad (2.78)$$

If $R = -1$ than the so called Wöhler or S-N (Stress - fatigue life) curve can be used to describe the fatigue behavior of GFRP composites. This curve relates the number of cycles to failure N_f with the amplitude of the stress cycles σ_{amp} . The parameters a_2 and b_2 are curve-fitting coefficients. [CUR2003-6, p78]

$$\log(N_f) = a_2 + b_2 \log(\sigma_{amp}) \quad \text{with } \sigma_{amp} = \sigma_{max} - |\sigma_{min}| \quad (2.79)$$

Because in many cases the S-N curve also touches the point ($N_f = 1; \sigma_{amp} = \sigma_{t;Rk}$), this equation can be rewritten to the following form, wherein γ_m and γ_c are material and conversion factors and σ_{Rk} is the characteristic design strength of the composite. k is the slope of the S-N curve and depends on the material used. For example for glass epoxy composite $k = -10$ and for glass polyester composite $k = -9$. Note that the expression below is direct method to calculate the fatigue life for any given stress amplitude and composite. [CUR2003-6, p77-79]

$$N_f = \left(\frac{\sigma_{amp} \gamma_m \gamma_c}{\sigma_{Rk}} \right)^k \quad (2.80)$$

To accommodate for the influence of the mean stress level during a stress cycles, a 'Goodman-diagram' is used. For any specific number of stress cycles it yields the relation between the stress amplitude σ_{amp} and the mean stress during the cycles σ_{mean} . Using the following formulae which include the material factor γ_m , the number of cycles to failure can be calculated, taking into account the mean stress, thus extending the above formulae for all R-values. [CUR2003-6, p79-81] With known k-values, stress values and material factors the expected fatigue life of any composite can be calculated with this formula.

$$\sigma_{mean} > 0: N_f = \left(\frac{\sigma_{amp}}{\frac{\sigma_{t;Rk}}{\gamma_m} \left[1 - \frac{\sigma_{mean}}{\sigma_{t;Rk}/\gamma_m} \right]} \right)^k \quad (2.81)$$

$$\sigma_{mean} < 0: N_f = \left(\frac{\sigma_{amp}}{\frac{\sigma_{t;Rk}}{\gamma_m} \left[1 - \frac{\sigma_{mean}}{\sigma_{c;Rk}/\gamma_m} \right]} \right)^k \quad (2.82)$$

2.6.11 JOINT DESIGN

In general three types of structural connections for FRP elements do exist. The first type of connection is the mechanical connection, using bolts, nuts and washers to connect two or more elements. Secondly, bonded connections are used. In bonded joints adhesives connect the FRP elements with each other. The last type of connection is the combined connection, using both adhesives as well as mechanical fasteners. The table below gives a general overview of the main advantages and disadvantages of the connection types. [B14, p128-129]

Mechanical joints	Advantages	Disadvantages
	Requires no special surface preparation	Low strength to stress concentrations
	Can be disassembled	Special practices required in assembly; results in time consuming assembly
	Ease of inspection	Fluid and weather tightness normally requires special gaskets or sealants
		Corrosion of metallic fasteners
Bonded joints	Advantages	Disadvantages
	High joints strength can be achieved	Cannot be disassembled
	Low part count	Requires special surface preparation
	Fluid and weather tightness	Difficulty of inspection
	Potential corrosion problems are minimized	Temperature and high humidity can affect joint strength
	Smooth external surfaces	
	Good fatigue resistance	
Combined joints	Advantages	Disadvantages
	Bolts provide support and pressure during assembly and curing	Structurally bolts act as backup elements - in an intact joint, bolts carry no load
	Growth of bond line defects is hindered by bolts	Requires special surface preparation

Table 27: Comparison of advantages and disadvantages of different FRP joint types [B14, p128-129]

In the following table some more in-depth information on FRP joint properties in comparison to each other will be given. Note that from this table it becomes clear that bonded joints cope best under corrosive, weather-intensive environments and under prone-to-fatigue applications. Thus, they are very suitable for application in traffic bridges. [B14, p128]

Property	Mechanical joints	Bonded joints	Combined joints
Stress concentration at joint	high	medium	medium
Strength to weight ratio	low	medium	medium
Seal (water tightness)	no	yes	yes
Thermal insulation	no	yes	no
Electrical insulation	no	yes	no
Aesthetics (smooth joints)	bad	good	bad
Fatigue endurance	bad	good	good
Sensitivity to peel loading	no	yes	no
Disassembly	possible	impossible	impossible
Inspection	easy	difficult	difficult
Heat or pressure required	no	possible	possible
Tooling costs	low	high	low
Time to develop full strength	immediate	long	long

Table 28: In-depth properties of FRP joint types [B14, p128]

2.6.11.1 BOLTED JOINTS

Bolted joints transfer shear forces between elements in a structure. They do this by friction between the regions that are compressed locally (in vicinity to the fastener). Therefore it is important that the composite material around the bolt(s) can withstand this compression force and that the bolt itself can take up this force. Next to that it has to be verified that the region surrounding a group of bolts cannot be torn out of the profile. Next to that the EUROCOMP Design code gives some important remarks on bolted FRP joints: Always use stainless or galvanized steel as fastener material, never use threaded bolts or screws. When pultruded profiles are joined with mechanical fasteners attention to the force direction in the connection must be given. [P32, p58]

The following failure modes of bolted FRP connections can be distinguished. Note that these failure modes are quite similar to steel connection failure modes. However since no official international code does exist yet, every profile manufacturer came up with their own system of rules and guidelines. In this study the Fiberline Design manual [B25] will be used.

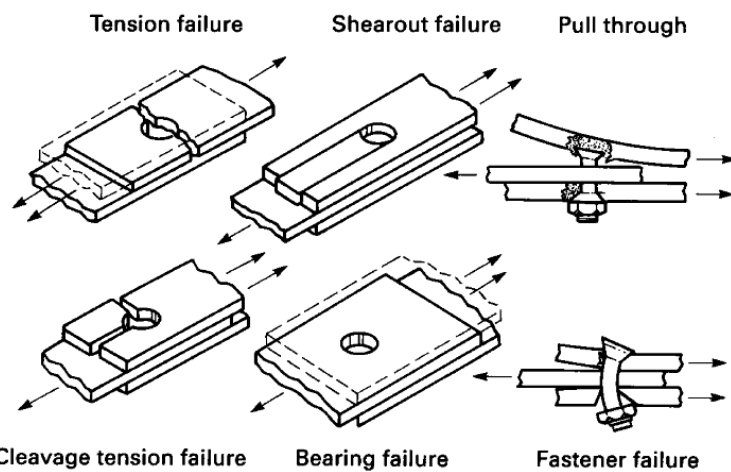


Fig. 64: Bolted FRP connection failure modes [P86, p114]

Of the six failure modes presented above some can easily be avoided by using correct edge distances, bolt diameter, head configurations and composite thickness. Pull-through can only occur if countersunk bolt heads are used. Fastener failure will only occur, when an incorrect-fastener-diameter to composite-thickness-ratio was chosen. A correct ratio is given by the following formula. [P86, p112]

$$1,5 < d/t < 3,0 \quad (2.83)$$

The other two failure modes that are cancelled out by using the right distances are shear-out failure, cleavage tension failure. The following scheme gives the appropriate dimensions [B25, p1.4.4]

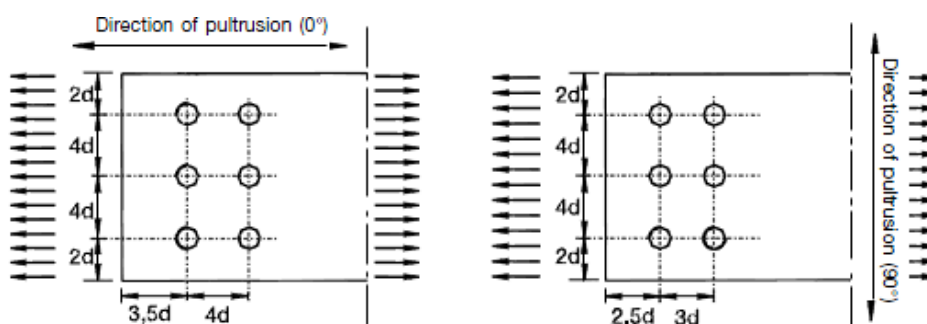


Fig. 65: Fiberline dimension scheme for bolted FRP connections [B25, 1.4.4]

Tensile failure

Tensile failure of bolted connections can occur in two ways, either by tearing of the bolt in the threaded cross-section, or by shear fracture of the composite at the rim of the washer. Failure of the bolt can be calculated by the following formula: [P32, p62]

$$P_d \leq \frac{A_s f_{yk}}{\gamma_m} \quad (2.84)$$

Failure of the composite in a bolted connection under tension is given by: [P32, p62]

$$P_d \leq \frac{2d\pi t f_\tau}{\gamma_m} \quad (2.85)$$

In the above formulae $P_d = \text{Design load}$, $A_s = \text{stress area of bolt}$, $f_{yk} = \text{tensile strength of bolt}$, $d = \text{diameter of bolt}$, $2d = \text{diameter of washer}$, $t = \text{composite thickness}$, $f_\tau = \text{shear strength of laminate}$.

Shear failure

For shear failure of a bolted joint in FRP several failure modes do exist, for more information on these failure modes the appropriate literature can be used [B25, p1.4.6-1.4.11] [B14, p142-151]. In the following only the two general formulae for shear in longitudinal direction (0°) and transverse direction (90°) of pultruded profiles will be given. These originate from the "Fiberline Design Manual". [P32, p60] [B25, p1.4.6, p1.4.9]

$$P_{B,d,0} \leq \frac{dt f_{cB,0}}{\gamma_m} \quad (2.86)$$

In the above formula $f_{cB,0} = \text{pin - bearing strength} = 150 \text{ N/mm}^2$ and $\gamma_m = 1,3 = \text{material factor}$. The formula below described the shear strength in transverse direction:

$$P_{B,d,90} \leq \frac{dt f_{cB,90}}{\gamma_m} \quad (2.87)$$

In this formula $f_{cB,90} = \text{pin - bearing strength} = 70 \text{ N/mm}^2$ and $\gamma_m = 1,3 = \text{material factor}$.

Reviewing the performance of mechanically bonded joints in FRP structures a number of problems arise: The load-direction is critical in connections bonded by bolts; large local stresses are very detrimental for the fatigue performance. Next to that, since steel is used for the fasteners, the corrosion-resistance decreases and the weight also grows. Especially in structures with a lot of connections, such as trusses, this poses a problem. Also the coated/ gel-coated surface of the composite is damaged by drilling holes, providing a vulnerable point in the structure. Finally the strict demands on distances between fasteners and between fasteners and the edge of the composite pose problems when large loads need to be transferred.[P86, p132]

2.6.11.2 BONDED JOINTS

Bonded joints in FRP structures transfer load between two or more joined elements via shear in the adhesive layer. For the adhesive layers only epoxy, silicone, polyurethane, phenolic and acrylic are used. Thus bonded joints are often considered to be the ‘natural’ way of connecting fiber reinforced polymer elements. [P86, p13] The schemes below show some options of means of connections for FRP elements: [B25, p1.5.3]

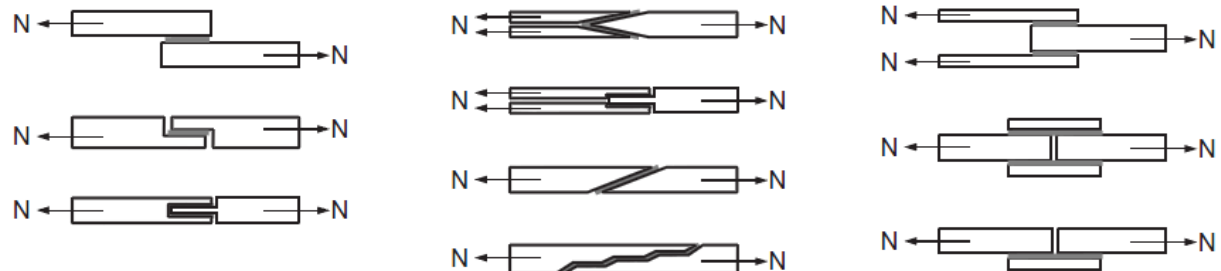


Fig. 66: Examples of bonded joints for FRP elements [B25, 1.5.3]

Glued joints are characterized by their high stiffness/rigidity, the ease to make aesthetic bonded joints, the extreme strength of some adhesives and thus the small needed contact area and their good reaction to dynamic loads. However it is important to notice that typical adhesives have properties that are time-dependent and influenced by environmental factors such as humidity. Next to that, bonded joints behave very brittle, meaning failure occurs suddenly, without warning. Finally, although the overlap length is one of the most important parameters in bonded joint design, the capacity of the joint only increases up until a certain boundary overlap length, after which the joint capacity stagnates. [B25, p1.5.3]

Three failure modes of bonded FRP joints are usually distinguished: Firstly, adhesive failure, which can be eliminated by choosing the right adhesive for the composite and cleaning the bonding surface thoroughly. Secondly, cohesive failure of adhesive, meaning rupture of the glue, can occur. The last failure mode of bonded joints is cohesive failure of the adherent, meaning rupture of the composite. The graph below correlates the bonded joint strength with the adherent thickness and shows the most probable failure mode. The strongest joint types are the stepped- and scarfed joints, the weakest is the single-lap joint, which is eccentric. [B14, p175]

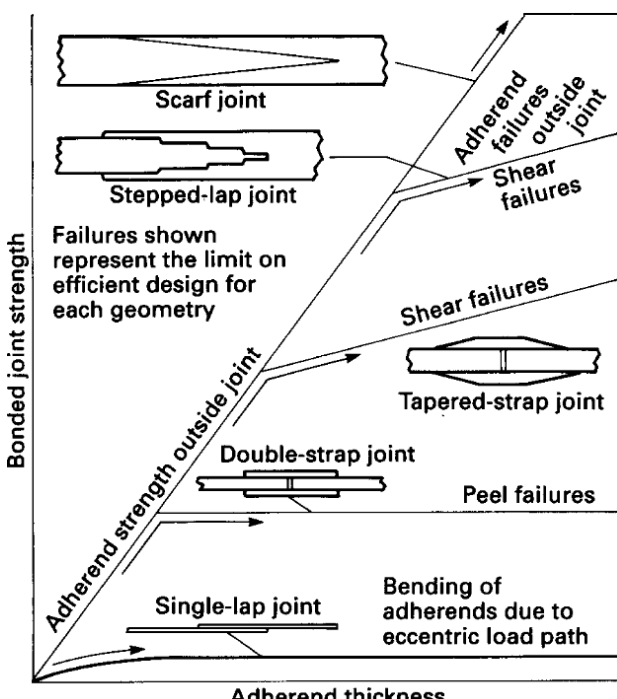


Fig. 67: Failure modes of different FRP bonded joint types [B14, p175]

The schemes below compare a bonded joint (epoxy) with a bolted joint (single M10 bolt) in tension. The different stress distributions are very clear. Note also the difference in the maximum stress occurring in both cases. The bolt connection induces stresses 5x-7x times bigger than the bolted connection. [P86, p10]

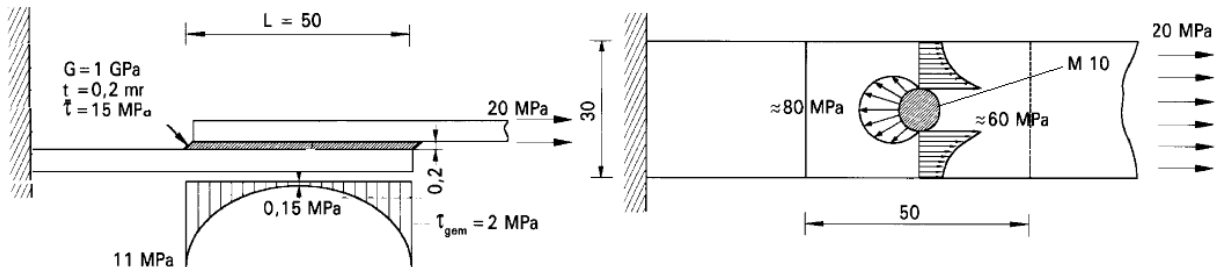


Fig. 68: Stress distribution for bonded (left) and bolted (right) joints under the same circumstances [P86, p10]

The most efficient adhesive layer thickness was found to be in the range of 0,1mm – 0,25mm. If thicker adhesive layers are needed, for example >1,5mm, the adherents need to be tapered. The optimum overlap-to-thickness-ratio lies at about 30:1. The maximum thickness of composite adherent that can be joined without stepping or scarfing is 4,5mm and tapering increases this limit to 6,35mm. [P86, p28-29] It is important to know the characteristics of the adhesive used. Although bonded joints are generally considered to behave brittle, there still exist large differences in the ductility of the adhesive. Adhesive that are considered to be brittle, have a shear failure strain of 0,1% while ductile adhesives have a shear failure strain up to 2,0%. [P86, 34]

The shear-and peel-stresses in bonded single- and double lap connections always have their maximum at the ends of the overlap or the ends of a step in a stepped joint. To minimize these stress peaks it is important to use identical adherents, highest possible in-plane laminate stiffness, longest possible overlap (not higher than the earlier discussed boundary overlap length) and using ductile adhesive with low tensile and shear elastic moduli. Next to that tapered adherents also reduce the peak stress. [P86, p37,38] For fatigue loading a life of 10^6 cycles can be expected if the peak stress is limited to about 25% of the static strength value for single lap joints, and about 50% for scarf joints.[P86, p39]

The formulae below are used to calculate the maximum stress that a single-lap joint can take up for a tensile force of P_o , w is the width of the joint, and l is the length of the adhesive layer. [P86, p41-42]

$$\sigma_{max} = \sigma_{av} + \sigma_{bend} = \frac{P_o/w}{t} + \frac{6M_o}{t^2} \quad (2.88)$$

$$M_o \cong P_t/2 \left(1 + \zeta^C + \frac{1}{6} (\zeta^C)^2 \right)$$

$$\zeta^C = \frac{P}{D} \quad (D = \text{adherent stiffness})$$

$$c = l/2$$

For more information on double lap joint calculation, stepped joint calculation and scarfed joint calculation reference is made to the appropriate literature. [P86, p50-70] [B14, p178-190]

Laminated joints

If the adhesive in a bonded joint is replaced by a matrix resin and sometimes also reinforcements it is called a laminated joint. Laminated joints form a solid structure, combining the joint and the adherents. The most typical configuration of a laminated joint is a butt-joint on which doubles are laminated, the result being a double-strap joint with no distinguishable adhesive layer. Manufacturing such a joint is very labor-intensive and thus costly. Next to that, laminated joints have some major disadvantages which make them not very suitable for large scale use: There is discontinuity in the mechanical properties of the joint, the adherent

and the double have different thermo-mechanical properties and typically a relatively thick layer of pure polymers is formed on the bonded surfaces. Also, the “EUROCOMP design guide” advises to perform detailed finite element analysis and/or testing before using laminated strap an tee joints, step-lap joints, scarf joints and angle joints. [P86, p71-82]

2.6.11.3 COMBINED JOINTS

In the “EUROCOMP design code” very limited information is given on the design of joints in which both bolts as well as glue is used. The reason for this lies in the fact, that the adhesive bond between the joined adherents behaves much stiffer than the bolted connection. Therefore the adhesive joint will take up all present loads, and the strength of the combined joint will not be bigger than that of a joint using adhesive only. [B14, p210]

This leads to the recommendation to design combined joints as if they were adhesive joints. Thus no load-sharing between the two connection types exists. However, some applications of combined joints do exist, where the combination of fastening methods makes sense: Bolts can prevent manufacturing defects and service-induced bond line defects from spreading. Furthermore bolts can provide the required clamping pressure during the bonding process. [B14, p210-211]

To conclude this section on combined joints a graph on the stress distribution within a bolted-bonded joints is given here. It can be seen that the bolts within the bond line have no influence on the stress distribution. The outer left bolt, which is outside the glued surface causes a small stress peak, which is still significantly lower than the stress peaks at the end of the glued surface. [B14, p506]

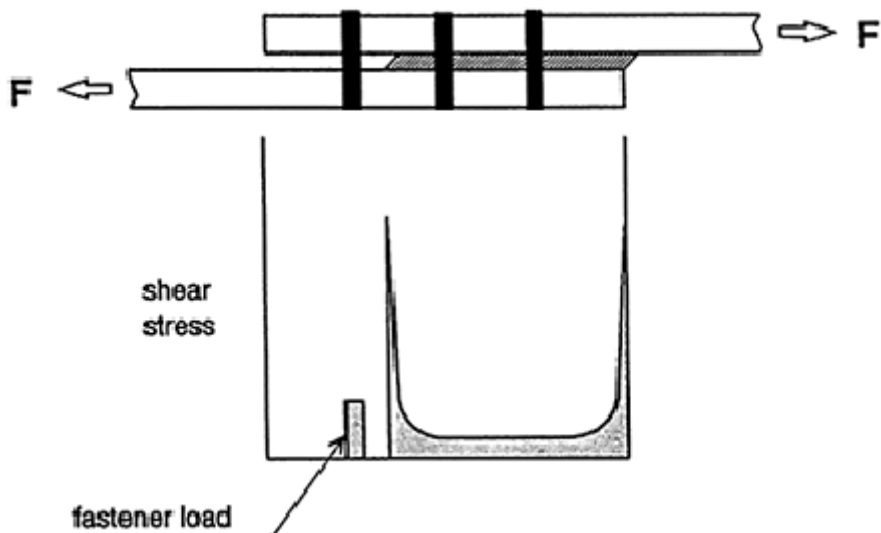


Fig. 69: Stress distribution in a combined bolted-bonded FRP joint [B14, p506]

3. TRAFFIC BRIDGES

In the past few hundred years many different types of bridges have been designed. In this topic the most common bridge types will be discussed. This description has the sole purpose to clarify where the fiber reinforced traffic bridge, which will be designed in the course of this thesis, stands in the field of traffic bridges.

Next to that this chapter will cover all deck types which can be used for the construction of fiber reinforced traffic bridges.

The last, but perhaps not important part of this chapter will concern the different kind of loads that have to be applied while designing traffic bridges in the Netherlands and in Europe. For this purpose the applicable codes will be thoroughly investigated.

3.1 TYPES OF BRIDGES

In this chapter the main types of traffic bridges will be shown. The general flow of forces will be shown, as well as the main characteristics, such as span length, weight and common applications.

3.1.1 ARCH BRIDGES

As the name describes, the main component of arch bridges is the arch. Usually an arch bridge is composed of two arches, to cope with lateral forces through the coupling wind braces.

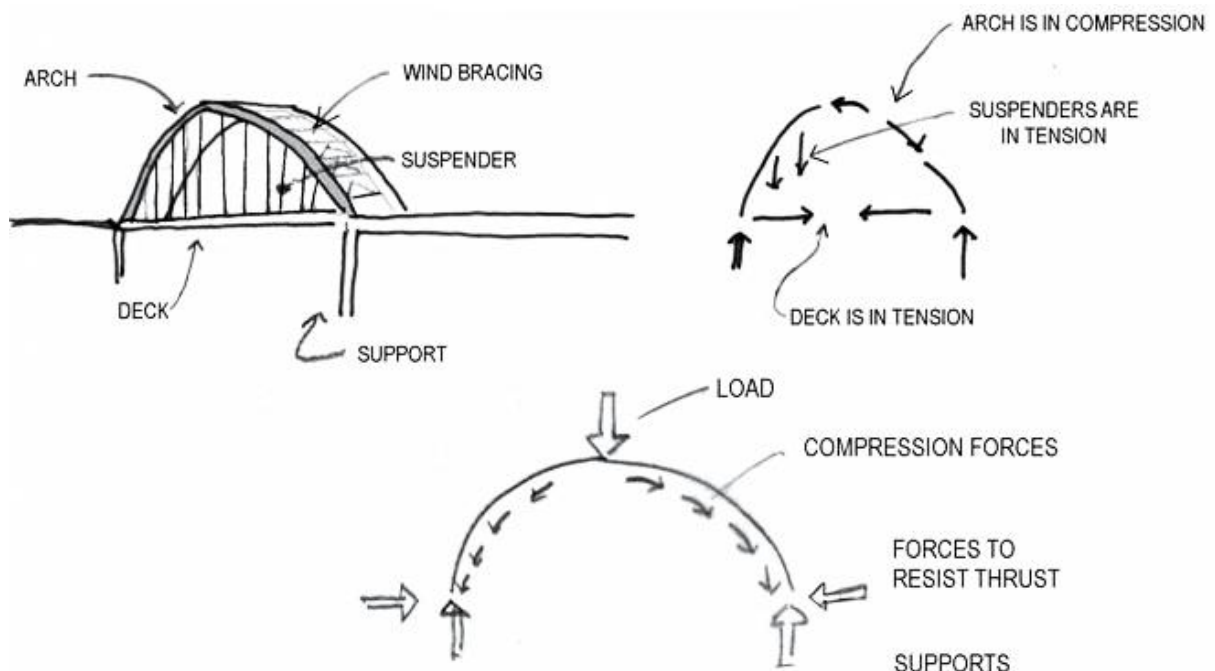


Fig. 70: General flow of forces in arch bridges

The arches are in compression, following nature's principle of compressive arches, which also occurs in rocky materials. The compressive force present in the arches has to be counteracted by either the

abutments/supports or by the bridge deck, which acts as tie, to hold the ends of the arch together. The deck is supported by an array of vertical suspenders. To prevent buckling in the arch it usually has a large cross-section, making it relatively heavy. Next to that the arch also has to cope with bending moments which arise due to non-uniform load conditions. More very heavy elements of arch bridges without tie are the very large abutments which have to resist the compressive forces.

Arch bridges have been in use for thousands of years, and are still very popular for medium to large spans up to 550m in the case of the "Lupu Bridge", Shanghai, China and 552m in the case of the "Chaotianmen Bridge", Chongqing, China. The most common span though is 50-150-300m. Arch bridges are used most often for highway traffic, though many railway-arch bridges also do exist.

Next to the given example of the bridge deck which is hanging under the arch, many other variants, such as bridge decks resting on top of the arch and bridge decks through the arch, exist. Often arch bridges are combined with other bridge types such as cable-stayed bridges or truss-bridges, leading to hybrid bridge system such as truss-arches or cable suspenders.

3.1.2 SUSPENSION BRIDGES

Suspension bridges function by hanging the bridge deck from an elevated cable. The force flow is reverse to that of an arch bridge. The cable is under tension, tied to the buttress through the backstays and laid over two towers. In that way the cable has a parabolic shape. The towers are in compression and the buttress resists the tensile force of the cable through its large own weight. For lateral stability two parallel cables are used in most cases.

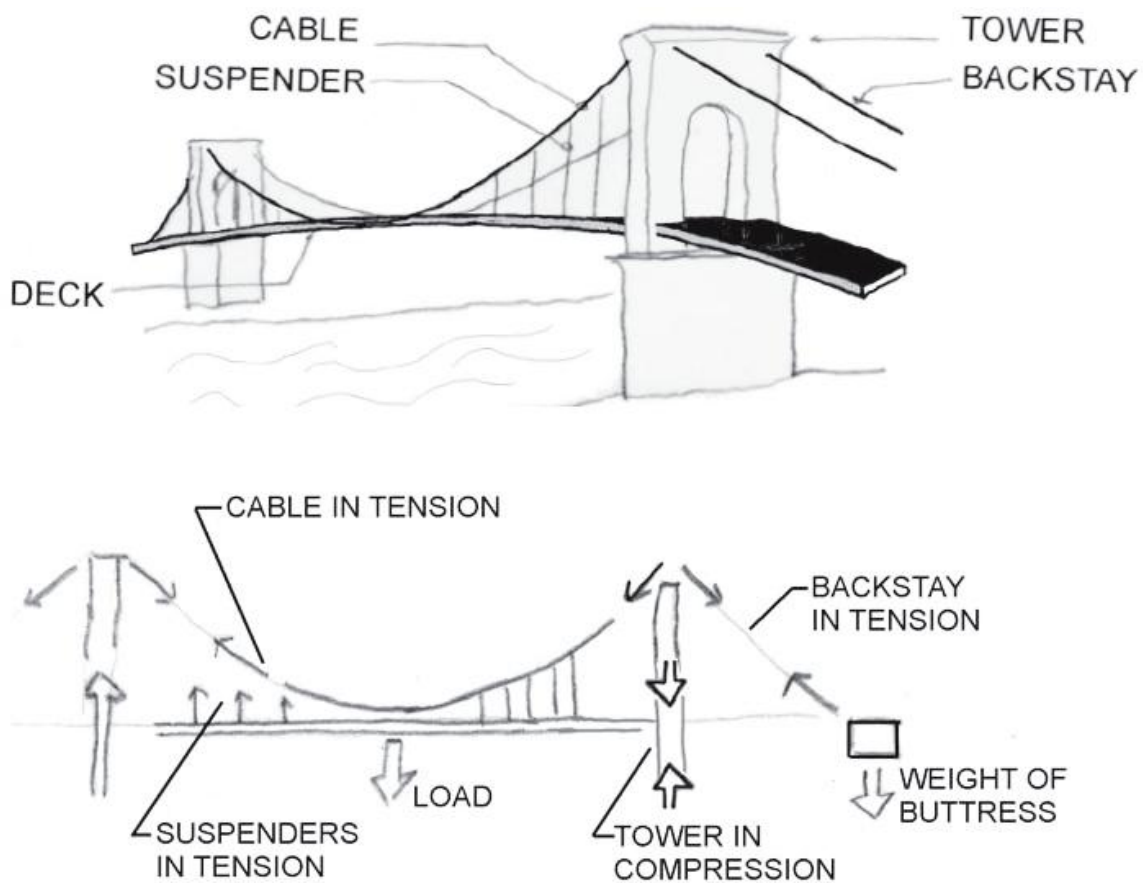


Fig. 71 General flow of forces in suspension bridges

Suspension bridges are very suitable for long spans up to 1991m in the case of the "Akashi Kaikyo Bridge", Kobe-Naruto, Japan. Partly due to the complex construction and the large buttresses needed suspension bridges are only used for large spans of 150-700-1200m. This makes them the largest span bridge type available. The reason that suspension bridges can reach such large spans is the low weight of the bridge, since no elements, except for the deck, are under flexure. The main cables as well as the suspenders are under tension. Due to the well-engineered joints of cables and tower, the tower is almost exclusively under vertical compression.

Of course the light weight also has some disadvantages: Vibration and aerodynamic resonance are some of the problems that can be encountered with these bridges. Suspension bridges are mostly used for highway traffic and not for railway traffic, due to the high concentrated loads and the low deck stiffness.

3.1.3 CABLE STAYED BRIDGES

Though cable stayed bridges look similar to suspension bridges they function in a different way. Cable stayed bridges behave like elastically supported continuous beams. The bridge deck is in this case the beam which is supported by the different cable stays, which are distributed over its length. The tower of the cable stayed bridge is under compression, leading the vertical forces on the bridge deck via tension in the cables to its foundation. The cable stays generate a compressive force in the bridge deck, pushing it from the outside in, towards the tower.

Cable stayed bridges have only been around for a mere 70 years and maybe are a modern example of bridge engineering. They mostly consist of two plane multi fan-shaped cables, though bridges with a singular plane are also common. Often single towers are used, for longer spans such as the longest span cable stayed bridge, the "Tatara Bridge", Japan with a span of 890m, two towers or even more are used. Most often they are used for spans of 110-350-600m. Just like the suspension bridges, cable stayed bridges are also light-weight, though the tower has to be much stiffer due to the forces exerted by the cable stays.

Cable stayed bridges are mostly used for highway traffic, mainly due the high concentrated loads and the low deck stiffness, as described before in the case of suspension bridges.

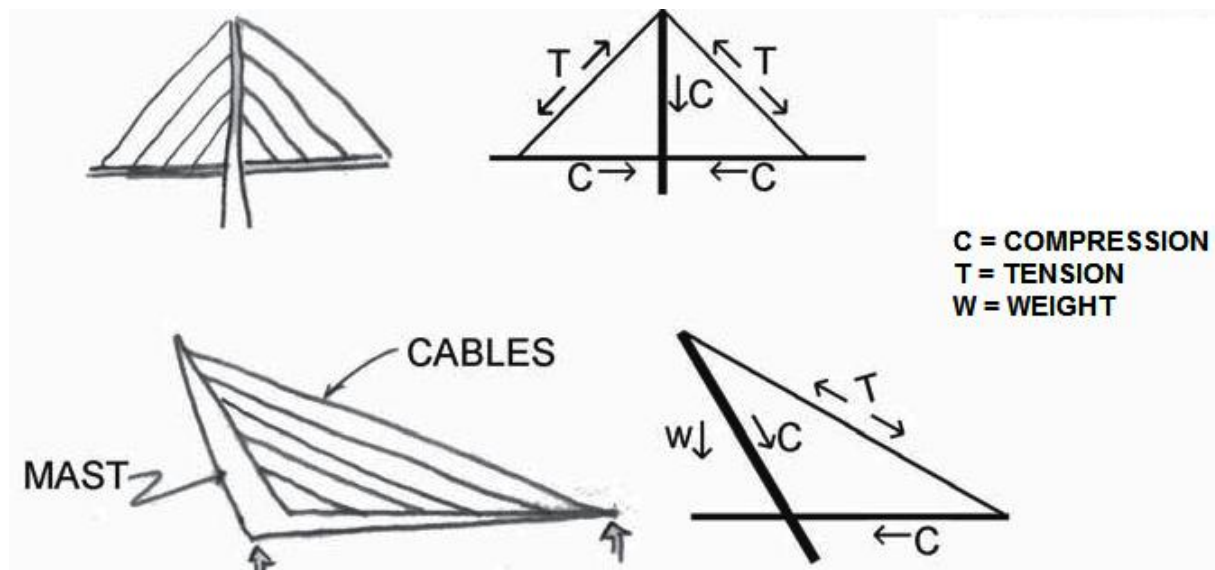


Fig. 72: General flow of forces in cable stayed bridges

3.1.4 GIRDER BRIDGES

Girder bridges are maybe the simplest form of bridges. They consist of a single girder which is loaded under flexure, leading to the underside of the girder being under tension and the topside being under compression. Due to their simplicity they have been around for thousands of years and are still vastly used. In fact girder bridges are worldwide the most used bridge type. Common spans are low to medium: 10-80-150m. Developments of new sections such as stiffened box- or plate-girders with a large height and therefore a very good bending stiffness have drastically increased span length. Examples for different steel cross-sections are I-girders (span: 25-30m) and box girders (span: 60-100m). For (pre-stressed) concrete cross-sections the following possibilities exist: simple slabs (span: 5-15m), T-girders (span: 12-18m), box girders (span: 15-36m), pre-stressed box girders (span: 30-180m) and pre-stressed I-girders (span: 9-40m). [T06, p23-26]

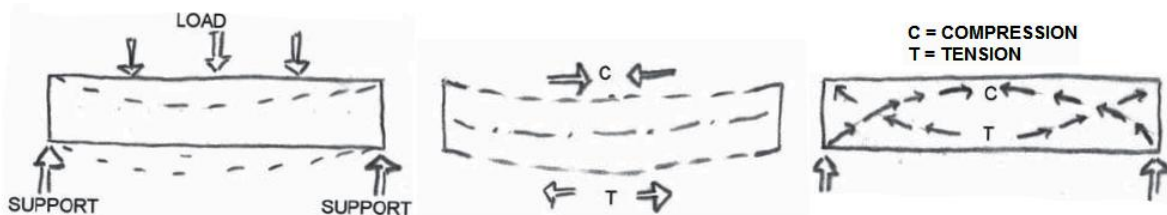


Fig. 73: General flow of forces in beam bridges

Due to the large array of possibilities in the shape and arrangement of girders many different applications exist: From small span pedestrian bridges to 100m+ spans for heavy weight railway traffic. The diversity is also present in the material use; concrete is more often used for smaller span bridges, due to its low costs. Steel is more often used for larger spans due its higher strength and lower weight.

3.1.5 TRUSS BRIDGES

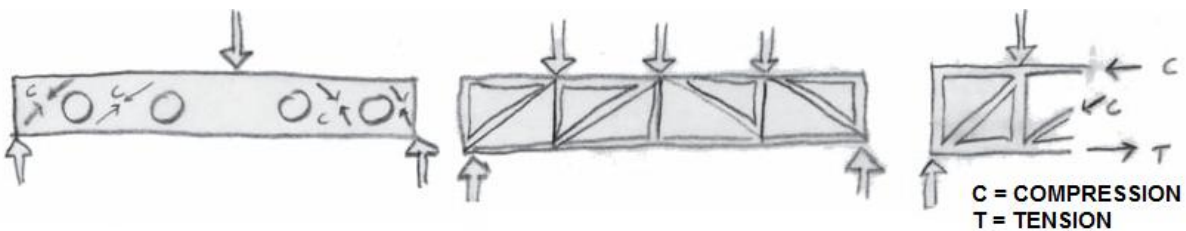


Fig. 74: General flow of forces in truss bridges

Truss bridges can be considered to be optimized beam bridges. The example of a castellated beam is given on the left side of the picture. The holes in the beam are cut out to reduce the weight of the beam whilst not decreasing the mechanical properties. Trusses are essentially beams, in which as much material as possible is left out. In this way even higher, and thus stiffer beams or trusses can be fabricated. The upper flange is under compression, the lower flange under tension. The vertical members are under compression, the diagonals can either be designed to take tension or compression.

Truss bridges are very versatile, due to the large number of possibilities in shape. Truss bridges are able to take even very high concentrated loads and are therefore often used for heavy railway traffic. Spans are usually in the range of 40-170-300m. As stated before with other types of bridges, combinations are also possible with truss bridges; a common example is the parabolic truss, a hybrid of truss- and arch-bridge.

3.1.6 BACKGROUND ON THE CHOICE OF BRIDGE TYPE FOR THE FIBER REINFORCED POLYMER BRIDGE

The bridge that is to be designed during the course of this master thesis will be of medium span, meaning a span length of not more than 50m. This immediately shows where the proposed fiber reinforced polymer bridge will lie in the field of bridge engineering. Bridge types that are common in very long spans, like the cable stayed bridge and the suspension bridge are certainly not very useful for a span of 50m. Next to that they would impose other problems such as vibrations and other air-induced effects, on which very little is known in the field of fiber reinforced polymers. These effects alone could be subject of another master thesis. So far, cable stayed all fiber reinforced polymer bridges have only been applied in very small numbers in low-load, limited span pedestrian bridges.

Since the arch bridge is primarily used for bridges with spans that exceed 50m by far, an arch bridge cannot be seen as a bridge type that would be efficiently applicable in the case of the proposed traffic bridge. Next to that arch bridges also have one element that is primarily loaded under compression. Production of a fiber reinforced element that large, that has to resist buckling and that has to be connected to the suspenders would be very complex and research on it would certainly be one the main objectives of the research. The Lleida-footbridge in Spain is until now the only all fiber reinforced polymer arch bridge. It too has a limited span and is only suitable for pedestrian use.

As described before in [chapter 1.2], the shape that is therefore most applicable for a design of this kind is a hybrid between a girder bridge and a truss bridge. Since even for this “simple” type of girder-bridge the use of fiber reinforced polymers has not been thoroughly investigated it should hopefully be a suitable material for efficient and feasible design and construction of heavy traffic truss-girder bridges.

3.2 FIBER REINFORCED POLYMER BRIDGE DECKS FOR FRP BRIDGES

Bridge decks are one of the most important applications of fiber reinforced polymers in bridge engineering. In the following chapter existing types of fiber reinforced bridge decks will be investigated. First of all a general introduction of advantages and disadvantage of fiber reinforced bridge decks will be given.

Fiber reinforced bridge decks have been regularly used for about 15 years. About 50 bridge decks have been installed in the USA alone since then. Fiber reinforced bridge decks are usually made by combining vinyl-ester- or polyester-resin with E-glass reinforcement. They are pre-fabricated in elements with large dimensions, the assembled and installed on site. The finalizing abrasion resistant layer is added here too. For the production of fiber reinforced bridge decks three different techniques are generally used: Pultrusion, Vacuum assisted resin transfer molding (VARTM) and hand lay-up. All of these techniques have their own advantages: Pultrusion offers excellent dimensional tolerances and high quality but also high costs and low customization ability. VARTM is comparably cheap, offers the ability to incorporate special features but has lower dimension tolerances. Hand lay-up is very customizable and cheap but offers lower quality and dimensional tolerances. [P61, p1-3][A33, p2]

3.2.1 ADVANTAGES OF FIBER REINFORCED POLYMER BRIDGE DECKS

Currently the production costs of fiber reinforced polymer bridge decks are still higher than conventional concrete or steel decks. However, certain other characteristics, like the corrosion resistance and the long service life can make fiber reinforced decks competitive or even cheaper than traditional decks. [P61, p3]

Another great advantage of fiber reinforced polymer decks is the lower weight. FRP bridge decks weigh about 20% of concrete decks. This lowers not only the requirements for the substructure but also the foundation requirements. Next to that a lower mass also means that with most bridge renovations FRP decks can be used without costly alterations of the substructure. Earthquake induced displacements also reduce significantly with lower mass of the bridge deck. [P61, p4][A38, p2]

Fiber reinforced polymer bridge decks exhibit a much better corrosion resistance to e.g. de-icing salts and a much better resistance to freeze-thaw cycles than traditional materials. Where concrete features cracks and spalls and steel corrodes after a long service life, fiber reinforced polymers are expected to have service lives in excess of 75 years. Due to the short time of application of FRP in practice this still needs to be verified with long-term field tests. Concrete decks are typically replaced at least every 15-25 years. [P61, p4-5][A38, p2][A08, p67]

Furthermore FRP bridge decks are among the most rapid installation bridge decks available. Since they are prefabricated to a large extent and are very light weight installation on site is straight-forward and does not need large machinery or long curing times. Rapid installation also reduces labor costs and minimizes traffic delays. Due to the solid surface that can be obtained when placing FRP bridge decks, abrasion resistant overlays and top layers can be placed very quickly (if not already provided in prefab). [P61, p5][A38, p2]

Another advantage of FRP bridge decks is the ability to tailor-make the deck sections according to the exact specifications of the bridge designer. Fiber type, fiber content, number of layers and fiber orientation; those are all properties that can be altered in width, length, and depth direction of the bridge decks. This makes very efficient use of materials and thus very good cost effectiveness possible. [P61, p5]

Some FRP bridge deck types are even capable of achieving composite action, due to very well designed connections between bridge decks and underlying girders. In this way bridge deck also contribute to the bending stiffness of the girders, thus increasing the bending resistance and decreasing deflections. [A38, p2]

To conclude the advantages section, a major advantage of FRP in bridge decks will be given. Bridge decks usually endure the most load cycles of all bridge elements. Typical load cycle numbers are in the range of millions or even tens of millions. This makes them prone fatigue damage. Especially orthotropic steel bridge decks had difficulties in coping with these high fatigue loads. Several tests on fatigue in fiber reinforced polymer elements have shown that FRP is a very promising material in respect to fatigue. The chapters on fatigue [chapter 2.6.10.3; chapter 3.3.4] give more information on fatigue in fiber reinforced polymers. [B17, p685]

3.2.2 DISADVANTAGES OF FIBER REINFORCED BRIDGE DECKS

One of the main reasons for the fact that FRP bridge decks are not yet widely used is the high initial cost that is linked to FRP. Many awarding authorities, engineering- and building companies are still not using cost-models to predict life-cycle costs and thus make a fair comparison between different building materials. Next to that the high initial costs have already dropped significantly since production techniques have become more and more efficient and application of FRP has become slightly more widespread than before. This process will certainly carry on and grow on in the future. [P61, p10]

Fiber reinforced polymers also have an inherent “problem” that is caused by their low modulus compared to for example steel. More specifically glass reinforcement suffers from this. In order to meet serviceability requirements for deflections, FRP systems have to be over-designed from a strength perspective. Although this leads to a very conservative and safe structural system, it is also quite inefficient since all of added strength of the material is not used under normal traffic loads. It has to be said though that many modern FRPs have better stiffness values and new shapes, manufacturing methods and hybridization with other materials can drastically reduce this problem. [P61, p10]

The last disadvantage that will be discussed here is the complexity of FRP elements. Typically manufacturers design their own products and the exact mechanical properties and material specifications such as fiber-orientation, -type, -content, etc. will remain company secrets. This leads to high degree of non-

standardization within the industry, which makes it very hard for the bridge designer to work with the materials, since they are “black box design” for him. Bridge engineers are usually no FRP-experts, so rather than struggling with FE-design of state-of-the-art fiber reinforced polymer sections, they will prefer to work with materials, of which the behavior is understood very well by the engineering practice. It is very likely that manufacturers will develop more and more standard products in the future. The introduction of national and international codes for FRP would certainly be beneficiary for this development. [P61, p10]

3.2.3 COMPARISON OF ADVANTAGES AND DISADVANTAGES

The table below gives a summary on the advantages and disadvantages of the application FRP bridge decks.

Advantages of FRP Bridge Decks	Disadvantages of FRP Bridge Decks
Low weight	High initial cost
Resistance to de-icing salts and other chemicals	Deflection driven design due to FRP low stiffness
Fast installation	No standard manufacturing process
Good durability	Little knowledge on thermal behavior
Lower user costs (lower maintenance costs)	Some failure of the wearing surface (i.e. cracking, debonding)
Long service life	The resultant tendency to creep over time
Fatigue resistance	Lack of long term performance data
Good quality due to fabrication in a controlled environment	Limited FRP experience within the engineering-and construction industry
Ease of installation	Lack of design standards

Table 29: Advantages and disadvantages of fiber reinforced polymer bridge decks [P29, p11-12]

3.2.4 TYPES OF FIBER REINFORCED POLYMER BRIDGE DECKS

Generally two different construction types of FRP bridge decks exist: firstly the multi-cellular deck panels made of adhesively bonded, mostly pultruded shapes. Most bridge decks that have been installed to this date use this system. The panels consist of differently shaped cross-sections: hexagonal, triangular, rectangular or trapezoidal cross-section are mostly used. The second construction type of FRP bridge decks is the sandwich panel with various core structure possibilities. Stiffened foams or thin walled cellular materials are most commonly used for the cores. These cores are often considered to be of a honeycomb type.

The picture below shows some of the most common cross-sections used as bridge decks. Of the eight given deck types only two do not have their origin in the USA. This illustrates that fiber reinforced bridge decks are most common in that part of the world. [P29]

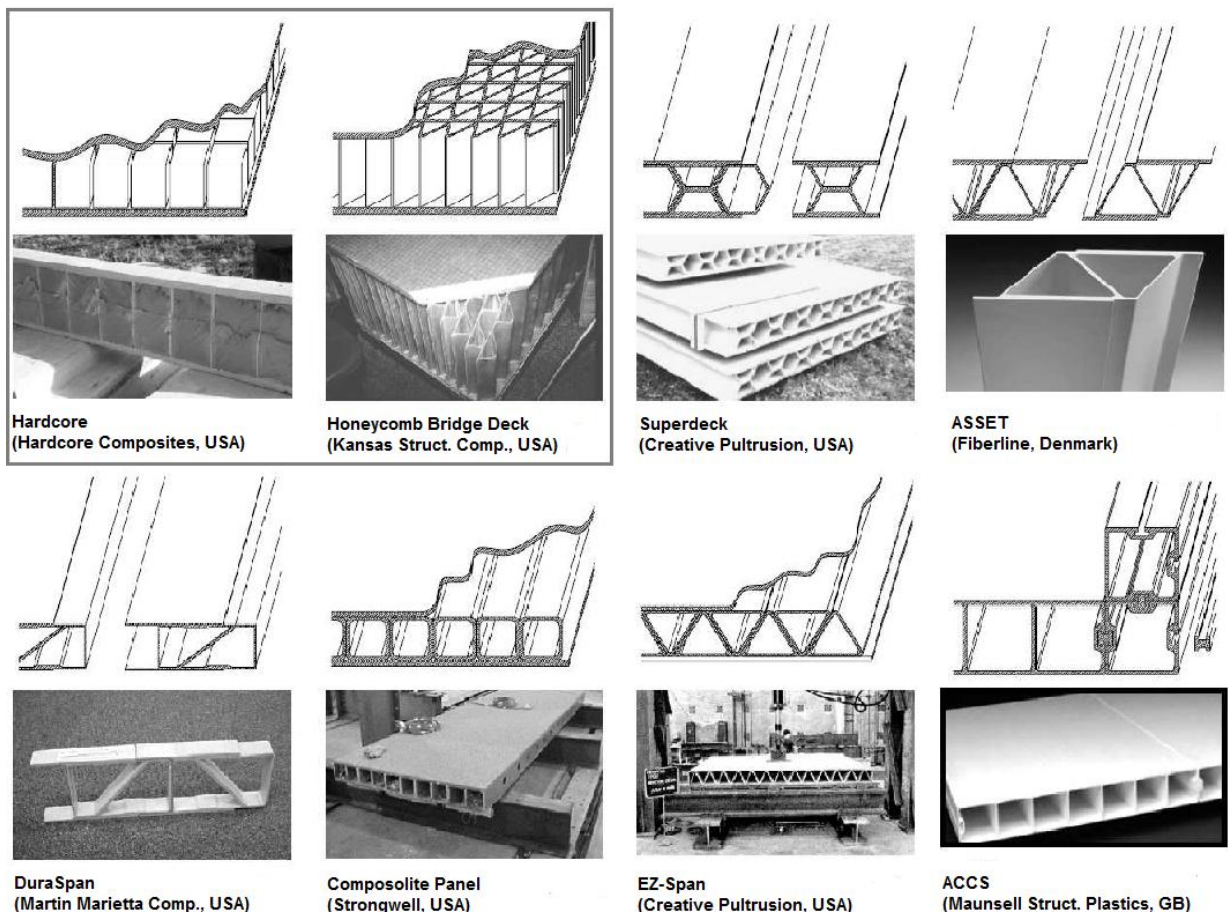


Fig. 75: Different fiber reinforced polymer bridge deck types [T07, p29]

The first two bridge decks are of the sandwich panel type. The “Hardcore panel” of “Hardcore Composites” is filled with foam and glass fiber reinforced vinyl ester resin. The top- and bottom layer is made of honeycomb sheets. The void between the two face sheets in the second product, the “Honeycomb Bridge Deck” of “Kansas Structural Composites”, is filled with a sinusoidal honeycomb of FRP sheeting. This bridge decks does not use inner foam. Both products share the advanteguous property of a various thickness, which makes them more versatile than the multi-cellular deck panels. Typical deck thicknesses of sandwich panels are 200-500mm, though even higher thicknesses are possible.

The other bridge deck types are produced using pultrusion or hand lay-up. Some recent developments have led to the introduction of pultrusion in combination with filament winding, which improves the mechanical properties in the lateral direction and generally strengthens the panel. [P12] The bridge decks shown differ mainly in the cross sectional shape, the member thicknesses and the connection method. The latter will be discussed later. The thinnest deck shown is the “Composolite Panel” by “Strongwell” with has a thickness of 171mm, followed by the “Duraspan Panel” with 190mm. The other panels all have thicknesses above 200mm. The “Superdeck” has a thickness of 203mm, the “EZ span” 216mm and the European “ASSET Deck” has a thickness of 225mm. The “Maunsell” bridge deck “ACCS” is available in different thicknesses. The manufacturer of “ASSET”, “Fiberline” of Denmark, one of the biggest FRP manufacturers in the world has recently introduced two other bridge types that are suitable for slightly lower loads than the “ASSET Bridge Deck”: the “FBD450” and the “FBD300 Bridge Deck”. The three deck types will be compared in the following table. Of the compared products the “FBD600 ASSET” is most likely to be applied as a bridge deck for a heavy traffic bridge. Of the three products it is the only one which is able to comply with the heaviest load class dictated by the Eurocode.

Property	Unit	FBD600 ASSET	FBD450	FBD300
Height	mm	225	130	80
Width (single unit)	mm	521	310,7	339
A	mm ²	15.644	6.156	7.118
I _x	10 ⁴ mm ⁴	125	16	7,2
I _y	10 ⁴ mm ⁴	229	30	79
W _x	10 ³ mm ³	1.114	246	164
W _y	10 ³ mm ³	87	193	462,4
Stiffness	N/mm ²	20.000	21.500	27.000
Weight	kg/m	29,9	11,5	14
Weight per m ²	kg/m ²	103,7	65,85	42,1

Table 30: Comparison between different Fiberline Decks [WEB: www.fiberline.com]

The load-carrying behavior of sandwich decks is normally bi-directional while the behavior of pultruded decks is basically unidirectional in the pultrusion direction. Since bridges are designed for concentrated loads, the bi-directional behavior is more favorable for this application. Due to the possibility of varying the depth of sandwich panels their maximum span is about 10m. Pultruded shapes are limited to a thickness of about 230mm which limits their span to about 3m. Bridge decks of this type therefore need more supporting girders with smaller spacing. Also, overhangs with pultruded sections are not possible. Since the proposed design is a tubular truss with an inner deck this should not be a problem. [P59, p2]

Nowadays solely glass fibers are used for bridge deck sections and design is always governed by the (live) load deflection criteria in the serviceability limit state. Due to this stiffness-driven design the stresses in the deck are usually small and can reach safety factors of 4-5 in the serviceability limit state. Thereby, failure modes are characterized by local buckling failures, following initial inter-laminar failures, such that the material strength cannot be fully exploited. Mostly these failures occur in the compression zones of the sandwich face panels or at load introduction points in the webs of pultruded sections. [P59, p2]

FRP bridge decks are generally very resistant to fatigue, though sandwich panels tend to be more sensitive than pultruded sections. Damages due to debonding failures between face sheets and core materials have been reported. Since this connection is somewhat more difficult to fabricate than the pultruded web connections it is expected that improvements in fabrication technology will increase the fatigue resistance of sandwich panel bridge decks. [P59, p2]

Since fiber reinforced bridge deck panels are usually processed as long, thin strips, the connection between these long strips becomes very important for the transverse properties, the load sharing behavior and the water tightness. The following picture shows for different connection methods of the bridge deck panels. The top left method ("Creative Pultrusion") uses a continuous glue layer as sole bonding method. This system is also used by "Fiberline" to connect for example the "FBD600 ASSET" deck panels. Next to the glue-only solution several other methods with additional FRP splice plates or FRP dowels also exist. The bottom left method ("Martin Marietta Composites") is the most used system in the USA. A problem with dowels and other mechanical fasteners such as bolts is the high local load induced at the point of connection. This problem is omitted when using glued bonds only. [P29, p53-55]

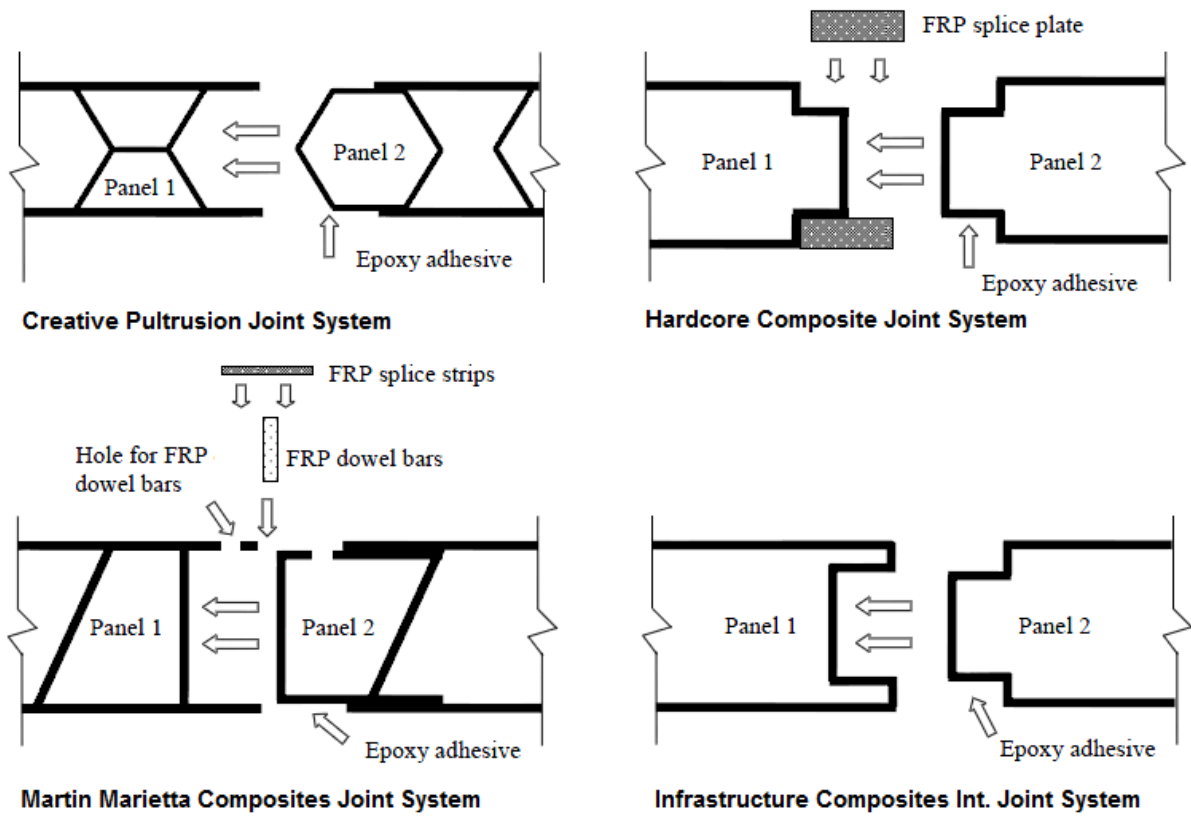


Fig. 76: Different methods to connect fiber reinforced polymer deck panels with each other [P29, p53-55]

Next to the connection of bridge deck panels to one another, they also have to be connected to the underlying girders. Since FRP decks have to compete with steel- or concrete bridge decks they also have to ensure similar composite behavior between the bridge deck and the underlying girder. Concrete bridge decks are connected to the main girders through dowels which ensure very good composite action, meaning that a certain width (the so-called "effective width") of the concrete deck above the girders contributes to the compressive strength of the upper flange of the main girders and thus to the total bending stiffness of the girder. Modern steel decks usually have an even better composite action with the girders, orthotropic steel decks are usually connected to the girder and therefore act in a similar way as concrete decks.[P29, p53-55]

To compete with traditional bridge decks FRP bridge decks also have to provide composite action. Else the main girders would have to be designed without or with less composite action. The different manufacturers have introduced several methods to ensure composite action between the two structural elements. The developed methods are very similar to the concrete deck methods. Strips in the bridge decks are cut open and filled with non-shrink grout. This grout encases metal studs welded to the underlying girder. Another method is the fastening of the deck to the girders via blind fasteners which are again encased by non-shrink grout. Though these methods lead to a certain degree of composite action, FRP bridge decks still do not guarantee an equal level of composite action such as concrete or steel decks. This is also caused by the significantly lower stiffness of the fiber reinforced polymer deck panels. This lower stiffness is further decreased by the transverse joints that are present in the panels. This is the reason that, when using traditional steel or concrete substructures for FRP decks the span is limited to about 20m.[P59, p2-3] Since this problem only occurs when steel or concrete girders are used it should not pose a limitation to the desired all-FRP design. The picture below shows the different solutions for FRP bridge deck – longitudinal girder connection.

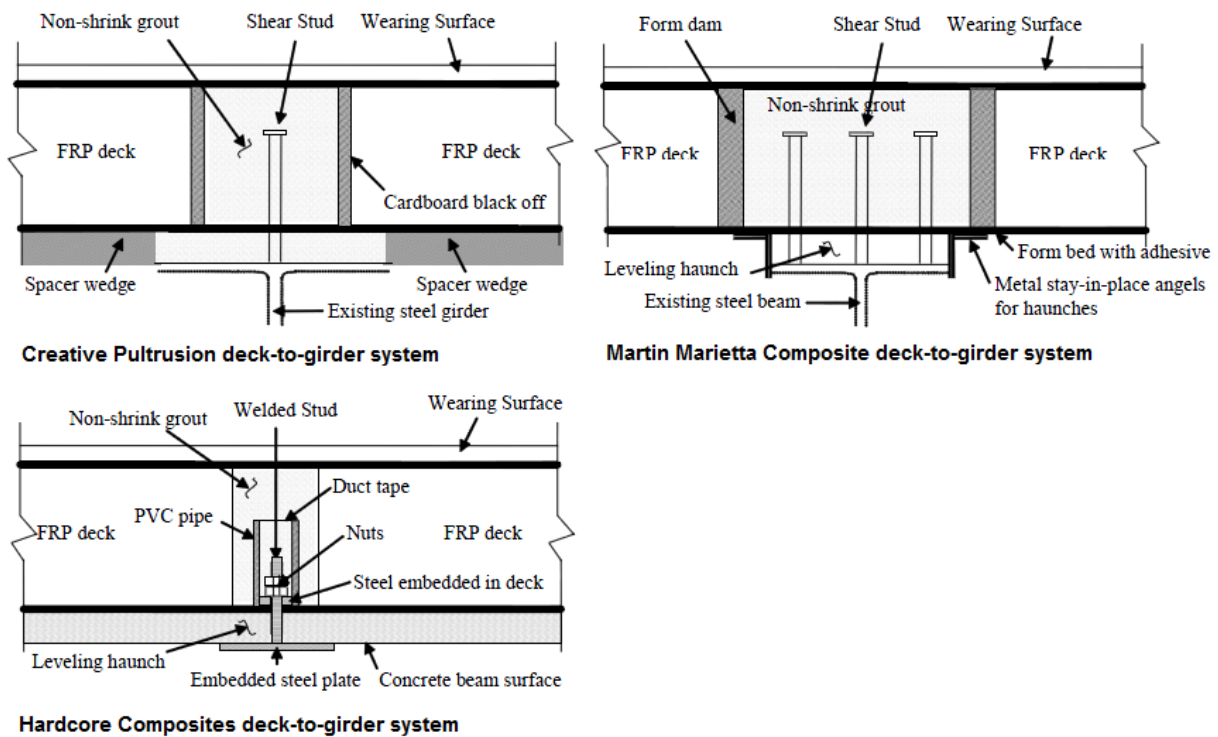


Fig. 77: Different solutions for deck-to-girder connection that deliver composite action [P29, p56-59]

To conclude this chapter some guidelines for the intended design will be given:

Material

First of all a choice has to be made on the material to be used. It seems rather obvious that an all-FRP bridge structure should also have a bridge deck made of this modern material. This point is even strengthened by the fact that in bridge design bridge decks are the part that is most often made of fiber reinforced polymers. The given examples show the diversity of available products. When using FRP as bridge deck material care has to be taken though: The fire behavior of fiber reinforced polymers is still an issue. Appropriate measures will have to be taken to ensure the fire safety.

Type of FRP bridge deck

As already mentioned two groups of FRP bridge decks exist: The multicellular pultruded panels and the sandwich panels. The sandwich panels have spans up to 10m which would make single transverse spans between the bridges sides possible. Multicellular panels would need additional supporting beams between the bridge sides because they have a limited span of about 3m. A disadvantage of the sandwich panels is their somewhat limited fatigue resistance compared to the multicellular panels, and the lower availability of commercial products. For now a slight preference exists for the multicellular panels in general and specifically the "Fiberline" products. Mechanical data of these products is readily available, and the fact that supporting beams for these panels would be needed can also be seen as an advantage: The supporting beam can increase the overall stiffness of the main cylindrical truss when properly connected.

Deck-to-girder connections

Before the composite action between bridge deck and underlying girders was discussed. This concept originates from traditional materials. If the bridge is designed to withstand all design loads without the composite action no problems should arise. This would make the design somewhat more inefficient, but would also enable easy replacement of the deck when the fatigue life is ultimately reached before the bridge design-life end. The design life of the load-bearing structure of the bridge is about 100 years, compared to 15-20 years in the case of the bridge deck. The deck-supporting girder in the cylindrical truss will be designed in such a way, that composite action is not needed to withstand design loads.

3.3 LOADS ON TRAFFIC BRIDGES

The applicable rules, actions etc. that have to be used during the design will be dictated by the Eurocode. The specific code that will be used is the NEN-EN1991: Actions on structures. The part that is most interesting in case of traffic bridge design is the NEN-EN1991-2: the Eurocode 1: Actions on Structures – Part 2: Traffic loads on bridges. Next to that the correction sheets of this code, the NEN-EN1991-2/C1 and the Dutch national annex, the NEN-EN1991-2/NB will be used.

The NEN-EN1991 or Eurocode 1 is part of the Eurocodes for the building industry which are shown below:

- EN1990 Eurocode: Basis of Structural Design
- EN1991 Eurocode 1: Actions on structures
- EN1992 Eurocode 2: Design of Concrete structures
- EN1993 Eurocode 3: Design of steel structures
- EN1994 Eurocode 4: Design of composite steel and concrete structures
- EN1995 Eurocode 5: Design of timber structures
- EN1996 Eurocode 6: Design of masonry structures
- EN1997 Eurocode 7: Geotechnical design
- EN1998 Eurocode 8: Design of structures for earthquake resistance
- EN1999 Eurocode 9: Design of aluminum structures

It has to be stated here that the above list does not contain a standard for fiber reinforced polymers as a building material. In one of the following chapters an investigation will be made, if other countries, maybe even outside of the European Union, do have national standards on the civil use of fiber reinforced polymers. Next to the traffic loads, the bridge also has to cope with other actions such as snow- and wind loads, thermal actions, actions during execution and accidental loads. The rules for these actions are all prescribed by other parts of NEN-EN1991 and will also be described in this chapter.

3.3.1 WIND LOADS

The lateral wind load on traffic bridges has to be calculated according to ‘Eurocode 1991-1-4, Actions on structures – General actions – Wind actions’ and the Dutch national annex of this code [NEN-EN 1991-1-4:2005/NB:2007]. Here, the general procedure will be given; the actual calculation of the values will take place during the design phase. The normal wind load F_w can be calculated using the following formula [NEN-EN 1991-1-4:2005, p27] :

$$F_w = c_f c_s c_d q_p A_{ref} \quad (3.1)$$

In this formula, q_p is the wind pressure, according to [chapter 3.3.1.1], A_{ref} is the reference surface of the structure according to [chapter 3.3.1.2], c_f is the force coefficient of the element according to [chapter 3.3.1.3] and $c_s c_d$ is the building factor according to [chapter 3.3.1.4]. The normal wind load can be transformed into a line load using the simple transformation:

$$q_{wind} = F_w / l_{bridge} \quad (3.2)$$

3.3.1.1 WIND PRESSURE q_p

The general formula for wind pressure is given by [NEN-EN 1991-1-4:2005, p24]

$$q_p(z) = \frac{\rho}{2} (v_m)^2 (1 + 7I_v) \quad (3.3)$$

Wherein: $\rho = 1,5 \text{ kg/m}^3$, which is the air-density according to [NEN-EN 1991-1-4,NB:2007, p9]. v_b is the base wind speed, and I_v is the turbulence intensity. Before the wind pressure can be calculated, first the ‘base wind speed’, the ‘roughness factor’, the ‘terrain factor’ and the ‘turbulence intensity’ need to be calculated. In the following the formulae for these parameters will be given. The premise for the procedure below is that the site for the bridge lies in The Netherlands, South Holland Province (Wind area II) in urban terrain (Terrain roughness III).

Base wind speed

The base wind speed can be calculated by the following formula: [NEN-EN 1991-1-4:2005, p21]

$$v_m(z) = c_r(z)c_o(z)v_b \quad (3.4)$$

Wherein: $c_r(z)$ is the roughness factor, calculated by the formula below, $c_o(z)$ is the orographic factor, which is set to $c_o(z) = 1$, for the Dutch flatlands. [NEN-EN 1991-1-4:2005, p21] The base wind speed $v_b = v_{b,0} = 27 \text{ m/s}$ for the Dutch province of South Holland, wind area II, according to [NEN-EN 1991-1-4,NB:2007, p3,4].

Roughness factor

In the case of a height above 7m ($= z_{min}$) above sea level and, in the case of terrain roughness III, urban area, $z_0 = 0,5m$ according to [NEN-EN 1991-1-4,NB:2007, p5]. The formula for the roughness factor $c_r(z)$ then becomes [NEN-EN 1991-1-4:2005, p21]:

$$c_r(z) = k_r \ln\left(\frac{z}{z_0}\right) \text{ for } z_{min} \leq z < z_{max} \quad (3.5)$$

In this formula k_r is the terrain factor, dependent on the roughness length z_0 .

Terrain factor

The terrain factor k_r is given by the following formula: [NEN-EN 1991-1-4:2005, p21]:

$$k_r = 0,19 \left(\frac{z_0}{z_{0,II}} \right)^{0,07} \quad (3.6)$$

Wherein $z_{0,II} = 0,05m$, the roughness length of terrain roughness category II, given by [NEN-EN 1991-1-4:2005, p22]

Turbulence intensity

The turbulence intensity I_v can be calculated using the following formula, according to [NEN-EN 1991-1-4:2005, p24]

$$I_v = \frac{\sigma_v}{v_m(z)} = \frac{k_r v_b k_l}{v_m(z)} \text{ for } z_{min} \leq z < z_{max} \quad (3.7)$$

Wherein σ_v is the standard deviation of the turbulence component of the wind speed. The standard deviation can be calculated using the value $k_l = 1$ for the turbulence factor according to [NEN-EN 1991-1-4:2005, p24].

3.3.1.2 REFERENCE SURFACE AREA A_{ref}

The reference surface area A_{ref} of the structure is the surface area of the truss bridge and can be calculated by the summation of the projected surfaces of all truss members in the vertical lateral plane of the bridge. In the form of a formula this is equal to: [NEN-EN 1991-1-4:2005, p72]

$$A_{ref} = \sum_0^n d_n l_n \quad (3.8)$$

The reference area can only be calculated when the exact dimensions of all bridge members are known. For preliminary design the conservative approach of taking $A_{ref} = A_c$, wherein A_c is the total surface area enclosed by the outer bridge edges, laterally and vertically projected. Another important value is the solidity ratio φ which denotes the ratio of reference surface area to total surface area. This ratio is needed in the calculation procedure of the force coefficient. [NEN-EN 1991-1-4:2005,p72]

$$\varphi = \frac{A_{ref}}{A_c} \quad (3.9)$$

3.3.1.3 FORCE COEFFICIENT c_f

The force coefficient c_f is given by the following formula [NEN-EN 1991-1-4:2005, p70]:

$$c_f = c_{f,0} \psi_\lambda \quad (3.10)$$

Wherein $c_{f,0}$ is the force coefficient of the truss without the so called end effects, $c_{f,0}$ can be derived from the design graph below for spatial trusses as a function of the solidity ratio φ : [NEN-EN 1991-1-4:2005, p71]:

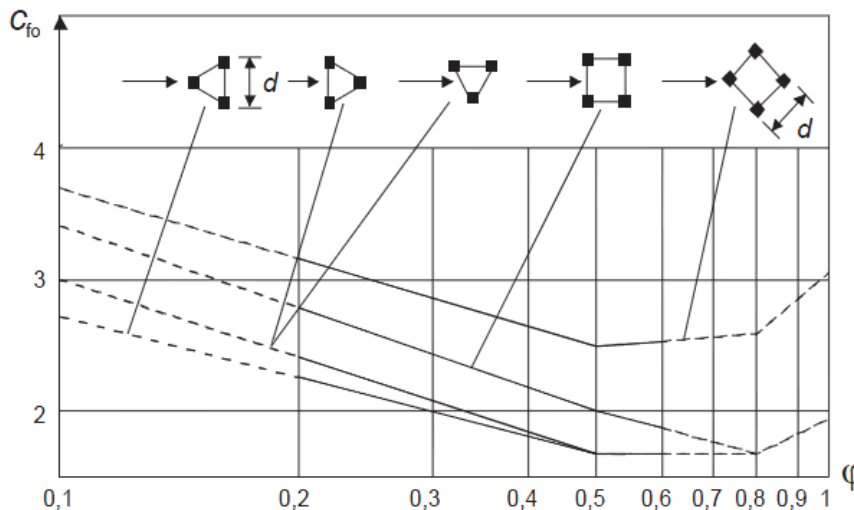


Fig. 78: Force coefficient for trusses without end effects as a function of the solidity factor [NEN-EN 1991-1-4:2005, p71]

The end effect factor ψ_λ for trusses as a function of the structure slenderness of the structure takes the smaller wind resistance of the structure at the ends into account. A conservative and safe value for this factor is $\psi_\lambda = 1$, assuming that there is no wind resistance reduction at the ends of the structure (See also [T09, p28]). The Eurocode uses the following formula for the slenderness λ of a truss girder: [NEN-EN 1991-1-4, Table 7.16, p74]

$$\text{Smallest value of } \lambda = 1,4 \frac{l}{h} \text{ or } \lambda = 70 \text{ for } l \geq 50m \quad (3.11)$$

$$\text{Smallest value of } \lambda = 2 \frac{l}{h} \text{ or } \lambda = 70 \text{ for } l < 15m \quad (3.12)$$

The values of λ for all span lengths between 15m and 50m need to be linearly interpolated. When the slenderness λ and the solidity ratio φ is known, the end effect factor ψ_λ can be derived from the following graph. [NEN-EN 1991-1-4, Figure 7.36, p75]

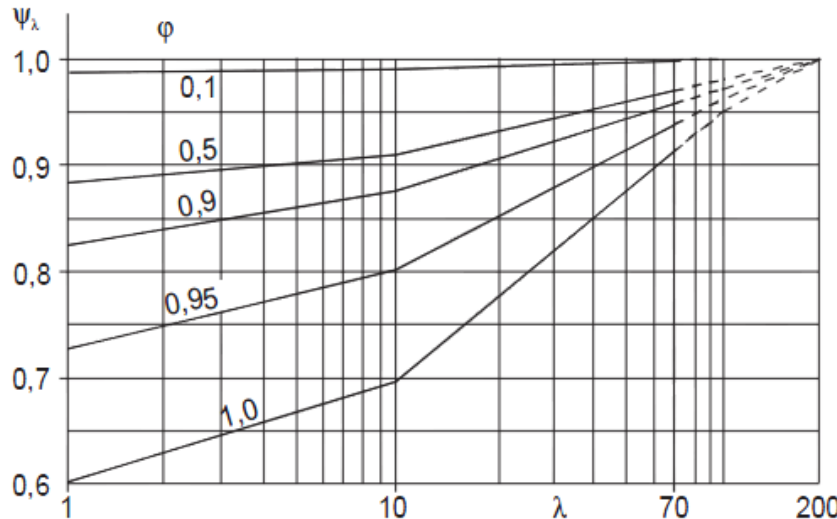


Fig. 79: End effect factor as a function of the slenderness λ and the solidity ratio φ [NEN-EN 1991-1-4, Figure 7.36, p75]

3.3.1.4 BUILDING COEFFICIENT $c_s c_d$

The building coefficient $c_s c_d$ takes account of the effects of the alternating wind pressure (c_s), as well as the vibrations caused by the wind turbulence (c_d). This coefficient takes into account all vibration effects due to wind load on a normal bridge. Since the part of the Eurocode on bridges [NEN-EN 1991-1-4:2005, chapter 8] as well as the Dutch national annex give no specific information on the calculation of this factor in the case of bridges, in this chapter the general procedure for civil engineering structures will be given, according to [NEN-EN 1991-1-4:2005, p29]. The calculation of this coefficient is time-consuming and requires knowledge on the structure, such as Eigen frequencies and mass per unit length, which can only be derived in a later design-stage. In the preliminary stage of design the value of the building coefficient will therefore be taken as $c_s c_d = 1$:

$$c_s c_d = I_v = \frac{1 + 2k_p I_v(z_s) \sqrt{B^2 + R^2}}{1 + 7I_v(z_s)} \quad (3.13)$$

Wherein k_p is the peak factor, denoting the proportion of the fluctuating part of the response and its standard deviation. B^2 is the background response factor and R^2 is the resonance response factor. z_s is the reference height for the building factor.

Resonance response factor

The resonance response factor R^2 can be calculated using the following formula: [NEN-EN 1991-1-4:2005, B.2, p95]

$$R^2 = \frac{\pi^2}{2\delta} S_L(z_s, n_{1,x}) R_h(\eta_h) R_b(\eta_b) \quad (3.14)$$

Wherein δ is the total logarithmic decrement of the damping is the sum of the structural damping $\delta = 0,04 - 0,08_s$ given for fiber reinforced polymer bridges by [NEN-EN 1991-1-4:2005, F.5, Table F.2, p134], the damping by a tuned mass-damper and the aerodynamic damping given by the following formula: [NEN-EN 1991-1-4:2005, F.5, p132]

$$\delta_a = \frac{c_f \rho b v_m(z_s)}{2n_{1,x} m_e} \quad (3.15)$$

Wherein $n_{1,x}$ is the first natural frequency of the structure; still to be calculated and m_e is the mass per length unit, also still to be calculated.

The value $S_L(z_s, n_{1,x})$ is the dimensionless spectral density function calculated by: [NEN-EN 1991-1-4:2005, B.1, p93]

$$S_L(z_s, n_{1,x}) = \frac{6,8 f_L(z, n)}{(1 + 10,2 f_L(z, n))^{5/3}} \quad (3.16)$$

Wherein $f_L(z, n)$ is a dimensionless frequency dependent on the Eigen frequency $n_{1,x}$ of the structure, the mean speed $v_m(z_s)$ and the turbulence length scale $L(z_s)$ derived by the following formula [NEN-EN 1991-1-4:2005, B.1, p93]

$$f_L(z, n) = \frac{n L(z)}{v_m(z_s)} \quad (3.17)$$

Wherein $L(z)$ can be derived using the following formula: [NEN-EN 1991-1-4:2005, B.1, p93]

$$L(z_s) = L_t \left(\frac{z}{z_t} \right)^{0,67+0,05 \ln(z_0)} \quad \text{for } z \geq z_{min} \quad (3.18)$$

Wherein $L_t = 300m$ which is the reference length scale and z_t is the reference height

The aerodynamic admittance factors $R_h(\eta_h)$ and $R_b(\eta_b)$ for a fundamental vibration are given by the following formulae: [NEN-EN 1991-1-4:2005, B.2, p95]

$$R_h(\eta_h) = \frac{1}{\eta_h} - \frac{1}{2\eta_h^2} (1 - e^{-2\eta_h}) \quad \text{with } R_h = 1 \text{ for } \eta_h = 0 \quad (3.19)$$

$$R_b(\eta_b) = \frac{1}{\eta_b} - \frac{1}{2\eta_b^2} (1 - e^{-2\eta_b}) \quad \text{with } R_b = 1 \text{ for } \eta_b = 0 \quad (3.20)$$

Wherein, according to [NEN-EN 1991-1-4:2005, B.2, p95]:

$$\eta_h = \frac{4,6h}{L(z_e)} f_L(z_s, n_{1,x}) \quad (3.21)$$

$$\eta_b = \frac{4,6b}{L(z_e)} f_L(z_s, n_{1,x}) \quad (3.22)$$

The background response factor B^2 describes the lack of a full correlation of the surface-pressure on the structure and can be calculated using the following formula. A value of $B^2 = 1$ is considered a safe, conservative estimate. [NEN-EN 1991-1-4:2005, B.2, p94]

$$B^2 = \frac{1}{1 + 0,9 \left(\frac{b+h}{L(Z_s)} \right)^{0,63}} \quad (3.23)$$

Wherein b, h are the width and height of the structure and $L(Z_s)$ is the turbulence length scale, given by [formula 3.18]

Peak factor

The peak factor k_p can be calculated using the largest value of the following formulae: [NEN-EN 1991-1-4:2005, B.2, p94]

$$k_p = \sqrt{2\ln(\nu T)} + \frac{0,6}{\sqrt{2\ln(\nu T)}} \text{ or } k_p = 3 \quad (3.24)$$

Wherein T is de median time of the reference wind speed, equal to $T = 600 \text{ sec}$. ν is the wind gust frequency given by:

$$\nu = n_{1,x} \sqrt{\frac{R^2}{B^2 + R^2}} \geq 0,8 \text{ Hz} \quad (3.25)$$

Wherein $n_{1,x}$ is the first Eigen frequency of the structure that thus first has to be calculated, before the exact value of the peak factor and thereby of the building coefficient can be derived.

Reference height

z_s is the reference height for the building factor, according to the following formula [NEN-EN 1991-1-4:2005, p30] for horizontal structures such as girders:

$$z_s = h_{base} + \frac{h_{structure}}{2} \geq z_{min} \quad (3.26)$$

3.3.2 SNOW LOADS

The normal design loads due to snow are given by the Eurocode 1 - Actions on structures – Part 1-3 – General Actions – Snow loads and the Dutch national annex [NEN-EN 1991-1-3:2003/NB:2007]. Special actions imposed on traffic bridges by snow are explicitly not covered in this code [NEN-EN 1991-1-3:2003, p9]. For an open tube type truss bridge, meaning the truss cells surrounding the bridge deck are not covered, it is assumed that the snow loads on traffic bridges can be assessed as snow loads on the ground according to [NEN-EN 1991-1-3:2003, chapter 4.3, p15]:

$$s_{Ad} = C_{esl} s_k \quad (3.27)$$

Wherein s_{Ad} is the calculation value of the snow-load on the ground for the considered location, C_{esl} is the coefficient for special snow loads and s_k is the characteristic value of the snow load on the ground for a specific location.

In the Netherlands, according to [NEN-EN 1991-1-3/NB:2007, chapter 4.1, p3] the characteristic value for the snow load on the ground for all Dutch regions and provinces has to be taken as:

$$s_k = 0,7 \text{ kN/m}^2 \quad (3.28)$$

The coefficient for special snow loads C_{esl} is given by [NEN-EN 1991-1-3:2003, chapter 4.3, p15] by:

$$C_{esl} = 2,0 \quad (3.29)$$

3.3.3 GENERAL LOAD CASES FOR TRAFFIC LOADS ON ROAD BRIDGES

The Eurocode defines four load models for vertical traffic loads on traffic bridges: Load Model 1 to Load Model 4. Next to that horizontal forces due to braking and accelerating and centrifugal forces are also considered. Bike- or pedestrian lanes are also covered. Traffic actions on road bridges, footbridges and railway bridges consist of variable and static loads, the Eurocode uses models that incorporate both load types in a single quasi-static load..

The described models are only valid for carriageways shorter than 200m. The models represent traffic loads due to cars, lorries, heavy vehicles and human crowds. To include traffic composition and density special adjustment factors have been introduced. The adjustment factors are part of the national annex, thus making them suitable for national traffic differences.

All load models have to be applied at the longitudinally most unfavorable place of the notional lane. Below the different load models will be described. Generally said, Load Model 1 and Load Model 2 are the most used load models. They cover the daily traffic loads, Load Model 3 and Load Model 4 are made for special occasion loads such as very heavy traffic or excessive crowd loading.

3.3.3.1 LOAD MODEL 1 (LM)

This model consists of concentrated as well as uniformly distributed loads, which cover most of the effects of the traffic of lorries and cars. This model should be used for general and local verifications. It consists of two partial systems: The tandem system and the UDL system. The denoted adjustment factors α are specified by the national annex. If they have not been specified, they should be set to unity. In the case of the Dutch national annex they are defined by [NEN-EN1991-2:2003/NB:2009, table NB.4.1, p6]

Tandem system

This system consists of two concentrated loads (tandem system) with each axle having the following weight:

$$\alpha_Q Q_k = \text{Axle weight} \quad (3.30)$$

$$\alpha_Q = \text{Adjustment factors}$$

Only one tandem may be set per lane. The tandem systems can only be applied as a whole, they should be placed centrally on the appropriate lane. The weight of the axle should be uniformly distributed between the wheels, defined by:

$$0,5\alpha_Q Q_k = \text{wheel weight} \quad (3.31)$$

The contact surface of wheels is square and 0,4m by 0,4m. The center of this square should be placed in a 2mx2m grid centrally in the lane. Adjacent tandems may not be placed closer than 0,5m to each other.

Uniformly distributed load system

The uniformly distributed loads system (UDL system) has the following weight per square meter of notional lane.

$$\alpha_q q_k = \text{Axe weight per } m^2 \text{ notional lane} \quad (3.32)$$

$$\alpha_Q = \text{Adjustment factors}$$

The UDL system has to be applied on the most unfavorable part of the notional lane.

Combination of Tandem System and Uniformly Distributed Load System

Both systems have to be applied simultaneously. The table below shows the prescribed loads for LM1.

Location	Tandem System	UDL system
	Axle loads Q_{ik} (kN)	q_{ik} (kN/m ²)
Lane Number 1	300	9
Lane Number 2	200	2,5
Lane Number 3	100	2,5
Other lanes	0	2,5
Remaining area	0	2,5

Table 31: Prescribed loads for LM1 [EN1991-2:2003, p37]

Two exemptions on the general LM1 rules exist: Where general and local effects can be calculated separately, the general effects may be calculated by using the following simplified alternative rules:

a) The second and third tandem are replaced by a second tandem system with axle weight equal to:

$$200\alpha_{Q2} + 100\alpha_{Q3} = \text{single replacement tandem weight} \quad (3.33)$$

b) For span length greater than 10m, each tandem system is replaced by a one-axle concentrated load of weight equal to the total weight of the two axles, denoted below.

$$600\alpha_{Q1} \text{ kN on Lane 1} \quad (3.33)$$

$$400\alpha_{Q2} \text{ kN on Lane 2}$$

$$200\alpha_{Q3} \text{ kN on Lane 3}$$

3.3.3.2 LOAD MODEL 2 (LM2)

Load Model 2 describes a single axle load applied on specific tire contact areas which covers the dynamic effects of the normal traffic on short structural members. The denoted adjustment factors β are specified by the national annex. If they have not been specified, they should be set to unity. LM2 consists of a single axle load. According to the Dutch national annex the value for β_Q is set equal to α_{Q1} . [NEN-EN1991-2:2003/NB:2009, Par. 4.3.3 (2)]

$$\beta_Q Q_{ak} = \text{Single axle load} \quad (3.34)$$

$$Q_{ak} = 400 \text{ kN} \text{ (including dynamic amplification)}$$

β_Q = Adjustment factors

This load should be applied at any location on the carriageway. When relevant only one wheel of $200\beta_Q$ kN may be taken into account. Next to expansion joints an additional dynamic amplification factor should be applied. The contact surfaces of the wheel should be set to 0,35m x 0,6m. These tire surfaces are different than in LM1, due to a different model. LM2 is normally the preferred model for orthotropic decks.

3.3.3.3 LOAD MODEL 3 (LM3)

Load model 3 is only used when special vehicles, like military or industrial vehicles use the bridge. A set of assemblies of axle loads representing special vehicles (e.g. for industrial transport) which can travel on routes permitted for abnormal loads have to be defined. Since it is not expected that special vehicles will use the bridge, Load Model 3 will not be used. If datasets of special vehicles that are likely to use the bridge, become available an additional analysis will be made. LM3 is intended for general and local verifications.

3.3.3.4 LOAD MODEL 4 (LM4)

Load model 4 is used to anticipate crowd loading in special occasions. It is intended only for general verifications. The load to be used is set to a uniformly distributed load of 5 kN/m^2 . This load includes dynamic amplification. It should be placed on all relevant parts of the bridge, including the central reservation. Load Model 4 is only applied when individual projects demand appropriate measures for such needs.

3.3.3.5 MULTI-COMPONENT ACTION

The above load models all have to be checked on simultaneity with each other and with other loads such as described in parts of [chapter 3.3.7]. Particularly horizontal forces such as braking and acceleration forces and pedestrian loads acting simultaneous to the earlier defined load models need to be checked. For this cause the Eurocode gives a table [NEN-EN1991-2:2003, p43, table 4.4a, "Assessment of groups of traffic loads (characteristic values of the multi-component action)"]. This table gives guidelines of which loads have to be applied in the case of combination of different load models. If Load Model 1 and pedestrian loads have to be checked, for example, all LM1 loads need to be applied together with a combination value of the vertical pedestrian loads, denoted by the national annex. In the case of the Dutch national annex the characteristic value for the distributed pedestrian load needs to be corrected with the factor $\Psi_0 = 0,4$.

3.3.4 FATIGUE LOADS ON TRAFFIC BRIDGES

A common governing load on bridges is the action of fatigue. Traffic running on bridges produces stress spectra which are dependent on the geometry of the vehicles, the magnitude of the axle loads, the vehicle spacing, the composition of the traffic and its dynamic effects. The Eurocode uses 5 fatigue load models: Fatigue Load Model (FLM) 1 to FLM5. FLM1 and FLM2 are the most general models, used to check whether the checked bridge has an unlimited fatigue life or not. FLM1 is more conservative, and FLM2 is more accurate when the simultaneous presence of several trucks on the bridge can be neglected. FLM1 and FLM2 are the most appropriate models for steel structures. Of the other three models, FLM5 is the most accurate model; it uses actual traffic data. FLM3, FLM4 and FLM5 are intended to be used for fatigue life assessment by reference to fatigue strength curves defined in other codes. They should not be used to check whether fatigue life is unlimited.

A traffic category on a bridge should be defined, for fatigue verifications, at least by the number of slow lanes and the number N_{obs} of heavy vehicles estimated per year and per slow lane. The following table shows the different categories, defined by the Eurocode:

Traffic categories		N_{obs} per year and per slow lane
1	Roads and motorways with 2 or more lanes per direction with high flow rates of lorries	$2,0 \times 10^6$
2	Roads and motorways with medium flow rates of lorries	$0,5 \times 10^6$
3	Main roads with low flow rates of lorries	$0,125 \times 10^6$
4	Local roads with low flow rates of lorries	$0,05 \times 10^6$

Table 32: Traffic Categories for Fatigue Load Models [EN1991-2:2003, p46, Table 4.5]

3.3.4.1 FATIGUE LOAD MODEL 1

FLM 1 has the same configuration as LM1. The axle loads however are equal to $0,7Q_{ik}$ and the values of the uniformly distributed loads are equal to $0,3q_{ik}$ and $0,3q_{rk}$. The maximum and minimum stresses $\sigma_{FLM,max}$ and $\sigma_{FLM,min}$ should be determined from the possible load arrangements on the bridge. FLM1 is thus a slightly less conservative model than the LM1.

3.3.4.2 FATIGUE LOAD MODEL 2

FLM2 consists of a set of idealized lorries, called frequent lorries. These frequent lorries are defined by the number of axles and the axle spacing, the frequent load of each axle, the wheel contact areas and the transverse distance between wheels. The maximum and minimum stresses $\sigma_{FLM,max}$ and $\sigma_{FLM,min}$ should be determined from the most severe effects of different lorries, separately considered, travelling along the appropriate lane. The frequent lorry specifications are defined by "table 4.6" of [EN1991-2:2003,p49].

3.3.4.3 FATIGUE LOAD MODEL 3

This model is also called the single vehicle model. Of the five models it is the most used model [T12, p29]. FLM3 consists of a set of four axles, each of them having two identical wheels. The weight of each axle is 120kN and the contact surface of each wheel is a square of 0,4m x 0,4m. The geometry is shown below:

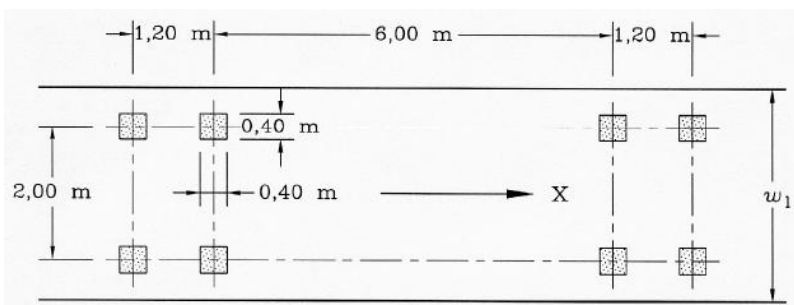


Fig. 80: Fatigue Load Model 3 geometry [EN1991-2:2003, p49, Fig.4.8]

3.3.4.4 FATIGUE LOAD MODEL 4

Fatigue load model 4 consists of a number of sets of standard lorries which together produce effects equivalent to those of typical traffic on European roads. The mix of traffic that is expected on the bridge has to be defined using tables 4.7 and 4.8 of "Eurocode 1" and the Dutch national annex [EN1991-2:2003, p51-52][NEN-EN1991-2:2003/NB:2009, p13]. In these tables 5 lorry types are defined, as well as 3 traffic types

and 3 wheel-axle setups. The maximum and minimum stresses $\sigma_{FLM,max}$ and $\sigma_{FLM,min}$ should be determined by the “Rainflow-“ or the “Reservoir-counting method”.

3.3.4.5 FATIGUE LOAD MODEL 5

If real recorded traffic data is available FLM5 can be used. Normally the data is supplemented by appropriate statistical and projected extrapolations. Exact specifications on the application of this model can be found in Annex B of Eurocode 1 [EN1991-2:2003, Annex B].

3.3.5 VIBRATIONS

The Eurocode prescribes the limitation of natural frequencies of structures and bridges in order to exclude vibrations due to traffic or wind which are unacceptable to pedestrians or passengers in cars using the bridge. Next to that fatigue damages due to resonance should be limited, as well as noise emission due to vibration. [EN1993-2:2006, p28]

The economic use of high-strength and lightweight materials in general and fiber reinforced polymers in specific has resulted in a trend towards more dynamically responsive structures. This trend is exacerbated by the emergence of new sources of vibration acting on buildings and bridges. As stated above, these vibrations have to be limited to ensure personal comfort. Vibrations mainly apply to the serviceability state and not to the ultimate limit state. However vibrations can lead to structural damage if damping is not sufficient and resonance occurs. [ISO 10137, pIV]

Since the vibration analysis for complex structures comes down to eigenvalue analysis of the complete stiffness matrix of the structure and the determination of the natural modes and -frequencies, the vibration analysis will be further discussed in the design phase, when FEM and FEA have been set up. In this chapter the characteristics of FRP vibrations, human induced- and vehicle induced vibrations will be discussed. Also some information on wind induced vibrations will be given.

3.3.5.1 VIBRATION OF FIBER REINFORCED POLYMERS

Not much research has been done on the vibration characteristics of FRP composites. In an American study [P31], the dynamic responses of a FRP bridge deck and a typical concrete bridge deck were compared. It turned out that dynamic impact on the FRP bridge was significantly lower than for the concrete bridge, leading to the conclusion that the dynamic impact factors used in the American AASHTO code for concrete bridge design can also be safely used for FRP bridge decks. In the same study it was also observed that the acceleration of FRP bridge decks is higher than that of concrete, but no conclusion on the effects of this on the long-term behavior of the bridge were made. [P31, p10]

Although not much information is available on the vibration energy absorption capabilities of FRP composites, it is expected that they exhibit high internal damping properties, which improve the vibration resistance of FRP structures. This aspect of composites may be relevant for traffic bridges, since they are predominantly subject to transitory, short-duration loads. [P08, p440R-11]

Another research on FRP vibration behavior [P77] showed that the joint type used (bolted or bonded) also greatly influenced the dynamic behavior of the FRP bridge. It showed that the lowest natural frequency of the Aberfeldy Footbridge was 26%-28% smaller for the bolted than for the bonded connection variant. This leads to the conclusion that bonded joints lead to higher natural frequencies, thus improving the vibration resistance. A drawback of bonded joints however was the lower damping ratio than the bolted joints, most probably because bolted joints exhibit a higher degree of friction during vibration. [P77, p10]

Finally, the laminate stacking sequence (LSS) of fiber reinforced polymer composite was also found to be influencing the vibration behavior of composites. Higher natural frequencies occur for plates with preferential stacking of $\pm 45^\circ$ plies in outer layers. The strongest improvement of natural frequency occurs

for rectangular plates in which the preferential stacking of outer plies is oriented perpendicular to the longest plate dimension. These laminates have the highest fundamental frequencies [B26, p5-94]

3.3.5.2 HUMAN INDUCED VIBRATIONS

The motion of walking and running may cause dynamic loading on structures such as bridges. In the past several light-weight pedestrian bridges, such as the London Millennium Bridge over the Thames have shown that human induced vibrations can give rise to significant vibrations, which can, in the worst case, lead to considerable structural damage of the bridge. Next to that, vibrations can also lead to large movements of the bridge structure, which cause considerable discomfort to the users. [B21, p136] The information in this chapter was derived from sources, describing the dynamic behavior of footbridges. It is expected that the added stiffness and dead weight of heavy traffic bridges will have a reductive effect on the susceptibility of the structure to dynamic effects. But since the low weight of FRP composites is something particularly new and unfamiliar in bridge design, the limits posed by human induced vibration will be considered here.

To analyze the effects of human movement on the dynamic behavior of the bridge, it is important to know the characteristics of human movement, and thus of pacing, walking, jogging and running in particular. The following table gives the typical vibration frequencies of human movement [B21, p137]

Type of walking	Pacing rate [Hz]	Forward speed [m/s]	Stride lengths [m]
Slow walk	1,7	1,1	0,60
Normal walk	2,0	1,5	0,75
Fast walk	2,3	2,2	1,00
Slow running (jogging)	2,5	3,3	1,30
Fast running (sprinting)	3,2	5,5	1,75

Table 33: Characteristics of typical human movement [B21, p137]

The above values are typical for human movement on bridge structures and it can be concluded that human pacing rates in the longitudinal direction out of the 1,5 Hz – 3,5 Hz region are very rare, and don't have to be considered for bridge design. [B21, p136] The lateral excitation frequency due to the sway of a person's center of gravity occurs at about half the pacing rate in the range of 0,75 Hz – 1,75 Hz. [B21, p1337]

To exclude the possibility of resonance with increasing amplitude due to human induced vibration, the Eurocode describes the following limits for the acceleration of footbridges. These limits are also called the "comfort criteria", defined in the Dutch national annex of NEN-EN1990 [NEN-EN 1990/A1:2005, p24]

$$0,7 \text{ m/s}^2 \text{ for vertical vibrations} \quad (3.35)$$

$$0,2 \text{ m/s}^2 \text{ for horizontal vibrations}$$

$$0,4 \text{ m/s}^2 \text{ for exceptional crowd conditions}$$

Furthermore the code postulates that the comfort criteria should only be verified for bridges when the fundamental frequency of the decks is smaller than the values described below. Note that the excluded values of natural frequency are exactly the values of human pacing. [NEN-EN 1990/A1:2005, p24]

$$5 \text{ Hz for vertical vibrations} \quad (3.36)$$

$$2,5 \text{ Hz for horizontal (lateral)and torsional vibrations}$$

During design the natural frequency of the bridge and its components will have to be analyzed using FEM-natural frequency analysis. It has to be guaranteed that the bridge will have a natural frequency above the above stated values.

3.3.5.3 VEHICLE INDUCED VIBRATIONS

The passage of highway vehicles over bridges can also induce resonant responses that are detrimental to ride quality, track stability or result in fatigue of structural members over time [B21, p136]

Typical highway bridges are seldom vulnerable to detrimental vibrations due to their configuration and mass, but occasionally it is necessary to check the response of a structure to vibrations caused by passing cars and trucks. The frequency of vibrations generated by highway traffic extends over a wide range depending on the vehicle configuration, speed and maintenance as well as the smoothness and state of the running surface. Highway traffic has been found to generally create vibrations with a frequency range of about 5 Hz – 25 Hz, which may excite individual elements on bridges, such as stay cables, external tendons or parts of the deck furniture but are seldom critical for the global behavior of the bridge. A possible exception is the combination of severe running surface defects with heavy traffic, which can generate significant impact loading.[B21, p141]

Since the dynamic effects of standard traffic loads are not particularly high and detrimental to normal traffic bridges the Eurocode does not give distinct restrictions on the damping and frequency response of traffic bridges. Instead, the dynamic effects of traffic loads are covered by the so-called ‘dynamic factor’, which is already included in the characteristic traffic load values described in [chapter 3.3.3]. [NEN-ENV 1992-2 :1996, p27]

Because of the low weight of FRP composites it has to be checked whether the natural frequency of the bridge does not lie in the range of the traffic frequency range of 5 Hz – 25 Hz. How this can be achieved will become clear during the design phase. Another important lesson learned during various researches [P31] was, that in order to reduce bridge vibrations generated by moving trucks and other traffic, the road roughness should be as small as possible. It is therefore vital to provide a very smooth road surface condition [P31, p10]

3.3.5.4 WIND INDUCED VIBRATIONS

When considering the dynamic response of structures to wind there are two main categories of mechanisms that may occur. Short-term variations in wind speed produce turbulent flow, or buffeting, that may result in resonant response of the structure. Excitation may also occur in smooth flow and these responses are categorized as aerodynamic instabilities.

All bridges are subject to the wind; however some types are more susceptible to dynamic response than others. For many simple bridge types their natural frequencies are sufficiently high as to avoid dynamic response. In this case it is usually sufficient to consider the wind to be a quasi-static load on the structure, as described in [chapter 3.3.1]. [B21, p122]

The Eurocode gives two important guidelines on the calculation of dynamic effects on bridges: First, the Eurocode regards dynamic calculations unnecessary for “normal road and railway bridge decks with a span of less than 40m. In this case normal means steel, concrete, aluminum or timber bridges, thus excluding fiber reinforced polymer bridges. [NEN-EN 1991-1-4:2005, p78] Secondly The Eurocode states that drag-effects due to wind may be neglected if the natural frequency of the affected structure at the windward side is larger than 1 Hz. [NEN-EN 1991-1-4:2005, p31] This limit

According to the Eurocode the first natural frequency of a simple plate girder or hollow section girder bridge may be estimated by the following formula. The factor K is $K = \pi$, for a single span bridge with two hinged supports, $K = 3,9$ for one cantilevered support, and $K = 4,7$ for two fixed supports. [NEN-EN 1991-1-4, p127] Note that this formula is only illustrative and may not be used instead of FEM natural frequency analysis for complex shaped bridges.

$$n_{1,B} = \frac{K^2}{2\pi L^2} \sqrt{\frac{EI_b}{m}} \quad (3.37)$$

L = span length

K = factor taking into account span and bound. cond.

m = mass per length unit

3.3.6 SERVICEABILITY LIMIT STATE DEFLECTION LIMITS

Since there do not exist clear deflection limits for FRP traffic and pedestrian bridges, first the limits of timber bridges will be given for illustration purposes. The Dutch national annex of “Eurocode 5” gives discrete limitations for girders, plates, truss-girders and for bridge decks [NEN-EN 1995-2:2005/NB:2009 Ontw., p6]:

- Girders, plates and truss girders: Maximum allowed deflection due to the characteristic traffic load: L/400
- Girders, plates and truss girders: Maximum allowed deflection due to pedestrian- or low-level traffic load: L/200
- Bridge deck: Maximum allowed deflection due to the characteristic traffic load: L/1400
- Bridge deck: Maximum allowed deflection due to pedestrian- or low-level traffic load: L/750

These are the Dutch deflection limits for timber bridges. For other materials no exact deflection limits are given in the appropriate Eurocodes; except for the vertical deformations of railway bridges, where the maximum vertical deflection measured along any track due rail traffic action may not exceed L/600 [NEN-EN 1990/A1, p27]. The reason for this is that deflection limits are serviceability criteria that are meant to control vibration according to the human tolerance to vibration. [P62, p50] The Eurocode gives these limits in the form of human comfort criteria which limit the acceleration of bridges, described in the national annex of Eurocode 1990 [NEN-EN 1990/A1:2005, p24], which have already been covered in [chapter 3.3.5.2].

A thorough research on different papers about FRP bridge engineering showed that most of them used the American AASHTO deflection limits for steel, aluminum and/or concrete structures for composite bridge design. These limits are described in the AASHTO LRFD Bridge Design Specifications [AASHTO-LFRD 1998]:

- Deflection limit due to vehicular load, general, on two-support span: L/800
- Deflection limit due to vehicular and/or pedestrian load, on two-support span: L/1000
- Deflection limit due to vehicular load on cantilever arm: L/300
- Deflection limit due to vehicular and/or pedestrian load on cantilever arm: L/375

The L/800 deflection limit for general vehicular load on two-support span was used by the following papers (the second number denotes the corresponding page): [P16, p30] [P18, p249] [P21, p323] [P29, p119] [P58, p10]. These papers concluded that the AASHTO limits provide safe, conservative results for FRP bridges and bridges with FRP decks. [P62, p68]

However, design of FRP bridges is usually controlled by deflection requirements, and meeting the same deflection requirement as conventional bridges, the L/800 requirement, may be uneconomical in many cases. Loosening this limitation, thus increasing them to L/400, has been suggested often in literature: [P31,

p419] [T12, p77] This limit also happens to be same deflection limit given for standard timber bridges under characteristic traffic loads by the Dutch Eurocode 5 annex. [NEN-EN 1995-2:2005/NB:2009 Ontw., p6]

To conclude this chapter an illustrative example of the all-FRP Aberfeldy footbridge, further described in [chapter 6.2.1], will be given. This pedestrian cable-stayed bridge was under scientific observation during construction and turned out to have a deflection of about L/1500 under a frequent live load of 2 kN/m². Also, the bridge had a first natural frequency of 2,7 Hz and viscous damping of 2,5% to 3,0% of critical damping. [P85 ,p5]

3.3.7 OTHER TRAFFIC LOADS ON TRAFFIC BRIDGES

Next to the general (vertical) load models of the Eurocode, several other (horizontal) loads have to be considered: Braking and acceleration forces, Centrifugal and other transverse forces. Since the carriageway of the bridge will be straight, thus will have no curvature in the length direction, the centrifugal forces will not have to be covered.

3.3.7.1 BRAKING AND ACCELERATION FORCES

A braking force Q_{1k} shall be taken as a longitudinal force acting at the surface level of the carriageway. The braking force is limited to 900 kN for the total width of the bridge. It should be calculated as a fraction of the total maximum vertical loads corresponding to the Load Model 1 likely to be applied in lane number 1, as follows:

$$Q_{1k} = 0,6\alpha_{Q1}(2Q_{1k}) + 0,10\alpha_{q1}q_{1k}w_1L \quad (3.38)$$

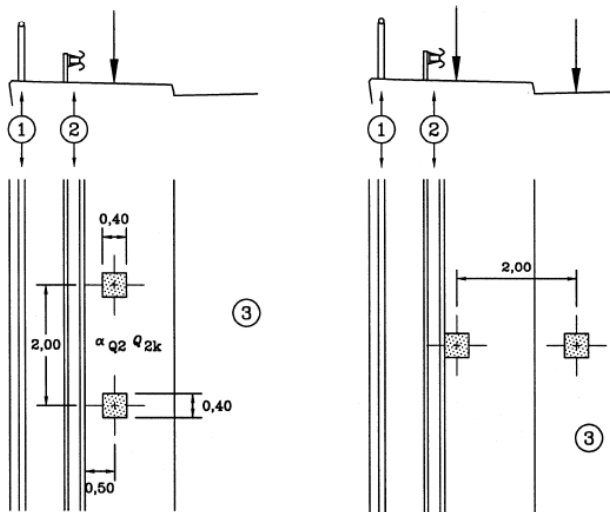
$$180\alpha_{Q1}(kN) \leq Q_{1k} \leq 900 (kN)$$

L = length of the deck (or part under consideration)

If Load Model 3 needs to be applied, specific braking forces of these vehicles need to be taken into account. The braking and acceleration force has to be applied along the axis of any lane.

3.3.7.2 VEHICLE ON FOOTWAYS AND CYCLE TRACKS

The event of a vehicle leaving the roadway has to be accounted for. The Eurocode provides the following rules: If appropriate safety-barriers (according to [NEN-EN1317-2]) are provided, wheel or vehicle loading between these barriers need not to be taken into account. In the case of providence of this barrier one accidental axle load corresponding to $\alpha_{Q2}Q_{2k}$ should be placed and oriented vertically on the unprotected parts of the deck such that the most adverse effect is achieved. This load should not be applied simultaneously with other load cases. The picture below shows the placement of the load. [EN1991-2:2003, p54]



Key
(1) Pedestrian parapet (or vehicle parapet if a safety barrier is not provided)
(2) Safety barrier
(3) Carriageway

Fig. 81: Placement of accidental vehicle loads [EN1991-2:2003, p54]

3.3.7.3 COLLISION FORCES

Vehicles colliding with parts of the bridge have to be taken into account. The Eurocode gives a guideline for the collision of vehicles with kerbstones: A horizontal load of 100kN has to be applied 0,05m below the top of the kerbstone. Next to that, in the unfavorable case, an additional vertical load of $0,75\alpha_{Q1} Q_{1k}$ has to be placed at the same position

The collision forces on the vehicle restraint system have to be taken into account by applying a load of the following magnitude; the classes described below depend mainly on the energy take-up of the restraining system. The load has to be applied as vertical line load a height 0,1m below the top of the restraining system with a length of 0,5m. An additional vertical load of $0,5\alpha_{Q1} Q_{1k}$ has to be applied simultaneously.

$$100kN \text{ for class } A \quad (3.39)$$

$$200kN \text{ for class } B$$

$$400kN \text{ for class } C$$

$$600kN \text{ for class } D$$

Collision forces on structural members that are not protected by restraining measures should also be taken into account. In the case of a cylindrical truss as main bridge structural system, the action may occur and will be taken into account. These forces are defined by the Dutch national annex: Non-concrete bridges should be able to take up a load of the following magnitude, choosing the one with the most adverse effect. This load has to be applied at a height of 1,20m above the deck, in a rectangle of 0,25xwidth(structure).

$$1000kN \text{ in longitudinal direction} \quad (3.40)$$

or

$$500kN \text{ in transverse direction}$$

3.3.7.4 LOAD MODELS FOR FOOTWAYS AND CYCLE TRACKS

The Eurocode prescribes three independent load conditions that all have to be checked:

$$q_{fk} = \text{a uniformly distributed load} \quad (3.41)$$

$$Q_{fwk} = \text{a concentrated load}$$

$$Q_{serv} = \text{loads representing service vehicles}$$

When the crowd loading load model (LM4) does not have to be applied, q_{fk} should be calculated by:

$$q_{fk} = 2,0 + \frac{120}{L + 30} kN/m^2 \quad (3.42)$$

$$q_{fk} \geq 2,5 kN/m^2; q_{fk} \leq 5 kN/m^2$$

The distributed load q_{fk} should only be applied in the unfavorable parts of the influence surface, longitudinally and transversally. The value for Q_{fwk} should be set to 7kN acting on a surface of 0,1m x 0,1m. The axle load of the service vehicle load should be taken as 25kN, having two axles at 3m apart, and each axle having two wheels spaces 1,75m. The contact surface for each wheel should be set to 0,25m x 0,25m. In the case of a traffic bridge, horizontal forces due to pedestrian or cyclists do not have to be taken into account.

4. FIRE SAFETY

Since polyester-, vinyl ester- and epoxy resins are based on organic substances composed of carbon, hydrogen and nitrogen atoms, they are inherently flammable to varying degrees. [A08, p66-67][B21, p498-499] Fiber reinforced polymers are often made up of such resins, therefore, in structural design this poses a problem, since the occurrence of fire and heat can never be ruled out from the scope of design loads. Generally said, the authorities require bridges to be structurally safe, even in the case of an occurring fire, for example due to a car- or lorry-explosion.

The picture below shows the extinguishment of a fire under a concrete heavy traffic bridge in Germany. After the fire, the bridge had to be closed for all traffic weighing over 7.500kg. These severe consequences of a fire under generally inflammable concrete bridges illustrate even more the necessity of fire safety engineering for fiber reinforced polymer bridges. [WEB, www.kfv-pinneberg.de]



Fig. 82: Bridge fire in Germany [WEB, www.kfv-pinneberg.de]

4.1 DEFINITION OF FIRE

Before discussing the fire properties of bridges and FRP in specific, first the general fire mechanism has to be covered. Typical fires are composed of turbulent flames consisting of three zones, divided from base to top in the solid flame region, the intermittent flame region and the thermal plume region. The lowest zone houses the main exothermic reaction of the flammable vapors. This is the zone where most heat is produced. The temperature in this region is about 800°C-900°C for most solid fuels and 1150°C-1250°C for hydrocarbon or gas fuels. In the intermittent zone the temperature drops gradually with increasing distance from the solid flame region. The boundary between the zones is not well defined and has a large amount of overlap. The temperature in the intermittent region is varying from 300°C-600°C, but on average about 400°C. The highest region is the thermal plume region where no flames are visible and the temperature drops with height. This region consists of hot gases, vapors and soot particles that are carried upwards by convective heat. [B7, p6]

The initiation and growth of fire is determined by several factors including the type and the caloric value of fuel, fuel load, fuel size (area of burning fuel), and oxygen content in the flame, the wind speed and whether the fire is in an open or confined space. In fiber reinforced polymers the material itself can be a very rich source of fuel that causes the temperature to rise and the flame to spread. [B7, p7]

During a fire five general stages can be distinguished. Below the classification of compartment-fire stages can be found:

Ignition

This is the point when the fuel source ignites and undergoes sustained flaming combustion.

Growth

The initial growth of a fire is dependent mainly on the fuel itself, with little or no influence from the combustible materials within the compartment. The fire will grow and the compartment temperature will continue to rise if sufficient fuel and oxygen are available. It is often in this stage that composite materials exposed to the flame will ignite when the temperature exceeds 350°C -500°C.

Flashover

This occurs when the fire is fully developed and all combustible items in the compartment (including any composite materials) are involved in the fire. Flashover (the point when all combustible materials/gases suddenly ignite) usually occurs when the average upper gas- temperature in the room exceeds about 600°C.

Fully developed fire

This stage occurs when the heat release rate and temperature of a fire are at their greatest. The peak temperature of a typical post-flashover room fire is 900°C -1.000°C, although it can reach temperatures as high as 1.200°C.

Decay

The final decay stage occurs as the fuel and combustible materials become consumed, causing the compartment temperature to fall. Obviously, decay can also be caused by active fire suppression systems, such as sprinklers. [B7, p7]

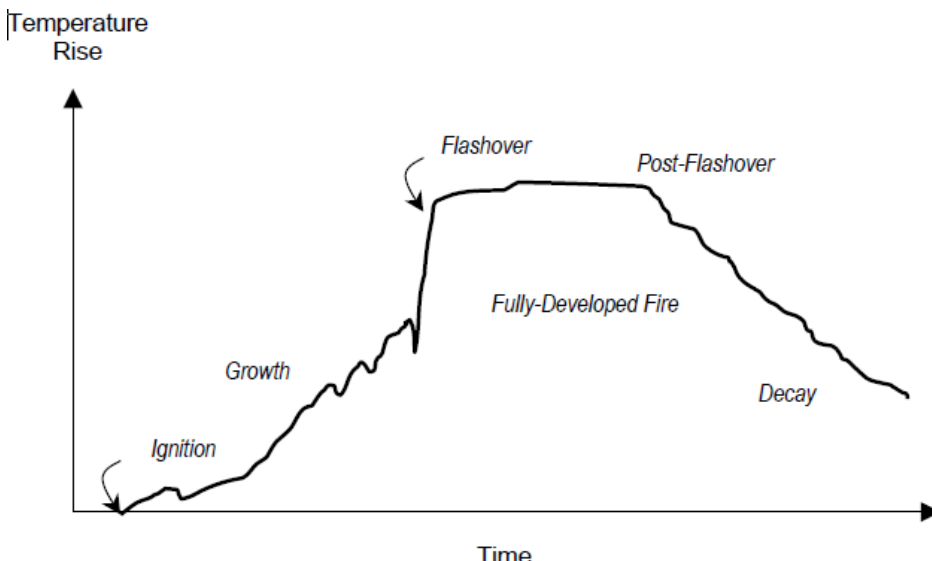


Fig. 83: Growth of a compartment fire with the different fire phases [B07, p8]

In the fire engineering practice it is more common to quantify the intensity of a fire by the radiant heat flux, rather than the flame temperature. Below some typical values for the radiant heat flux in the case of different fires can be found.[B7, p9]

- Small smoldering fire: 2-10 kW/m²
- Trash can fire: 10-50 kW/m²
- Room fire: 50-100 kW/m²
- Post-flashover fire: > 100 kW/m²
- Gas-jet fire: 150-300 kW/m²

4.1.1 FIRE CURVES

In the past several fire curves have been developed for several different purposes in the fire safety industry, such as building design, road- and rail-tunnel design etc. The fire curves model different heating conditions. The fire curves below have been implemented in the applicable Eurocode [NEN-EN 1991-1-2]. The curves shown below will be briefly described in the following. All descriptions are based on the same code, as mentioned before.

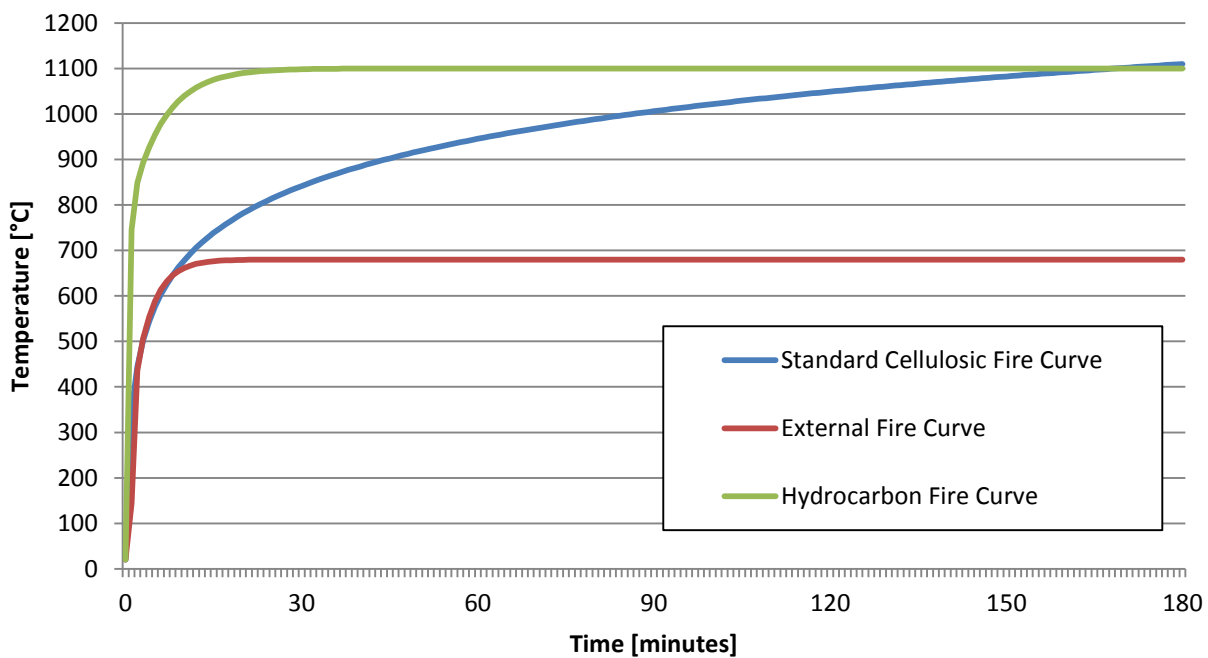


Fig. 84: Standard fire curves [NEN-1991-1-2-2002, p23]

Standard Cellulosic Fire Curve

$$\theta_g = 20 + 345 \log_{10}(8t + 1) \quad (4.1)$$

θ_g = gas temperature [°C], t = time [min]

$$\alpha_c = 25 \text{ W/m}^2\text{K} \text{ coefficient of heat transfer} \quad (4.2)$$

The International Organization for Standardization (ISO) developed this curve to describe ventilated controlled compartment natural fires, for example fire in a normal building. This curve concentrates on fire of materials normally available in typical buildings, such as timber and paper. Therefore it has a quite shallow increase of temperature compared to the other curves. The temperature reached after 30 min is 842°C. This is the most used fire curve for normal building fires.

Hydrocarbon Fire Curve

$$\theta_g = 1080(1 - 0,325e^{-0,176t} - 0,675e^{-2,5t}) + 20 \quad (4.3)$$

θ_g = gas temperature [°C], t = time [min]

$$\alpha_c = 50 \text{ W/m}^2\text{K coefficient of heat transfer} \quad (4.4)$$

This is the designated fire curve for more severe fires, involving flammable materials like petrol gas, chemical, gasoline etc. The burning rate is well in excess of that of the cellulosic curve. The hydrocarbon curve is applicable when petrol fires could occur, such as for example car fires, petrol or oil tankers and chemical tankers. The hydrocarbon fire curve reaches its maximum temperature of 1100°C just under 30 minutes, making it the most severe fire loading curve of NEN-EN-1991-1-2.

External Fire Curve

$$\theta_g = 660(1 - 0,687e^{-0,32t} - 0,313e^{-3,8t}) + 20 \quad (4.5)$$

θ_g = gas temperature [°C], t = time [min]

$$\alpha_c = 25 \text{ W/m}^2\text{K coefficient of heat transfer} \quad (4.6)$$

This fire curve emulates the occurrence of a fire on the outside of an enclosed space, thereby exposing the outer structural elements to heat. Because the heat can freely dissipate in the open, this fire curve imposes much less severe fire loads on the structure it is used for. The external fire curve reaches its maximum temperature of 680°C in about 20 minutes. Since the bridge to be designed will be placed in an outside environment, this could very well be the most suitable curve for bridge design. However, traffic bridges are also prone to possible fuel fires, making the more severe hydrocarbon curve applicable.

Other fire curves

Other fire curves for more specialized applications do exist. Especially the need for adequate fire safety in extremely confined spaces, such as traffic tunnels, call for even more severe fire curves. For example “Rijkswaterstaat” of the Netherlands developed the “RWS Fire Curve” for road and rail tunnels which reaches its peak temperature of about 1350°C in about 60 minutes. Germany and France have also developed similar fire curves for road- and rail-tunnels. The fire curves for tunnels will not be covered in this research, due to the very different nature of tunnel fires concerning the spread of fire in general, and the heat dissipation profile in specific, compared to bridge fires.

4.2 FIRE SAFETY OF BRIDGES IN GENERAL

In this chapter the fire safety will be discussed, especially for the case of fire safety for bridges in general and traffic bridges in specific.

4.2.1 FUNDAMENTALS

The basic principles of fire-safety design and related fire-safety objectives can be applied in any other phenomenon associated with fire, for example fire growth, hot gases and effluents movement, structural and compartmentalization behavior. The general fire safety objective can be summarized in the following points: [NEN-ISO 23932:2009, p1]

- Safety of life
- Conservation of property and structural integrity
- Continuity of operations
- Protection of the environment
- Preservation of heritage

This chapter will be started with a very general approach on the actions that fire engineers must take in order to obtain sufficient fire safety in any structure. The following flowchart will address the different steps that need to be taken during the fire safety design of any structures:

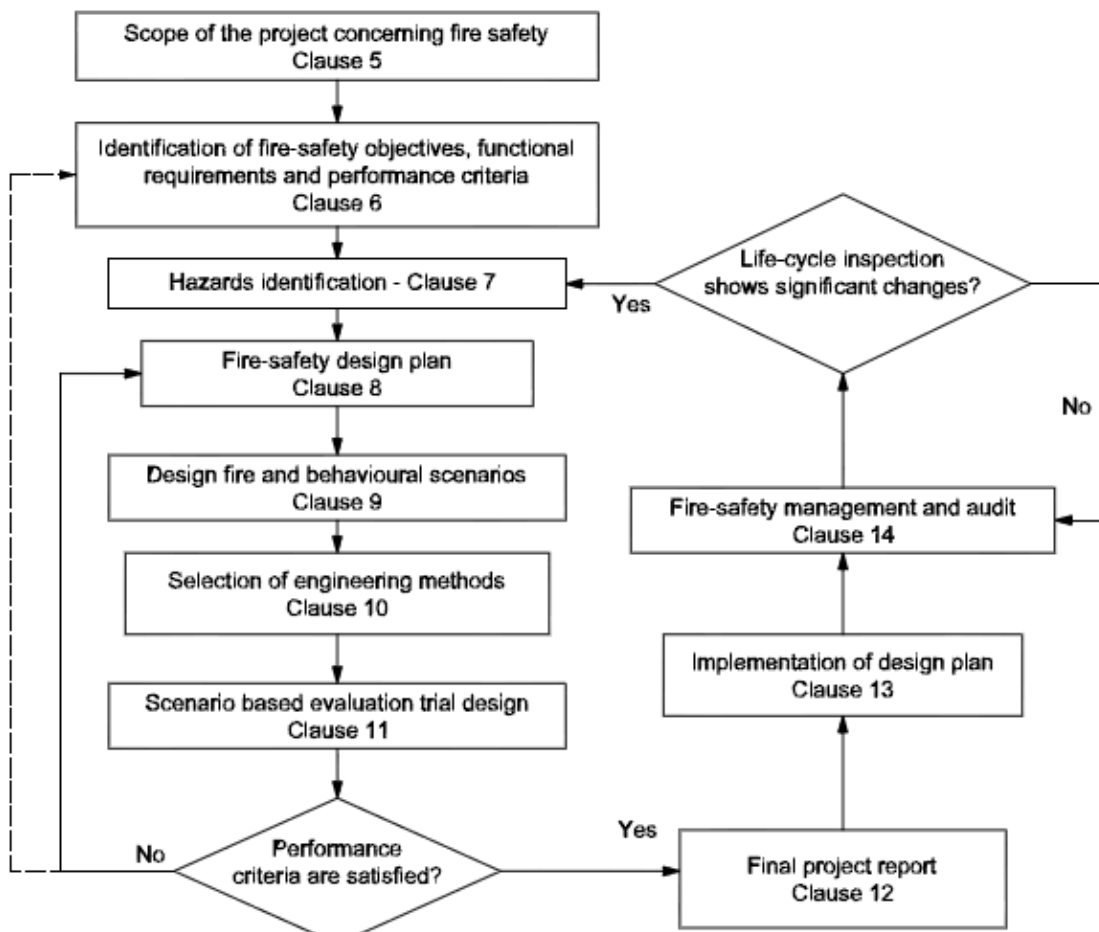


Fig. 85: General flowchart illustrating the fire-safety engineering process for design, implementation and maintenance [NEN-ISO23932:2009, p4]

The flow chart above shows the various steps required for the development of a fire-safety engineering process that fully meets the requirements of all interested/affected parties. After having defined the scope of the project (Clause 5), the first step (Clause 6) involves the development of fire-safety objectives, related functional requirements and quantitative performance criteria for the various design functions (e.g. fire protection) that are required to achieve the fire-safety objectives. A specific fire-safety design plan is then developed (Clause 8), containing trial design elements that can potentially satisfy the quantitative performance criteria according to a preliminary hazards identification (Clause 7).

It is necessary to agree on a set of design fire scenarios that can be used to challenge the performance of these design functions (Clause 9). Whether the performance criteria are, in fact, satisfied is determined by an engineering analysis of the trial design, as described in (Clause 11), making use of engineering methods selected as indicated in (Clause 10). If the performance criteria are not satisfied by the trial design, modifications are required until a final design plan in line with requirements is achieved. The final project report, including the necessary documentation, is produced and validated (Clause 12).

The implementation of this final design plan leading to the erection of the built environment is discussed in (Clause 13). Even after the implementation is completed, the fire-safety engineering process continues with periodic inspections and ongoing fire-safety management procedures as described in (Clause 14). [NEN-ISO 23932:2009, p3]

The described code also gives three important questions, which summarize the fire safety engineering processes and -measures very clearly: [NEN-ISO 23932:2009, p5]

What are the required/desired outcomes of all foreseeable fire safety measures?

This question addresses the objectives of the fire safety design.

How will these outcomes be achieved by design functionality?

This question focuses on the actual functional requirements and measures that have to be taken to achieve the earlier set goals.

How will the adequacy of the design be measured in engineering terms?

The last question considers the actual performance criteria of the design: It quantifies the fire safety measures taken and compares them with the goals set in the first question.

4.2.2 SPECIFIC BRIDGE FIRE SAFETY

Extensive research on different codes and regulations showed that there is very little prescribed on the fire safety of bridges. The only way of achieving sufficient fire safety is to revert to the performance based design, just like mentioned in [chapter 4.2.1]. of the last section. This means that the fire safety engineer has to choose specific needs of the fire design. This can mean a fire safety period of 30 minutes for example, which means that the structural integrity must be fully guaranteed in the first 30 minutes of a fire. These needs can only be defined in a later stage, during the design of the fiber reinforced polymer bridge. It is important to mention that a bridge with a bridge deck which is fully enclosed by a cylindrical truss has a very different, most probably worse, heat dissipation profile than a bridge with an open bridge deck. During design, this has to be considered, possibly by applying design rules for the fire safety of tunnels.

The following list shows the actions and their order that can induce fire damage on any traffic bridge. This general flow of actions can be used for most traffic bridges. [P90, p3]

- Initial accident
- Release or spill of fuel or other flammable contents
- Ignition of the flammable materials
- Fire and/or explosion
- Fire exposure of unprotected bridge elements

- Severe damage to the bridge

These actions clearly show that bridges can be damaged, even by little accidents. These accidents can cause the follow up actions such as spill of fuels, and may have devastating consequences on the bridge and its users. The reasons why sufficient fire protection is always necessary in the case of traffic bridges can be found below: [P90, p8]

Protect people

The fire protection measures are necessary to protect the people, their lives and their health. That means that possibilities of egress should always be provided. Traffic disruption should also be minimized to stop more people from getting hurt in the case of an occurring accident.

Protect assets

The fire protections should always be aimed at maintaining the existing infrastructure. Next to that the threat of elements being exposed to fire should be minimized. Also the fire protection measures should extend the useful life of the bridge and aim at maintaining stable usage, thus not overloading the bridge.

Protect environment

Finally, the fire protection measures should also protect the environment. This means that in the case of fire no excessive smoke or liquid spill should pollute the environment.

4.2.2.1 METHODS OF PROTECTING BRIDGES

Several methods exist to protect bridges; here they will be discussed. Specific fire protection methods for FRP will be discussed more in detail in chapter 4.3. The two most obvious measures are also often hard to realize in an environment with set design parameters and boundary conditions: First, the under-passing traffic should be limited to low-limit vehicles, e.g. no tankers. Secondly, the over-passing height of the bridge should be increased, thereby reducing the proximity of the bridge to possible under-passing fire sources. [P90, p9]

The next possible method to protect bridges from fire damage is to eliminate the exposed and unprotected elements of the bridge. Also, active fire suppression measures such as sprinklers; CO₂ gas installations etc. can be installed. [P90, p9]

The perhaps most often used method of fire protection is the utilization of passive fire protection measures such as for example the application of inorganic, gypsum, silicate or magnesium oxychloride panels that are inflammable and are very heat resistant. One can imagine that the option of providing protective panels is not very applicable in the case of curved trusses composed of circular hollow sections. The added cost of such panel systems is generally mediocre. [P90, p10-12]

The next method of passive fire protection is the application of formed in place materials, such as added layers of concrete, which have the disadvantage of being thick and heavy and having only a limited corrosion resistance. The formed in place materials are at about the same magnitude of cost as the panel systems. [P90, p13] In the same family of protection measures are the spray applied materials, which are mostly thinner and lighter than the former method. Often they consist of sprayed fibers and cementitious lightweight materials such as cement/sand/vermiculite mixtures. They have the great advantage of low cost. Both methods described in this section are not very useful to be applied on smooth circular hollow sections, that are always visible and are supposed to be visible and visually attractive to the user of the bridge. [P90, p14]

The last method of passive fire protection to be described here is the intumescent coating fire protection, where structural elements are coated in a thin (max. 1-2mm) layer of so called intumescent materials. These materials foam up during fire and swell up to about 40-100 times of their initial thickness, thereby protecting the underlying structural material. These coatings are very well suited to protect structural

elements without being visibly obstructive. [P90, p15] In chapter 4.3 on FRP specific fire protection these coatings will be discussed in more detail.

4.2.2.2 PRACTICAL GUIDELINES AND CODES

First of all, the European code Eurocode 1: Actions on structures – General actions – Actions on structures exposed to fire [NEN-EN 1991-1-2:2003/NB:2007] gives a general guideline on the fire design of structures in general: [NEN-EN 1991-1-2:2003/NB:2007, chapter 2.1, p19]

- Choice of the applicable design fire scenario
- Determination of the corresponding design fire
- Calculation of the temperature increase within the structural elements
- Calculation of the mechanical behavior of the structure that is exposed to fire

Next to the general code described before the European codes on fire design of steel structures, and steel-concrete composite structures also give a lot of valuable information. The codes are the Eurocode 3: Design of steel structures – Part 1-2: General rules – Structural fire design [NEN-EN 1993-1-2:2005/NB:2006] and Eurocode 4: Design of composite steel and concrete structures – Part 1-2: General rules – Structural fire design [NEN-EN 1994-1-2:2005/NB:2007]

As mentioned, for bridges, a vehicle fire with possibly leaking fuel must always be considered as a possible scenario during service life. Especially bridges with the main support structure lying above the bridge deck need to be properly protected against failure due to fire. Of course, in the case of bridges passing over roads, burning vehicles and fuel from the road below also need to be considered. For fast response to small occurring fires on the bridge itself fire extinguishing measures must be placed in short distances. The structural elements need to be sufficiently redundant such that no collapse of the complete structure occurs if only a few elements are damaged. [B06, p138] The redundancy of the different elements must of course always be accompanied by excellent fire reaction and fire resistance properties, which will be described in [chapter 4.3] for fiber reinforced polymer materials.

The American code “NFPA502” issued by the ‘National Fire Protection Association, USA’ gives some information on the provisions that need to be taken for the fire protection of bridges and elevated highways. The measures described in chapter 6 of this code are mainly focused on traffic control, emergency communication, signage, water supply and drainage. Some of the rules will be described here:

When the distance to the nearest water source to any point on the bridge exceeds 120m, the bridge needs to be equipped with a standpipe system [NFPA502, par. 6.5].

Closure of the bridge should be possible; fast evacuation of the vehicles present on the bridge need to be possible at all times. [NFPA502, par. 6.4]

Another important provision that needs to be taken is the supply of drainage systems, such that spilled flammable liquids can be removed from the bridge deck in a fast and efficient way. Furthermore expansion joints need to be designed such that fuel, possibly burning cannot spill on roadways beneath the bridge. [NFPA502, par. 6.6]

The American code furthermore gives some general fire data for typical vehicles present on traffic roads. The values shown in the table below correspond well with European fire data for these vehicles.

Cause of fire	Equivalent size of gasoline pool [m ²]	Heat Release Rate [MW]	Smoke Generation Rate [m ³ /sec]	Maximum Temperature [°C]
Passenger Car	2	8	20	400
Van	5	15	40	550
Bus or Truck	10	30	60	700
Gasoline Tanker	30-100	120	100-200	1000

Table 34: Fire loads due to different road vehicles fires [NFPA502, p19]

4.3 FIRE SAFETY OF FIBER REINFORCED POLYMERS

Despite all the advantages of fiber reinforced polymer composites that were covered in [chapter 2], there is one major disadvantage of composite materials: The performance in fire is generally very poor. When composites are exposed to high temperatures, above 300°C, the organic matrix quickly decomposes with the release of heat, smoke, soot and toxic volatiles. When organic fibers such as aramid or polyethylene are used as reinforcement, the fibers also decompose and contribute to the heat and smoke release. [B07, p3]

Next to that, composites also soften, creep and distort at even lower temperatures, above 100°C-200°C, which can result in buckling and eventually failure of load-bearing structures. Due to the release of heat, smoke and gases firefighting becomes extremely hazardous during FRP fires. This disadvantageous property of fiber reinforced polymers is the main reason for the very infrequent application of this material in the infrastructure sector. [B07, p3]

However, in the aerospace industry, high tech plastic composites are often used as heat shields for space-crafts re-entering the earth's atmosphere. This somewhat contradicts to the earlier statement that FRP composites behave very poorly under elevated temperature conditions. Composites have excellent thermal insulation properties and conduct heat much slower than steel or other metals. Next to that FRP can be tailor-made to have improved resistance against pyrolysis. Properties that can be improved with alteration of matrix composition include ignition time, heat release rate, heat of combustion, smoke production and toxic potency of gas products. An added fact is the availability of thousands of different matrix compositions which all have very different fire properties. Some burn quick and violent whilst others can withstand temperatures over 1.300°C. [B07, p3] [B23, p406]

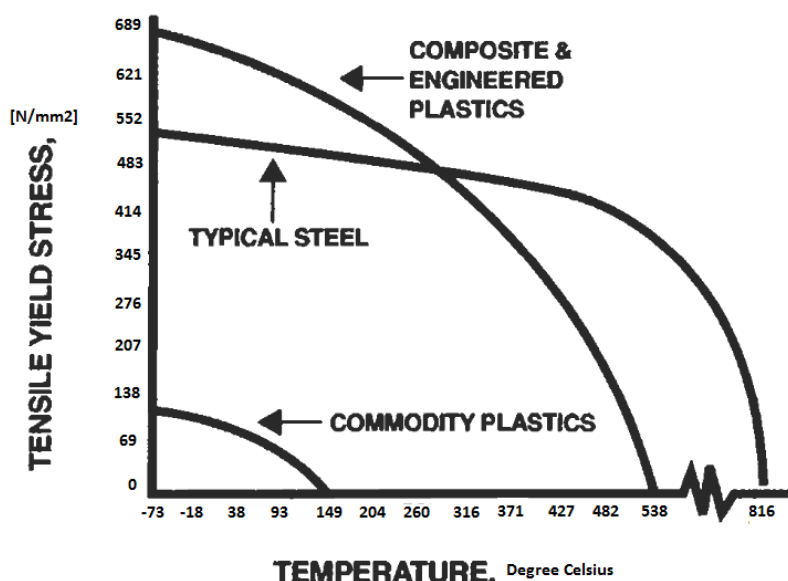


Fig. 86: Tensile Yield Stress vs. Temperatures for plastic, engineered plastics and structural steel [B23, p407]

Although, due to the variance in possible matrix compositions it is very hard to put a single value onto the fire resistance of FRP, the above graph shows a general view on the yield strength of plastics under elevated temperatures. Note the extremely low yield strength at temperatures over 100°C. Steel shows the known behavior and loses all strength at about 816°C. Composites lose their strength at about 540°C, which makes fire protection measurements indispensable.

This chapter will cover all important topics of fire safety in fiber reinforced polymers. First the mechanism of fire will be discussed, followed by the important parameters describing fire properties of materials in general. Afterwards the fire decomposition mechanism of some commonly used matrices and fiber reinforcements will be covered. Following, the fire reaction and fire resistance of FRP materials will be discussed, as well as the perhaps most important topic, the improvement of the fire properties of FRP composites.

4.3.1 CHARACTERISTIC VALUES DESCRIBING THE FIRE PROPERTIES OF A MATERIAL

The fire hazard of materials is often defined by their fire reaction and their fire resistance. Fire reaction is used to describe the flammability and combustion properties of a material that affect the early stages of fire, generally from ignition to flashover. Fire reaction also describes the smoke toxicity of a combustible material. Fire resistance defines the ability of a material or structure to impede the spread of fire and retain mechanical integrity. In other words, fire resistance describes the ability of a construction to prevent a fire from spreading from one room to neighboring rooms. Fire resistance also describes the ability of a construction to retain structural integrity (i.e. shape, load-bearing properties) in a fire. [B07, p4-5]

4.3.1.1 FIRE REACTION

Heat release rate

The single most important parameter that defines the fire reaction of a material is the heat release rate, it is considered to be the best indicator of the fire hazard of a combustible material. It is a quantitative measure of the thermal energy released by a material per unit area when exposed to a fire with a constant heat flux as described in the preceding chapter. The unit for heat release rate (HRH) is kW/m². Because the HRH is not constant, but varies with exposure time to the fire, as the material is progressively consumed, the HRH is composed of two parameters: The average HRH, which is the averaged value of the HRH over a short period of time (3-5 minutes) and the peak HRH, which is the maximum amount of liberated heat, measured over a very short period of time (<5 seconds). A material with low values for peak and average HRH are most suitable for high fire risk applications to minimize the growth and spread of fire. [B07, p4]

Time-to-ignition

The second important parameter defining the fire reaction is the time-to-ignition, which is the period that a combustible material can withstand exposure to constant radiant heat flux before igniting and undergoing sustained flaming combustion. The ignition time can be used as an approximate measure for the flammability resistance of a material. Logically, long time-to-ignition values are better. [B07, p4]

Flame spread rate

The flame spread rate describes the speed at which the flame front travels over the surface of a combustible material. The flame spread rate can only be determined experimentally, which results in varying values for this rate, dependent on the type of test used. Low flame spread rates are better. [B07, p4]

Limiting Oxygen Index

This value is defined as the minimum oxygen content in the fire environment required to sustain flaming combustion of a material. Materials with high oxygen index should be used in high fire risk applications,

particularly for internal structures and components, because they offer the potential to self-extinguish when the fire becomes deprived of oxygen. [B07, p4-5]

Smoke density and gas toxicity

These two parameters are the most important parameters for the probability of human survival in fire conditions. Most fatalities are not caused by heat and flame, but are due to thick, toxic smoke, induced by the fire. Smoke density is defined as the concentration of smoke particles within the plume of a fire. Gas toxicity is a term that describes the concentration and lethality of gas products within the smoke plume. Low values for both parameters are better in fire behavior of materials. A large number of toxic gases can be released from composite materials including asphyxiates, irritants and carcinogens. [B07, p5]

4.3.1.2 FIRE RESISTANCE

As opposed to fire reaction properties, fire resistance properties are becoming the more important parameters in the later (post flashover) stages of a fire.

Heat insulation

Heat insulation is the resistive property that describes the rate of heat conduction through a material when exposed to fire (or extreme heat). Materials that are good heat insulators are best suited for slowing the spread of fire from room-to-room or compartment-to-compartment. Composites are generally more heat insulating than metals.

Burn-through resistance

This is the time needed for a flame to penetrate a material and emerge from the opposing side. Composites generally have better burn-through resistance than metals that melt at temperatures below the flame temperature, such as aluminum alloys.

Structural and mechanical integrity

For this research this is maybe the most important fire resistance property, it defines the ability of a material or structure to retain mechanical properties such as strength, stiffness, creep resistance when exposed to fire and after the fire has been extinguished. [B07, p5]

4.3.2 THERMAL DECOMPOSITION OF COMPOSITES IN FIRE

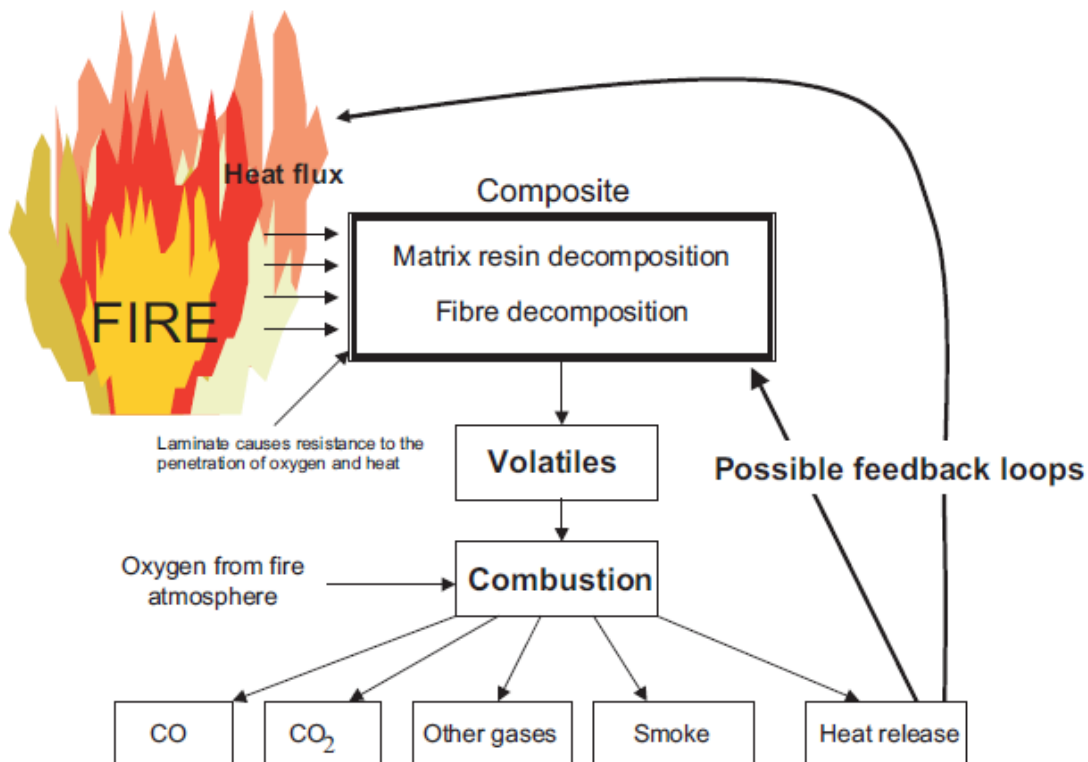


Fig. 87: Scheme depicting the composite decomposition during fire [B07, p21]

When the composite is exposed to a sufficiently large heat flux the (polymer) matrix and the organic fibers will decompose and yield volatile gases, carbonaceous char and airborne soot particles (smoke). This process is shown in the above scheme. Note that the heat release caused by the decomposition can accelerate this decomposition process, thus forming a circular flow. The decomposition usually starts at temperatures in the range of 250°C - 400°C. [B07, p135]

The volatile gases consist of a variety of vapors and substances, both flammable (e.g. carbon monoxide, methane, low molecular organics) and non-flammable (carbon dioxide, water). The gases diffuse into the flame zone, where they react with oxygen leading to the final combustion products, such as water, carbon dioxide, smoke particles and small amounts of carbon monoxide, of course accompanied by heat release, thus forming a self-sustaining process. [B07, p20]

To give a short overview over the chemical processes occurring in polymer composites during fire: The main mechanisms that reduce molecular weight during fire are random chain scission, chain-end scission ('unzipping') and chain stripping (removal of side groups) of the polymer chains. Two other thermally induced processes, cross-linking and condensation, have the opposite effect of increasing molecular weight. Although decomposition often involves more than one of the scission mechanisms, the dominant reaction in most polymer systems is random chain scission. [B07, p20]

In general only a few percent of the bonds need to rupture to drastically degrade the mechanical properties. A bond rupture level of about 10% is generally sufficient to generate organic compounds that are volatile in a fire. [B07, p20-21]

The temperature range over which polymers decompose increases with the heating rate. The decomposition temperature of the polymer matrix and any organic fibers in a composite exposed to fire will therefore not be uniform, but instead will decrease in temperature from the hot to cold surface. [B07, p24] In the following the fire decomposition properties of several thermoset matrices, thermoplastic matrices and organic fiber reinforcements will be discussed.

4.3.3 FIRE DAMAGE TO COMPOSITES

In this chapter the two main fire damage mechanisms in polymer composites will be discussed. The most important mechanisms are char formation and delamination or matrix cracking. The other important mechanism of softening and degradation of the matrix and organic fibers will be discussed in the next chapter. [B07, p47]

4.3.3.1 CHAR FORMATION

The formation of a char layer is an important process because it can promote significant flame retardation. Polymers with high char yield generally possess longer ignition times, lower heat release rates, slower flame spread rates, and generate less smoke and toxic gases than low char-forming polymers. The picture below shows the char depth one the left, and a photo of the corresponding, partly charred composite laminate. The decomposition region is a zone where the matrix is fully decomposed but not yet charred. [B07, p48]

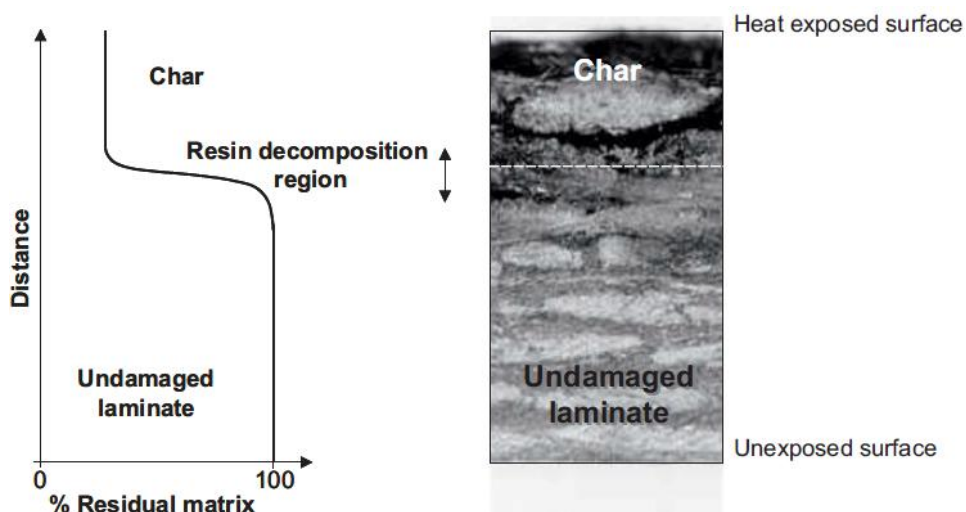


Fig. 88: Different damage zones in a fire-damaged laminate [B07, p48]

The limiting oxygen index increases with the char yield. This is because char reduces flammability in several ways. The picture below shows the char yield linked to the limiting oxygen index.

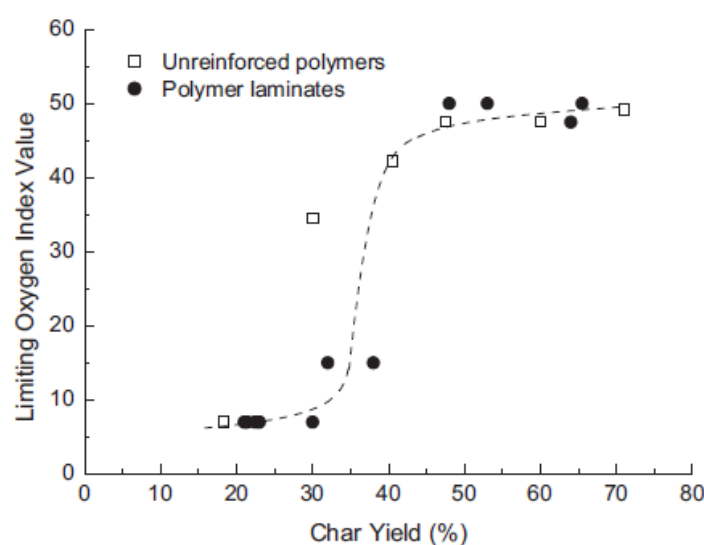


Fig. 89: Char Yield increases the limiting oxygen index value [B07, p50]

This beneficial property of the char production in composites has several reasons: Firstly, the char often acts as a thermal insulation layer because the thermal conductivity of char is mostly lower than the

conductivity of the virgin composite material. [B07, p48] Secondly, char can also improve fire resistance by limiting the access of oxygen from the atmosphere to the region of the composite undergoing decomposition, which slows down the combustion rate. Thirdly, char can act as a barrier against the flow of volatiles from the decomposition zone, thereby delaying ignition, slowing flame spread, and reducing the heat release rate. [B07, p50] Finally, char can help retaining the structural integrity of a fire-damaged composite by holding the fibers in place after the polymer matrix has been degraded.

However, for char to be effective in providing fire retardation it must form a continuous network structure that possesses low thermal conductivity and gas transportation properties. Furthermore the char must adhere strongly to the underlying composite; otherwise it can flake off and expose virgin material directly to the fire. A discontinuous char structure will enable the escape of flammable volatiles into the flame, and thereby reduces the effectiveness of the char layer to provide fire protection. [B07, p51]

4.3.3.2 DELAMINATION DAMAGE

Delamination cracking between the ply layers and matrix cracking within the plies often occurs ahead of the char zone when composites are exposed to fire. This damage may be confined solely to the reaction zone, or may spread through the reaction zone and underlying virgin material. It is believed that the cracking is in part due to the internal pressure build-up in the material due to volatile formation and, in some cases, vaporisation of trapped moisture. The temperature in the delamination cracking region is well above the glass transition temperature in most polymer systems used in composites, so the phenomenon can be readily explained by the combination of pressure build-up and matrix softening. [B07, p53]

Delamination, and to a certain extent matrix cracking, can be expected to have a significant effect on fire behavior due to the formation of non-bonded interfaces between plies. Matrix cracks can also provide pathways for the rapid release of combustion gases. Furthermore, when laminates are located above a fire source or in a vertical orientation, delamination can cause plies to fall off, thereby exposing fresh material to fire. [B07, p53]

4.3.3.3 DECOMPOSITION OF THERMOSETS UNDER FIRE LOAD

Thermoset resins as matrix material are most used for engineered, reinforced polymer composites. In this section the thermal decomposition parameters of five of the most common thermosets will be covered.

Unsaturated Polyester Resins

Of the thermosetting resins, unsaturated polyester resins are the most used in the fiber reinforced polymer industry. The reason for this lies in their moderate cost, good mechanical properties, reasonable environmental durability, low viscosity at room temperature and good low-temperature cure properties. [B07, p25-26]

The thermal decomposition process of all unsaturated polyesters is governed in the initial stages by scission of highly strained portions of the polystyrene cross-links, inducing a chain reaction of free radicals that then go on to promote further decomposition. This results in a variety of low molecular weight volatiles, including CO, CO₂, methane and others. 90%-95% of the original mass of the unsaturated polyester matrix is decomposed into the mentioned volatiles, rather than char. This is the main reason for the relatively high flammability and heat release of polyester composites. [B07, p32]

In addition to flammability and heat release, another disadvantage of styrene-based solvent monomer systems in fire is that the styrene component itself tends to produce smoke. Furthermore these resins tend, during decomposition, to pass through a 'liquid' or low viscosity stage that can result in the formation of flaming droplets. These disadvantages can be somewhat alleviated by applying high reinforcement- or filler content. [B07, p33]

Another way of counteracting the fast decomposition of unsaturated polyester resins is the addition of halogen fillers to the resin. Despite environmental concerns, this method is highly effective in reducing flammability and is still the main measure by which low-flammability general-purpose resins are realized.

Halogenated resins are of little benefit in established fires where the polyester component is not the source of the fire. In this case the resin will burn alongside the other flammable components and release heat and toxic products. Halogenated resins are also known to have slightly poorer mechanical properties compared to conventional polyesters. To improve the environmental, non-toxic performance of the low-flammability polyester resins other methods have been found, like for example resins in which part or all of the styrene has been replaced by methyl methacrylate, and the resin is highly filled with alumina trihydrate (ATH). The flame retardant properties of these polyester systems are similar to the modified acrylics, described later in this chapter. [B07, p31]

Vinyl Ester Resin

The fire behavior of vinyl ester resins is very similar to the polyesters, although, due to the slightly higher styrene content, the time-to-ignition, heat release rate and smoke generation may often be slightly higher. As with unsaturated polyesters, most of the polymer is decomposed into volatiles and only 5%-10% of the original mass is converted into char. [B07, p33]

Modified Acrylic Resins (MODAR)

Just like the resin discussed before, MODAR is also based on the solvent monomer principle. The distinguishing features of MODAR resins are their low viscosity in the uncured state and the very fast nature of the cure reaction. This limits the applicability mainly to 'closed mold' processes, such as resin transfer molding and pultrusion.

An advantage of the low viscosity is that it enables relatively high levels of fillers, usually alumina trihydrate (ATH), to be incorporated, while retaining process-ability. It is mainly this characteristic that accounts for the very good fire performance reported for composites based on the MODAR-ATH system. It also has a lower tendency to produce smoke than styrene-based resins. It should be noted, however, that the high levels of ATH can limit the structural performance of this type of resin, which poses a large disadvantage in the application as load-carrying FRP bridge superstructures. [B07, p34]

Epoxy Resins

Decomposition of most epoxies occurs via random chain scission reactions over the temperature range of about 380°C to 450°C. The scission reactions decompose 80- 90% of the original polymer weight into almost 100 different volatile, partly flammable compounds. These substances provide a fuel source for the decomposition reaction to continue until the epoxy is completely degraded. Only 10% to 20% of the original polymer weight is transformed into a highly porous char. As with polyester composites, the high yield of flammable volatiles produced in the decomposition reaction is the main reason for the relatively poor fire performance of epoxy matrix composites. [B07, p38]

Phenolic resins

Unlike the other resins discussed earlier, the retained mass of phenolic resins decreases with increasing temperature in several stages which is indicative of a multiple-order decomposition process. Above 300°C the scission process commences, which mainly involves scission reactions along the chain, with elimination of some volatile byproducts. The reaction rate reaches a maximum in the second stage, and a variety of volatile gases are produced including CO, methane and phenol. The picture below compares the retained mass during heating up of Epoxy/Glass composite with Phenolic/Glass composite. Note the mass/temperature differences.

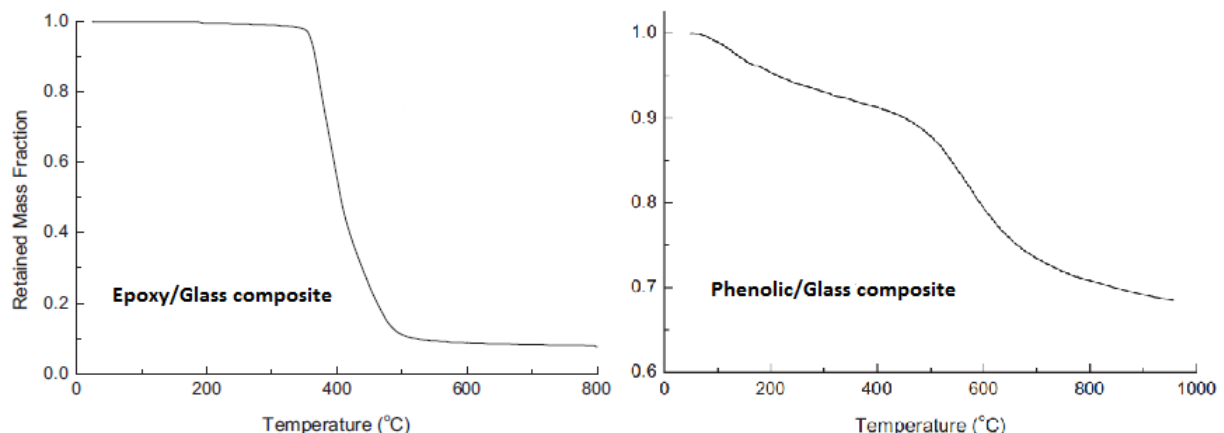


Fig. 90: Comparison of retained mass at elevated temperature for Epoxy and Phenolic composites [B07, p38, 40]

In contrast to many other thermosetting systems, much of the higher molecular weight aromatic material remaining after the scission reactions is able to condense to form a solid material. When a phenolic matrix composite is exposed to fire then the char formation temperature will decrease quickly with distance below the hot surface. 40%-60% of the original mass of phenolic resins is transformed into char, resulting in a much lower yield of flammable volatiles compared to other polymers: hence the superior fire performance and low flammability of phenolic composites. [B07, p40-41]

4.3.3.4 DECOMPOSITION OF THERMOPLASTICS UNDER FIRE LOAD

Although thermoplastics are less often used than thermoset resins in the fiber reinforced polymer industry, some of them possess better fire decomposition properties than thermosets, next to that, they also gain more and more market-share in the industry. Below 3 common thermoplastics will be discussed in short.

Poly Propylene (PP)

All olefin polymers tend to decompose completely into volatile products, leaving no char. In the presence of oxygen, free radical formation is accelerated which reduces the temperature at which the onset of decomposition takes place. The poor thermal stability of PP can be altered by the addition of free radical absorbing stabilizers. These also improve resistance to degradation during high temperature processing and to UV attack at ambient temperature, the latter being a problem with all olefin polymers. The stabilizer compounds are rendered ineffective during the process of absorbing free radicals so, unfortunately, their effect on hindering decomposition is not permanent. [B07, p42]

Poly Ether Ether Kethone (PEEK)

PEEK has a very good thermal stability and a high melting point for a thermoplastic of 380°C and is often used in elevated temperature applications due to these reasons. The decomposition of PEEK begins at about 500°C by a primary random chain scission reaction of the ether bonds and ketone linkages. PEEK appears to degrade in a single-stage process between 500°C and 640°C.

An important feature of the decomposition reaction is the high yield of char (~60% of the original mass) This high char yield of PEEK, with the consequent reduction in combustible volatiles, results in flammability resistance superior to most other thermoplastics as well as the styrene or solvent monomer-based thermosets. [B07, p42-43]

Poly Phenylene Sulphide (PPS)

PPS decomposes in a single-stage reaction over the temperature range 380°C to 500°C. Decomposition occurs by random scission along the PPS chain. The major volatile products are cyclic tetramer, linear trimers and di-mers and benzene. With 60%, the char yield of PSS is very high. A distinct feature of many thermoplastics used in composites is their high char yield. PPS and PEEK both yield a high fraction of char that is comparable with phenolic resin. [B07, p43]

4.3.3.5 DECOMPOSITION OF FIBER REINFORCEMENTS UNDER FIRE LOAD

In this chapter the fire decomposition of fiber reinforcements will be discussed. Although for most common reinforcement types the decomposition turns out to be much less problematic than for the associated matrix material, there are some organic reinforcements that are susceptible to fire decomposition.

Glass Fibers

E-glass fiber, which is the most used type of glass fiber, remains unaffected by fire until temperatures of about 830°C (1050°C for S-glass), when softening and viscous flow starts. Melting occurs at 1070°C (1500°C for S-glass). However, the mechanical properties such as strength and creep resistance decrease over a range of temperatures well below the softening temperature. Since the temperature of most fires is typically in the range of 500°C-1.100°C, common glass fibers have excellent fire resistance properties. Upon cooling the molten glass can fuse, which can slow the rate of heat conduction and acts as a barrier against the release of flammable volatile gases. Under these conditions, fused glass fibers can even reduce the flammability of composite materials. [B07, p44]

Carbon Fibers

Oxidation of carbon fibers starts at temperatures of 350°C-450°C. In that case impurities and irregularities in the fibers can cause axial splitting other fibers into small fibrils under fire load, which can become a health hazard when released from a burning composite into the smoke plume where they can be inhaled. However, in most types of fire the extent of oxidation is small because most carbon fibers within a composite are protected by char. It is usually only fibers at the hot composite surface are directly exposed to the fire. Only in oxygen-rich environment carbon fibers experience significant oxidation, and this is the only case, when the heat flux is high. [B07, p44]

Aramid Fibers

Decomposition of aramid fibers starts quite rapidly at temperatures of 450°C-500°C in air and nitrogen, respectively, involving a substantial break-down of the main polymer network structure by a random scission process. The fibers yield a high amount of char of 40% of the original mass, as a by-product of the decomposition reaction when heated in nitrogen. Despite the thermal instability, aramid fibers are inherently flame resistant with very good oxygen limit value. [B07, p45]

Poly Ethylene (PE) Fibers

The decomposition process of polyethylene into organic volatiles makes the fibers much more flammable than aramid fibers. The table below compares the time-to-ignition, heat release rates, smoke density, yields

of CO and CO₂ gases, and mass loss of polyethylene and aramid fibers when tested in an air-environment at an incident heat flux of 50 kW/m². It can be seen that the polyethylene fibers ignite more rapidly, have much higher peak and average heat release rates, and yield higher amounts of smoke, CO and CO₂ gases, which clearly demonstrates their inferior fire performance. [B07, p45-46]

Fire Reaction Property	Unit	Poly Ethylene Fibers	Aramid Fibers
Time-to-ignition	sec	31	185
Peak Heat Release Rate	kW/m ²	691	63
Average Heat Release Rate	kW/m ²	275	50
Average Smoke Extinction Area	m ² /kg	426	66
Average Carbon Monoxide Yield	kg/kg	0,019	0,0018
Average Carbon Dioxide Yield	kg/kg	2,11	1,09

Table 35: Comparison of PE- and Aramid-fibers under a heat flux of 50 kW/m² [B07, p46]

4.3.3.6 FIRE REACTION PROPERTIES OF FIBER REINFORCED POLYMER COMPOSITES

In 4.2.5, the characteristic values describing the fire properties of a material were already covered in general. In this chapter all parameters of the fire reaction will be discussed for fiber reinforced polymers in specific. As in the chapter before only the most common thermoset- and thermoplastic matrix resins will be discussed.

4.3.3.7 HEAT RELEASE RATE

The “Heat Release Rate” (HRR) is not only the single most important fire reaction parameter for composites, it also influences other parameters such as the surface spread of flame, smoke generation, and carbon monoxide emission. In composites the heat release rate is not constant but has a clear path of development. In the induction period no heat is released, because the exposure time to external heat is insufficient to heat the composite up to decomposition reaction temperature. After this initial period the heat release rate rapidly increases in only a few seconds. This increase is caused by a sudden, short-term release of heat from the ignition of flammable volatiles from the resin-rich surface of the composite. The curve continues to rise to a peak HRR, after which the heat release is slowed down due to the formation and growth of char at the hot surface. After a certain amount of burning time the HRR becomes negligibly small due to the complete depletion of flammable fuels. At this stage the polymer matrix is completely depleted. The graph below, on the left shows the different stages of the heat release process for a glass vinyl-ester composite under a constant heat flux of 50 kW/m². [B07, p72-73]

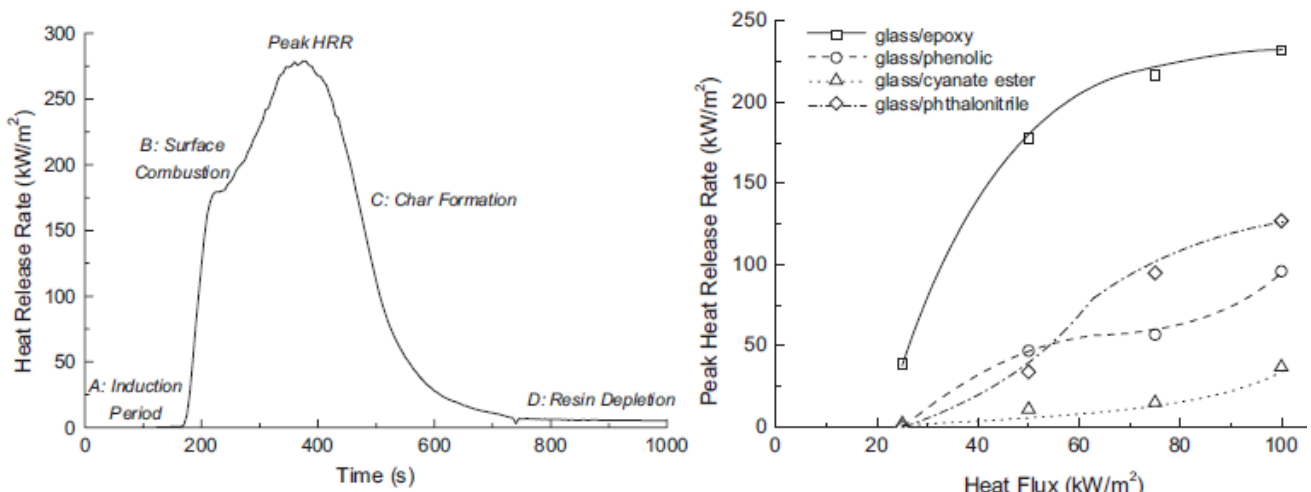


Fig. 91: Left: Typical heat release process for glass vinyl ester composites under constant heat flux of 50 kW/m². Right: Comparison of HRR's of normal and high fire performance composites. [B07, p72-73]

More fire resistant composites, such as for example glass phenolic composites show a slightly different behavior than that depicted in the curve. First of all, the peak HRR is about 4x times smaller than for glass vinyl-ester composite and secondly, the induction period lasts about 50% longer. [B07, p73-74]

The graph above, on the right compares normal thermoset composites, such as glass epoxy, with high fire performance composites, such as phenolic, cyanate ester and phthalonitrile. The high performance composites possess not only a much smaller HRR, but also feature a smaller increase of HRR with increasing external heat flux. [B07, p74]

As for the ignition time, the fiber content also influences the heat release rate. An increase from 0% to 60% glass fiber reinforcement content in a polyester composite reduces the peak HRR by about 70%, from 1050 kW/m^2 to 300 kW/m^2 . [B07, p76] The laminate thickness also has great influence on the HRR of the composite. Thicker elements lead to a much smaller total heat release for epoxy, vinyl ester and polyester composites. However the thickness effect becomes much smaller for high fire performance matrices such as phenolic. The graph below quantifies these statements. [B07, p78]

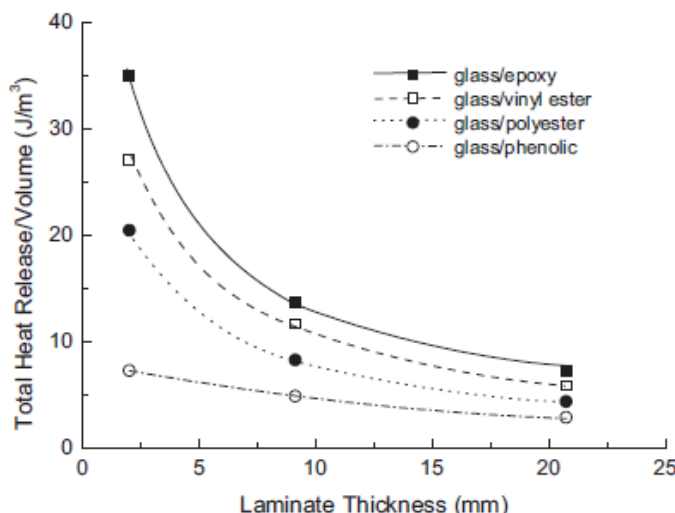


Fig. 92: Influence of the laminate thickness on the total heat release [B07, p79]

4.3.3.8 TIME-TO-IGNITION

Because most organic resins used in composite can ignite within a very short time of being exposed to fire and following ignition, will burn with large high-temperature flames, time-to-ignition is a very important parameter for the fire reaction of FRP composites. In composites, ignition is mostly triggered when a critical amount of flammable volatiles is generated by the endothermic decomposition of the matrix. The ignition time depends on the availability of oxygen, the temperature, the chemical- and thermo-physical properties of the matrix, the reinforcement and finally, the initial heat flux. [B07, p59-60]

Most resins do not ignite when the initial external heat flux lies under a certain value. This value is called the threshold heat flux and lies at about 13 kW/m^2 for polyester, vinyl ester and epoxy composites. Phenolic laminates have a higher threshold heat flux of 25 kW/m^2 . [B07, p60]

The graphs below shows a comparison of the time-to-ignition of different thermoset resin based glass fiber composites on the left. Phenolic resins clearly have the best behavior of all standard thermoset resins. On the right some thermoplastic and thermoset resins are compared at a constant heat flux of 75 kW/m^2 . Note the very good ignition times for most thermoplastics.

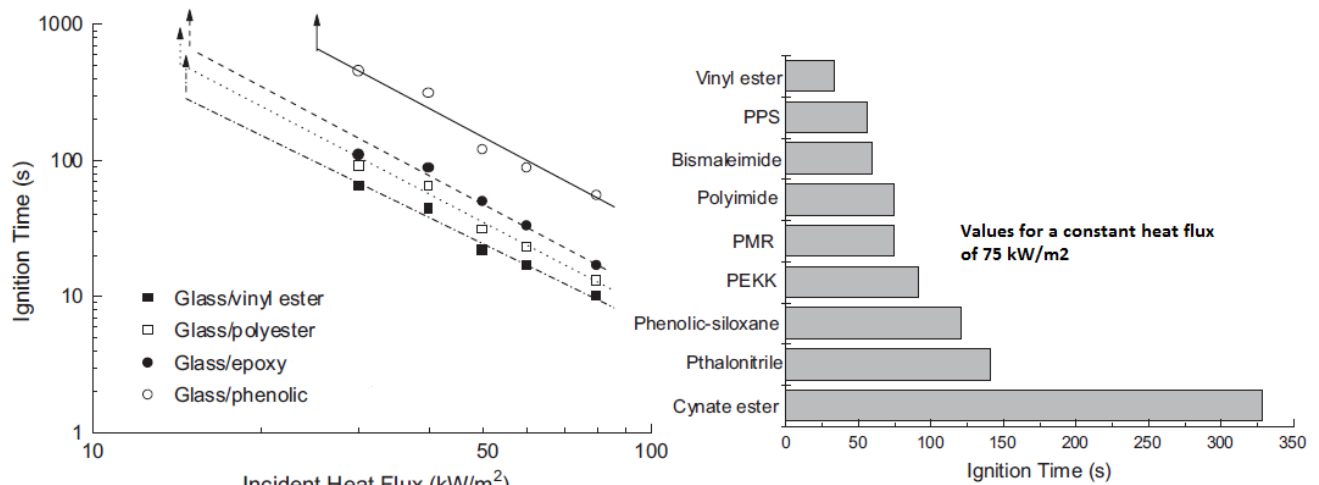


Fig. 93: Time-to-ignition of different thermoset (left) and thermoplastic (right) resin based composites. [B07, p61,62]

The fiber reinforcement in composites can also influence the ignition time, although glass and carbon fibers are inert to fire when the heat flux is below $100-125 \text{ kW/m}^2$. Therefore, the amount of reinforcement present in the composite (the fiber content) substantially increases the ignition time. However the binders and coatings which are often used to reinforce fibers can have an adverse effect on the ignition time, since they are mostly organic and thus not inert to fire. Chopped Strand Mats for example, which are heavily coated/impregnated by nature decrease the ignition time drastically, particularly at low to medium heat fluxes ($< 50 \text{ kW/m}^2$). The difference in ignition time of CSM glass fiber/polyester composite compared to woven glass fiber/polyester composite is about 40%. [B07, p63-65]

Although not much research was conducted on organic reinforcements such as aramid and PE, it is expected that they will decrease ignition times. The graph, below on the left, shows the difference in ignition time for glass, aramid and PE-reinforcements. [B07, p63-65]

Another important parameter influencing the ignition time of fiber reinforced polymer composites is the thickness of the material. As shown in the graph below, on the right, the thickness particularly is of great influence for low heat fluxes of about 35 kW/m^2 .

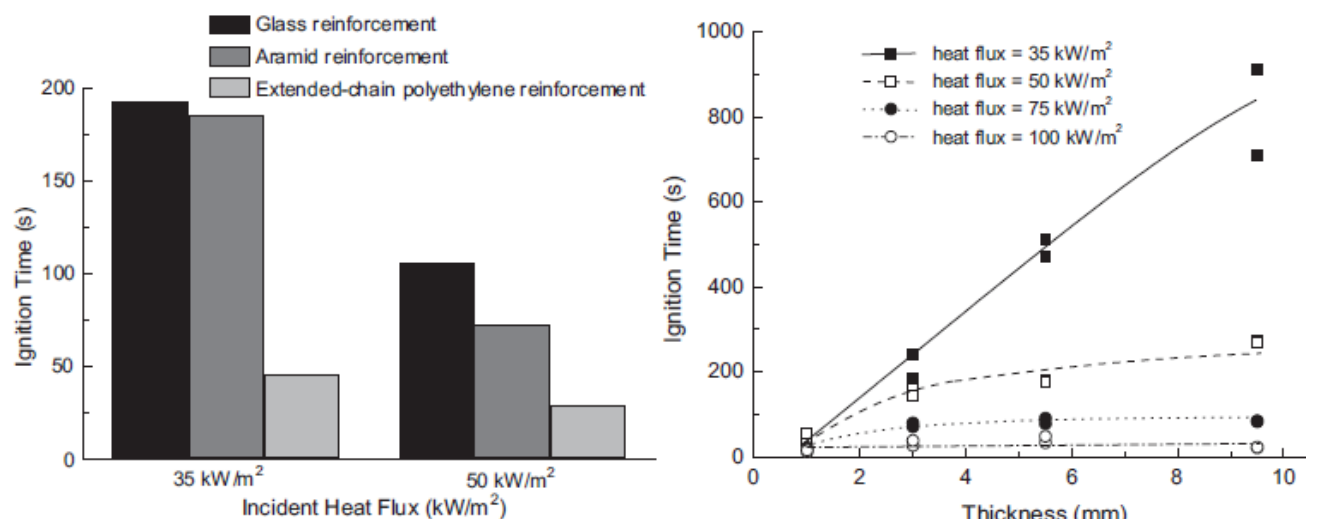


Fig. 94: Left: Comparison of ignition times for different reinforcements. Right: Influence of thickness on the ignition time [B07, p66,67]

4.3.3.9 SURFACE SPREAD OF FLAME

Due to the high flammability of many composites, there is a serious safety concern that flames will quickly spread and thereby increase the difficulty in containing and extinguishing a fire. This is one of the key concerns of fire safety authorities with the use of composites in high fire-risk applications.

In flame spread tests it can be observed that the flame propagates readily down the surface of glass/polyester and glass/epoxy laminates, and this is caused by the high flammability of these materials. However, the flame is unable to spread down the glass/phenolic laminate, and this material can be regarded as self-extinguishing. Phenolic laminates thus again have excellent resistance of flame spread, and this is another outstanding fire reaction property of these materials that makes them suited for many high fire risk applications. Other composites with a bismaleimide, polyimide or high-temperature thermoplastic, like PEEK or PPS, matrix display excellent flame spread resistance. Next to that, composites have much higher flame spread speeds when reinforced with combustible fibers (e.g. aramid, polyethylene) rather than non-combustible fibers, such as carbon or glass. [B07, p94]

The greatest influence on the flame spread rate of composite materials is their heat release rate. The higher the peak HRR, the higher the flame spread speed. The graph below on the left shows the flame spread distance over time for three different thermoset based composites. Note that phenolic composite allows no flame spread at all, thus, as mentioned before, can be considered self-extinguishing. [B07, p94]

The graph below on the right correlates the Flame Spread Index (FSI) with the peak HRR, normalized by the ignition time. The flame spread index is a parameter often used to quantify the downward flame spread rate, the higher the value, the faster the flame spread. The FSI is directly linear correlated to the normalized peak HRR. Polymers with a high HRR also have a high flame spread index. [B07, p94-95]

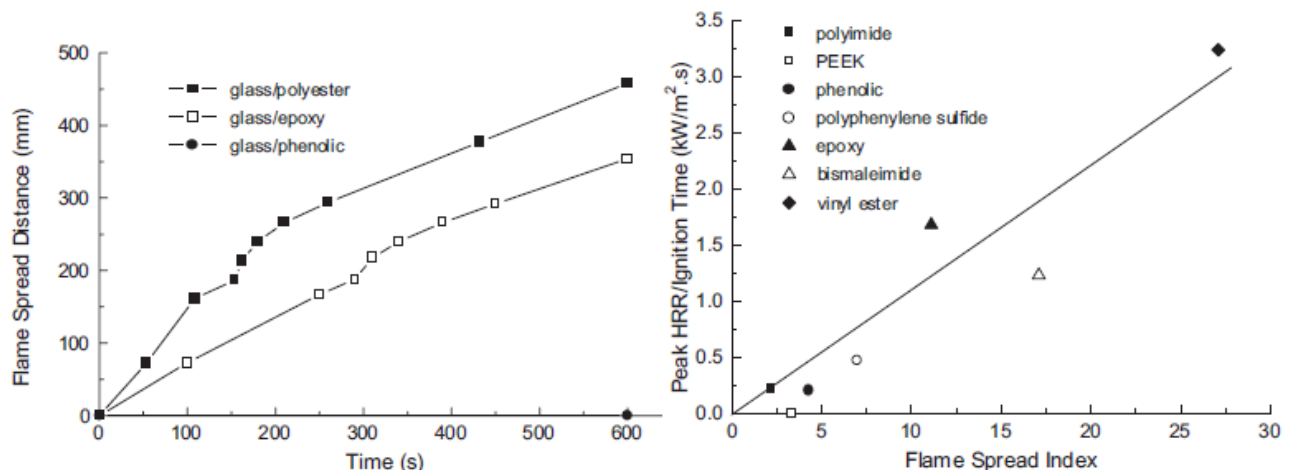


Fig. 95: Left: Flame spread distance for different polymers over time. Right: Flame Spread Index correlation with normalized peak Heat Release Rate for different polymers [B07, p95]

4.3.3.10 LIMITING OXYGEN INDEX

The Limiting Oxygen Index (LOI) is often used to rank the relative flammability of fiber reinforced polymer composite materials. The LOI values for a range of thermoset and thermoplastic composites are presented in the graph below, on the left. It is seen the LOI values for highly flammable composites, such as polyester-, vinyl ester- and epoxy-based materials, are below about 30. Composites with highly stable or aromatic polymers have much higher index values. It is generally recognized that the LOI values for polymers and polymer composites increase with their ability to yield char in a fire. [B07, p90-91]

The LOI index values shown in the graph, below left, were determined at room temperature. However, a composite material will reach much higher temperatures in a fire. Different studies have shown the LOI-values of composites are dependent on the test temperature. The values can change dramatically with temperature, usually decreasing with increasing temperature, and often changing the relative ranking of

some materials. It is therefore questionable to use LOI values measured at room temperature to assess the flammability of composite materials. The graph below, on the right shows the effect of temperature from 25°C to 300°C on the LOI of two glass fiber composites. The index values increase with temperature up to 100°C, but at higher temperatures there is a steady reduction in the values because less heat is needed to sustain decomposition and burning. [B07, p91]

While the LOI is often used to characterize the fire performance of composites, there is no clear correlation between the index value and other fire reaction properties, for example the HRR. Therefore it is not valid to use the index value as a quantitative measure of fire resistance, although it can be used to rank the relative flammability. [B07, p91]

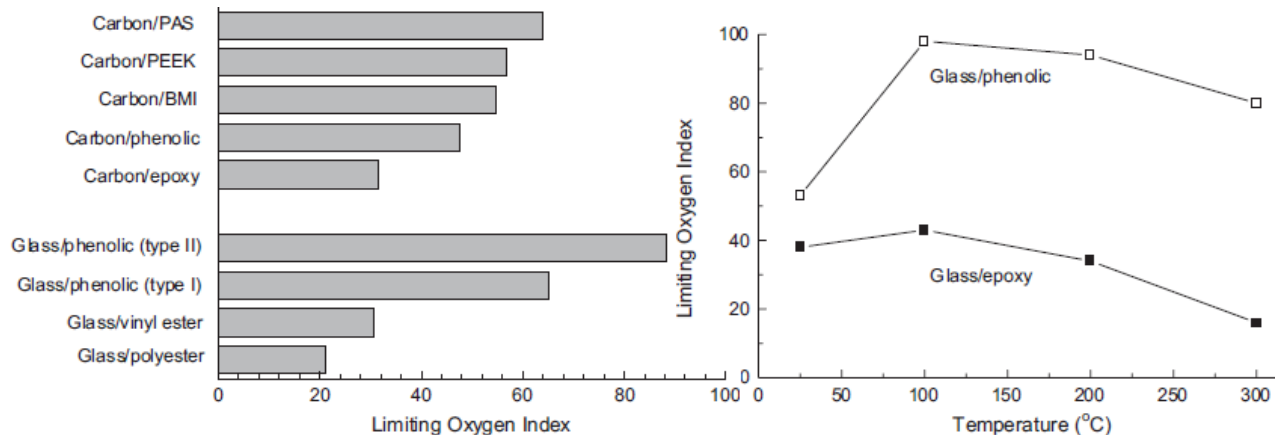


Fig. 96: Left: Limiting Oxygen Index for different composites. Right: Temperature dependence of LOI for two composites [B07, p92]

4.3.3.11 SMOKE GENERATION

Smoke is one of the main safety concerns when using FRP composites. It consists of a mix of small fragments of fiber and ultra-fine carbon soot particles. The toxicity of this smoke will be covered in the next chapter, in this chapter the smoke density, and thereby the reduced visibility for trapped people and firefighters will be the main concern. For application in a non-enclosed bridge the smoke generation poses less of a problem than in enclosed spaces. However the smoke generation will also be covered in this thesis, since the possibility of a fully enclosed bridge is still left open.

Smoke generation is measured by the Specific Extinction Area (SEA). This value is a measure of how effectively a given mass of flammable volatiles released by combustible material is converted into smoke. A larger value for the SEA thus means a higher smoke density. Polymer matrices, such as polyester, epoxies and vinyl esters produce a much denser smoke than phenolic resins. The graph below, on the right compares the SEA of vinyl ester with the SEA of phenolic. It is clearly visible that the maximum SEA is about 4x times higher for the vinyl ester composite than for the phenolic composite. [B07, p85-86]

The graph below, on the left shows the maximum smoke density for some low smoke emission thermoplastics compared to the smoke emission of some typical thermoset polymers. Note that the smoke density for PEEK/PAS/PES is even lower than that of phenolic. Generally said, a polymer which yields much char has a low smoke generation. [B07, p85-86] Thick, continuous char layers also limit the release of ultra-small fiber fragments. High fiber contents reduce the smoke generation, because less organic material is available to produce smoke. [B07, p87]

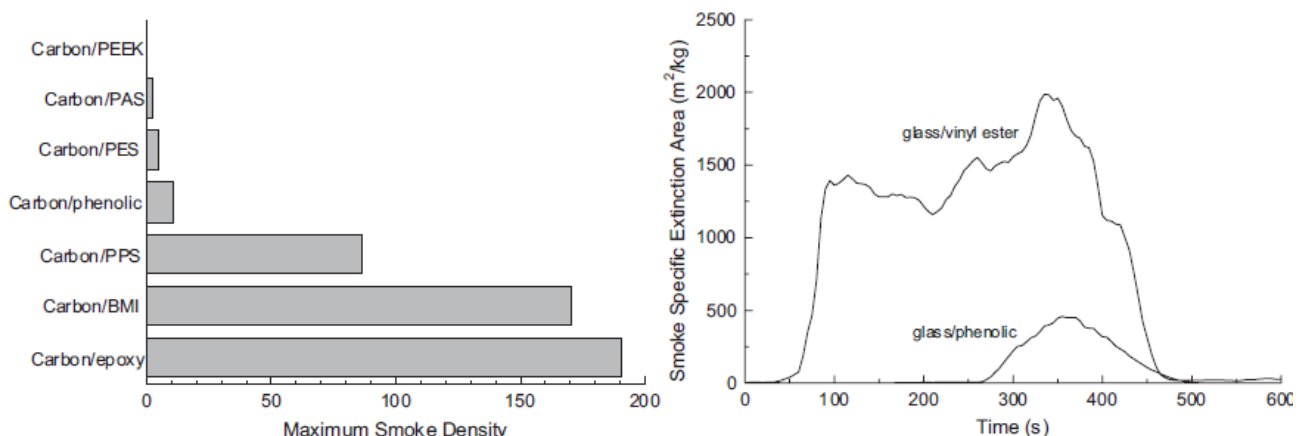


Fig. 97: Left: Maximum Smoke Density for different thermoplastic/thermoset carbon composites. Right: Comparison of SEA's for phenolic and vinyl ester glass composites [B07, p86, 87]

The graph below shows the correlation between external heat flux and the average smoke density. Although smoke density increases with growing heat fluxes, the increase is not so dramatic as with the heat release rate for example. [B07, p88]

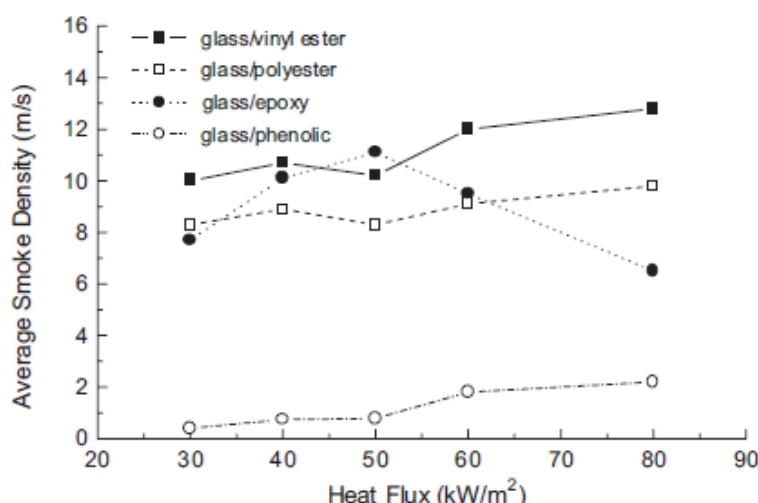


Fig. 98: Correlation between heat flux and average smoke density for different thermoset polymer composites [B07, p88]

4.3.3.12 SMOKE TOXICITY

Toxic gases released during combustion often pose the greatest health hazard in fires. Inhalation of toxic smoke is the number one death cause in compartment fires. Carbon monoxide is one of the most dangerous substances that is generated during a FRP fire. Concentrations as low as 1.500 'parts per million' (ppm) are deadly for humans after only one hour, compared to 50.000 ppm for carbon dioxide. [B07, p88] For application in a non-enclosed bridge the smoke toxicity poses less of a problem than in enclosed spaces. However the smoke toxicity will also be covered in this thesis, since the possibility of a fully enclosed bridge is still left open.

Next to the already mentioned CO and CO₂ gases, other gases like toluene, methane, acetone, propane, benzene, benzaldehyd, styrene, and aromatic volatile compounds are also released by thermoset resins during fire. More dangerous corrosive and toxic gases such as HCl and HCN are also released. However, since the emission of these gases is much lower than the emission of CO, the level of released CO (and CO₂) is considered to be a good measure for the toxicity of the emitted smoke. [B07, p89]

The table below shows typical values for the emission of CO, CO₂, HCN and HCl gases. It is interesting to see that even a high fire performance thermoset like phenolic does not perform better than other thermosets.

Thermoplastics produce significantly less smoke than the thermosets. Carbon PEEK composite is the best performing composite considering smoke toxicity, emitting only traces of CO and CO₂. [B07, p90]

Composite	CO (ppm)	CO ₂ (vol%)	HCN (ppm)	HCl (ppm)
Glass/ Vinyl Ester	230	0,3	not detected	not detected
Glass/ Epoxy	283	1,5	5	not detected
Glass/ BMI	300	0,1	7	trace
Glass/ Phenolic	300	1,0	1	1
Glass/ Polyimide	200	1,0	trace	2
Glass/ PPS	70	0,5	2	0,5
Glass/ Phthalonitrile	40	n.a.	n.a.	n.a.
Carbon/PEEK	trace	trace	not detected	not detected

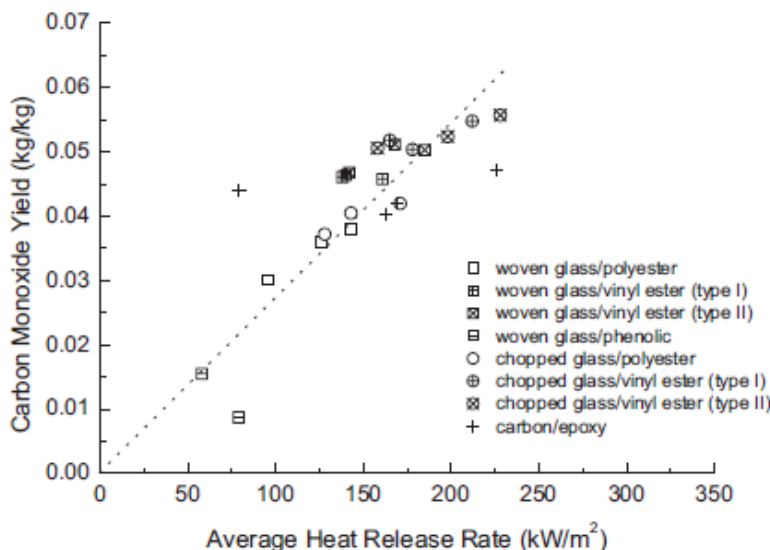
Table 36: Emission of toxic gases of different fiber reinforced composites [B07, p90]

Another table is presented which compares the toxicity of different gases. It can be seen that the exposure limits for Carbon Monoxide and Carbon Dioxide are much higher than the limits for the other toxic gases.

Toxic Gas Species	Chemical	Exposure limit [ppm]
Carbon Monoxide	CO	1.500
Carbon Dioxide	CO ₂	50.000
Hydrogen Cyanide	HCN	50
Hydrogen Chloride	HCl	30
Sulfure Dioxide	SO ₂	30
Nitrogen Oxides	NO _x	30

Table 37: Toxic gas exposure limit [B07, p367]

The amount of CO produced is also very much influenced by the heat release rate properties of a composite. The CO-level correlates linearly with the heat release rate, which suggests that the toxic hazard caused by the release of CO can be minimized by using composites with low heat release rates. The graph below shows this correlation. [B07, p90]



4.3.4 FIRE RESISTANCE PROPERTIES OF FRP COMPOSITES

In this chapter the fire resistance properties, heat-transmission and burn-through-resistance of fiber reinforced composites will be discussed. The mechanical properties of composites under fire load will be discussed in the next chapter.

4.3.4.1 BACK-FACE TEMPERATURE BUILD-UP

In fire resistance one of the most important parameters used is the general build-up of the back-face (unexposed face) temperature and specifically the time taken for the back-face temperature to reach 160°C, at which point the fire is likely to spread from one compartment to another. The graph below on the left shows the back-face temperature build-up for glass polyester and glass phenolic composites exposed to the standard cellulosic fire curve. It is seen that the temperature rise at the back-face of the phenolic laminate over the initial 30-40 minutes is lower than the polyester composite. At longer times the temperature of the phenolic increases faster. This is due mainly to explosive delamination damage caused by the internal pressure build-up from the vaporization of entrapped water in the phenolic matrix. [B07, p96-97]

The graph below, on the right shows a more important value for the back-face temperature, it correlates the thickness of different composite laminates with the time to reach 160°C at the back-face. To obtain this graph the more common (and severe) hydrocarbon fire curve was used. The time to reach 160°C rapidly increases with growing thickness of the test specimens. It is clearly visible that unprotected FRP composites reach the critical back-face temperature in very short times, mostly under 20 minutes. It can be seen that phenolic behaves much better than polyester resin. [B07, p97]

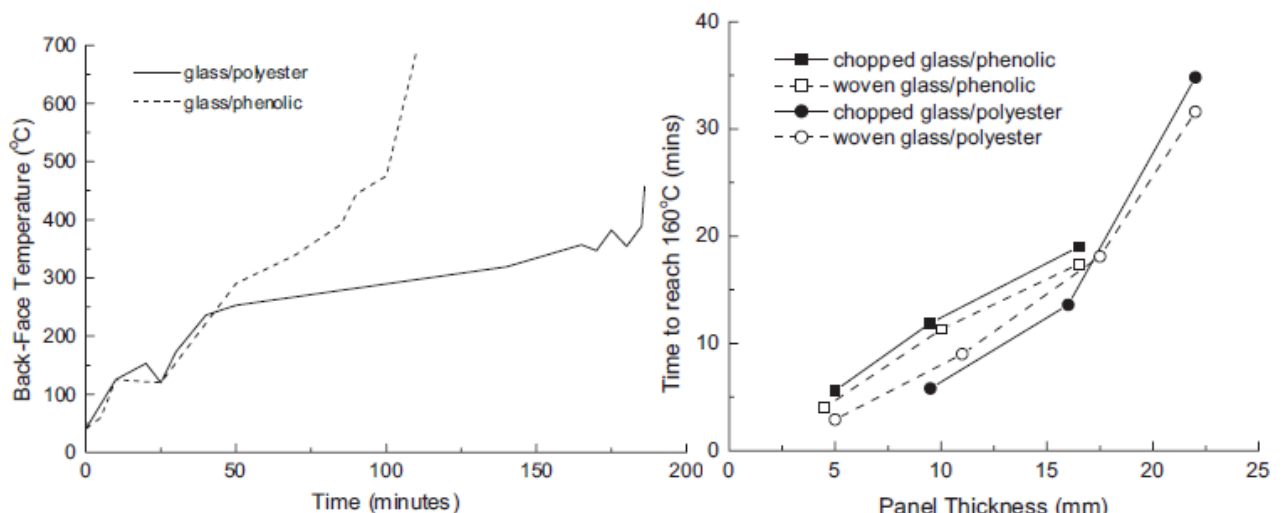


Fig. 100: Left: Back-face temperature build-up in cellulosic fire conditions. Right: Comparison of time to reach a back-face temperature of 160°C correlated to the member thickness for different composites. [B07, p96,97]

4.3.5 MECHANICAL PROPERTIES OF COMPOSITES UNDER FIRE LOAD

Not much is known about the fire resistance properties compared to the fire reaction properties, especially when the structure is loaded. Moreover it is not possible to estimate the fire resistance behavior based solely on the known fire reaction properties. A composite that has good fire reaction properties, may not necessarily have good fire resistance properties. For example, phenolic laminates generally show better fire reaction properties than unsaturated polyester laminates, including longer ignition time, lower heat release rate, slower flame spread and less smoke, but their mechanical properties can often degrade more rapidly in fire. [B07, p163]

Until recently, little was known about the structural properties of composites in fire. Understanding the structural performance in fire is a critical safety issue because the loss in stiffness, strength and creep resistance can cause composite structures to distort and collapse; possibly resulting in injury and death. [B07, p163] There are relatively few references in the literature to the fire behavior of moderately sized composite structures under load. [B07, p164] With thermally stable, post-cured laminates, changes in properties with temperature can be considered reversible up to the point where decomposition of one of the phases, usually the polymer matrix, begins. With fire it is necessary to consider changes beyond this point. [B07, p174]

Although some theoretical models exist, such as the 'Kulkarni and Gibson model' [B07, p175], the 'Mahieux and Reifsneider model' [B07, p176] and the 'Arrhenius models' [B07, p177, 178], they all share the property that they are relationships based on curve-fitting on data from different experiments with various resin and reinforcement types. The general advice is to use the model which best fits the experiment data, which implies that experiment data is needed to interpolate or extrapolate further properties under temperature load. Also, most models contain several fitting constants, which need to be derived experimentally. [B07, p178]

Because the available models on the structural performance of fiber reinforced composites are still in an experimental phase this chapter will concentrate on some available experimental data. The graph below, on the left shows the temperature dependence of the elastic modulus of an unidirectional reinforced glass polyester pultrusion and its components. The unidirectional core comprises about 60% by volume of the total section; the other parts are foremost comprised by the random swirl mats. It can be seen that the modulus declines with about 40% up to 200°C, where the decline flattens out. The most rapid drop of modulus can be found in the temperature range of 75°C to 175°C [B07, p182, 183]. Note also that most predictive models use the modulus as a basis for the prediction of the decline of other mechanical properties as well. [B07, p175]

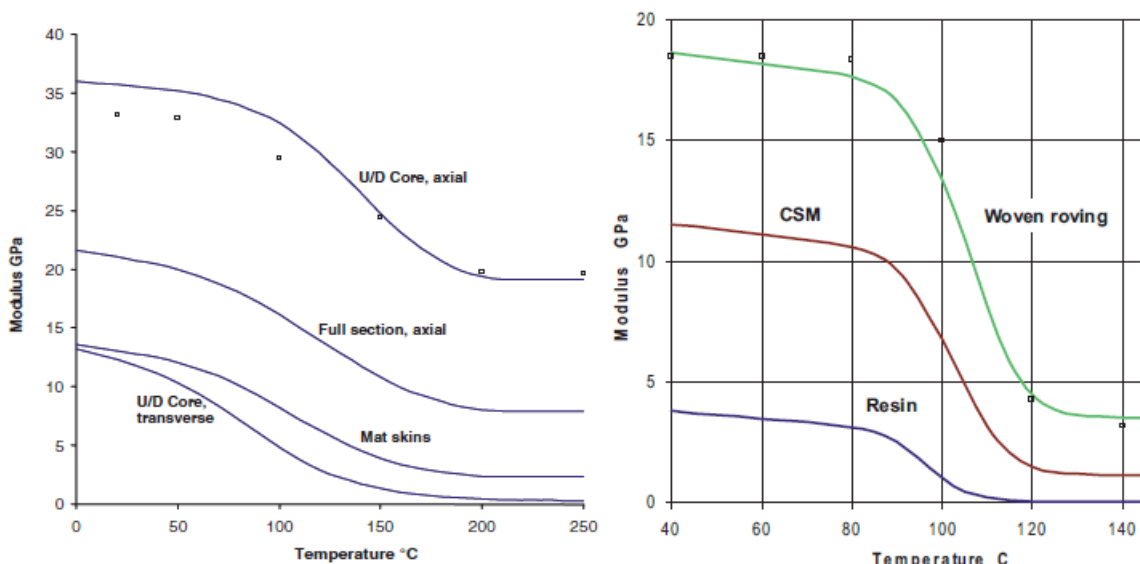


Fig. 101: Left: Young's modulus of UD- 60% reinforced glass polyester pultruded section (including its components) and random swirl mat correlated to the temperature. **Right:** Young's modulus of woven glass vinyl ester laminate and its parts correlated to the temperature [B07, p183, 185]

The graph above, on the right shows a similar relationship as the previously described graph. However it describes several vinyl ester resin based composites. It can be seen that decrease of modulus for vinyl ester resins is even bigger than for polyester resins. The modulus of the isolated resin drops to zero at about 120°C. [B07, p185]

Because the temperature under fire conditions is usually higher than the described 150°C to 250°C some information on composite behavior under higher temperatures is also needed. The graph below, on the left shows some test results on the tensile strength under temperatures up to 400°C. Three types of woven fabric laminates are investigated: Glass vinyl ester, glass polyester and glass polypropylene. Although the

vinyl ester composites behaved worse than the polyester composites in the latter paragraph, it can be seen that the behavior under temperatures of 200°C to 400°C is similar for both and show a total decrease of tensile strength of about 40%. Polypropylene composites exhibit a much worse strength decrease of about 80%. [B07, p187, 188]

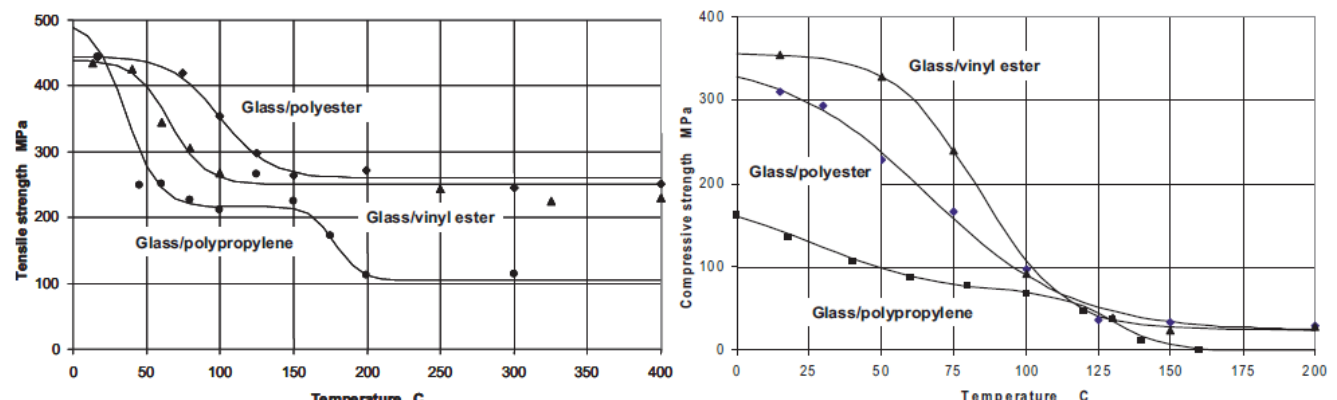


Fig. 102: Left: Tensile strength of different glass reinforced composites at elevated temperatures. Right: Compressive strength of the same glass reinforced composites at elevated temperatures [B07, p188, 190]

The graph shown above on the right shows the development of the compressive strength under elevated temperatures. It can be seen that for all composites, the compressive strength drops much more rapidly than the tensile strength. Polyester- and vinyl ester composites show drops of >90% for temperatures greater than 150°C. Polypropylene composites have a compressive strength of zero at temperatures over 160°C. These very rapid decreases of compressive strength are caused by the reduction of shear properties of the resin, which leads to a loss of interaction of the fiber strength and thus delamination failure. [B07, p190]

Furthermore some tests have been done on the time-to-failure under increasing tensile loads under a constant heat flux. The two graphs below show the results of experiments for tensile and compressive loads. Again, polyester, vinyl ester and polypropylene glass composites are compared. The constant heat flux used is 75 kW/m². The tensile load bearing capacity (depicted on the left) rapidly drops, however for low stress levels at about 50 N/mm² to 200 N/mm², depending on the composite, a time-to-failure in excess of 1000 seconds (16 minutes) is possible. [B07, p191]

A different story holds for the compressive stress values, here it can be seen that the rate of decline is about the same as for tensile load. However, the time to failure is only about 100 seconds at stress levels of 0 N/mm² to 50 N/mm² (depending on the composite). This clearly illustrates that the behavior under compression is clearly the most concerning issue regarding composites under fire load (!) [B07, p192] In compression, the strength is much more dependent on the role of the matrix, which is a cause for this behavior. [B07, p223]

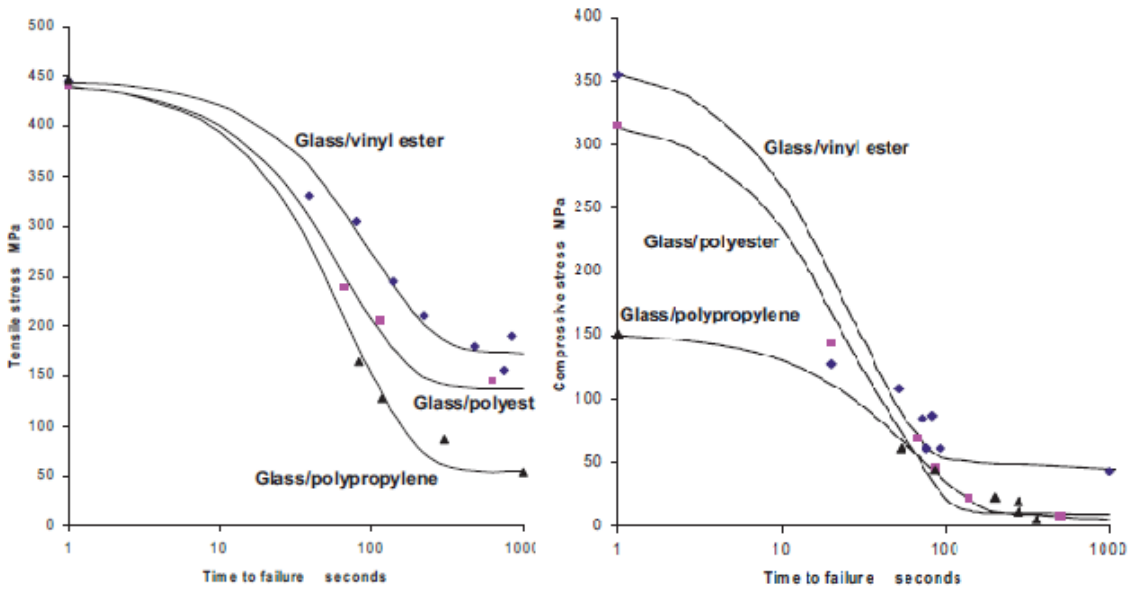


Fig. 103: Failure times of different composites under tension and compression [B07, p193, 194]

The graphs below compare the normalized tensile (left) and compressive stresses (right) of vinyl ester (top) and phenolic (bottom) glass resins under different fire loads. The failure times of the phenolic laminate are the shortest, which is interesting considering its lower flammability. The less favorable performance of the phenolic laminate was attributed to heat-induced delamination and matrix cracking, which is more extensive than for the vinyl ester laminate. Comparison of the tensile failure curves with those for compression loading underlines the significantly longer failure times for the tensile case. [B07, 191-197]

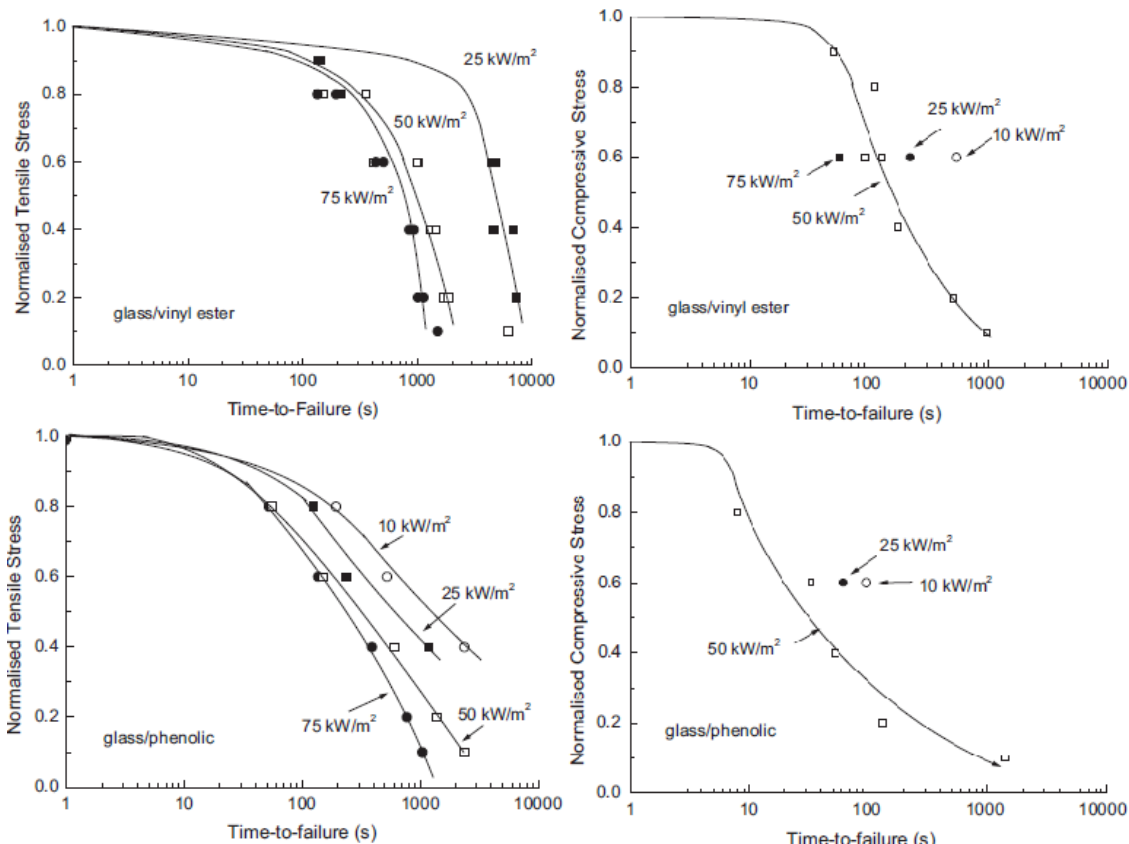


Fig. 104: Failure times under normalized tensile (left) or compressive (right) stresses of different resins [B07, p195, 196]

4.3.6 POST-FIRE PROPERTIES OF COMPOSITES

After a fire is extinguished, it is important to know the residual properties of a burnt composite at room temperature in order to determine the mechanical integrity and safety of a fire-damaged structure. Progress towards characterizing the post-fire properties has been slow, and there is much that is not known. [B07, p215] A standard fire test method for characterizing the residual properties of laminates following fire has not been established. [B07, p216]

The graphs below show the post-fire flexural strength of different thermoset (left) and thermoplastic- and epoxy composites (right). The test specimens were loaded with a constant 25 kW/m^2 heat flux for twenty minutes. For the thermoset composites a generally very high reduction in strength can be seen. A disturbing feature is that the post-fire strength of epoxy based composites diminishes very rapidly, due to the flammability of the epoxy matrix. This is a large problem because epoxy is often used for high strength applications such as bridge engineering. [B07, p217] The thermoplastic resins (right) are able to retain a much higher strength than the thermoset resins. Most probably this is due to the higher decomposition temperature. [B07, p225]

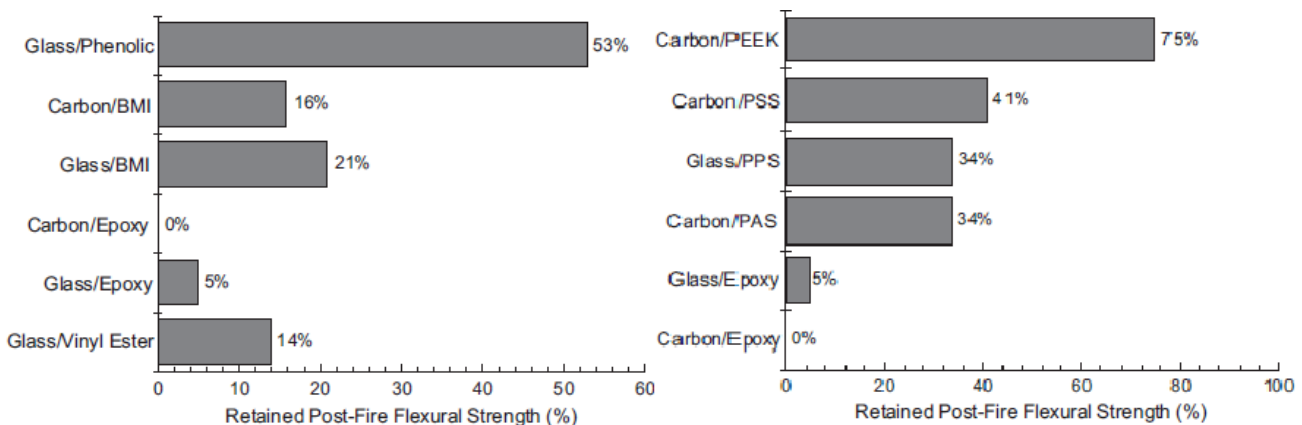


Fig. 105: Retained post-fire flexural strength of different thermoset (left) and thermoplastic (right) composites [B07, p217, 226]

The graphs below show the results of another fire test. The left graph shows the dependence of the normalized post-fire flexural strength on the heating time. It is visible that the behavior of phenolic composites is similar to the more flammable vinyl ester composites, despite the fire reaction properties of phenolic. The same holds for the right graph, where the normalized post-fire flexural strength is correlated to increasing heat fluxes. It can be concluded that phenolic loses significant strength, even without igniting. [B07, p218-219]

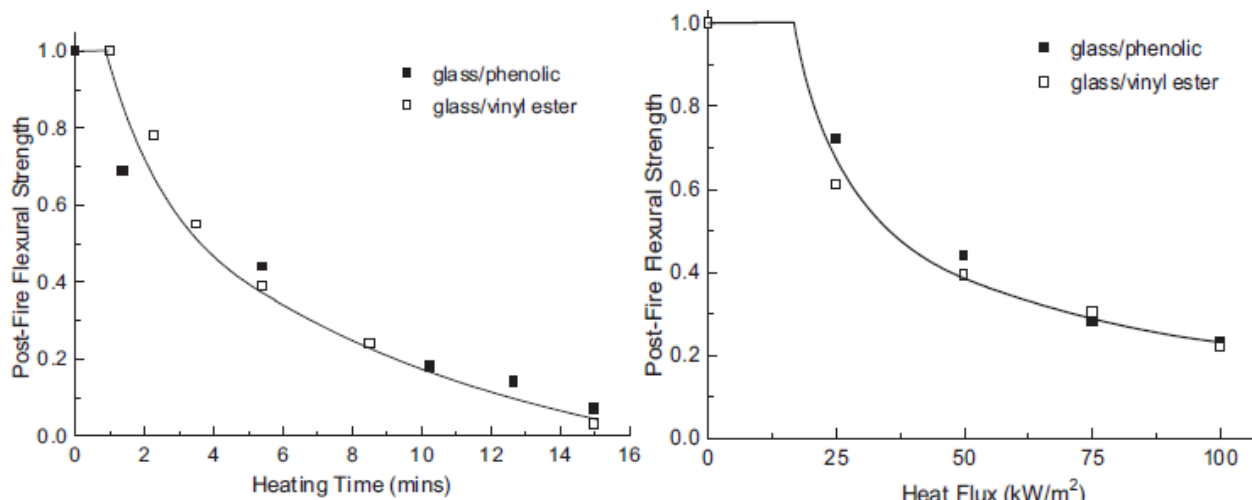


Fig. 106: Dependence of the post-fire flexural strength on heating time (left) and heat flux (right) [B07, p220]

4.3.6.1 TWO-LAYER MODEL FOR THE POST-FIRE MECHANICAL PROPERTIES PREDICTION

Although no standard procedure does yet exist for the calculation of the post-fire mechanical properties of composites, it is already known that these properties depend mainly on the char-depth. The portion of the composite cross-section which has been totally decomposed and turned into char during the fire cannot contribute significantly to the strength of the material, because char has strength and stiffness properties very close to zero. [B07, p222] These assumptions were used in the ‘two-layer model’ by Mouritz and Mathys to predict tension, compression and flexure properties of laminates that had been exposed to uniform one-side-only heating in a fire. The damaged laminate is assumed to consist of two regions; firstly the char region where the resin matrix is thermally degraded and secondly the virgin, unburned region. The picture below shows these layers. The decomposition zone between the char zone and the virgin region is assumed to be very thin compared to the other zones and is thus ignored. [B07, p226]

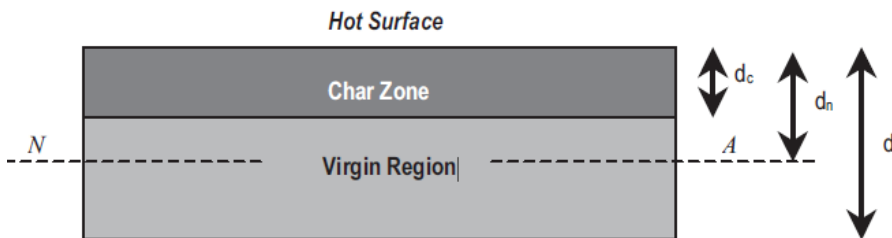


Fig. 107: Two-layer model by Mouritz and Mathys [B07, p227]

Using the two-layer model, the post-fire elastic moduli for tension, compression and flexure can be described with the following formulae:

$$E_t = \left(\frac{d - d_c}{d} \right) E_{t(o)} + \left(\frac{d_c}{d} \right) E_{t(char)} \quad (4.7)$$

$$E_c = \left(\frac{d - d_c}{d} \right) E_{c(o)} + \left(\frac{d_c}{d} \right) E_{c(char)} \quad (4.8)$$

$$E_f = \frac{4E_{f(o)}}{d^3} \left[(d - d_n)^3 + (d_n - d_c)^3 + \frac{E_{f(char)}}{E_{f(o)}} (d_n^3 - (d_n - d_c)^3) \right] \quad (4.9)$$

$$d_n = \frac{d_c^2 (E_{f(o)} - E_{f(char)}) - E_{f(o)} d^2}{2d_c (E_{f(o)} - E_{f(char)}) - 2E_{f(o)} d^2} \quad (4.10)$$

Wherein $E_{t(o)}$, $E_{c(o)}$ and $E_{f(o)}$ are the tensile, compressive and flexural moduli of the virgin region, assumed to be the same as the original material. $E_{t(char)}$, $E_{c(char)}$ and $E_{f(char)}$ are the tensile, compressive and flexural moduli of the char, which must be empirically determined, but lie between 0 GPa and 0,01 GPa for glass polyester char and at about 0,27 GPa for glass phenolic char. [B07, p222] It is thus conservative and safe to assume them to be zero. d_n needs to be calculated when the post-fire flexural modulus is needed. [B07, p227-228] Similar formulas have been derived by Mouritz and Mathys for the post-fire tensile strength σ_t and compressive strength σ_c and the flexural failure load P_f . [B07, p229-230]

$$\sigma_t = \left(\frac{d - d_c}{d} \right) \sigma_{t(o)} + \left(\frac{d_c}{d} \right) \sigma_{t(char)} \quad (4.11)$$

$$\sigma_c = \left(\frac{d - d_c}{d} \right) \sigma_{c(o)} + \left(\frac{d_c}{d} \right) \sigma_{c(char)} \quad (4.12)$$

$$P_f = \frac{8\sigma_{f(0)} b}{3L^*} \left[(d - d_n)^2 + \frac{(d_n - d_c)^3}{(d - d_n)} + \frac{E_{f(c)}}{E_{f(0)}} \frac{(d_n^3 - (d_n - d_c)^3)}{(d - d_n)} \right] \quad (4.13)$$

For the case of thin laminate beams that may fail by buckling, the Euler buckling load P_c can also be calculated using this method, assuming ideal column behavior of an isotropic material. C in formula 4.5 is a constant determined by the restraint conditions at the beam ends. Formula 4.6 defines the slenderness ratio (l/r) [B07, p230]

$$P_c = \frac{C\pi^2 Eb(d - d_c)^3}{12L^2} \quad (4.14)$$

$$(l/r) = \frac{l\sqrt{12}}{(d - d_c)} \quad (4.15)$$

The above formulas were compared with an array of test results and it showed that the formulae yielded very similar numerical values as derived in the experiments. The graph below on the left shows the Euler buckling strength as a function of the slenderness ratio for various size glass polyester plates and beam following exposure to a fuel fire. The graph on the right shows the reduction of the tensile, compressive and flexural strength during exposure to a constant heat flux of 50 kW/m^2 . [B07, p230-231]

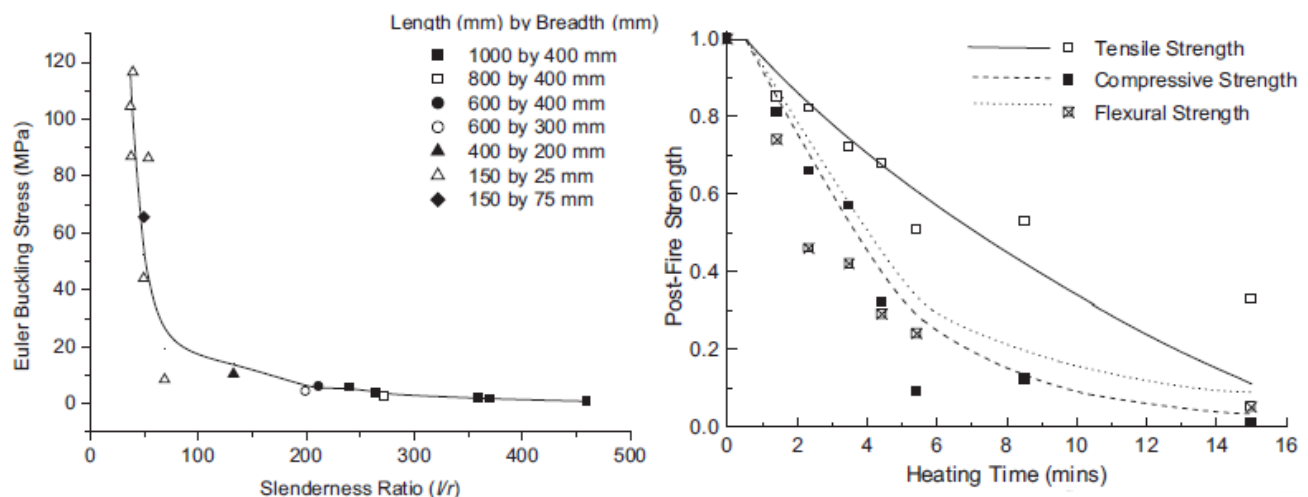


Fig. 108: Left: Euler Buckling strength as function of the slenderness ratio for various test specimens. Right: Reductions of the tensile, compressive and flexural strength of a slender glass polyester composite beam due to a constant heat flux of 50 kW/m^2 . [B07, p230]

4.3.7 IMPROVEMENT OF FIRE PROPERTIES OF FRP COMPOSITES

The previous chapter showed clearly that the mechanical properties of most fiber reinforced composites drastically reduce under the influence of fire and/or heat. Several tests have shown that the compressive strength in particular is dramatically reduced, for medium heat fluxes up to 75 kW/m^2 most thermoset composites have failure times under 100 seconds. The low mechanical properties under fire load call for measures to protect the composite elements against the negative influence of fire. In other words measures to improve particularly the mechanical properties under fire.

This chapter will be focused on various means to achieve improved mechanical properties under fire load. Furthermore also the improvement of fire reaction and fire resistance will be covered. The methods used are extraordinary diverse, and vary in complexity from simple additive compounds blended into the polymer matrix or heat-resistant coatings, through to sophisticated methods that involve chemical

modification of the matrix or heat-induced intumescence of the composite surface. Another group of methods that is described, are the methods where the thermal stability and fire resistance of organic fibers are improved.

The graph below gives an important first impression of what fire protection measures can mean to the post-fire mechanical strength of fiber reinforced composites. The data below was derived in an experiment with a thin glass fiber vinyl ester laminate that was exposed to a heat flux of 25 kW/m^2 for twenty minutes. The post-fire flexural strength was increased with about 800% for the best-performing protective measures. [B07, p233]

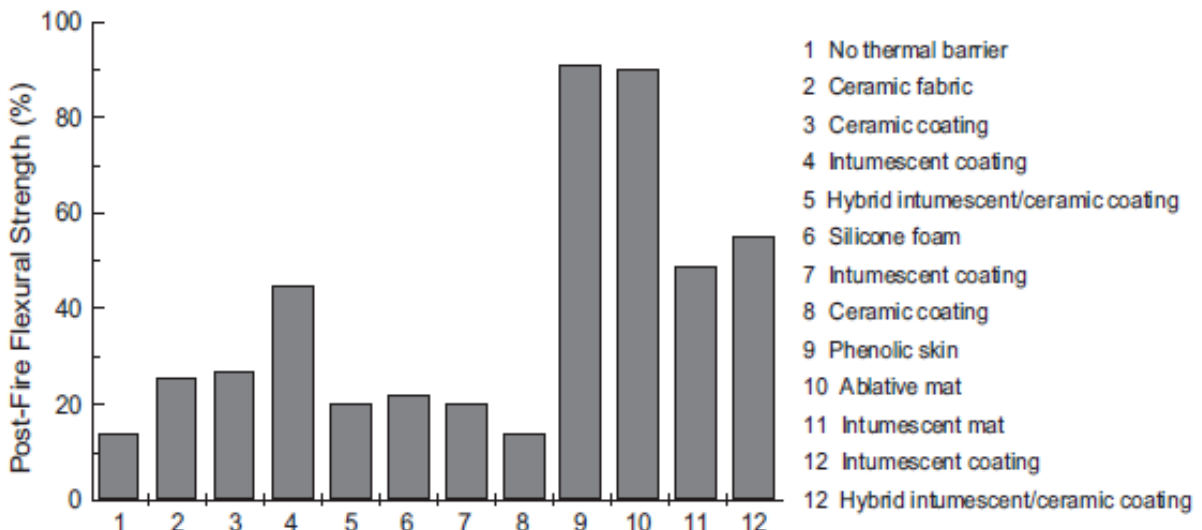


Fig. 109: Post-fire flexural strength of a glass fiber vinyl ester composite protected against fire by various means. The test sample was exposed to a heat flux of 25 kW/m^2 for twenty minutes. [B07, p233]

Flame retardant polymers are often classified as ‘condensed phase’ or ‘gas phase’ active, depending on whether they disrupt the decomposition of the polymer or combustion in the flame. The most effective retardants operate in both phases at the same time. Condensed phase activity encompasses several flame retardant mechanisms, which include: diluting the amount of combustible organic material by the addition of inert filler particles, reducing the temperature of the composite by acting as a heat sink, reducing the temperature by the addition of fillers that decompose endothermically, reducing the heat release rate by using polymers that decompose via endothermic reactions, increasing the aromaticity of the polymer in order for it to decompose into an insulating surface layer of char.[B07, p239]

Polymer composites that are flame retardant in the gas phase operate by interfering with the combustion reaction, thus reducing both flame propagation and the amount of heat returned from the fire to the material. The most widely employed flame retardant mechanism in the gas phase is usually the release of bromine, chlorine or phosphorus based radicals that terminate the exothermic combustion reactions by removing H and OH radicals from the flame. [B07, p240]

Flame retardants are by far the largest group of additives used in polymers. They account for about 27% of the plastic additive market, and this exceeds other types of additives including heat stabilizers (15,6%), antioxidants (7,6%), lubricants (6%) and UV stabilizers (5%). [B07, p240]

Flame retardants are classified as additive or reactive compounds. Additive compounds are intimately blended into the polymer during processing, but do not chemically react with the polymer. The chemical composition of many of these compounds is based on the following elements: antimony, aluminum, boron, phosphorus, bromine or chlorine, which all confer a high level of flame retardation. It is estimated that about 90% of all additive compounds are based on these elements, and are used in the form of antimony oxides, alumina trihydrate and boron oxides. Less often, additive compounds are used that contain barium, zinc, tin, iron, molybdenum or sulfur. [B07, p240]

Reactive compounds are polymerized with a resin during processing to become integrated into the molecular network structure. Reactive fire retardants are mainly based on halogen (bromine and chlorine), phosphorus, inorganic and melamine compounds. Until recently, bromine and chlorine were the common retardants because of their potency in quenching flames. During the last years, however, there is strong pressure from governments and environmentalists to use non halogenated flame retardants because of health and environmental concerns with bromine and chlorine vapor compounds. Phosphorus is a highly effective flame retardant that operates by reducing the amount of combustible gases released from a decomposing polymer by promoting char formation. [B07, p240]

To conclude this introduction it must be stated that it is common practice to use a combination of flame retardants in polymer composites in order to maximize the flammability resistance while minimizing the adverse effects on the mechanical properties, smoke-production and -toxicity. [B07, p240]

4.3.7.1 FLAME RETARDANT FILLERS

Fillers are inorganic non-reactive compounds that are added to the polymer during the final stages of processing to reduce the flammability of the finished product. The filler particles are under 10 µm in diameter, and often in the submicron range. The particles are blended into the liquid resin. Most polymers require a high loading of filler to show an appreciable improvement to their flammability resistance, and the minimum volume content is usually about 20% and the average content is typically 50 to 60%. Fillers are often used because of their low cost, relatively easy addition into the polymer, and high fire resistance. It is important to note that fillers are rarely used alone, but instead are used in combination with other flame retardants to achieve a high level of flammability resistance. There are two classes of fillers – inert- and active flame retardants – which are distinguished by their mode of action. [B07, p241]

Inert flame retardant fillers

Inert fillers reduce the flammability and smoke yield by one or more of the following mechanisms. The main mechanism is the reduction of the fuel load by diluting the mass fraction of organic material in a composite by the addition of a non-combustible filler. Obviously, for this mechanism large filler loadings of 50% to 60% are needed. The second mechanism of inert fillers is the absorption of heat by the filler. To be an effective heat sink the filler must have a greater heat capacity than the polymer host. The third mechanism to be described here is the formation of an insulating surface layer by the filler. This layer reduces the rate of heat conduction to the underlying composite material and thereby slows the decomposition rate of the polymer. Most available fillers operate by reducing the flammable mass and by forming a heat sink. The most commonly used composites are silica, calcium carbonate and carbon black. Sometimes simple hydrated clay silicates such as talc, gypsum or pumice are used. [B07, p242]

Active flame retardant fillers

Active fillers are more effective than inert fillers because they do not only operate as flammable mass reducer and heat sink, they also function in the condensed phase by decomposing at elevated temperature via an endothermic reaction that can absorb large amounts of heat. The decomposition of the filler also yields a large amount of inert gases, such as water vapor and carbon dioxide, which diffuse into the flame where they dilute the concentration of flammable volatiles. To achieve a substantial reduction in flame retardancy, medium to high filler loadings of 20% to 60% are needed. A diverse range of metal oxides and metal hydroxides are used as active flame retardant filler, although the most common is aluminum trihydroxide, Al(OH)_3 . Other types of aluminum oxide compounds are also used, as well as oxide compounds containing antimony (SbO_3 , Sb_2O_5), iron (FeOOH , FeOCl), molybdenum (MoO_3), magnesium (Mg(OH)_2), zinc and tin. [B07, p242-243]

Aluminum trihydroxide fillers

Aluminum trihydroxide (ATH) also known as aluminum trihydrate is the active flame retardant filler compound that is most often used in polymer composites. The amount of ATH used is greater than the combined amount of all other flame retardant fillers. ATH is popular due to its low cost, good flame retardant properties and its non-toxic smoke. For most resin systems a fill grade in excess of 50% is needed

to obtain substantial results. High fill-grades degrade the mechanical and durability properties, thus ATH is often used in lower concentration in combination with another flame retardant. [B07, p243]

ATH is active in both the condensed and gas phases of the combustion process, and when used in a large amount, it is remarkably effective in suppressing flaming combustion and (in some cases) smoke. The main condensed phase mechanism of ATH is the absorption of heat when the filler decomposes. ATH decomposes between 220°C and 400°C by an endothermic reaction which absorbs about 1kJ of heat per gram of ATH. [B07, p243]

The main endothermic peak of the reaction occurs at about 300°C, which means the reaction is absorbing the most heat at a temperature at which most polymers used in composites do not decompose. Further mechanisms that ATH undergoes under fire load are the release of water vapor, functioning as a heat sink, due to its high heat capacity and the production of a refractory Al₂O₃ layer in the polymer. The last mechanism only occurs in the case of very high ATH loading.

The graphs below show the high effectiveness of ATH in lowering the peak- and average heat release rate. The rate of reduction lies at about 15% to 40%, depending on the heat flux. The reduction of the heat release becomes greater at high heat fluxes.

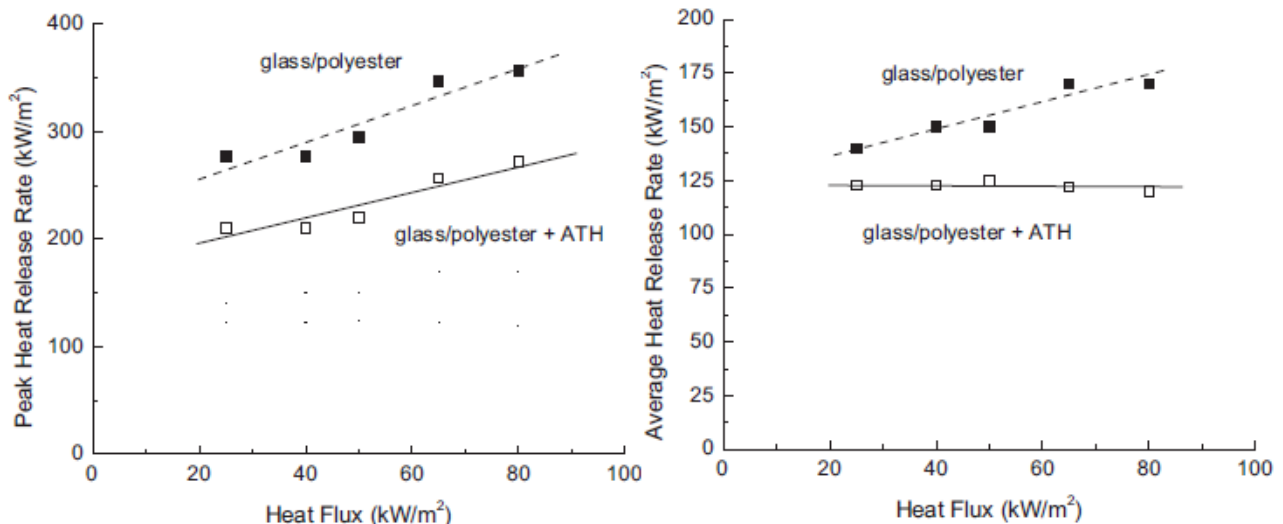


Fig. 110: Reduction of peak- (left) and average (right) heat release due to the addition of ATH [B07, p246]

In various tests it was found that ATH is particularly effective when used in combination with modified acrylic resins or MODAR. Due to the low viscosity of MODAR very high loading rates of ATH can be achieved. Highly ATH filled MODAR resins are superior in terms of toxic gas emission and mechanical properties to phenolic resins, which makes them suitable for use in flame resistant structural composite materials. When ATH is used in combination with polyester resins, for example at 50% loading rate, the polyester composite still behaves worse than phenolic composites, concerning only the fire properties. [B07, p244]

When ATH is used in combination with phenolic resin systems very good results can be gained with lower loading levels. The graph below shows some of the improvements on fire reaction properties due 30% fill ratio of ATH in glass phenolic composite subjected to a heat flux of 50 kW/m².

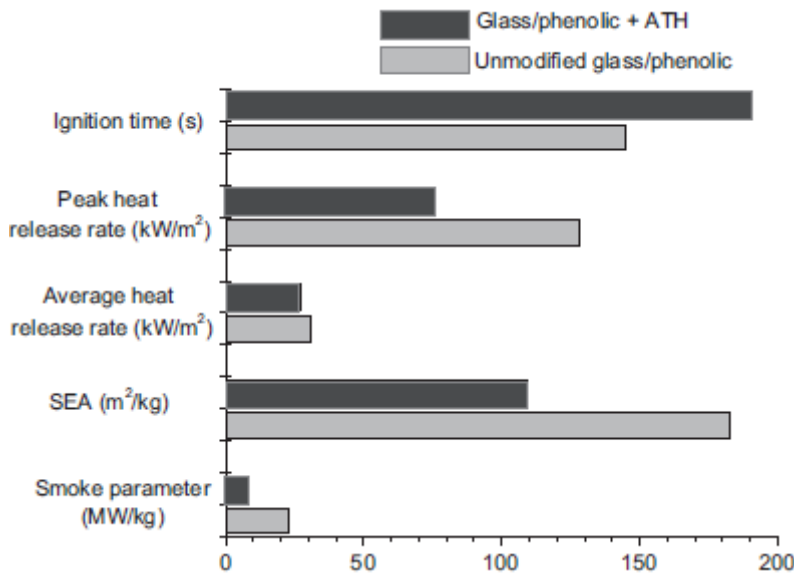


Fig. 111: Effect of 30% ATH fill on the fire reaction properties of a glass phenolic composite subjected to a heat flux of 50 kW/m² [B07, p248]

Magnesium oxide fillers

Magnesium hydroxide ($\text{Mg}(\text{OH})_2$) and a hydromagnesite ($\text{Mg}_4(\text{CO}_3)_3(\text{OH})_2\text{H}_2\text{O}$) hunite ($\text{Mg}_3\text{Ca}(\text{CO}_3)_4$) hybrid compound are active fillers suited to polymer composites that need to be processed above the decomposition temperature of ATH. Magnesium hydroxide is thermally stable up to 330°C -340°C, and therefore can be used in most types of high temperature thermoplastics without decomposing during processing. This is what makes them more suitable to increase the fire properties of thermoplastics than ATH. Both magnesium compounds act as flame retardants in a similar manner to ATH. As with ATH, they need to be present in a large amount (30% to 60%) to provide significant flame retardancy. The magnesium compounds undergo a highly endothermic decomposition reaction that slows the heating rate of the host material in a fire. [B07, p248]

Magnesium compound fillers are effective in prolonging the ignition time and reducing the amount of smoke produced by high temperature polymers. However, magnesium compounds are generally less effective and more expensive than ATH compounds. When used in one of the many engineering polymers such as polyesters, vinyl esters and epoxies the efficiency of magnesium compounds drops because the decomposition temperatures of the filler and the host matrix are very similar. [B07, p249]

Antimony oxide fillers

Antimony oxide fillers (Sb_2O_3) are used because of their good flame retardant properties. They function by releasing reactive molecules such SbOH and SbO , which scavenge the H-radicals, thus slowing the exothermic reaction. This reduces the flame temperature. Antimony oxides can be used alone in polymers, but are much more often used in combination with flame retardant halogen compounds. [B07, p251]

Iron-based fillers

Organometallic and inorganic iron compounds, such as ferrous oxides, ferric oxides and ferrocene are used as flame retardants and smoke suppressors in polymers. However, these materials have not been thoroughly tested in engineering polymer composites. They are believed to decompose at elevated temperatures and thus promote the formation of char. The increased char yield reduces the amount of flammable organic volatiles released by the decomposing polymer, lowering the fuel load. Most iron-based fillers have only been tested with commodity plastics such as PVC or ABS. Because these plastics are not used in polymer composites, these tests will not be covered here. [B07, p251]

Zinc oxide and borate fillers

Zinc stannate (ZnSnO_3), zinc hydroxystannate ($\text{ZnSnO}_3\text{H}_2\text{O}$) and zinc borates are used occasionally in halogenated polymers. Of the three groups of fillers, zinc borates are used most often due to their low cost and good flame retardant properties in certain polymers. It is interesting to point out that Zinc oxides require substantially lower loading levels than the fillers described earlier. The table below shows some results on the fire properties of a polyester resin filled with only 2% zinc hydroxystannate (ZHS). Generally the properties are improved, except for the carbon monoxide yield. [B07, p253]

Property	Unit	Virgin Polyester	Polyester + ZHS filler	Improv. Percentage
Ignition time	s	24	22	-8%
Peak heat release rate	kW/m^2	202	126	38%
Average Heat Release Rate	kW/m^2	115	68	41%
CO Yield	kg/kg	0,06	0,12	-100%
CO ₂ Yield	kg/kg	0,70	0,69	1%
Smoke extinction area	m^2/kg	825	415	50%

Table 38: Fire reaction properties of polyester resin with and without 2% ZHS fill [B07, p253]

Zinc oxide and borate fillers work by decomposing at elevated temperatures, reacting with H radicals released by the heated polymer, reducing the flame temperature. Zinc borates also release water vapor during fire, diluting the concentration of flammable volatiles. After decomposition the residual borate also forms a viscous surface layer, which slows the mass transfer of flammable volatiles into the flame. Other types of boric flame retardants are also used, such as boric acid (H_3BO_3) and borax ($\text{Na}_2\text{B}_4\text{O}_7\text{H}_2\text{O}$). These fillers also possess intumescence properties, meaning that they swell at elevated temperatures. Especially borax is reported to be an excellent flame retardant. [B07, p253]

Intumescence flame retardant fillers

Intumescence fillers are a relatively new way of improving the fire resistance of fiber reinforced polymer. When exposed to heat, the intumescence particles decompose in a reaction that yields large amounts of non-flammable, non-toxic gases that remain trapped in the host matrix. As these gases accumulate they cause the already softened polymer to foam and swell. As the composite continues to heat up the foamed polymer matrix itself begins to decompose and thus produces a highly porous char layer that insulates and protects the underlying virgin composite material. The fibers in the intumescence char prevent it from spalling or flaking. The scheme below illustrates the intumescence flame retardant process. [B07, p254]

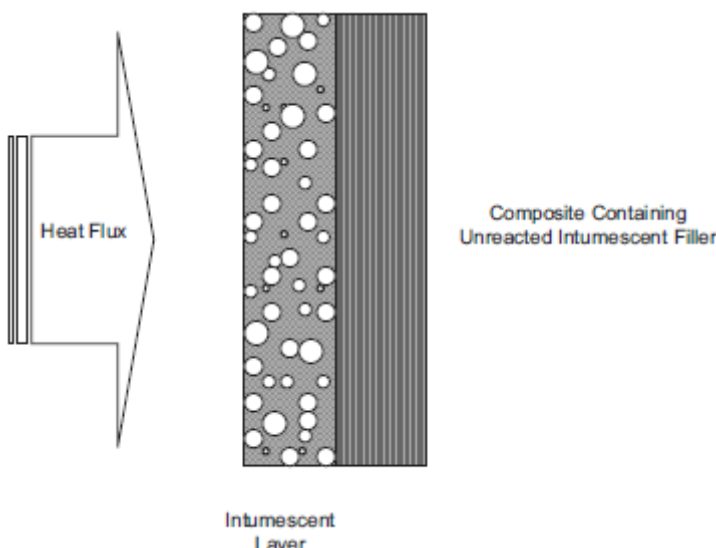


Fig. 112: Mechanism of flame resistance in composite filled with intumescence filler [B07, p254]

For optimal fire resistance it is important that the foaming process of the intumescence occurs only when the polymer is in a soft viscous state. When the intumescence particles decompose in a state where the host

matrix is still rigid, the matrix cannot swell and foam, leading to cracks and delamination in the composite, having adverse effects on the fire resistance. The same holds for decomposition of the filler in a too-late-stage, when the matrix is already softened too much. This causes the intumescent gases to escape from the composite, thus not foaming and swelling it. [B07, p254]

Another important limitation of intumescent fillers is that they can only effectively produce an insulating layer of char if the host matrix itself yields large amounts of char under elevated temperatures. Phenolic resins have this property, and the graph below shows the dramatic reduction of back-face temperature in a glass phenolic composite filled with intumescent filler particles. [B07, p255]

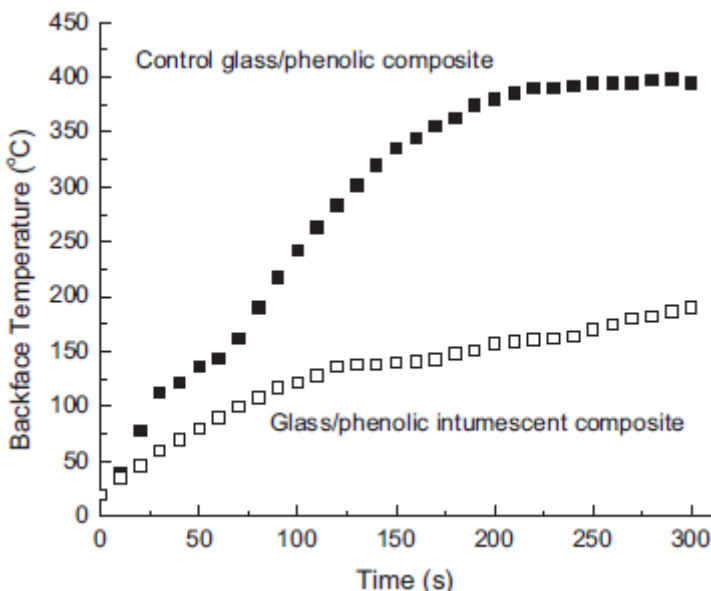


Fig. 113: Comparison of back-face temperature time profiles for glass phenolic composites with and without intumescent filler [B07, p255]

Tests have shown that phosphate intumescent particles combined with polysilicate fiber (Visil) fillers that promote char forming can lead to much lower peak heat release rates and reduced smoke yields in polyester, vinyl ester, epoxy and phenolic composites. It has to be stated though, that the development of intumescent filler systems is still in an early phase and much research still has to be conducted. Further information on intumescent systems will be given in [chapter 4.2.9.5] on fire protective surface coatings. [B07, p256]

4.3.7.2 FLAME RETARDANT ORGANIC POLYMERS

Structural modification of the polymer chains is an effective technique for improving flammability resistance. The thermal stability of a polymer is determined by the bond energy between atoms on the main chain. Polymers containing large amounts of hydrogen, nitrogen or oxygen display high flammability because of their low bond enthalpy with carbon. The thermal stability of a polymer can be improved by increasing the strength of the chain bonds. Thermal stability is increased by incorporating aromatic and heterocyclic ring structures into the main chain, and minimizing the presence of H, N and O. Not only is the decomposition temperature of a polymer increased by this modification, but the mass fraction of flammable volatiles is reduced which lowers the heat release rate. In this chapter the three main methods to improve the inherent flame resistance of polymer matrices will be discussed. The methods are firstly the incorporation of the halogens bromine and chlorine into the molecular structure, secondly the incorporation of phosphorous compounds into the polymer. Thirdly the modification of the molecular network by graft copolymerization will be discussed. Even more modern techniques that incorporate nanotechnology, such as embedding nanotubes in the matrix will be separately discussed in a later chapter. [B07, p256-258]

Halogenated polymer composites

The chemical modification of polymers using organohalogen compounds is one of the more common and effective methods for reducing the flammability of composite materials. Halogen-based compounds contain bromine or chlorine. Halogenated polymers are made by incorporating halogen into the molecular network structure of the resin via co-polymerisation. For example, flame retardant polyesters are produced by a polymerisation reaction between polyester and a brominated monomer such as terebromophthalic anhydride, dibromoneopentyl glycol or terebromobisphenol A. As another example, flame retardant epoxy can be produced using a brominated monomer derivative of bisphenol A (tetrabromobiphenol A). [B07, 258]

The main flame retardant action of halogenated polymers is the disruption of the gas phase reactions that control the flame temperature of a fire. Reactive halogen species are released from a decomposing brominated or chlorinated polymer into the flame where they terminate the exothermic decomposition reactions of organic volatiles, and thereby lower the temperature. [B07, 259] It is important that this release of halogen radicals occurs at lower temperatures than the decomposition of the non-brominated part of the polymer. This is necessary to slow the release rate of flammable volatiles, thereby starving the flame. Another important mechanism is the ‘blanketing effect’ that is induced by heavy halogen gases from the polymer. This ‘blanket’ limits the access of oxygen to the surface and thereby promotes char-formation. [B07, p261]

The table below compares different fire reaction properties of non-brominated and brominated glass polyester composites at different heat flux intensities. It can be seen that ignition time, heat release rate and smoke parameter all drastically improve due to the bromination of the polymer. Generally improvements are better than when using flame retardant fillers. Note that for good flame retardant properties the bromine content in the polymer must be over 20%. [B07, p261]

Property	Heat Flux	Non-brominated Composite	Brominated Composite	Improv. Percentage
Ignition Time	35 kW/m ²	41 s	93 s	441%
	50 kW/m ²	25 s	62 s	403%
	70 kW/m ²	13 s	31 s	238%
Peak Heat Release Rate	35 kW/m ²	327 kW/m ²	112 kW/m ²	292%
	50 kW/m ²	374 kW/m ²	159 kW/m ²	235%
	70 kW/m ²	471 kW/m ²	174 kW/m ²	271%
Average Heat Release Rate	35 kW/m ²	78 kW/m ²	38 kW/m ²	205%
	50 kW/m ²	115 kW/m ²	49 kW/m ²	235%
	70 kW/m ²	109 kW/m ²	83 kW/m ²	131%
Smoke Parameter	35 kW/m ²	338 MW/kg	94 MW/kg	360%
	50 kW/m ²	374 MW/kg	155 MW/kg	241%
	70 kW/m ²	457 MW/kg	175 MW/kg	261%

Fig. 114: Comparison of fire reaction properties of a non-brominated and brominated glass polyester composite [B07, p262]

Halogenated polymers, and brominated and chlorinated polymers in specific, are often combined with flame retardant fillers to improve the combined flammability resistance dramatically. The combination of fillers with halogens can have additive, antagonistic or synergistic effects. In the case additive effects, the combination of flame retardancy of both substances is equal to the sum of the two. Both substances function alongside and without interaction. For example, some inert fillers work additively with halogen polymers. The halogen improves the flammability resistance in the gas phase while the filler operates in the condensed phase by reducing the fuel load or acting as a heat sink. An antagonistic effect is when the efficiency of the filled polymer system is less than the additive efficiencies of the individual components. The best situation is when the halogen and the filler have a synergistic flame retardant action, meaning that the combined flame retardancy of the system is greater than the sum of the filler and halogen

flame retardancy. Examples of systems that work synergistic are halogen combined with antimony oxide (most common), bismuth oxide, molybdenum oxide, tin oxide and boron compounds. [B07, p262-263]

A major concern with halogenated polymers and polymer composites is the release of smoke containing corrosive, acidic and toxic gases that are serious health and environmental hazards. Halogens produce toxic gases that are extremely hazardous. Chlorinated polymers release copious amounts of HCl gas that attack the respiratory system and eyes, which impairs the ability of people to escape from fire. Chlorinated polymers also produce chlorinated dibenzodioxins and related dioxin compounds that are highly toxic. A further concern is that dioxins can enter the eco-system where they remain stable for many years during which time many animals and plants can be affected. Therefore, these polymers are gradually being phased-out in many countries, and are being replaced with more environmentally-friendly flame retardant polymers containing brominated indan, tris(tribromophenyl) cyanurate, and tris(tribromoneopentyl). [B07, p266]

Halogen antimony oxide synergistic compound

Antimony oxide (Sb_2O_3) is a weak flame retardant when used alone. When used in halogenated polymer composites the flame retardant efficiency drastically improves. The improvement is achieved by synergistic interactions between both flame retardant mechanisms. Next to the synergistic action, antimony oxide also dilutes the flammable organic content of the polymer system. The critical loading point of antimony oxide filler lies at about 20%, after which the fire reaction does not intensify anymore. The graphs below show the flame spread index, the limiting oxygen index and the specific optical density of a brominated glass vinyl ester composite filled with different metal oxide fillers. It can be seen that antimony trioxide performs best for the fire spread index and the limiting oxygen index. [B07, p263-265]

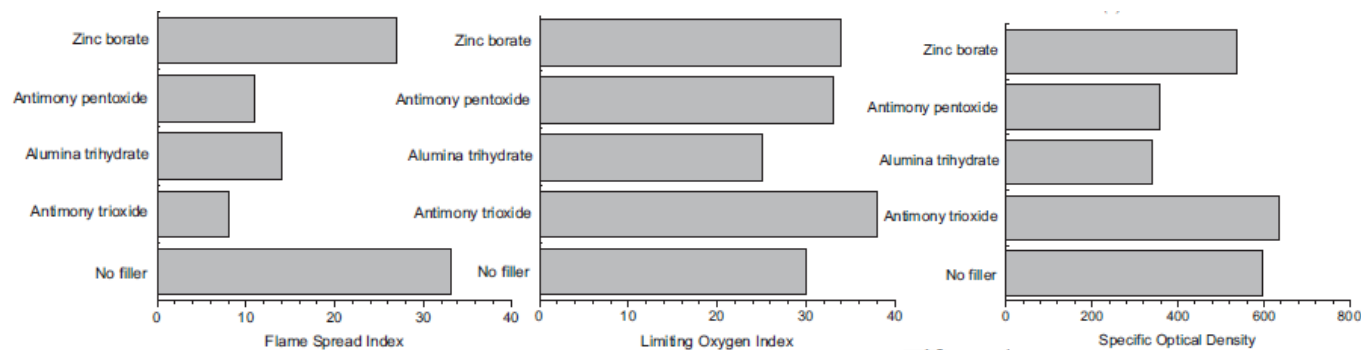


Fig. 115: Effect of flame retardant metal oxide fillers on the flame retardant properties of brominated glass vinyl ester composite [B07, p265]

Phosphorous polymer composites

The flammability resistance of polymers and polymer composites can be greatly improved by the addition of phosphorus. The most common method for adding phosphorus is blending phosphorous filler compound into a polymer during processing. The most common types are elemental phosphorus, ammonium polyphosphates and triarylphosphates. Phosphorus can also be incorporated into the molecular structure by copolymerization of the resin with a reactive organic phosphorous monomer or halogenated phosphate. The polymerization method is used to produce many varieties of flame retardant polymers suitable for use in composite materials. [B07, p266]

Phosphorus acts as a flame retardant in the gas and condensed phase, depending on the chemical nature and thermal stability of the host polymer. The gas phase mechanism dominates in most thermoplastics and non-oxygenated thermoset polymers. This mechanism involves the release of phosphorus radicals from the polymer at elevated temperature, although to be effective the volatilization process must occur below 350°C to 400°C, otherwise the polymer itself will decompose. Phosphorous polymers also make use of the 'blanketing effect', described earlier for the halogen polymers. Since the efficiency of phosphorous polymers depends greatly on the base polymer a simple rule has been derived to predict the effectiveness: The flame retardant efficiency of phosphorous increases with the oxygen content of the polymer. [B07, p266-267]

The graphs below illustrate the flame retardant properties of phosphorous carbon epoxy composites. The left graph shows the vertical burn time for various phosphorous contents. This is the time of self-extinguishment of a vertical composite strip after the removal of a heat source. The graph on the right shows the average heat release rate correlated to the phosphorous content, when exposed to a heat flux of 50 kW/m^2 . It can be seen that very small amounts of phosphorous lead to the best results, the vertical burn time does not substantially reduce for more than 3% phosphorous content. The heat release rate shows best results for about the same amount of phosphorous. [B07, p267-268]

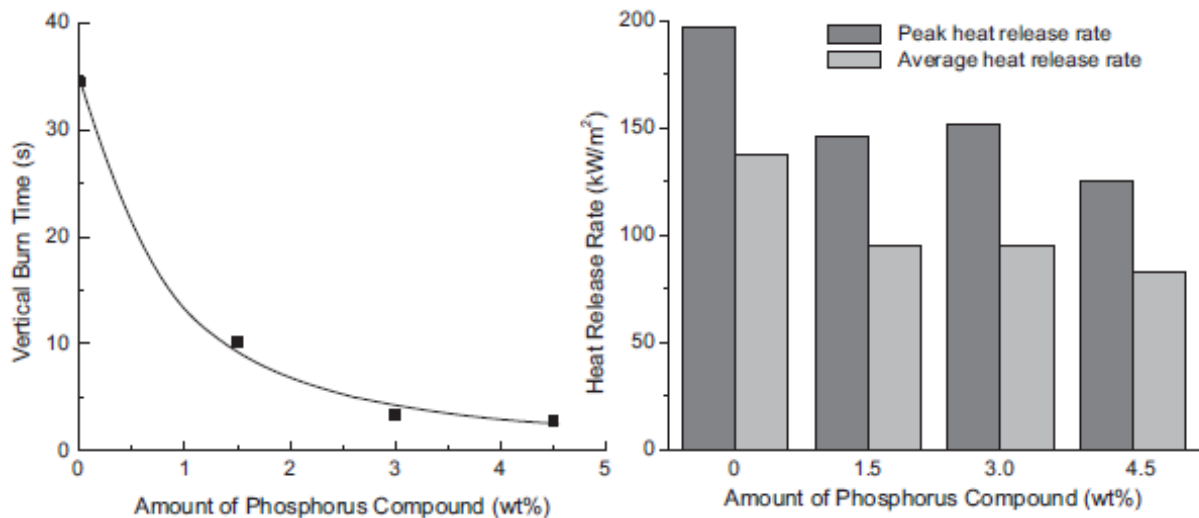


Fig. 116: Left: Vertical burn time for a phosphorous carbon epoxy composite. Right: Heat release rates for a phosphorous carbon epoxy composite subjected to a heat flux of 50 kW/m^2 . [B07, p268]

Graft copolymerization composites

Graft copolymerization is an emerging technique for the production of flame retardant polymers. This technique basically involves attaching a monomer, which is a strong char former, onto the polymer chain. The copolymerization process can occur via two routes known as 'grafting from' and 'grafting onto'. Regardless of the process, it is essential that the monomer thermally decomposes at a lower temperature than the host polymer, and yields a large amount of char that provides protection of the polymer.

Graft copolymerization is a promising technique for producing flame retardant polymers; however it is an emerging technology that requires further development. While a variety of flame retardant thermoplastics can be produced using the technique, the graft copolymerization of engineering thermoset polymers commonly used in structural composites requires further research and development.

4.3.7.3 FLAME RETARDANT INORGANIC POLYMERS

The use of specialty inorganic polymers in composites is another emerging flame retardant technology. Several inorganic polymers, most notably geopolymers, POSS (polyhedral oligomeric silsesquioxanes) and FyreRoc (inorganic metallosilicates) have considerable promise because they can be processed and cured into fibrous composites under conditions similar to organic resins, are reasonably inexpensive, and have outstanding flammability resistance. These inorganic polymers are also often called ceramics, ceramic polymers or ceramic composites.

Geopolymers are potassium aluminosilicate compounds prepared from a two-part system consisting of an alumina liquid suspension and silica powder. When the components are mixed into a paste the geopolymer has a sufficiently low viscosity to enable it to be applied as a binder onto reinforcing fabrics. Geopolymers are extremely resistant to fire, and will not ignite, spread flame, release heat or cause flashover. The table below shows the fire reaction properties of several organic polymer carbon composites as well as the inorganic polymer carbon composite. The values for the geopolymer are extraordinary. The material is completely infusible, releases absolutely no heat, does not burn and does not smoke. [B07, p271]

Property	Unit	Geopolymer	Epoxy	Phenolic	PPS	PEEK
Ignition time	s	0	94	94	173	307
Weight Loss	%	0	24	28	16	2
Peak Heat Release rate	kW/m ²	0	171	177	94	14
Average Heat Release Rate	kW/m ²	0	93	112	70	8
Smoke extinction area	m ² /kg	0	-	253	604	69

Table 39: Fire properties of different carbon thermoset and thermoplastic composites compared to geopolymers carbon composite [B07, p271]

Next to geopolymers the other important inorganic polymer is POSS, which is hybrid inorganic-organic polymer nanocomposite composed of the inorganic intermediate silica ($\text{SiO}_{1.5}$). The molecular structure of POSS has a cage-like configuration. POSS is still in development, but it is already known that it provides excellent thermal and oxidation stability and provides high flammability resistance when used in composites. [B07, p271]

Although inorganic polymers seem to solve all problems regarding flammability resistance they are some hurdles to be overcome in the future. The first problem is the application of the ceramic composites. Up until now they are only used in small scale applications such as nuclear power plants and aerospace application and have never been produced or tested in large scale application, such as needed for the bridge engineering industry. Furthermore not much research has been carried out on the fatigue resistance of ceramic composites, which is vital for the application in traffic bridges.

4.3.7.4 FLAME RETARDANT FIBERS

The most commonly used fiber reinforcement, glass fiber, is considered to be incombustible and carbon fibers remain stable over the temperature range of most fires when not exposed to an oxygen atmosphere. Despite these facts some alternative fibers were developed, that have even better fire resistant properties. Firstly continuous basalt-based fibers have been developed which have somewhat better mechanical properties than commonly available E-glass fibers. The basalt fibers are claimed to be fire resistant up to 1500°C. [B07, p272]

Organic fibers have more flame reaction issues than inorganic fibers. Aramid fibers are the most commonly used organic fiber in engineering composites, but still have better flammability resistance than many polymer matrix systems. When the fiber content of aramid fibers is increased in composites, this often results in reduced heat release and smoke formation, due to the higher char yield, as described in [chapter 4.2.4.5]: 'Decomposition of fiber reinforcements under fire load'. There has not been much research on the improvement of the flame retardancy of aramid fibers.

Another group of organic fibers that is often used are the polyethylene (PE) fibers. They are more flammable than aramid fibers, and thus the need for the improvement of their fire properties was greater, resulting in more research on the topic. Methods include halogenation, chlorination and phosphorylation of the polymer chains. However results of these tests have not yet been scientifically quantified and thus are not helpful for the design practice. [B07, p273]

4.3.7.5 FIRE PROTECTIVE SURFACE COATINGS

A common method to protect composites from fire is to use an insulating coating. The ideal coatings should possess the following properties: non-flammability, low thermal conductivity, strong adhesion (with similar expansion coefficient) to the composite substrate, environmentally durable, wear resistant, light-weight, thin and inexpensive. There are hundreds of coating materials that are commercially available for use on composites, although none possess all of the properties required for an ideal coating. [B07, p273]

There are three major classes of insulating coatings: flame retardant polymer coatings, thermal barriers, and intumescent coatings. Flame retardant polymer coatings are inherently fire resistant organic resins or inorganic materials, applied as thin film. Thermal barriers are usually ceramic-based materials that are non-

flammable and have low heat conducting properties. Examples are silica and Rockwool mats and sprayed films such as zirconia. Intumescent materials provide fire protection by foaming and swelling under elevated temperatures. The graphs below show the impressive results that can be achieved with fire protective surface coatings. The left graph shows the post-fire flexural strength of glass polyester composite with different surface coatings. Note that under a heat flux of 100 kW/m^2 the normalized flexural strength of the composite even exceeds 1,0 due to the excessive swelling. The right graph shows the correlation between heating time and post-fire flexural strength of protected and unprotected glass polyester composite. It can be seen that a protective intumescent layer drastically improves the post-fire strength. [B07, p234, 273-274]

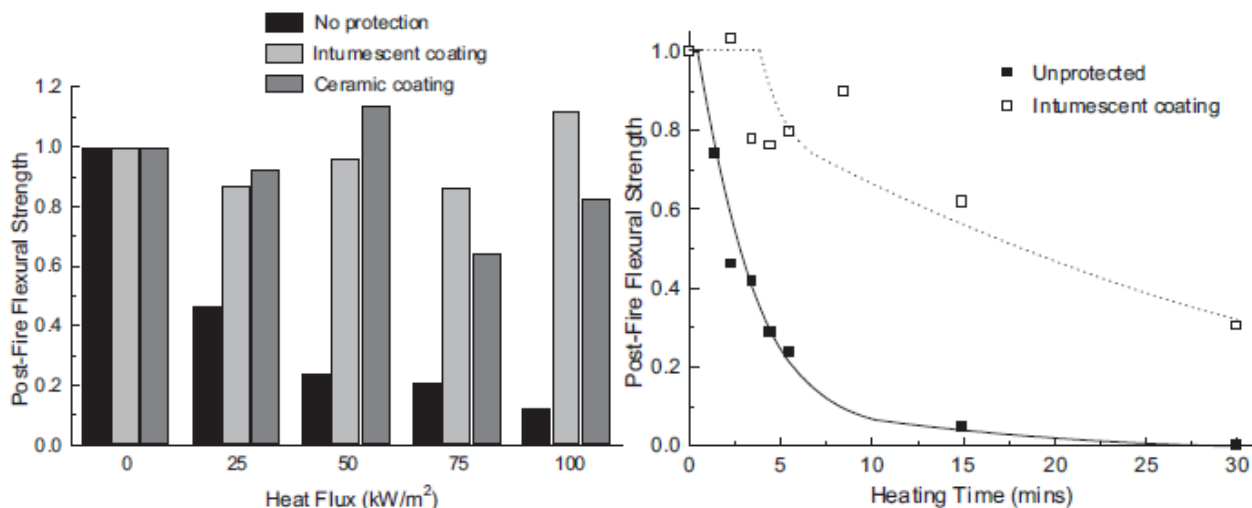


Fig. 117: Post-fire flexural strength of glass polyester composites with different coatings. Right: Correlation between heating time and post-fire flexural strength of protected and un-protected glass polyester composite. [B07, p234]

Flame retardant polymer coatings

A variety of organic polymers can be used, the most common being phenolic, brominated resins and alkyd resins, often with a high loading of flame retardant filler, to improve the fire retardant properties of composites. Organic polymer coatings are usually applied by brushing or spraying the liquid resin directly onto the composite substrate or coating the tool surface with the flame retardant resin and then over-laminating with the composite in a process similar to the application of a gel coat. The benefits of organic polymer coatings include moderate cost, light-weight and good chemical compatibility with the composite substrate that ensures good adhesion. However, a limitation of the application techniques is that the maximum coating thickness is usually very thin (under 2-3 mm), which can only provide short-term protection against high temperature fires. [B07, p274]

The graphs below show the peak heat release rate (left) and smoke extinction area (right) of a glass vinyl ester composite fitted with a protective phenolic skin. Although the graphs show a great improvement of the measured properties, they do not show the limited protection time that a thin phenolic skin can only offer.

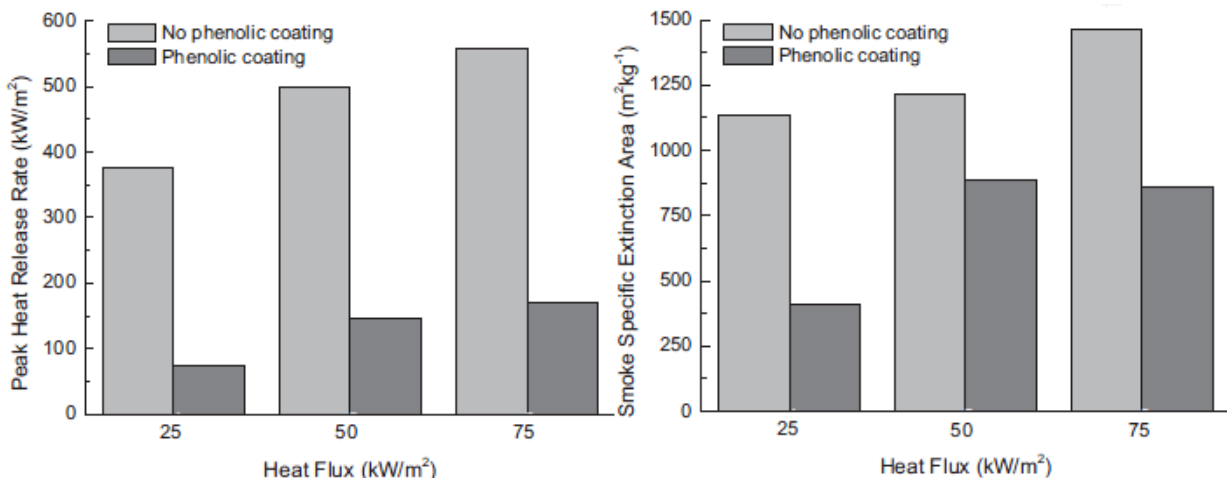


Fig. 118: Two fire reaction properties of a glass vinyl ester composite with and without phenolic skin [B07, p275]

Recently inorganic polymers have been introduced as flame retardant coatings. Geopolymers, POSS and Tecnofire (which is a char-forming graphite mat) are for example potentially interesting coating materials. Inorganic polymer coatings provide better fire protection than organic flame retardant polymers because of their higher resistance to pyrolysis and heat conduction. The most common method for applying inorganic coatings is by brushing the uncured polymer directly onto the composite. However, some inorganic resins are viscous which makes it difficult to brush, although the high viscosity makes it is possible to apply coatings up to 8-10 mm thick. [B07, p276]

The fire protection offered by inorganic coatings improves with their thickness, and therefore the ability to apply thick coatings is important. For example, the graph below shows that the peak heat release rate of a sandwich composite drops rapidly with increasing thickness of a geopolymer coating. It is essential, however, that the coating is strongly bonded to the substrate to avoid spalling and flaking. [B07, p276]

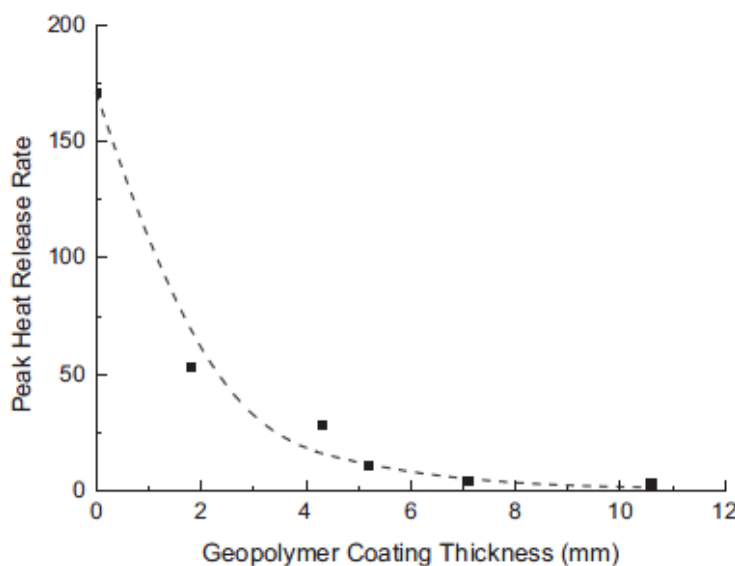


Fig. 119: Effect of the geopolymer coating thickness on the heat release rate of a sandwich composite [B07, p277]

Fire protective thermal barrier coatings

Thermal barrier coatings provide fire protection by having excellent insulating properties and sometimes heat reflective properties that direct heat back towards the fire. The most commonly used coatings consist of mineral fiber or ceramic wool mats, and these are bonded using a high-temperature adhesive to the composite substrate. It is also possible to bond the mat directly onto a composite while the polymer matrix is still curing. [B07, p276]

Two examples of commercial thermal barrier materials are Rockwool® and Structogard. These are widely used for fire insulation in ships and buildings. The graph below on the left side shows the effectiveness of a ceramic fiber barrier material in providing thermal protection to glass polyester composite. The thermal barrier greatly increases the ignition resistance of the composite, even at very high heat flux. Furthermore, the minimum incident heat flux needed to ignite the composite is increased from about 15 to 35 kW/m² due to the excellent insulation of the coating. The protection provided by thermal barriers also improves the fire resistance properties of composites, including increased burn-through time and higher structural properties in fire (!). [B07, p277]

The graph below on the right compares the char growth rates in a glass polyester composite with and without a thermal barrier coating. Charring starts to occur after about 30 seconds in the unprotected composite, and at longer heating times the char-layer grows through the material until it is completely burnt-through after 17 minutes. A long delay in charring and burn-through occurs when the composite is protected with the thermal coating. Charring does not start until after 11 minutes and the materials still does not completely burn-through, even not after 30 minutes. [B07, 277]

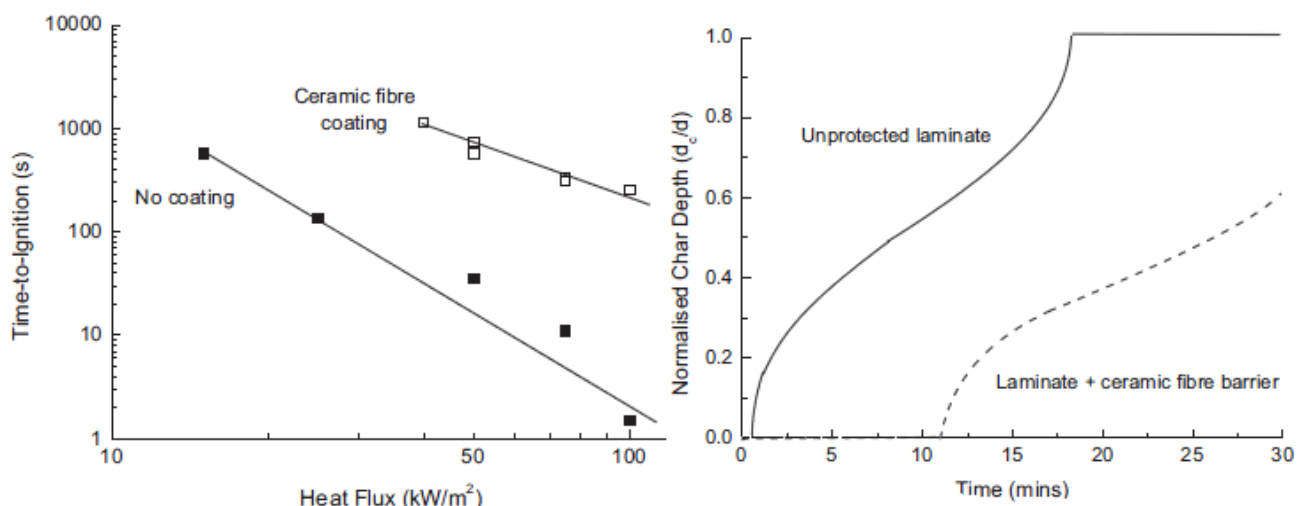


Fig. 120: Improvement of time-to-ignition (left) and char depth properties of a glass polyester composite with and without ceramic fiber coating/barrier [B07, p278]

The major drawback when using ceramic fiber coatings in composites is the large thickness needed. To obtain substantial long-term fire protection, thicknesses of about 10mm to 20mm are needed. [B07, p279] This adds to the weight and dimensions of the structure and is not advantageous in the case of a truss traffic bridge with a lot of surface area. Next to that, the price of most ceramic coatings is also very high, making large-scale application costly.

Another approach to use ceramic coatings is application of the ceramic substance as a thin film, sprayed directly on the elements, using techniques such as plasma- or liquid spraying. Any type of ceramic can be applied provided it can adhere strongly to the composite substrate. Often used spray-on ceramics are zirconium oxide and alumina. The graph below shows some test results on the fire reaction properties of a carbon epoxy composite with and without zirconium oxide coating. Despite the improved fire resistance, ceramic spray-on coating are rarely used because they can be expensive and prone to cracking and spalling due to thermal expansion mismatch with the composite substrate. [B07, p279]

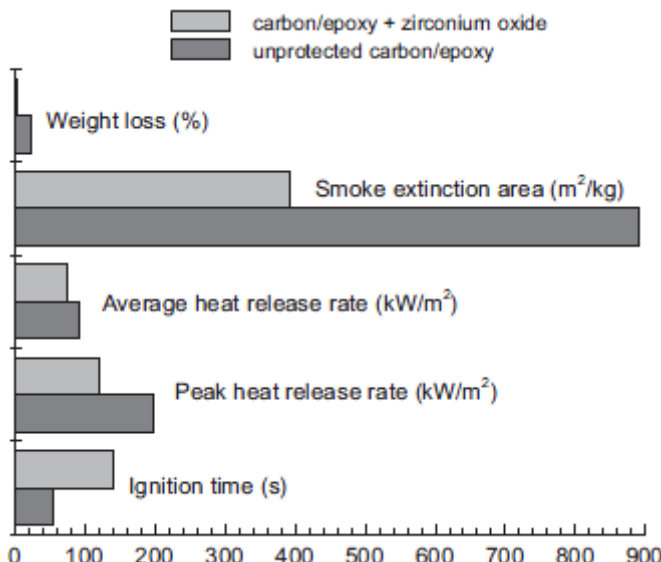


Fig. 121: Fire reaction properties of carbon epoxy composite with and without zirconium oxide coating [B07, p279]

Fire protective intumescent coatings

Intumescent coatings provide fire protection by undergoing an endothermic decomposition reaction process at elevated temperature that causes the material to swell and foam into a highly porous, thick and thermally stable char layer. The high void content and thickness of the coating allows it to act as an insulation barrier to the underlying composite against flame and heat. Intumescent coatings can be applied by painting or spraying liquid compound directly onto a composite element. Afterwards the intumescent coated elements need to be cured to form a solid encasing intumescent film. The maximum thickness for this method is about 5mm. Thicker intumescent coatings can be achieved using fibrous intumescent mats that are bonded to the substrate by high-temperature adhesive paste. [B07, p280]

Three reaction processes happen during heating of the intumescent. Firstly, the coating material decomposes, secondly the inert gases, evolved from the decomposition reaction drive back hot convective air currents and thirdly, the coating expands into a highly porous char layer with a high resistance to heat conduction from the flame into the underlying composite substrate. Intumescent coatings consist of a multitude of compounds. The four main types of compounds are carbon-rich (carbonific) compound, inorganic acid or acid salt, organic amine or amide and a blowing agent (spumific). These compounds undergo a series of decomposition reaction and physical processes almost simultaneously in order to function well as fire retardant. In the scheme below the order of processes in the intumescent is shown. [B07, p280]

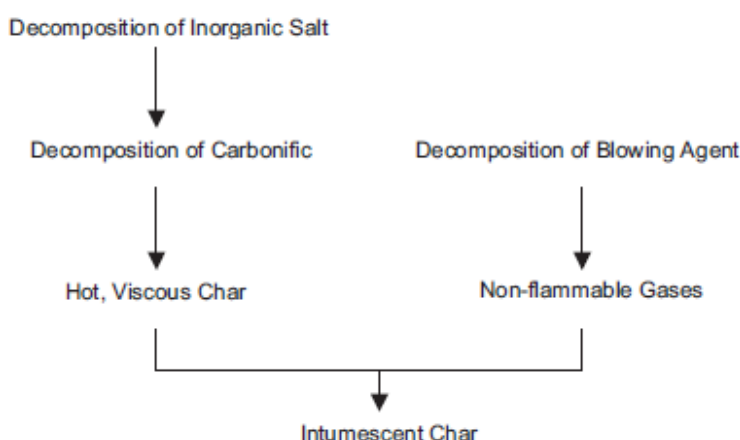


Fig. 122: Sequence of the fire protective intumescent coating reaction [B07, p281]

The first step in the intumescence reaction is the decomposition of the inorganic or acid salt, it must only start at temperatures sufficiently high, such that normal external heating like warming-up due to direct sunlight does not start the decomposition. Yet it must not be that high that the substrate composite starts to decompose first. Often used salt compounds such as zinc borate, ammonium phosphate, melamine phosphate, organic esters and salts of ammonium, amide or amine have decomposition temperatures roundabout 100°C to 250°C. Often catalysts like organic amides or amines, such as urea, melamine and dicyandiamide are used to improve the decomposition reaction. [B07, p280]

In the next stage the carbonic compound starts to decompose by a dehydration reaction with the previously decomposed inorganic salts. This reaction converts the carbonic into a carbonaceous char. The carbonic is a carbon-rich polyhydric compound that yields large amounts of char. Usually carbonics are polycarbonates, such as starch or polyhydric alcohol or phenol, such as phenol-formaldehyde. It is important that the now hot and viscous char is immediately expanded and drastically increased in volume. This happens when the blowing agent decomposition starts simultaneously with the carbonic decomposition. Blowing agents decompose in an endothermic reaction that produces large amounts of non-flammable gases that cause the char-melt to swell. Often used blowing agents are nitrogen compounds such as urea, dicyandiamide, guanidine, melamine and glycine that yield ammonia, carbon dioxide and water vapors during decomposition. Sometimes chlorinated paraffin is also used. The gases collect into small bubbles that cause the char to swell and foam. The coating eventually solidifies into a thick multicellular material that drastically slows the heat conduction from the fire into the composite substrate. [B07, p281]

Good intumescent coatings expand to 50 to 200 times of their original volume under fire load. They thereby form a fine-scale multicellular network with cell sizes of 20 µm to 50 µm and a wall thickness of 6 µm to 8 µm. A recent development in the field of intumescents is the addition of graphite flakes, which expand up to 100 times on heating and improve the effectiveness of the insulating layer. Several additives can be incorporated into the intumescent mix, including agents that control the cell thickness, antioxidants, thickeners, pigments and milled fibers for structural reinforcement. The pictures below show an intumescent of 0,8 mm thickness (left) which has expanded about 65 times to a thickness of 52 mm after fire load (right) [B07, p281-282]

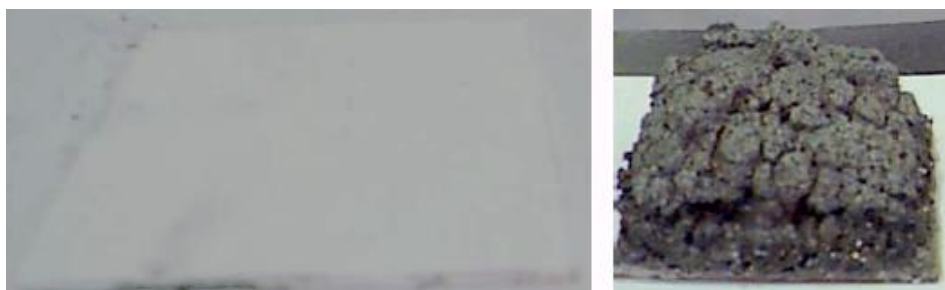


Fig. 123: Intumescent coating before (left, thickness = 0,8 mm) and after (right, thickness = 52 mm) fire loading [B07, p282]

Intumescent coatings are excellent heat insulators that slow the rate of heat transfer into composite laminates in fire. They can also be extremely effective in delaying combustion, suppressing flame spread, reducing the heat release rate, and lowering the smoke density of composite materials. The graph below on the left compares the temperature rise in a composite panel with and without such a coating. The temperature was measured at the back-face of the panel. The results are impressive, even after an exposure time of 60 minutes the intumescent protected composite temperature does not rise over 200°C (compared to furnace temperature of almost 1000°C). The graph below, on the right shows the effect of incident heat flux on the ignition time of glass polyester composite with and without an intumescent coating. Ignition was delayed considerably by the intumescent coating, with the thick mat providing greater protection because it was able to swell more than the film. [B07, p282]

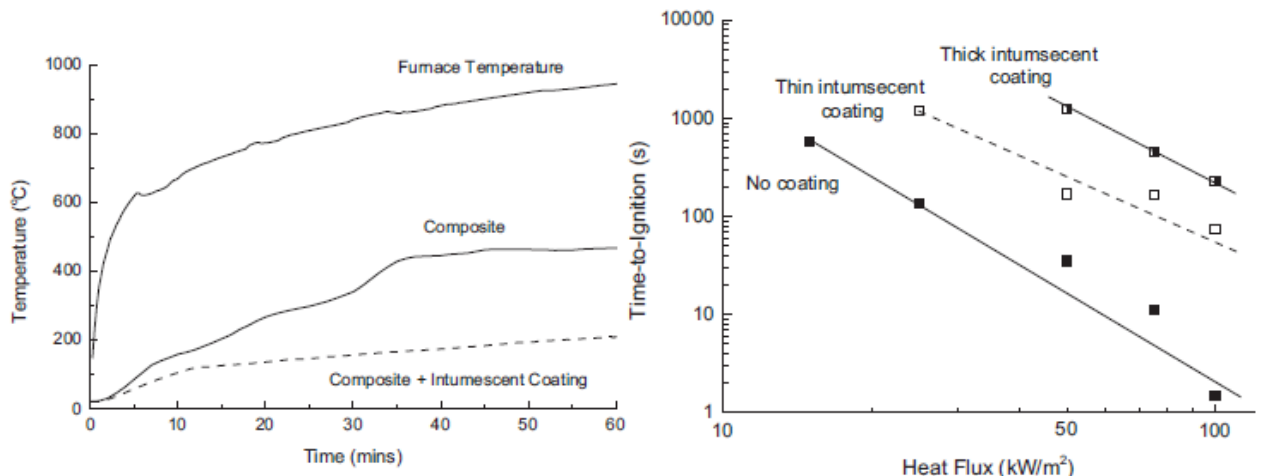


Fig. 124: Left: Back-face-temperature of an intumescence protected composite panel. **Right:** Ignition time of a glass polyester composite protected with thin and thick intumescence coatings at different heat fluxes [B07, p283]

Of course intumescence coatings also have several disadvantages: a major problem with many commercial coating products is that they do not bond strongly with the substrate, and often fall off during swelling, exposing the underlying composite directly to the flame. For a tubular truss composed of intumescence coated composite beams, this could be a serious issue. Thorough bonding is therefore essential. Durability and rapid ageing by weathering are also issues that need to be addressed by using separate coatings for this purpose. [B07, p282-283]

4.3.7.6 FLAME RETARDANT POLYMER NANOCOMPOSITES

The term nano-composite describes a composite in which one of the components, the so-called nano-material has at least one nano-scale dimension and it is completely dispersed throughout the polymer. The three main groups of nano-composites are polymer-clay nano-composites, single-wall and multiple-wall nanotubes and nano-scale spherical particles. [B07, p287]

A general advantage of flame retardant nano-composites is the low loading level required, compared to normal micro-level fillers. The reason for this is that for similar loading-levels, smaller particles have a bigger surface area, which reduces the material needed, because the reactive surface is bigger. [B07, p287-288]

The incorporation of nano-materials reduces the polymer flammability by several mechanisms, such as limiting fuel transfer to the flame and formation of a protective char layer. However, these polymer nano-composites still burn with very little, if any, reduction in total heat release, and time to ignition is generally not improved and can even decrease for some nano-composites. In other words, nanoparticles have to be used in combination with other flame retardant agents in order to achieve the required fire performance levels. Next to that, although some applications exist for thermoset resins, most research up until now was done on the incorporation of nano-materials in thermoplastic resins. [P84, p23]

Amongst the nano-materials used in composites, the nano-scale spherical particles and the nano-clay most certainly offer the greatest potential for a quick and efficient application in thermoset resins. Nano-tubes are still in a very fundamental scientific phase and are not very much available in the industry.

Polymer-clay nano-composite

The first interest in polymer-clay nano-composites emerged when it was found that low loading-levels in the range of 3% to 5% of layered silicate materials, such as montmorillonite, hectorite and bentonite can greatly improve the mechanical properties, enhance the barrier properties and improve the fire retardancy of polymers. The most often used nano-clay is montmorillonite (MMT). Nano-clay is already commercially available as thermoset epoxy composite, for example at 'Nanocor'. [B07, p288]

To improve dispersion of the clay nano-particles within the polymer matrix, natural clays are modified using organic substances. This leads to the formation of organo-modified nano-clays such as oMMT. The incorporation of a relatively low quantity of organomodified nano-clay in the polymer matrix creates a protective layer during combustion. Upon heating, the viscosity of the molten polymer/layered silicate nano-composite decreases with increasing temperature and facilitates the migration of the clay nano-layers to the surface. Moreover, heat transfer promotes thermal decomposition of the organomodifier which can actively catalyze the formation of a stable char residue. Therefore accumulation of the clay on the surface of the material acts as a protective barrier that limits heat transfer into the material, volatilization of combustible degradation products and diffusion of oxygen into the material. Thus, the main fire retardancy mechanisms in polymer/clay nano-composites are the formation of a barrier against heat and volatiles by migration of the clay nano-layer toward the material surface, followed by char formation, together with increased melt viscosity nano-composites. The incorporation of nano-clays generally retards and decreases the peak heat release rate, but does not reduce the total heat involved and may also decrease the time to ignition. [P84, p15-16]

Concerning nano-composites like the thermoplastic ethylene vinyl acetate (EVA), it was discovered that the heat release is reduced by 70–80% when nano-composites with high level of clay-delaminations filled with tiny amounts of organo-clays (2–5%) are burned. [P84, p16]

Nano-tubes

The most widely studied nano-fibrous materials with respect to polymer flame retardancy are carbon nanotubes (CNT). Thanks to their high aspect ratio (length divided by diameter), CNTs percolate to form a network at very low loading in the polymer matrix and lead to substantial enhancement of several functional properties such as mechanical, rheological and flame retardant properties.

There are two different types of CNTs, small-diameter (1–2 nm) single-walled nanotubes (SWNTs) and larger-diameter (10–100 nm) multi-walled nanotubes (MWNTs). Both can be seen in the schematic picture below. CNTs are an interesting alternative to the use of conventional flame retardants and nano-clays. Their incorporation at low loading rates (0,5% to 3 %) has been reported to improve the flammability of a large range of thermoplastic polymers such as EVA, PS, PMMA, PA-6, LDPE and PP. [P84, p19]

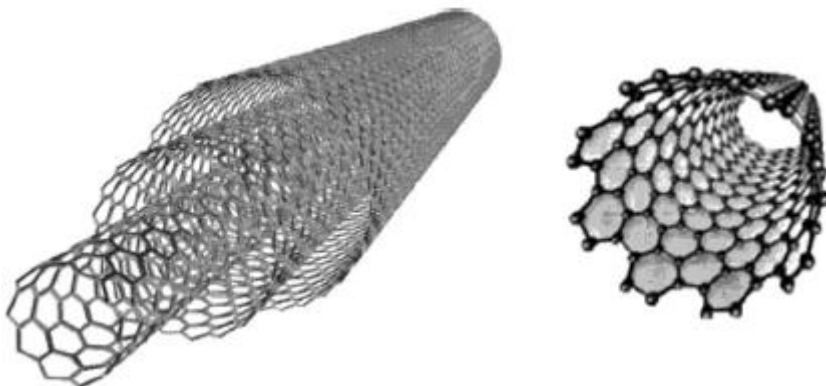


Fig. 125: Multi-walled (left) and single-walled carbon nano-tubes (right) used in polymer nano-composites [P84, p19]

The flame retardant properties of thermoplastic MWNT nano-composites appear to be governed by two distinct physical processes. Firstly, the structured network layer acts as a shield and re-emits much of the incident radiation back into the gas phase, decreasing the polymer degradation rate. Secondly, the presence of carbon nanotubes decreases the thermal conductivity of the polymer. As a result, the time to ignition and the peak heat release rate of the thermoplastic MWNT composite increase with the MWNT content. The lowest heat release rate is attained with the sample containing 1 % MWNT, most likely due to a balance between thermal conductivity and shielding effects. The formation of such an efficient and compact layer is favored by the use of MWNT with a high aspect ratio, i.e. length-to-outer diameter ratio. [P84, p20]

Nanoscale spherical particles

Another family of additives consists of nanoparticles of metal oxides, silica and polyhedral oligomeric silsesquioxane (POSS). As described earlier, the last example POSS already found its way into the industry and some manufacturers, such as for example the company 'HybridPlastic', that offers thermoset POSS epoxy resins. Nano-scale particulate additives are characterized by their isometric dimensions and have also proved to be very interesting with regard to flame retardant polymer systems. [P84, p21]

POSS is an inorganic silica-like nano-cage. On combustion of such a polymer composite, POSS acts as a precursor forming thermally stable ceramic materials at high temperature. These inorganic nano-cages are also referred to as pre-ceramic compounds. The incorporation of POSS in polymers modifies both the viscosity and the mechanical properties of the molten polymer. In addition, it also affects the thermal stability and fire performances by reducing the quantity of heat released upon combustion. For instance, the incorporation of 10 wt% of methyl phenyl POSS in a special polyamide thermoplastic led to a 70% decrease in peak HRR during tests carried out at 35 kW/m².[P84, p22]

5. FEA/FEM OF FRP

Whether concrete-, steel- or FRP-structures have to be designed: it is most likely that complex shapes such as shell structures, space frames or lattice tubes will not be calculated analytically by hand. To obtain a good design of a cylindrical truss traffic bridge in FRP, FEM software is indispensable. The main goal of this thesis is to make a feasible design of a FRP cylindrical truss bridge. Since the design of such a structure involves hundreds or even thousands of individual girders, plate elements and connections, a calculation by hand becomes very time-consuming. Another goal of this thesis is to optimize the structure both geometrically and in terms of material-build-up and -usage. Such optimizations are most efficiently done using state-of-the-art FEA- and FEM-software. In a quick scan of the FEM-software-world the following programs, that could be suitable, were found.

5.1 SPECIAL FEATURES OF FRP IN FEA DESIGN

Since fiber reinforced polymers are a new building material, their implementation in most software packages is not complete yet. Some of the software described in this chapter does give some added functionality on composite design, however an incorporation of different standard profiles, which is the case for steel for example is not yet available.

5.1.1 INHOMOGENEITY

An important difficulty for the application of FRP materials in FEM design is inhomogeneous nature of the material. Not only does a composite consist of reinforcement fibers and resin matrix, it also contains additives and fillers. All of these materials have different mechanical properties, which all have a certain influence on the mechanical properties of the fully assembled composite element. One cannot simply add up the mechanical properties of the ingredients by volume fraction. [Chapter 2.6.2; chapter 2.6.6] give more information on scientific approaches to solve this problem can be found in.

5.1.2 ANISOTROPICITY

Another property of common composites is their anisotropy. Most of the strength and stiffness of composites is contained in the reinforcements. Since the reinforcement is mostly of a fibrous form, one can imagine that pulling the fibers in their length-direction yields more resistance than pulling them in the perpendicular direction. This anisotropic behavior is not only limited to the tensile strength and stiffness, but is also present in shear strength and stiffness, compressive strength and stiffness, bending strength and stiffness, temperature effects etc. In short, fiber reinforced polymers behave completely different in respect to the direction of the applied force than for example steel, where the force application direction has little to no influence (isotropic behavior). More information on approaches to cope with anisotropy can be found in [chapter 2.6.2].

5.1.3 LAMINATE BUILD-UP

Due of the earlier-described anisotropy most applications of composites feature a so-called laminate build-up, in which a laminate is composed of several layers (or plies) of different composite materials. In that way designers can achieve quasi-isotropicity by combining several layers and varying the fiber direction within the plies. A difficulty with the application of laminates is the interface between the different layers. The

designer aims at full bond strength, thus at behavior-as-one, but in practice this will never be achieved. How this can be modeled in finite elements models depends on the sophistication level of the software package. More information on laminate theory can be found in [chapter 2.6.6].

5.1.4 CONNECTION DETAILING

Considering the complexity of a typical composite with a laminate build-up it is not hard to imagine that FE-design of FRP connections will be much more of a problem than for typical steel connections. The advantage of tailor-making composites, adapting them to the local stresses by incorporating more fibers in the right direction at connections is engineering-wise a great advantage, but calls for very complex finite element modeling solutions. For more information on fiber reinforced polymer composite joint design see [chapter 2.6].

5.2 FEA/FEM SOFTWARE PACKAGES

In the following several available software products will be covered. They will be compared by the FEA-possibilities, the FRP-specific features and the popularity in the industry. The 4 software packages are only a small selection of available FEA/FEM packages. This selection though incorporates two of the most common programs specialized on bridge engineering. Therefore these examples of software should give enough information to justify the choice for a particular software package.

5.2.1 LUSAS

“LUSAS” is world-leading finite element analysis software, which originates from the Great Britain. “LUSAS” originally only offered “LUSAS Bridge”, a complete design tool for bridge engineering. Later other software was added to their portfolio: “LUSAS Civil & Structural”, a design stool for buildings and civil structures like stadiums, towers and tunnels. Next to that “LUSAS Analyst” was developed, a FEA tool for mechanical engineers. The most interesting tool for this thesis though is the recently developed “LUSAS Composite” tool: This tool is specialized in the design and analysis of complex (polymer) composite structures. The program incorporates functions such as lay-up definition, composite matrix failure modeling, composite delamination and the Tsai-Hill, Hoffmann, Tsai-Wu and Hashin failure criteria. [WEB, www.lusas.com]

An example for a structure calculated with “LUSAS Bridge” is the “Greenside Place Link Bridge” in Edinburgh, discussed in [chapter 6.1.5]. This structure is of the same type as the structure that is to be designed. “LUSAS Bridge” is capable of a range of modeling properties, such as CAD-import, automatic meshing, multiple section libraries, box-girder property calculator, tapering beams modeling. All modeling is done in a Windows-based graphic user interface. Of course all Eurocode Load Cases are also incorporated in “LUSAS Bridge”. Concerning analysis, “LUSAS” is capable of linear-static analysis, buckling analysis, all kinds of dynamic analysis, modal analysis, non-linear analysis, creep modeling and vehicle-load optimization. [WEB, www.lusas.com]

“LUSAS” is used very widely throughout the industry. Applications of “LUSAS Composite” include the design of composite floor panels for military aircraft, design of carbon fiber mast, turret and boom components for a yacht rig and analysis of glass fiber reinforced plastic, aluminum bolted T-joints. “LUSAS Bridge” was used for dozens of bridge projects. Arch bridges, Cable-stayed bridges, prestressed box-girder bridges and small-scale pedestrian bridges, for all of these examples of analysis and design with “LUSAS Bridge” can be found.

5.2.2 MSC – NASTRAN

According to the manufacturer, “MSC Nastran” is the most widely used Finite Element Analysis solver. “MSC” is a spin-off of “NASA” and became independent in the 1960’s. “MSC” offers several different products capable of every analysis from acoustic simulation and multi-body dynamics simulation to Computational Fluid Dynamics and thermal simulation. It is this large spectrum of application fields that made “MSC” so successful. “MSC Nastran” is the general solver for structural FEA. It includes a tool for design and analysis of composites. Thus it is perfectly capable of calculating with composites. Although this software is so widely used, it is not specially made for bridge design. Most applications of “MSC” can be found in the field of mechanical engineering, such as car design, turbine design, aviation and aerospace. [WEB, www.msccsoftware.com]

Since “MSC Nastran” is not used for bridge design it lacks the structural- and bridge-design specific features such as pre-defined loads and section properties. The capabilities of MSC concerning composite design and analysis are though among the best in the world. It is perfectly suitable for composite lay-up design and stress-optimization. It can calculate linear- as well as non-linear responses and includes all failure-models including progressive failure and incorporates micro-mechanical failure models. [WEB, www.msccsoftware.com]

Since “MSC” is made for smaller scale products of the automotive-, energy-, medical- and aerospace industry it is most probably not very well suited for the FEA of the bridge that is to be designed. It could however come in handy for the design and analysis of particular elements such as connections or single girders of the bridge.

5.2.3 ANSYS STRUCTURAL

“ANSYS” is another US-American company that devoted itself into providing FEA/FEM solutions for different fields of application. Next to “MSC”, “ANSYS” is one the biggest FEA-software developers of the world. ANSYS offers several software packages that are intended for industries like the automotive-, aerospace-, heavy machinery- and electronics industry. “ANSYS” also offers several products for the building industry. The company is specialized in detailed structural analysis of special elements of a build as well as blast design, fire and smoke propagation simulation and structural building design. The latter can be designed and analyzed using “ANSYS Civil” FEM. Several bridges, tunnels and stadiums have been designed using this tool. [WEB, www.ansys.com]

“ANSYS” also offers a special composite design tool, called “ANSYS Composite Prep Post”. This software is specifically designed to calculate composites layer by layer, with all layers having different properties. All known failure criteria are incorporated in the program. “ANSYS Composite Prep Post” can analyze a composite structure globally or very detailed, down to single plies of the laminate. [WEB, www.ansys.com]

Just like “MSC”, “ANSYS” is not specialized on the structural design and analysis of bridge structures. Although some examples of bridge design using ANSYS are available, more specialized software such as “LUSAS” are more suitable for general structural design. An advantage of “ANSYS” is the detailed composite tool, which could be used for single special composite elements of the FRP-bridge. Next to that the ability to simulate fire and smoke propagation could be used for the fire design of the bridge or elements of the bridge.

5.2.4 MIDAS CIVIL/ TNO DIANA

“MIDAS” is a relatively young South-Korean software developer, that is specialized in FEA/FEM of bridge structures. Over the years “MIDAS” has grown significantly and broadened its product scope, now offering also solutions for building- and structural engineering, geotechnical engineering and mechanical

engineering. In 2005 "MIDAS" started a strategic partnership with "TNO DIANA", the famous FEA solver from Delft. This solver is now integrated in the "MIDAS" software. [WEB, en.midasuser.com]

Since "MIDAS Civil" is a direct competitor of "LUSAS", it features the similar capabilities and tools. "MIDAS Civil" is capable of a range of modeling properties, such as CAD-import, automatic meshing, multiple section libraries, box-girder property calculator, tapering beams modeling. All modeling is done in a Windows-based graphic user interface. Of course all Eurocode Load Cases are also incorporated in "MIDAS Civil". Concerning analysis, "LUSAS" is capable of linear-static analysis, buckling analysis, all kinds of dynamic analysis and modal analysis. For advanced non-linear detail analysis of civil structures, "MIDAS" developed "MIDAS FEA" that works with the "TNO DIANA" solver. [WEB, en.midasuser.com]

Since the author has already gained some experience with the "MIDAS Civil" software in bridge design during his BSc thesis, this could well be a suitable solution. A disadvantage of "MIDAS" compared to "LUSAS" is the lack of special design tools for design and analysis of FRP composites. When "MIDAS" would be used together with element design in "ANSYS" or "MSC" this disadvantage could be overcome. "MIDAS" is used widely in the bridge engineering and construction industry. Examples of bridges that were (partly) designed using "MIDAS" are the state-of-the-art cable-stayed 'New Wear Bridge' in Sunderland, Great Britain, the 'Young Jong' Suspension Bridge, Incheon, South Korea and the box girder 'La Jabalina Bridge' in Durango, Mexico. [WEB, en.midasuser.com]

6. CASE STUDIES

In this chapter several examples of comparable bridge structures will be discussed. First a number of cylindrical truss bridges will be covered. Most of the cylindrical truss bridge examples are made of steel. Trusses made of FRP are a totally new concept.

After the cylindrical trusses several all-FRP bridges will be discussed. Although many applications of FRP in bridge engineering exist, and several hundred bridges that involve FRP exist, the number of all-FRP bridges is somewhere around 50-70. [T07, p62-67]

To conclude the case study chapter examples on the fire safety of bridges will be given. Since bridges are mostly open, non-confined spaces the number of examples for bridge fire safety is not too large either.

6.1 CYLINDRICAL TRUSS BRIDGES AND SHELL BRIDGES

Cylindrical truss bridges or tubular lattice girder bridges are a very recent shape for bridges. Functioning in a similar way as traditional truss bridge they combine the efficiency of trusses with the elegance of cylinders. The reason that cylindricaltrusses have only been applied for a mere 10 years probably lies in the complex geometric nature of their design, which calls for computer aided design and finite element analysis.

In the following, six examples will be discussed, which are all tubular trusses or at least resemble this form in a close way. Except from one all structures are intended for pedestrian/cyclist use only. The railway viaduct in The Hague, The Netherlands is the only cylindrical truss that is used for heavy traffic loads.

6.1.1 SINGAPORE MARINA BAY FRONT PEDESTRIAN BRIDGE

The “Singapore Helix Bridge” is a pedestrian bridge with a total length of 280m. It uses a reverse double-helix exoskeleton stainless steel structure to carry the 6m wide deck, spanning 65m between the peers. The bridge deck is carried by a double helix tube via an array of steel hangers. The helix structurally functions as a tubular lattice girder. [A29, p15] The Marina Bay Front Pedestrian Bridge was designed by the engineering firm ‘Arup’ in close cooperation with the architects ‘The Cox Group’ and ‘Architects 61’ and opened in 2009. The bridge connects the Singapore Bay front with the Marina Centre complex. Arup made vast use of FEM, FEA and BIM during the design. The whole geometry was derived using Bentley® systems to speed up the design process and make the planning and construction more efficient. Part of the difficulty was the complexity of the structure due to the longitudinal and horizontal curvature, the vertical incline and the 4 viewpoint alongside the bridge. Next to that parts of the bridge were also covered with a mesh of steel wire and glass panels to provide enclosure for the pedestrians on the bridge. [A28, p1-2]

The material use of the bridge is very efficient due to the cylindrical lattice-work. This was also needed because the tubular sections of the bridge are completely made of, rather expensive, stainless steel. The use of stainless steel has a similar advantage in maintenance costs as fiber reinforced polymer. Both materials are less sensitive to environmental influences than normal structural steel or concrete. The bridge was built together with an adjacent road bridge; this combined project totally cost about € 98 million. [T09, p13]

In the following some pictures can be found that accurately describe the nature and structural system of the “Singapore Marina Bay Front Pedestrian Bridge”.



Fig. 126: Impressions of the Singapore Marina Bay Front Pedestrian Bridge [WEB, www.marinabay.sg]

6.1.2 SINGAPORE HENDERSON WAVES BRIDGE

This project is not a typical tubular truss. Structurally it functions more as an arch bridge, but since it is comprised as a lattice of steel and timber and it has a very striking and unique shape, it was chosen as an example structure. The “Singapore Henderson Waves Bridge” is a pedestrian bridge spanning a total of 284m above the six-lane “Henderson Highway” on the southern coast of Singapore. It also has a vertical ascent of 21m in total. The bridge has seven spans, six of which with a 3,5m high arch. The seventh arch is bigger, it has a height of 6m and measures 57m in length. [A27, p20] The Henderson Waves Bridge’s design concept is based on a folded three-dimensional surface-shape created by mathematical formulas. Because the overall shape of the bridge could be defined by single parametric formula using ‘Math CAD’, the transfer of the geometry between different CAD and FEM/FEA programs was very straight-forward. [A27, p21]

Engineering of this bridge was done by ‘Adams Kara Taylor (AKT)’, the architectural design was made by ‘IJP Architects’. Construction of the bridge was finished in May 2008. The load-bearing system of the bridge consists of a central spine, made of a steel box girder, which is the main load-bearing element in this design; edge members, which support the open areas to the decks; the central arch, whose steel sections rise and fall, thus working in compression and tension; lateral mid-height members, which form a shallow arch to support the central arch and curved steel restraints, which also support the central arch, forming a continuous connection between the arch member, the mid-height member, the central spine and the edge member. To summarize: steel is the main material for structural strength and stiffness, whereas timber is used mainly for aesthetics. [A27, p22]

The Henderson Waves Bridge is part of ‘Southern Bridges’ trail that links parks along the southern coast of Singapore. This project took 2 years to complete and cost about € 16 million to complete.

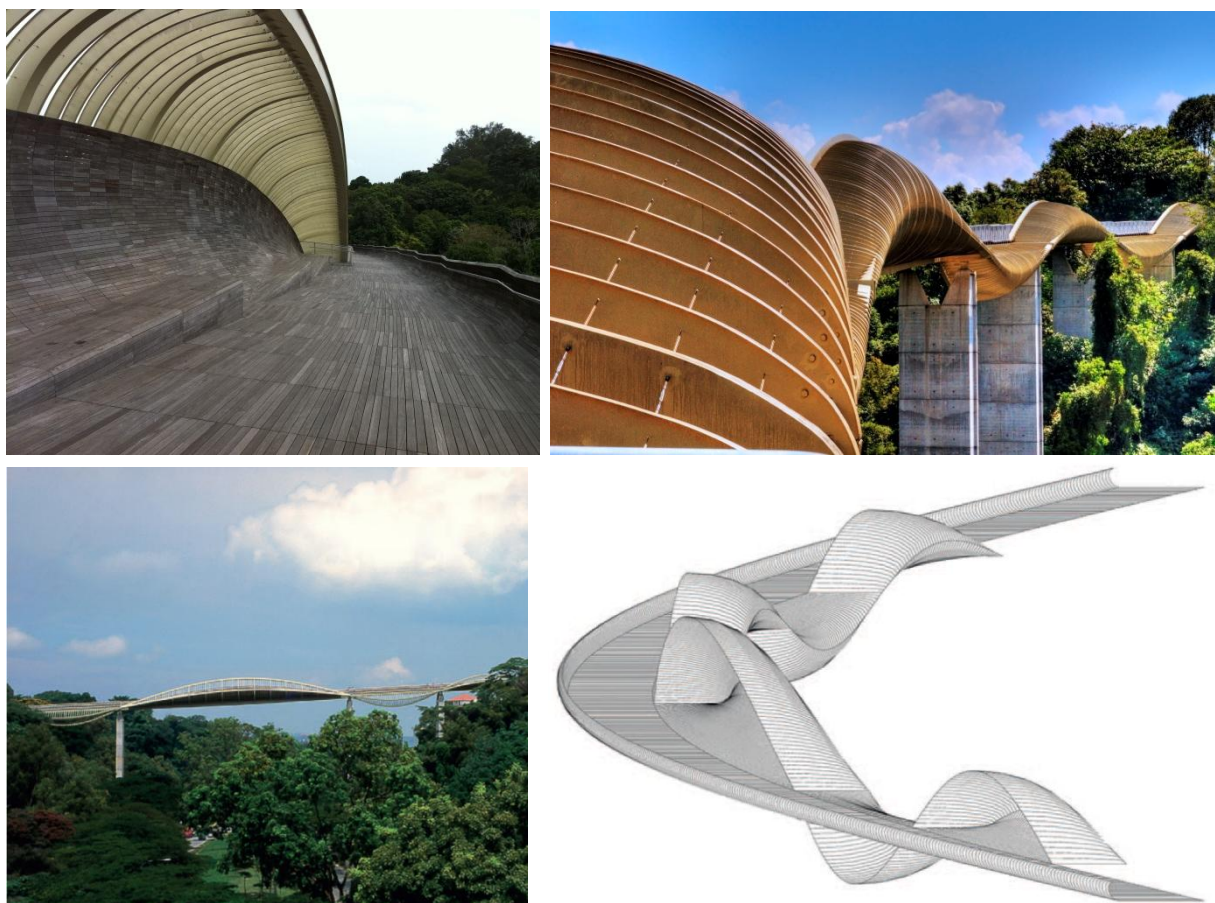


Fig. 127: Impressions of the Singapore Henderson Waves Bridge [A27]

6.1.3 LIGHTRAIL VIADUCT BEATRIXKWARTIER THE HAGUE

This is the only example of a heavy traffic bridge built with a tubular lattice girder used as load bearing system. This bridge was designed by "Zwarts & Jansma Architects" and the engineering was done by "Gemeentewerken Rotterdam". It was finished by the contractor "BAM" in 2006. The total costs for the viaduct without installations were €32 million. [WEB, www.dearchitect.nl]

The elliptical space-frame cylindrical structure of this bridge is built up by steel CHS sections. Together with steel-plate rings they form the cylinder with a diameter of approximately 10m. The inner diameter, free of obstructions is 7,5m. [WEB, www.denhaag.nl] Due to this construction height the bridge has large spans of 40m and 50m. The total length of the bridge is 400m and the intermediate supports are V-shaped concrete columns. The bridge is used for the light rail RandstadRail and features two tracks. [WEB, www.architectenweb.nl]

Inside of the tubular steel truss 2 light-rail tracks are placed on precast concrete beams with elliptical cross-sections. The concrete girders have a width of 2,4m. The steel rings used in the tubular truss are cut from 40mm steel plates and form the tubular truss together with the 324mm diameter circular hollow steel sections. All steel-to-steel connections in the truss are welded. The steel tubular truss forms the main load bearing system for this viaduct. The concrete girders mainly provide resistance to vibrations and reduce the noise emission through their large mass. [WEB, www.architectenweb.nl] [WEB, www.cobouw.nl, March 2006]

An interesting fact is, that in the middle of the viaduct where a light-rail station is situated, the load-bearing system is made up by heavy concrete girders and not by the steel tubular truss. The reason for this was the added width needed, which made it more difficult to carry all loads through the steel truss. [WEB, www.cobouw.nl, March 2006]



Fig. 128: Impressions of the Lightrail Viaduct, Beatrixkwartier, The Hague [WEB, www.zwarts.jansma.nl]

6.1.4 PEACE BRIDGE CALGARY

This bridge designed by "Santiago Calatrava" is still under construction. The expected date of finishing lies in the beginning of 2012. It has been designed as a pedestrian and cyclist bridge and symbolizes the commitment of the people of Calgary to a healthy, active and beautiful city. It is expected that over 20.000 cyclists/pedestrians will use the bridge on a day-to-day basis. The bridge deck has a width of 6,2m. The bridge has one large single span of 126m and the load-bearing system is an oval steel tube girder with a width of 8m and a height of 5,85m, which is composed of steel RHS sections. [A39, p2] The bridge deck will be a combination of pre-cast- and cast-in-place- concrete. [WEB, www.calgary.ca] The peace bridge has a design-life of 75 years and was designed to resist the Calgary one-in-100-year flood-cycle. [A39, p2]

When finished, the bridge deck of this bridge will be completely enclosed and shielded from the environment. The space between the RHS sections will be spanned by glass panels. Therefore the bridge can also be used by pedestrians and cyclists in the cold Calgary wintertime. The ability to easily fabricate an fully enclosed space within the cylindrical load bearing system of a tub-type ridge is very advantageous, especially concerning the harsh, cold and wet Canadian winter-conditions. [WEB, www.calgary.ca]

The total costs of this bridge lie at about € 19 million, of which about € 14 million are construction costs. [A39, p1] In the construction phase a temporary bridge is used, over which the fully assembled, coated, painted and glazed bridge is then launched via a hydraulic sliding mechanism.



Fig. 129: Impressions of the Peace Bridge in Calgary, Canada [WEB, www.calgary.ca]

6.1.5 GREENSIDE PLACE LINKE BRIDGE

The Greenside Place Link Bridge is situated in a modern neighborhood of Edinburgh, Scotland. The architectural design was done by 'Broadway Malyan Architects & Designers'. The structural engineer of this project was 'Buro Happold'. The bridge connects two buildings which are separated by a busy street. The bridge was finished and placed in 2004. The total costs of this bridge were € 2,6 million. [T09, p1-2]

The bridge was designed to be a self-standing independent structure that does not use the adjacent buildings for stability. Next to that the bridge had to be fully enclosed and the S-shaped profile was chosen for aesthetic reasons. Because the bridge had to be fully enclosed a spiraling cylinder was chosen as main load-bearing structure. The bridge consists of three spans: a middle-span of 31,5m and two side-spans (above the V-shaped supports) of 7,9m, leading to a total span of 47,3m. The bridge cross-section is an ellipse with a height of 4m and a width of 5m, making a bridge deck of 2,7m width possible. This deck is composed of extruded aluminum panels. The main structural system is made of spiral S355 CHS sections with a diameter of 139,7mm and a wall thickness of 10mm and six horizontal S355 CHS sections with a diameter of 193,7mm and a wall thickness of 16mm. The steel spiral is continuous and the horizontal steel tubes are connected via a short cylindrical welded section. At the supports and the ends of the bridge an extra ring was placed inside the spiral to stiffen the bridge at this point of introduction of large shear stresses. The ring sections have the same diameter as the horizontal sections, but an increased wall thickness of 20mm. General stability of the bridge was achieved by clamping the concrete columns from which the steel V-shaped supports emerge. [T09, p2-9] a

'Buro Happold' made excessive use of FEA-tools in designing this bridge. The software of choice for these engineers was the finite element program 'LUSAS', already discussed in [chapter 5.2.1]. During the analysis the eigen-frequencies for horizontal and vertical vibrations were also calculated, they were 6,3hz and 2,5Hz respectively. Due to the relatively light weight of the total structure and the accompanying low lateral natural frequency it was necessary to improve the natural frequency by adding X-braces to the V-shaped supports. [T09, p9-10]

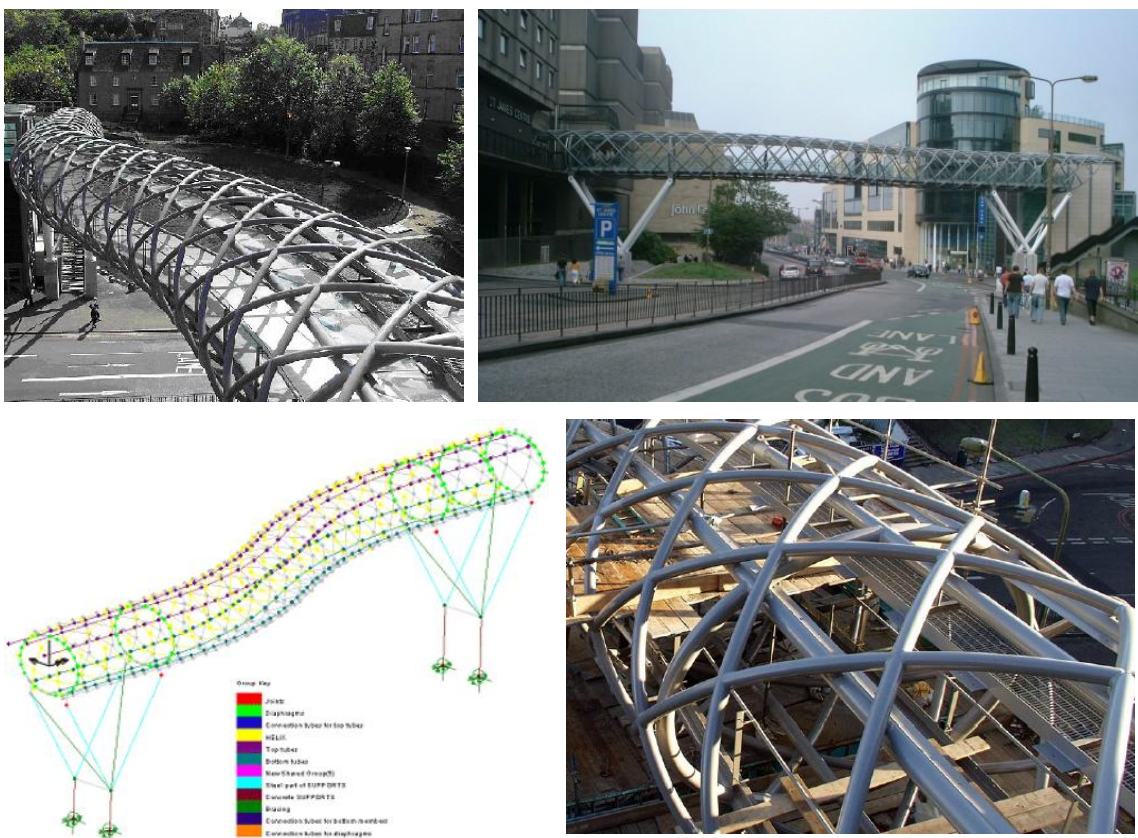


Fig. 130: Impressions of the Greenside Place Link Bridge, Edinburgh [T09][WEB, en.estructurae.de]

6.1.6 DESIGN PAPENDORPSE BRUG, UTRECHT, ABT

The bridge that is to be discussed in this chapter, in fact was never built. It was a design made by the Dutch architects 'Hans van Heeswijk' and 'Bureau West 8' and the structural engineering firm 'ABT'. The design was proposed in a design competition for the Papendorpse Brug with a free span of 150m over the Amsterdam-Rijn canal. The completion was won by another competitor and thus the bridge was never built.[A30, p1]

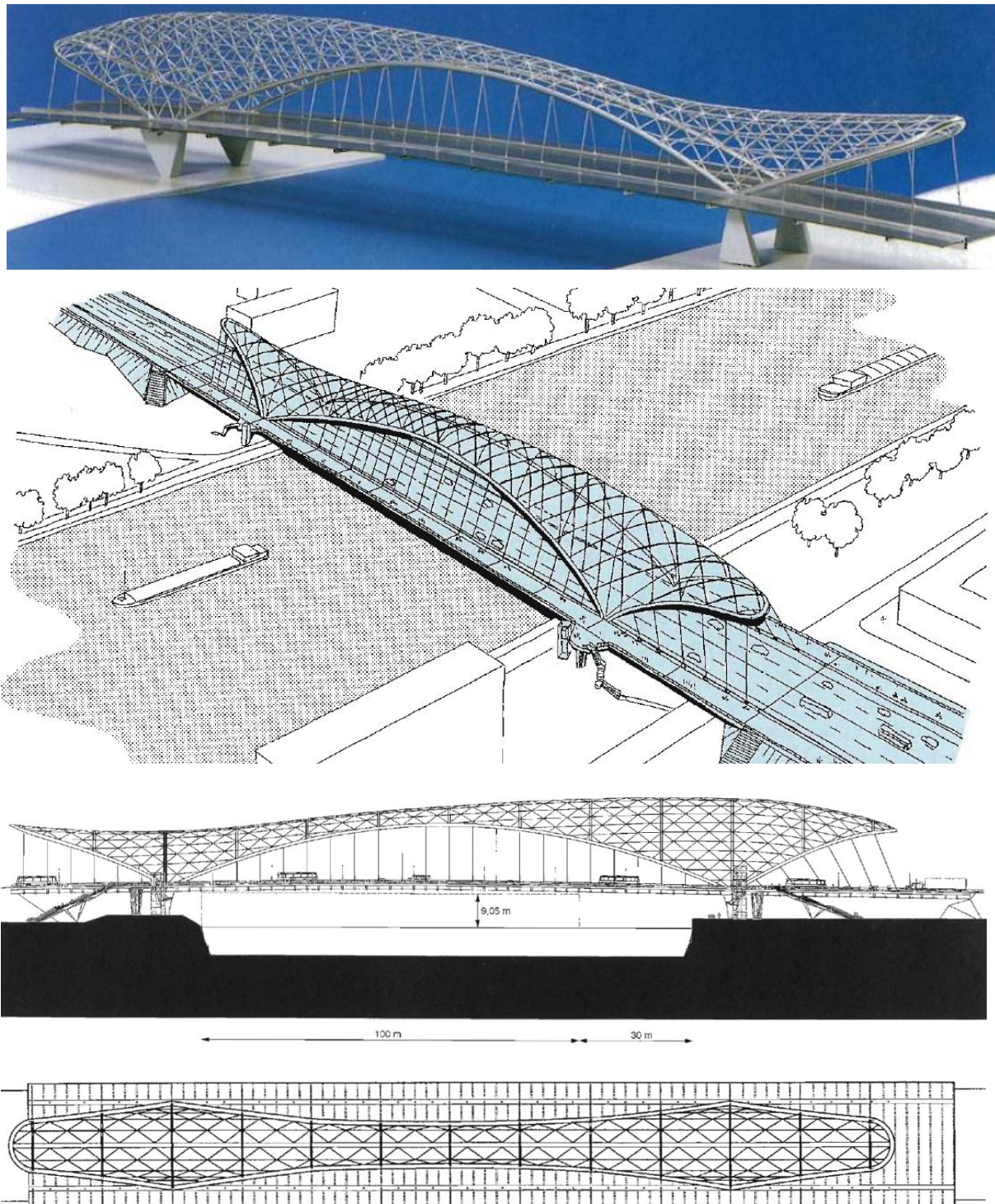


Fig. 131: Impressions of the design of the Papendorpse Brug, Utrecht by ABT [A30]

In the above pictures the special nature of this design becomes evident quickly. The main structural system is a steel grid-shell composed of CHS sections with a diameter of 323mm. The edge of this grid shell is formed by large-span steel arches. The grid-shell, which is situated above the bridge-deck is strongly asymmetrical, with one concave part and a larger convex part. The whole edge of the shell is made up by a steel member with a large stiffened rectangular cross-section of 900x1.800mn, which acts as an arch at the two long sides of the shell. The bridge-deck is supported via steel cables with a diameter of 90mm from the edge beams. Next to the grid sections two large longitudinal steel welded IPE girders with the dimensions 1000x2.000mm are used. [A30, p2-6]

The bridge deck, which also carries the horizontal loads induced by the grid-shell at the four base points, is composed of longitudinal and transverse steel beams and a concrete bridge deck. The total width of the deck is 33m, of which 2x5,1m are cantilevered at the sides. Since the bridge design was halted in preliminary design stages, exact cost estimations could not be made.

6.1.7 ROCHE-SUR-YON PEDESTRIAN BRIDGE

This cylindrical truss pedestrian bridge was designed by the architects 'Hugh Dutton Associates' and 'Bernard Tschum Architects & Planners' and engineered by 'HAD Paris'. The bridge cost about € 5,5 million. The structure has a length of 67m with three supports, leading to two free spans of 31,8m and one of 35,2m. It weighs about 160 tons. The bridge was placed in 2009 over an array of TGV railway tracks and provides pedestrians with a safe crossing. The structure was prefabricated in few parts and hoisted into place. Pedestrians can reach the 6m high bridge deck via one of the three stairs or elevators. [WEB, www.complexitys.com]

The structural system of the bridge is composed by a complex lattice work which is arranged in a cylindrical shape. The diagonal lattice members are T-shaped profiles, the profiles at the top of the tube being the heaviest, and getting smaller at the underside of the tube. The lowest diagonal members are cables. The vertical rings are H-shaped profiles with constant dimensions. At the supports steel plates are placed between the lattice members, to handle the increased shear stresses. Due to the array of different cross-sections many tons of steel were saved making the bridge more sustainable. The bridge deck is made of concrete and the bridge is enclosed by a polycarbonate sheets between the lattice members. [WEB, www.complexitys.com]

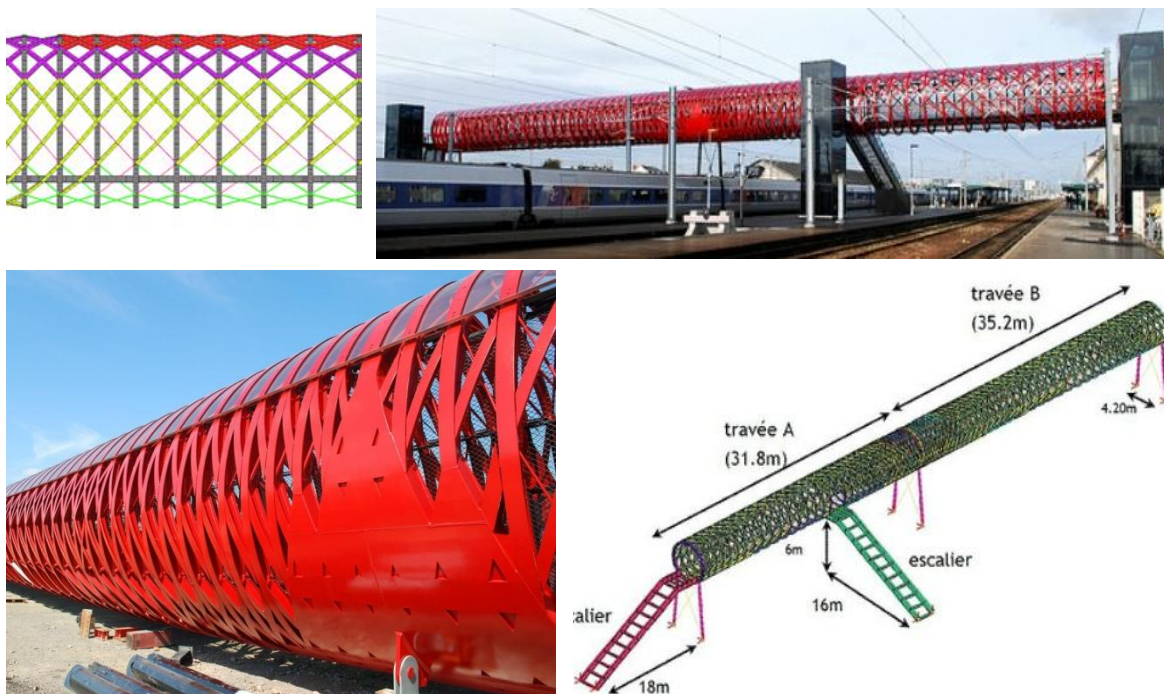


Fig. 132: Impressions of the Roch-sur-Yon Pedestrian Bridge, France [WEB: www.complexitys.com]

6.1.8 OTHERS

To conclude this chapter a number of other tubular truss bridges will be covered very briefly; a short description will be given as well as a few descriptive photos.

6.1.8.1 LUTON GALAXY LINK BRIDGE

This bridge was designed by AKT UK and connects the “Luton Galaxy Shopping Center” to a multi-story car park. The bridge has a single free span of 46m and is composed of a cylindrical “Vierendeel truss” made of steel CHS sections. It is fully enclosed, using curved polycarbonate sheets. The bridge was prefabricated in three parts before hoisting it into place. The light bridge deck hangs from the tubular truss. The total costs for this bridge were € 3,5 million. [WEB, www.akt-uk.com]



Fig. 133: Impression of the Luton Galaxy Link Bridge by AKT UK [WEB, www.akt-uk.com]

6.1.8.2 T. EVANS WYCKOFF MEMORIAL BRIDGE

This 2008 pedestrian bridge at the ‘Museum of Flight’ in Seattle has a free span of 104m. It was inspired by an airplanes contrail, the stream of crystallized vapor created in a plane’s wake. The bridge was designed by the architect ‘SRG Partnership’ and the structural engineer ‘Magnusson Klemencic Associates’. The load bearing structure is composed of a tubular truss that is formed by connecting multiple hoops, inclined at 45°, made of steel CHS sections with a diameter of 127mm. The resulting cross-section is elliptical and the bridge weighs 190t in total. This low weight was partly achieved by using a bridge deck made of extruded aluminum panels. The walkway is enclosed by a glass box which was placed inside the tube. [A40, p38][A41, p1-2]

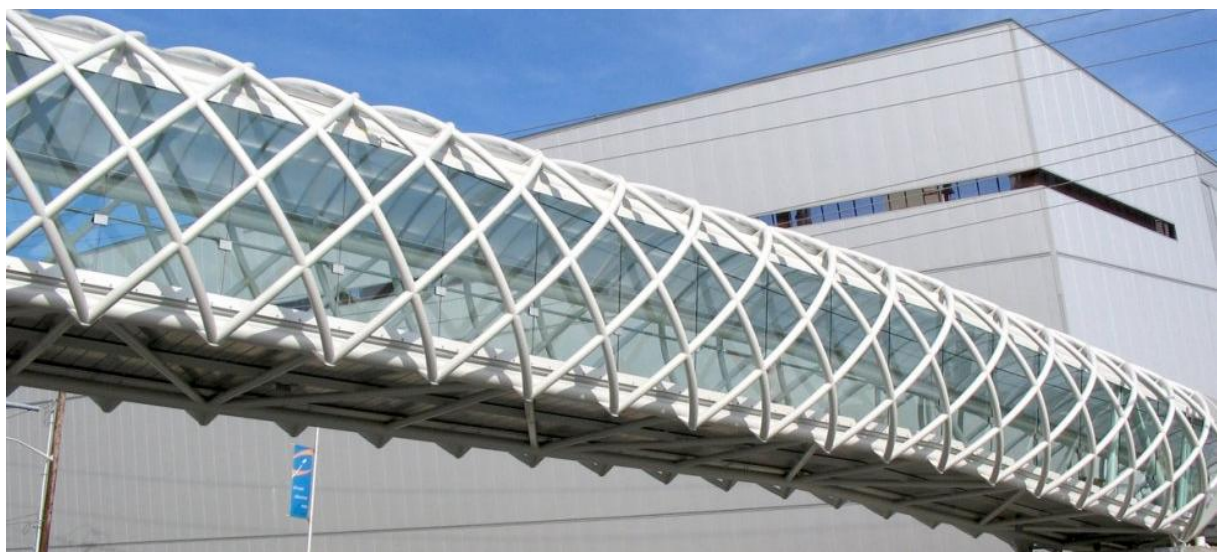


Fig. 134: Impression of the T. Evans Wyckoff Memorial Bridge, Seattle [WEB, www.museumofflight.com]

6.1.8.3 HARTHILL FOOTBRIDGE

This tubular truss bridge was designed by the structural engineering firm ‘Buro Happold’ and has a free span of 70m over the M8 motorway near Glasgow, Scotland. It was placed in 2008 and cost about € 6 million. The structural system is composed of a helical truss that is formed by steel CHS sections. The walkway is fully enclosed by glass panels. Like the Greenside Link Place Bridge, this bridge is also supported by two V-shaped supports with X-braces. Next to that the structural system is very similar to it. Since both bridges were designed by the same structural engineer, this most likely was no coincidence. [WEB, www.happypontist.blogspot.com]



Fig. 135: Impression of the Harthill Footbridge in Glasgow, Scotland [WEB, www.happypontist.blogspot.com]

6.1.8.4 WEBB BRIDGE

This state of the art pedestrian bridge was finished in 2003 in Melbourne, Australia. The design was made by the architect ‘Denton Corker Marshall’ and the structural engineer ‘Arup’. The bridge cost about € 2,7 million. In contrast to the other examples, this bridge uses the tubular truss primarily as aesthetic element. The main load bearing system is made up by steel box beams that follow the curve of the bridge, the bridge-deck is a cast in place concrete type. The steel hoops have a varying diameter, in width from 5-8,7m and in height from 4-8,9m. They are made of 15x150mm steel sections. [A02, p2]



Fig. 136: Impression of the Webb Bridge in Melbourne, Australia [A02]

6.2 ALL FRP BRIDGES

Fiber reinforced polymers have undergone a significant development during the last 10 to 20 years. This development also took place in the field of bridge engineering. Since the first applications of plastics in bridges several projects have been initiated that involved FRP composites in some way. This chapter will focus on bridges that are entirely made of FRP composites.

In the following, four examples will be discussed, which are all bridges made completely of fiber reinforced polymers. Three of the four examples are pedestrian bridges with spans in the range of 20m to 40m. One of the discussed bridges is a heavy traffic bridge with a span of 12m. The example bridges are situated in the Netherlands, Spain and Scotland. The discussed bridges are mainly based on glass-fiber polyester composite. In total about 50-60 all-FRP bridges exist throughout the whole world, of which 90% are pedestrian bridges. [T07, p62-67]

6.2.1 ABERFELDY FOOTBRIDGE



Fig. 137: Two views of the Aberfeldy footbridge over the river Tay in Scotland [P22, p1]

The Aberfeldy footbridge was constructed in 1992 in Aberfeldy in Scotland, crossing the local river Tay. After a preliminary evaluation by the University of Dundee under Prof. Harvey it became evident that traditional materials would not be sufficient to meet all desired needs, such as light weight and large span. As a result "Maunsell Structural Plastics" were appointed as lead structural engineers and it was decided to take on the challenge and build the first all-FRP footbridge in the world. "Maunsell" used their newly developed "Advanced Composites Component System" (ACCS), a system which uses prefabricated FRP panels joined by a combination of mechanical fasteners and bonded joints. The ACCS modular system relies on cold-cure adhesive bonding with an epoxy adhesive and a mechanical toggle system to join the individual plank units or cells. For an impression of this system, see the picture below on the left. [B21, p504] [P22, p1-2].

Due to the low dead-weight of the bridge a unique method of erection could be applied, using no cranes at all. The light-weight nature of the footbridge also minimized the foundation costs. The bridge is completely built-up of glass fiber reinforced polymer composite (GFRP) with weather- and wear-resistant coatings, providing a life-to-first-maintenance of over 20 years. The GFRP is made of E-glass fiber with isophthalic polyester resin. [A03, p1][T05, p27]

The bridge is a cable-stayed bridge with two A-frame GFRP pylons, weighing only 2.500 kg per frame. They were prefabricated in two pieces per frame. The frames carry the load on the deck via a fan-shaped array of

'Parafil' Kevlar (aramid) cables to the foundation. The cables are manufactured from a core of parallel Kevlar-49 fibers with polyethylene matrix and are connected to 10 primary cross-beams, made up of 2x2 ACCS cells.

The bridge deck consists of longitudinal edge beams and lateral cross-beams, which are both constructed from ACCS. The edge-beams consist of 5 ACCS cells, while the secondary cross-beams consist of only one ACCS cell. The top planks of the bridge deck are comprised of an ACCS layer with a thickness of one cell. The picture below, on the right shows the build-up of the bridge decks, as well as the connection of the cables to the primary cross-beam and the edge beams. [T05, p27]

The main-span of the Aberfeldy footbridge is 63m, which is quite large for the application of an all new technology such as FRP. The 113m long fully bonded light-weight deck was assembled on site in only 8 weeks. The design load of this bridge is a live load of 5,6 kN/m². The dead weight of the bridge is only 2,0 kN/ m², which includes 1,0 kN/ m² ballast. The total weight of the bridge without foundations is only 14.500 kg. [A03, p1]

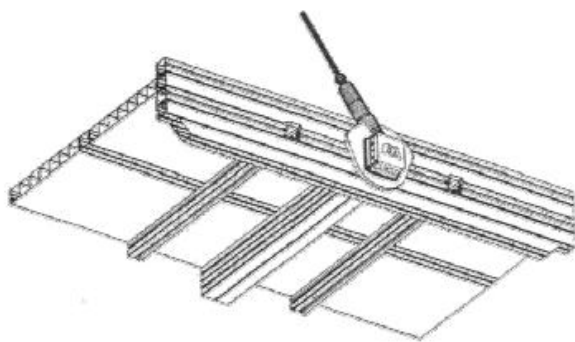
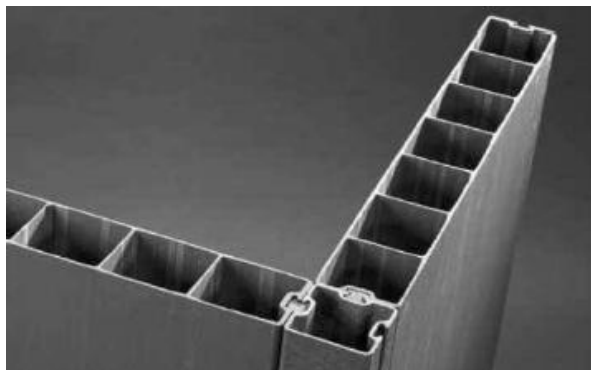


Fig. 138: Left: Maunsell Structural Plastics, ACCS modular system used for the Aberfeldy Footbridge. **Right:** Build-up of the Aberfeldy bridge-deck. [P22, p3]

During service life it became evident that the bridge behaves very lively even at a gentle walking pace and soon develops a highly noticeable bounce. The Kevlar cables appeared to be under quite low tension and the dynamic problem exhibited is clearly partly a result of the low mass of the system. Due to the close involvement of the Dundee University, whose students also had a part in the design and construction of this bridge; it is still an object of constant surveys and research. These researches show that, even with a minimum amount of service being performed, the structural system of this bridge is still completely intact, except for some minor cosmetic problems, such as the growth of algae. [P22, p10]

6.2.2 LLEIDA FOOTBRIDGE

The Lleida footbridge is located about 2 km from the city of Lleida in Spain. It crosses an existing roadway and a high-speed railway line between Madrid and Barcelona. The bridge is intended for pedestrians, requires minimum maintenance, and posed little disturbance to the railway traffic during construction. Construction of the bridge was finished in 2001. The picture below shows the Lleida footbridge right after the construction finished. [P85, p1]



Fig. 139: Lleida footbridge near Lleida, Spain [P85, p2]

The Lleida bridge is completely made of glass fiber reinforced polymer (GFRP) profiles. The bridge has a total span of 38m. The structure is a double-tied arch with a rise of 6,2m (height/span ratio of 0,16). The total width of the bridge is 6,1m, of which the bridge deck makes up 3m. The weight of the bridge is only 19.000 kg. All profiles of the bridge are made of plastic composite. The reinforcement is a combination of E-glass fibers, woven mats and complex mats. The matrix is made of isophthalic polyester and the minimum fiber content anywhere in the bridge elements is 50%.

The elements have a longitudinal modulus of elasticity of 23.000 to 27.000 N/mm², depending on the profile type. The tensile and compressive strength in longitudinal direction is 240 N/mm², which is comparable to that of typical S235 construction steel. The strength in transverse direction is much lower at about 50 N/mm² to 70 N/mm². [P85, p2]

Both arches, as well as the tied longitudinal bridge deck girders are made up of a rectangular hollow cross-section, which is made of two U-profiles (U-300x90x15mm) joined with two glued flat plates (180x12mm) to form a RHS girder. At the arch birth the arches are forked out into two branches to reduce horizontal deformation due to wind loads. The hangers are I-profiles (I-160x80x8mm) and the diagonal bracings between the two arches are square tubes (100x100x(6-8)mm). The bridge deck is made of transverse I-beams (I-200x100x10mm) with 0,6m c.t.c. distance, which directly support the 40mm thick deck panels, which form the roadway surface. The bridge deck also has a bracing system of diagonal U-section members (U-160x48x8mm) which reduces lateral distortion. The drawing below gives an overview of the structural system. Due to the lack in experience of the designer in glued connections, it was chosen to connect all members by mechanical means. All connections were bolted with stainless steel bolts and brackets. [P85, p3-4]

The bridge was designed for a nominal uniform load of 4 kN/m². Because GFRP is a relatively new material in bridge engineering, very conservative safety factors were chosen: For the normal stresses a partial safety factor of 2 was used, for shear stresses a factor of 3 was used. Buckling stability and the modulus of elasticity were calculated with a safety factor of 2. The design of most elements was governed by deformation (due to the low modulus of elasticity) and in some parts of the arch by buckling stability. The calculated maximum deflection under frequent loads (2 kN/m²) is about 24mm (L/1580). The measured deflection of 26mm was about the same. Special attention was given to the dynamic behavior, the first calculated natural frequency is 2,69 Hz. The maximum acceleration was limited by introducing diagonal cross-braces between the arches and the two ties. This resulted in a stiffer structure. The first natural frequency measured was 2,75 Hz and the viscous damping was 2,5% to 3,0% of critical damping. [P85, p5]

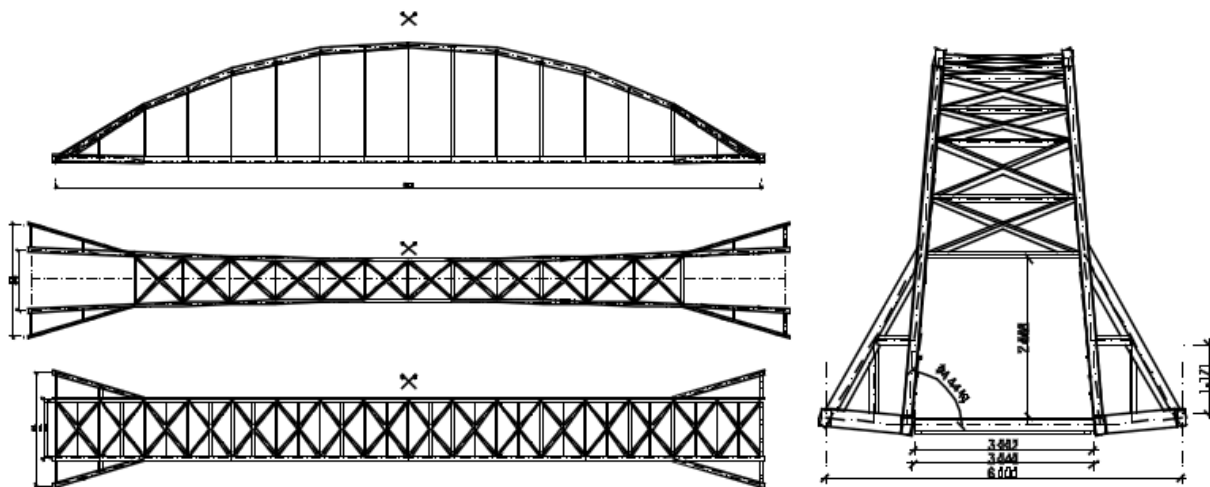


Fig. 140: Structural system of the Lleida footbridge in Spain. [P85, p2]

Generally spoken, the structure behaved considerably stiffer than indicated by theoretical predictions. This was explained by the profiled members having a higher deformation modulus than presumed and the connections being stiffer than expected. [P85, p5]

All GFRP elements of the bridge were prefabricated by 'Fiberline' in Denmark and transported to Spain. The maximum prefab element length was 9m. The GFRP part of the bridge was fully assembled and painted alongside the destination place. After the concrete foundation and piers were installed, the whole bridge was hoisted onto its final supports. This construction process resulted in very short disturbance time for the underlying rail- and roadway. The total hoisting process and thus the closure-time of the railway took only 3 hours. [P85, p6]

6.2.3 OOSTERWOLDE HEAVY TRAFFIC LIFT BRIDGE

According to the manufacturer of this bridge, 'Fibercore Europe', this is the first vertical lift bridge made completely of FRP, in the world. The bridge was designed for a maximum vehicle weight of 60 tons, in that way it can carry all traffic, including heavy trucks. The vertical lift is provided by a hydraulic riser, which is located in the pylon. The cable stays are purely for esthetics, they don't have a structural function. The load bearing system is composed of simple beams on two supports and an intermediate support at the pylon. The height of the pylon is thus only used for the vertical lift and does not carry the deck via support cables. [A45, p3, p5-6]



Fig. 141: Oosterwolde heavy traffic lift bridge [A45] [WEB: www.fibercore-europe.com]

The bridge construction was finished in June 2010 and the involved companies were, next to the manufacturer and composite designer 'Fibercore Europe', the engineering firm 'Witteveen & Bos' and the main contractor 'Knol Akkrum'. The design was backed up by the civil engineering department of Delft University of Technology, for which Dr. M.H. Kolstein performed several static load tests with FRP test specimens of the manufacturer. [WEB: www.infracore.nl]. In the list below the most important design data of this eccentric heavy traffic bridge can be found: [A45, p4]

- Date of completion:	June 2010
- Span:	Two spans of 3,3m and 8,42m
- Width:	11,2m – 12,5m
- Thickness bridge deck	0,5m -0,6m
- Width waterway:	7m
- Bridge weight:	65 tons (including ballast)
- Height pylon:	10,5m
- Class:	60 tons fast traffic
- Material:	'Fibercore' Infracore (100% glass fiber reinforced polymer)
- FRP production technique:	Vacuum bag/Pressure Bag/Hand-lay-up

6.2.4 HARBOURBRIDGE HARTELHAVEN ROTTERDAM

This glass fiber reinforced polymer composite bridge is intended for pedestrian use only. It is the first bridge which is composed of a completely monolithic FRP structure. The bridge is intended for pedestrian use only and therefore has no glued or bolted joints. Because of this monolithical bridge character, the connections between the bridge deck and the handrail structure are extremely stiff, thus enabling the complete structure to work as if it were a single beam. In other words: the height of the handrail is also used as part of the load-bearing structure to make a maximum span of 20m possible. Another advantage is that the bridge can be completely prefabricated and transported to site in one go. The first bridge of this type was placed in the Hartelhaven in the summer of 2011. It was designed in a cooperation between Fibercore Europe and Havenbedrijf Rotterdam and uses the well-known Infracore system of Fibercore. This bridge in particular will have two spans of 15m. [A18, p1]



Fig. 142: Fibercore harbourbride Rotterdam. [A18, p2]

6.3 FIRE SAFETY IN BRIDGE ENGINEERING CASES

In the chapter on fire safety the lack of bridge fire safety standards, codes, regulations, papers and general information on this subject was already covered. However a few examples do exist where fire safety engineering played an important role in the design process. Generally fire safety becomes more important when firstly many people and large crowds use the bridge, and secondly, when the bridge forms an enclosed space, from which heat cannot dissipate as quick as from bridges with open design. Thirdly the bridge has to structurally function even under (short term) fire loads. Especially when vital structural elements are situated above the bridge deck, and a fire occurs on the bridge deck, these structural elements should be protected and thus fully functional for a specified amount of time, the fire resistance time. The examples cover all of these situations.

6.3.1 HAFENSTRASSENUNTERFUEHRUNG , FRANKFURT AM MAIN, GERMANY

The following example covers the renovation of a very wide bridge carrying 30 railway tracks and the a complete turnout-area of the 'Frankfurt am Main' main railway station. The original bridge had a span of 15m and a width of 220m. After the renovation the bridge was supposed to have a span of 30m and the bridge deck was raised by 1,3m. The load-bearing system was composed of several stiffened steel I-girders width a height of 1,3m, a varying width of 2,3m to 2,9m and wall-thicknesses of 30mm to 60mm. On site, the girders were assembled into 25 7m to 15m wide pre-assemblies, before they were slid into place using 44 temporary portals. The 'Hafenstrassenunterfuehrung' was finished in the end of 1999 for a total building sum of about €45 million. The picture below shows the old bridge portals (black) as well as the new portals (colored). [A23, p1]

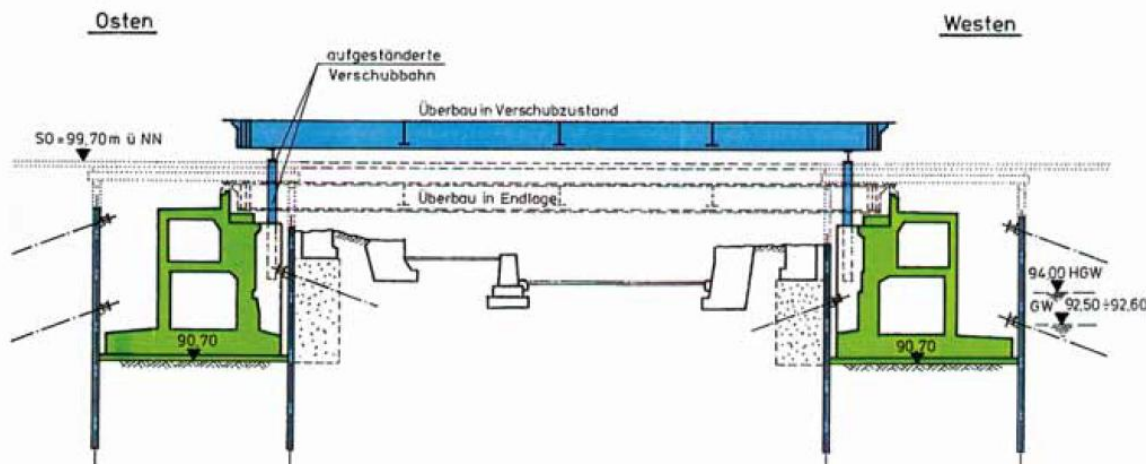


Fig. 143: Old and new load-bearing system of the Hafenstrassenunterfuehrung, Frankfurt am Main, Germany [A23, p1]

Because of the large covered area of about 6500m² the authorities demanded a fire resistance class of F30 according to DIN4102. This corresponds to a fire resistance of at least 30 minutes. One could also argue that the underside of this bridge behaves visually and functionally more like a tunnel than a bridge. Because the underside of the steel girders was directly exposed and the height of the fire resistance measures was limited, this called for special measures. The contractor 'Dyckerhoff & Widmann' therefore chose a (at that time) new method of the application of a thin layer of intumescent coating at the underside of the bridge. The upper side was already protected from fire by a thick layer of rocky railway ballast. [A23, p1]

The coating was provided by 'Peramatex GmbH and the system used was 'Unitherm ESA 38092'. This type of coating can achieve fire resistance times of 30 min to 60 min. Chemically it functions by extracting an inorganic acid under heat load. This acid dehydrates the also present polyalcohol, which produces a carbon-

free residue that, together with the molten binder is foamed up by the gaseous propellant induced by heat. Following this principle, the coatings foams up under heat load, reaching volumes up to 50-100 times of the original volume. The resulting foam is inflammable and fire-resistant. The example of the Hafenstrassenunterfuehrung was one of the first applications of intumescent coatings in the bridge engineering industry. Due to the stringent fire safety regulations, intumescent coatings are primarily used in the building industry in high-rise projects. [A23, p3-4]

After finishing, cleaning and perfecting the steel beams the contractor used three 'Airless'-guns to spray up to coating on a total surface of 34.000 m². The whole process took about 10 weeks. The coating had a thickness of 0,5mm to 2mm resulting in a total amount of 40t of 'Permatex Unitherm ESA'. Compared to the total weight of the steel beams of 5.400t this led to no significant added dead load. Afterwards thorough quality checks were performed to guarantee the obliged fire safety and –resistance. The coating was then finished with two layers of protective white paint. [A23, p2-3]

During application of the intumescent coating workers needed to use respiratory masks and protective glasses and clothing. Should a fire occur under a coated bridge, the foamed up intumescent layer can easily be removed from the steel surface using only normal tools. The foam though has to be disposed as hazardous waste. Whether the underlying steel is structurally still fully functioning depends on the intensity and length of the fire. [A23, p4]



Fig. 144: Application of the intumescent coating (left) and the finished, coated and pointed product (right) [A23, p2]

6.3.2 BRIDGE PAVILION, EXPO2008 ZARAGOZA



Fig. 145: Artist impression of the bridge pavilion at the EXPO 2008 in Zaragoza, Spain [A42, p1]

The Bridge Pavilion (or 'Puente Pabellón'), designed by 'Zaha Hadid Architects', was conceived for a dual purpose; to serve as the main pedestrian access route for the EXPO2008 in Zaragoza, Spain, as well as to house some of the exhibitions of the event. Next to that, it also provided access for emergency vehicle traffic. The design of the bridge is very complex, partly due to the requirement of delivering an iconic building for the renowned World EXPO. The bridge is composed of 4 oblong pods which are placed adjacently to each other. The total length of the bridge is 280m with two individual spans of 155m and 125m. [A25,p1]

The load bearing structure is composed of a complex array of light-weight steel space frames, arches and ribbed elements. The picture on the right shows the composition of the steel load bearing system. The depth of the cylindrical truss steel (or 'tube girder') varies from 13m at pod 4 to 30 at the central support. The bridge deck is supported by shaped steel box-beams. Next to that the arches of the central spine and the side-arches are also composed of steel box-sections. Furthermore diaphragm elements were placed at strategic points. The secondary ribs are made of steel I-beams with 3,6m c.t.c. distance.[A42, p4-7]

This complex structural design was made by 'Arup', making use of state-of-the-art CAD and FEM/FEA technology. Since 'Arup' is well-known for their broad engineering expertise, they were also asked to deliver a fire safety design. The complexity of the project, the presence of large pedestrian crowds during service-life and the high level of enclosure of the bridge decks called for a special fire safety engineering approach.

As during the design, in the years before 2008 no prescriptive fire safety codes for these kinds of structures existed in Spain, a performance based design (PBD) design approach was chosen. One of the problems to be overcome was the classification of Pod-1 and Pod-3 as exhibition space and space for general public assembly which harshened the demands for (fire)safety. Pod-2 and Pod-4 were classified as spaces for public thoroughfare. The division of the bridge in several pods had the advantage that fire engineering design could be made assuming that fire-spread between the individual pods was not possible. [A42, p8-10]

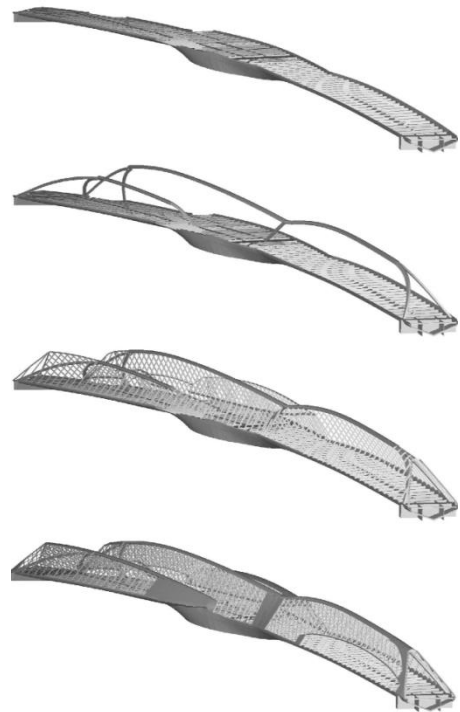


Fig. 146: Main structural system of the Bridge Pavillon [A42, p7]

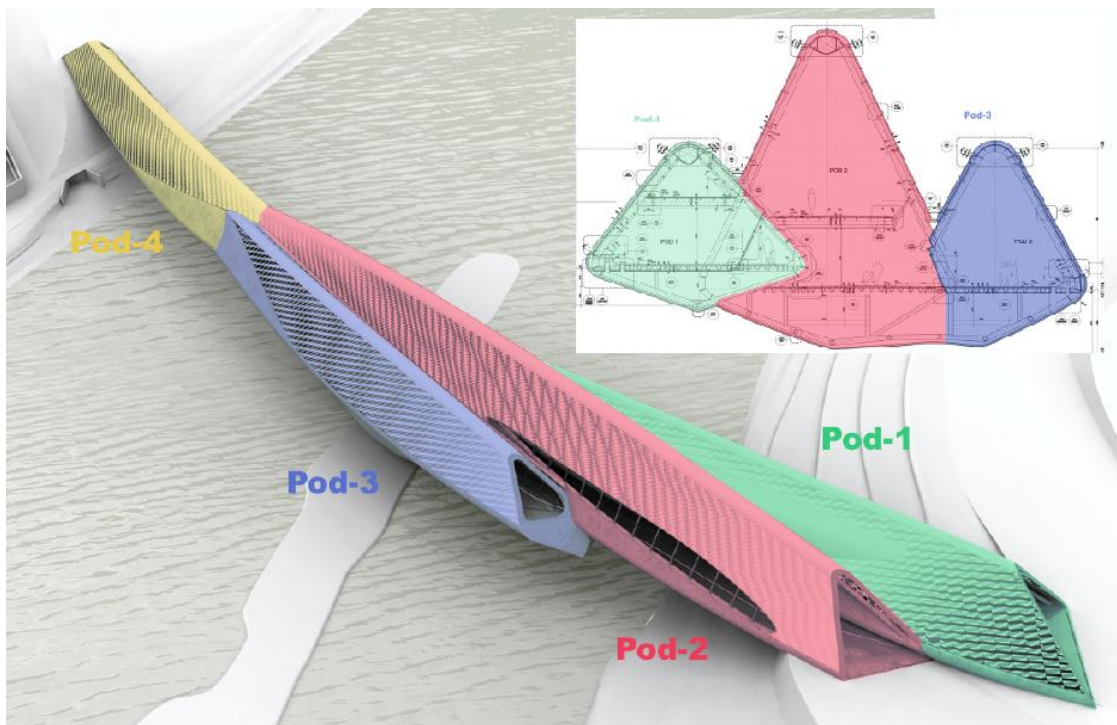


Fig. 147: Arrangement of pods in the Bridge Pavilion [A42, p16]

The criterion that was chosen to base the PSD on was the fire resistance R90 criterion from the general building code. This criterion dictates structural intactness for the first 90 minutes of an occurring fire. It was soon found that this criterion was appropriate for Pod-1 and Pod-3, since they were housing large public crowds during service. The R90 criterion was limited to R45 for the other pods, due to the lower fire load, the better ventilation and the transport character of the pods. [A42, p11-12]

For the actual fire protection of the steel elements two strategies were chosen. The non-exposed elements were covered with low-cost cementitious spray and insulations products such as gypsum boarding. The exposed elements such as most of the ribs, and the steel diagrid that carried the façade, were painted with intumescent products in different qualities. The highest quality of intumescent paint that was used was able to guarantee the R90 criterion. A special approach was chosen for the steel cables that supported several walkways in the bridge. They are not covered with intumescent paint; instead the design of the cable supports was made redundant, such that loss of a single or several cables does not cause the structure to fail. [A42, p12-14]

One of the important effects that always accompany fire is smoke. Smoke production and propagation is often considered more deadly than the heat that is produced by the fire. Although the pods of the "Bridge Pavilion" are interconnected they were designed such that smoke cannot propagate from one pod to another. Next to that the 'peak'-shaped pod section and the ventilated façade ensure fast smoke extraction. The façade was also designed by 'Arup', leading to a very well integrated design. This example also shows the need for special design approaches in the case of one-of-a-kind enclosed structures that are used by large crowds at the same time.[A42, p15-18]

6.3.3 CABLE STAYED BRIDGE FIRE SAFETY, PAPER JOFPE 2009

This example is not focusing on a real built bridge, instead it relates to the paper 'Evaluation of the Impact of Potential Fire Scenarios on Structural Elements of a Cable-stayed Bridge' published by "I.Bennetts and K. Moinuddin" in the "Journal of Fire Protection Engineering, Vol. 19, May 2009" [P39]. In this paper an interesting research on different fire scenarios for cable-stayed bridges and the modeling of the loss of structural strength in the high-strength cable stays was performed. Particularly the different fire scenarios can be of large interest for the design of other traffic bridges, such as the proposed fiber reinforced polymer traffic bridge. In this case-study the different fire scenarios proposed in the paper will be discussed.

A fire associated with a bridge will most likely be the result of a vehicle fire caused by a burning truck, bus or train on or below the bridge. The reasons that a cable-stayed bridge is more vulnerable to fire than a regular beam-action bridge, and fire should therefore be considered as a genuine load-case lies in the following: Firstly, loss or closure of the bridge for a significant time may lead to unacceptable commercial consequences. Secondly it may be impossible to undertake repairs if significant damage occurs. Whether these two points only hold for cable-stayed bridges or also hold for other bridge types can be doubted. That is the reason why the proposed fire scenarios are dealt with here. [P39, p3]

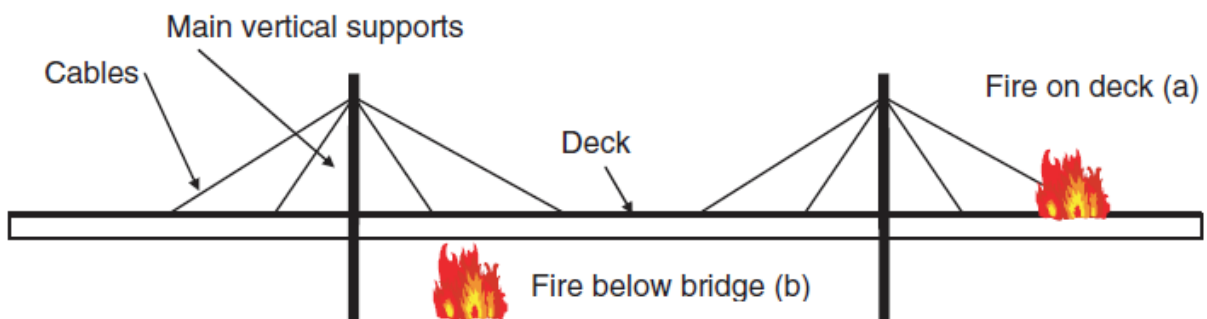


Fig. 148: Two different fire scenarios (a and b) for cable-stayed bridges [P39, p4]

The above figure shows the two most likely places where fire can occur, on deck (a) and below the bridge (b). The fire below the bridge deck can have significant effect on the girders above, with the temperature reached by the girders being a function of the height of the girders above the roadway, the mass and configuration of the girders and the heat release rate (HRR) and duration of the fire below the bridge. In case of fire on deck (a) the girders carrying the bridge deck will be shielded from the fire by the (mostly concrete) bridge deck. [P39, p4]

Because cable-stayed bridge decks are mostly high above ground, the b) case was not considered in the discussed paper. Also due to the shielding function of the bridge deck concerning the bridge girders, the fire load was only considered to be acting on the cable-stays and the cable supports. In the case of the FRP bridge that is to be designed both cases will have to be considered, the bridge will most probably not be placed in such great heights, that the fire probability can be out ruled for case b) and the a) case will have direct effects on the trusses adjacent to- and above the decks and possibly even on the truss underneath the deck, because the heat-shielding function of the (FRP) deck is not known yet. The paper remarks that most bridge decks (possibly even FRP decks) are covered with a porous layer of bitumen, which will most likely absorb much of the spilled fuel and because oxygen is needed for combustion, fire will only be present on the surface of the deck. [P39, p4-5]

According to the author about 2% of heavy traffic on major traffic routes are flammable liquid tankers and 1% are LPG tankers. The range of fire severities (HRR and duration of burning) of the associated truck fires is difficult to obtain, thus for estimating the magnitude of the occurring fires the paper proposed three different scenarios that induce the worst effects on the load-bearing elements of the bridge structure. All fire scenarios have a model duration of 2 hours. [P39, p6]

I) A heavy truck fire located close to the supports or cables (LT)

For this scenario the trailer length is taken as 20m with the maximum height above ground of 4,6m. From empirical relations a flame height of 12m to 15m above the trailer is assumed. The HRR values associated with this flame height are between 20MW and 50MW. However, due to the lower heat and flame intensity at the top of the fire a smaller radiation area with constant flame temperatures of 800°C to 1000°C can be used. The proposed model uses a radiating heat panel with dimensions 20m x 12m and a flame temperature of 900°C. Next to the static situation, a dynamic situation covering added convective and radiant heating due to wind load has to be taken account of. The convective heat transfer coefficient is taken as recommended by the standard fire test exposure: 23,2 W/m²K. [P39, p6-7]

II) An oil or flammable liquids tanker that catches fire when directly adjacent to the main supports or cables. (TF)

This scenario could be the result of rupturing, or the following due to a collision or accident. A tanker fire could cause sudden release of heat energy, but this will not have as detrimental effect as an associated pool fire caused by the leakage of fuel on to the roadway. This is due to the fact that a large fireball will only heat the structure for a very short period of time. A pool of 15m diameter is taken to be representative for a tanker fire. With added safety factors the emissive power of the pool fire flame is calculated as 90 kW/m². Again, for the worst case scenario of added wind load, and the pool being situated directly under the cable-stays this emissive power can grow to 170 kW/m². This value has been determined experimentally. [P39, p7-8]

III) A gas jet fire resulting from pipe fracture and ignition of fuel from a LPG tanker vehicle, most likely following a collision (LPG)

As for II) this scenario could cause a sudden release of heat due to a large fireball; however since this heat release would have a very short durance it is not the most severe sub-scenario. Of the three scenarios, this is the most unlikely one. Tests on 50mm pipes releasing 8 kg/s of gas at 13bar pressure have been conducted. Flame lengths up to 35m were obtained with gas temperatures of 1300°C at 4m and 1200°C at 12m of the source. The latter corresponds to a total heat flux of 250 kW/m². [P39, p8-9]

These fire scenarios were analyzed together with different numerical layer models of the cables and the cable supports. The heat in each layer was calculated in dependence of the other layers. Next to that the material strength values were also incorporated. To give a short impression of the results the figure below shows the results for the temperature effects of the different fire scenarios on the unprotected cable supports. It is clearly visible that the LPG gas jet fire has the most adverse effect: it reduces the load bearing capacity of the support to zero within 30 min. The capacity cut in half in little over 10 min. The tanker fire has slightly less adverse effects: it halves the capacity in about 16 minutes. The most probable fire to occur has also the least adverse effects for the supports: the capacity is cut in half in about 40 minutes. Note that in this example only one side of the support was exposed to fire and thus loses strength rapidly, the other sides of the support are much cooler than the directly exposed side. [P39, p22] This example shows usable fire scenarios as well as models to incorporate the heat transfer between different layers of the structural elements. It can be helpful when analyzing the fire resistance of the fiber reinforced polymer bridge to be designed.

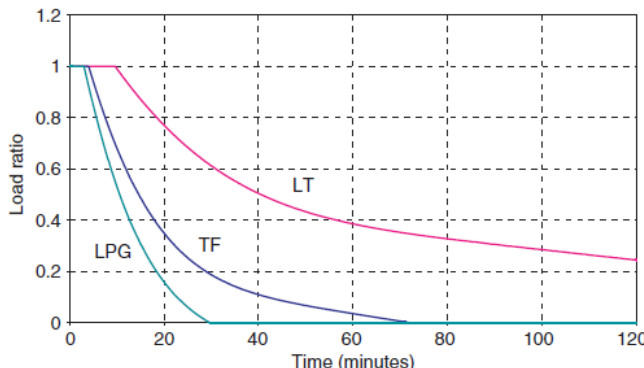


Fig. 149: Temperature effects of the fire scenarios on the bridge cable supports [P39, p22]

6.4 ISOTRUSS CFRP CYLINDRICAL TRUSS STRUCTURES

To conclude this case study chapter a final case study is given, which certainly deserves special attention. The so called “IsoTruss system” is an extremely lightweight and up to 12x times stronger than steel lattice structure (depending on the application). It is typically constructed of carbon filaments that are interwoven in an open-lattice design. The “iso” and “truss” in “IsoTruss” represent the isosceles triangles that truss the pyramids that ultimately give the structure its strength and stiffness. Next to the lightweight CFRP composite buildup, especially the three-dimensional spider web-like structural design eliminates the weight of comparable structures, such as solid wood and tubular metal poles. In essence, a 45 kg “IsoTruss” composite structure could replace a 500 kg steel structure and still offer equivalent strength. The “IsoTruss” system was developed by Prof. David Jensen of Brigham Young University Utah, USA in the mid-1990s. [WEB: www.sti.nasa.gov]

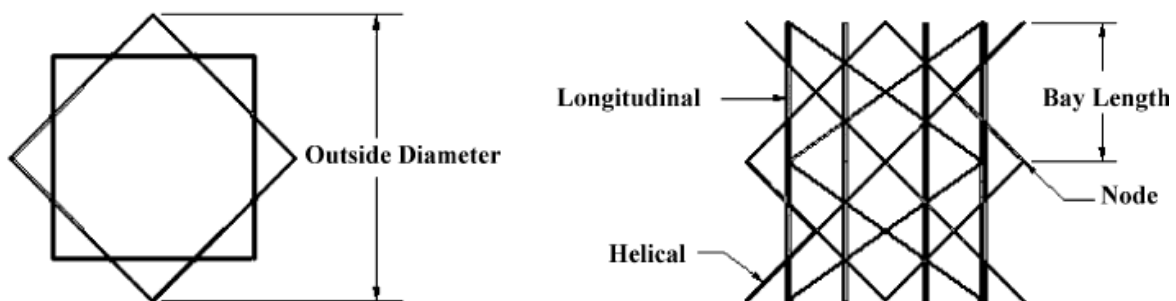


Fig. 150: Geometry of typical 8-node IsoTruss buildup. Left: Cross-section. Right: Side-view [P93, p2]

As depicted above, an IsoTruss structure is a three-dimensional tubular circumferentially and longitudinally periodic grid structure that is particularly well suited for fabrication with advanced composite materials, such as carbon fiber, aramid fiber, or glass fiber, with epoxy, vinyl ester, polyester, or polyurethane resins. These structures exhibit a tremendous performance to weight ratio.

The longitudinal members are the straight members, parallel to the length of the IsoTruss. They carry the axial and bending loads. The helical members are piecewise linear members spiraling around the longitudinal axis. The helical members resist torsion and shear loads and improve the compressive strength of the structure by decreasing the buckling length of the longitudinal members. [P93, p1]

The IsoTruss system was developed as follow-up on the two-dimensional Isogrid structures developed in the 1970s. Isogrids still are the typical and most common layout for any space-frame structure. Due to their unique layout, Isogrids are quasi-isotropic in their plane by nature. IsoTruss structures feature similar repeating triangles but these are arranged in a radial or tube-like configuration in which the triangles form a truss of pyramids that exhibit multiple radial symmetries. The result is an orthotropic material, which by definition has at least two orthogonal planes of symmetry (with right angle intersections), where material properties are independent of direction within each plane, giving the design performance advantages over conventional solid tubular structures. [WEB: www.compositesworld.com]

The triangles and pyramids redistribute shear- or bending-loads on the tube into the members as axial tensile and compressive force, similar to normal truss behavior. This axial and compressive loading leverages the advantages of composite materials thereby increasing load bearing characteristics of the structure at the absolute minimum weight. This principle is shown in the sketches below. [WEB: www.altuspoles.com]

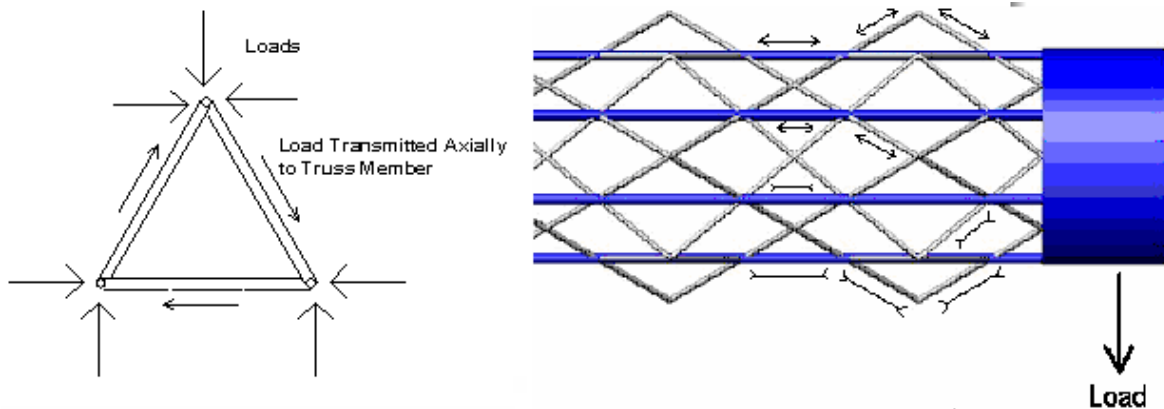


Fig. 151: Force diagram of an IsoTruss under bending load [WEB: www.altuspoles.com]

“IsoTruss” structures are currently manufactured by filament-winding only. The structure is wound over a custom-designed, collapsible and segmented metallic mandrel, using a lengthened single-head filament winder. Winding patterns are computer-controlled by advanced software. Single or multiple tows of continuous fiber, either in epoxy prepreg form or in a wet winding process with a range of resins, are wound over the mandrel. The thickness of a completed single wound element ranges from 6,5mm - 13mm. [WEB: www.compositesworld.com]

The largest IsoTruss products made to date are 40cm – 60cm in diameter. The maximum segment length produced up to date is 6,2. The segments can be fabricated with solid tube ends, which could be adhesively bonded together, making structures with lengths in excess of 80m possible. In terms of scaling up to structures larger than 62cm in diameter, well-proven mechanics show that it's scalable. [WEB: www.compositesworld.com]

A current application of the IsoTruss system is the development of carbon epoxy composite frames by the American company “Delta 7”. “Delta 7” manufactures “ultra-light” carbon fiber frame bikes using IsoTruss grid structures to offer a lightweight and efficient alternative to traditional steel, aluminum and composite structures. The IsoTruss structures provides an attractive, efficient, and damage-tolerant design. The open grid enables a variety of standard and innovative connections. The pictures below show how the connections of these IsoTrusses are realized, and how the finished product looks like. The frame below weighs about 9% of a comparable steel tubular frame, while having equivalent bending stiffness and buckling resistance. [WEB: www.delta7bikes.com]



Fig. 152: Close-up of the carbon epoxy composite “IsoTruss” structure of the “Delta 7 Ascend Road Bike” [WEB: www.delta7bikes.com]



Fig. 153: General view of the 7 IsoTruss elements used in the frame of the Delta 7 Arantix mountainbike frame [WEB: www.delta7bikes.com]

Although it is very unlikely that a full-size road bridge can be filament-wound in one go, the IsoTruss system offers an interesting view on efficient mesh design and build-up of cylindrical trusses. The IsoTruss layout could very well be scaled-up and used as a guide to design an efficient mesh layout for the cylindrical truss heavy traffic bridge, as intended in this research.

7. DURABILITY & SUSTAINABILITY

Various environmental and load conditions affect the durability of fiber reinforced polymers in terms of strength, stiffness, fiber-matrix interface integrity and cracking. There are numerous influential factors such as water, sea water, chemical agents, prolonged freezing, thermal cycling (freeze-thaw cycles), elevated temperature exposure, UV radiation, creep and relaxation, fatigue, fire etc. [P32, p21] Creep and fatigue are not covered in this chapter, they are covered in the appropriate [chapter 2.6.8; chapter 2.6.9]

A major advantage of most composites is that their corrosion-resistance is remarkably better than that of the traditional building materials concrete and steel. This is why the general agreement on durability of FRP composites is that their durability is better overall than that of traditional materials. However it is also clear that durability of FRP composites is still an area which does require further research in order to gain a greater understanding of the characteristics over longer periods of time. [B21, p497] A scientific knowledge-gap analysis performed by a cooperation of several US universities proves this assumption for most reinforcement and matrix-materials. [P10]

A real-world example

A practical application of glass fiber reinforced polyester panels with a isophthalic polyester gel-coat that were used as exterior cladding for the 'Mondial House' in London, UK in the 1970s showed that degradation of these panels over a life-span of 33 years was very moderate and the panels are expected to be able to have a design-life of at least another 20-30 years, bringing the total design life to 50-60 years. It has to be said though that these panels had no load-bearing function. Minding the fact that these panels where developed and installed in the 1970s, it is evident that modern resins and gel-coats are able to guarantee even longer design-life spans. [A06, p33]

7.1 MOISTURE AND ALKALINE SOLUTION EFFECTS

Moisture diffuses into all organic polymers, leading to changes in the thermo-physical, mechanical and chemical characteristics. It has been shown that moisture affects not only the polymer, but also the matrix-fiber interface and thus the bond-strength and in some cases even the fibers themselves. Aramid fibers for example absorb moisture and must be sufficiently protected by proper resin systems. Since in most civil engineering applications the composite material will always come in contact with moisture and/or water, it is essential that both short- and long-term effects on the composite are known and understood. [P10, p4] Moisture absorption depends on the type of polymer matrix, laminate composition, thickness, laminate quality, curing conditions, fiber-matrix interface and manufacturing process. In general, over short-term loading, moisture effects cause degradation in strength rather than stiffness. Epoxy resins are less sensitive to moisture compared to matrices of polyester or vinyl ester. [T03, p10-11]

To decrease the possibility of rapid movement of moisture and chemicals into the composite and towards the fiber-surface it is critical that a resin-rich surface exists in all FRP structures, this role is often fulfilled by the gel-coat. The gel-coat needs to have sufficient ductility to prevent cracking. Considering the lack of knowledge, "V.M. Karbhari (et al.)" advise to calculate with very conservative values for the guaranteed design strength of composites: 25% of the guaranteed design strength for GFRP, 30% for AFRP and 40% for CFRP. [P10, p4-5] Although FRP composites can come into contact with alkaline media through interaction with a variety of sources, including chemicals, soil or solutions diffusing through the soil, and concrete, the main concern at the present time is the potential degradation effect of concrete pore water on FRP

reinforcement bars. It is known that bare glass fibers are severely degraded in such an environment, which even amplifies the need for sufficiently thick and ductile resin layers to protect the fibers. Next to that it is important that before application in FRP-concrete composites, the composite is fully cured, since under-cure can improve the moisture-susceptibility of the composite. [P10, p5] Tests on CFRP reinforcement rods showed that a concrete alkaline environment has very little influence, reducing the ultimate capacity with only 4% [T03, p11]

7.2 THERMAL EFFECTS

Here, only the effects of thermic cycles (freeze-thaw cycles) and mildly increased temperatures due to radiation of the sun are considered. FRP composites under fire load are covered in chapter 4. Freeze-thaw cycles, especially in cold regions are known to change the material properties of FRP composite. Matrix hardening, matrix micro-cracking and fiber-matrix bond degradation can occur during a freeze-thaw cycling situation due to differences in the coefficients of thermal expansion of the fibers and the resin. The difference in coefficients of fibers and matrix has the most deteriorating effect on the fiber-matrix bond and can lead to delamination failure. [P62, p31][P10, p6]

Also tests in which a 2m x 0,3 m x 0,2 m section was cyclically tested under three-point bending at temperatures as low as -55°C showed that at these temperatures, the stiffness of the specimen decreased by 11,5% compared to room temperature. Acoustic emission tests confirmed matrix hardening, matrix micro-cracking, and fiber-matrix debonding. The strength-reduction ranged from 10% to about 27%. [P62, p31]

Care has to be taken if FRP composites are subjected to elevated temperatures due to sunlight radiation. Failure is possible if the laminating resin softens excessively. The upper use boundary temperature of the resin should always be followed in practice. This temperature typically lies at the point at which the flexural strength decreases to half the original flexural strength. Also, FRP composites should never be used at a temperature higher than 30°C below the glass transition temperature.

7.3 UV-RADIATION

Ultraviolet light may cause photo-oxidative reactions in the matrix, causing micro-cracking in the FRP composite. This susceptibility is caused by the fact that most polymers have bond dissociation energies in the order of 290-400nm, which is about the same wavelength as that of UV-light. The effects of ultraviolet exposure are usually confined to the top few microns of the surface. However, degradation is known to affect mechanical properties disproportionately. It is expected that this behavior is caused by stress concentrations which arise at the UV-flaws and initiate fracture at stress levels much lower than those for virgin material. [P62,p30][P10, p8]

Normally, to protect FRP elements from the effects of UV radiation often UV-resistant filler materials are used. Another common method to protect the composite is the application of a gel coat or other protective coating to shield the surface of the FRP from direct exposure. The polymeric coating does not act preventive of UV-induced damage; moreover it functions as a sacrificial layer, comparable to for example cathodic protection of steel elements. This means that it needs to be possible to maintain the UV-resistance of this coating. [P10, p8]

Nowadays it is known that most of the damage inflicted by UV-radiation does not occur because of the UV only, it is rather caused by the combination of UV-damage and moisture ingress in the damaged regions. This means that for proper protection UV-resistant polymer matrix systems need to be developed in the future. For now, protective coatings are the only way of providing adequate protection for FRP composites. [P10, p9]

7.4 QUANTIFICATION OF ENVIRONMENTAL EFFECTS

Many attempts have been made to quantify the deteriorating effects of the environmental factors described in this chapter. Research has shown that GFRP is more susceptible to degradation than CFRP, foremost in the following fields: alkaline effects, acid effects, salt effects, fatigue and UV-radiation. This fact can also be seen in the proposed table of environmental reduction factors for aramid-, glass- and carbon fiber reinforcement of epoxy composites. [P32, p22-23] Carbon fibers are very durable in most aspects. One of the biggest advantages is that the composite does not corrode. The durability problems that can be identified in are mostly connected to the matrix. Epoxy is a polymer that withstands deterioration fairly well in most aspects. Epoxy does not absorb water significantly, contrary to other polymers. [T02, p18]

In the following two main approaches will be covered, the first approach is the approach developed for the Eurocomp Design code in the mid-1990s. In this design code which is applicable for GFRP only the environmental reduction is dependent on the operating temperature of the composite and the heat distortion temperature of the polymer matrix. Generally said, a low operating temperature beneath 25°C combined with a high heat distortion temperature of the matrix yields the lowest environmental reduction factors. Furthermore this approach distinguishes short-term and long-term loading, yielding reduction factors in the range of 0,3-0,4 for long-term-loading. In comparison with the other approaches the results seem a little conservative. [B14, p30]

Operating temperature [°C]	Heat Distortion Temp. [°C]	Env. Reduction short term loading	Env. Reduction long term loading
25-50	55-80	0,83	0,33
	80-90	0,90	0,36
	>90	1,00	0,40
0-25	55-80	0,90	0,37
	80-90	1,00	0,39
	>90	1,00	0,40

Table 40: Environmental reduction factors of GFRP according to Eurocomp [B14, p30]

The other approach is presented by the Swiss "EMPA" ('Swiss Federal Laboratories for Material Science and Technology'). Their approach is more recent but only compares the environmental reduction of several epoxy composites. However in contrast to the Eurocomp approach, other reinforcement fibers such as aramid and carbon are also considered. Three exposure conditions are considered in the EMPA approach: Interior exposure, exterior exposure and aggressive environment exposure. The environmental reduction of glass fibers is generally the worst (ranging from 0,50 to 0,75), aramid performs much better (ranging from 0,70 to 0,85). Carbon fiber copes best with the environmental influences (ranging from 0,85 to 0,90). It is not clear for which time span these values are applicable. [P32, p22]

Exposure Condition	Fiber / Resin type	Environmental reduction
Interior exposure (in buildings and normal factories)	Carbon / Epoxy	0,95
	Glass / Epoxy	0,75
	Aramid / Epoxy	0,85
Exterior exposure (bridges, piers, parking garages)	Carbon / Epoxy	0,85
	Glass / Epoxy	0,65
	Aramid / Epoxy	0,75
Aggressive environment (chemical plants)	Carbon / Epoxy	0,85
	Glass / Epoxy	0,50
	Aramid / Epoxy	0,70

Table 41: Environmental reduction factor for different FRP systems and exposure conditions [P32, p22]

Two other environmental reduction factor approaches are known to the author, one by the NAVFAC (the US-American Naval Facilities Engineering Command), which advise an environmental durability factor of 0,65, which may be applied to account for degradation of GFRP material properties over time. [P16, p12] The second approach is that of the British researcher "T. Stratford", who performed a study on: "Aberfeldy

Footbridge: 16 years in service, Long Term in Service Performance of FRPs in construction." He proposes an environmental reduction factor of 0,71 for GFRP and 0,83 for AFRP [P22, p6]

7.5 SUSTAINABILITY

The key point of sustainability is the balance and consideration of economic-, human- and environmental factors in order to meet our needs today, without compromising the resources available for future generations. [A47, p1] The illustration below shows the three factors. The white area where these areas join is the general target of any approach on sustainability.

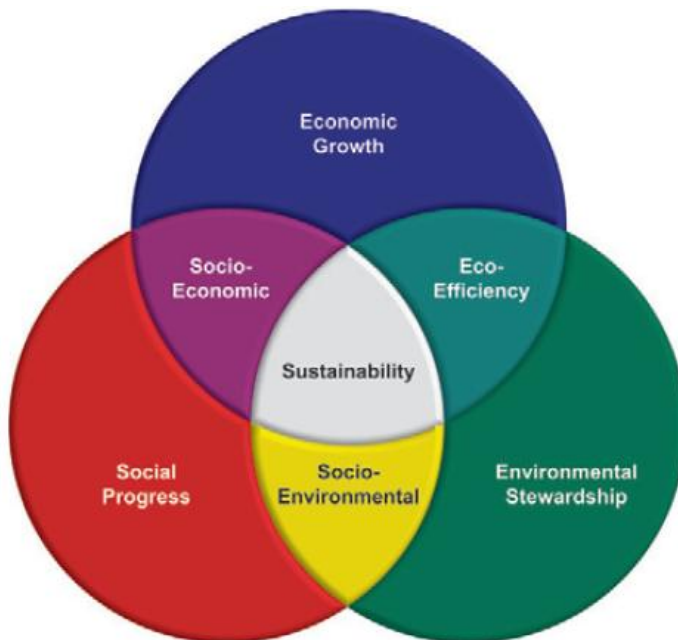


Fig. 154: Balance of People, Planet and Prosperity in the sustainability chart [A47, p1]

The most used method to assess sustainability is the 'Life Cycle Assessment' (LCA). It is used to compare the environmental impacts for a number of different attributes rather than comparing a single aspect, such as recycled contents. The LCA considers the raw material production, product manufacturing, distribution, use phase, disposal phase and the impact of transportation. This approach is often also referred to as 'cradle-to-grave'. Some of the factors that are considered in a typical LCA are: total consumed energy, global warming, greenhouse gases, acidification, soil and water (use), smog production, ozone depletion, excess nutrients to water bodies, eco- and human toxicology and depletion of minerals and fossil fuels. [A47, p2]

In the following, a spider diagram will be discussed, which compares the sustainability of a large-scale aquarium fish tank considered for purchase by the "Monterey Bay Aquarium Research Institute" in FRP composite compared to a normal concrete fish tank. 'Kreysler & Associates' was asked to make a LCA for both options and came to the conclusion that a tank made of FRP had a much better sustainability value, reducing all sustainability factors significantly. [P89, p7] Next to that, the study also showed that the total life cycle costs of the FRP tank were almost 20% lower than that of the concrete tank (1,56 million US\$ compared to 1,85 million US\$). [P89, p4]

This leads to the following key factors that positively influence the sustainability value of FRP materials in general: The excellent weight/strength ratio possibly has the greatest influence on the sustainability; composites can deliver embedded energy savings, when compared to a traditional material such as concrete on a functional unit basis. [P88, p13, p18]

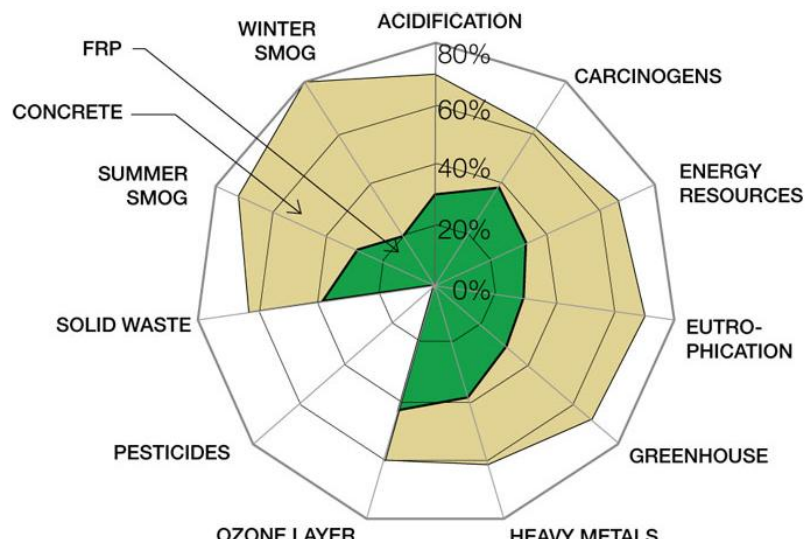


Fig. 155: Spider diagram comparing a composite fish tank to a concrete fish tank [P89, p22]

The same comparison also holds with aluminum parts made with virgin aluminum and steel primarily because the composite delivers better strength-to-weight. It is assumed that as more recycled content is added to the aluminum and steel, their energy use and environmental footprint is closer to the composite components. As might be expected, timber materials have a significant environmental advantage over composites, with a 50 percent lower embodied-energy footprint. An important fact on the impact that is represented by a composite part increases as its percentage of resin increases. Therefore, increasing fiber content and/or reducing styrene in the resin can make the product more sustainable. For structural applications, such as bridge engineering, where high strength and thus high fiber contents are needed this poses a great sustainability advantage. [P97, p20-21]

The table below gives a comparison of the embodied energy of three different construction materials: steel, aluminum and GFRP. It can be seen that virgin FRP is, compared to 25% recycled steel and 50% recycled aluminum. Still, the composite contains 2x-3x times less embodied energy, compared to the other materials on a functional unit basis. In the case of steel, a large part of the energy is used during field install and maintenance (among others due to the heavy weight and bad corrosion resistance), whereas the raw material production of aluminum takes up most energy in the aluminum life cycle. Composites also feature high raw material production energy uptake, but have the advantage that further processing, transport and maintenance embodies very little to no energy. [P88, p18-19]

Property	Unit	Steel	Aluminum	Composite
Primary raw materials		25% recycled	50% recycled	Glass & resin mix
Primary raw materials Energy	MJ/kg	26	101	70-74
Secondary operations		Hot/Cold/Section roll	Extrusion or other	Composite manufacture
Secondary operations Energy	MJ/kg	4-6	40-50	4-6
Field Install		Blast & Paint		
Field Install Energy	MJ/kg	30-35	0	0
Maintenance & Use phase		Blast & Paint		
Maintenance & Use phase Energy	MJ/kg	30-35	0	0
Total	MJ/kg	90-106	141-151	74-80
Total compared to a composite element of 1,9 kg weight	MJ/kg	270-318	169-181	74-80
		at 3,5 kg	at 1,2 kg	at 1,0 kg

Table 42: Total energy use of steel, aluminum and composite structural parts. [P88, p18-19]

In the last few years there have been some developments in the improvement of the sustainability of composites. An example of these developments is the 'Advantex' E-glass fiber made by 'Owens & Corning'. The two spider diagrams below compare a traditional E-glass fiber with the newly developed 'Advantex' glass fiber. It can be seen that the optimized E-glass fiber reduces fluoride and particulate emissions by 85% to 90%, while also reducing the nitrogen oxide emissions by 65%. Next to that, the other sustainability factors are also significantly reduced. The diagrams are the result of a comprehensive 'Life Cycle Analysis'. [P88, p16]

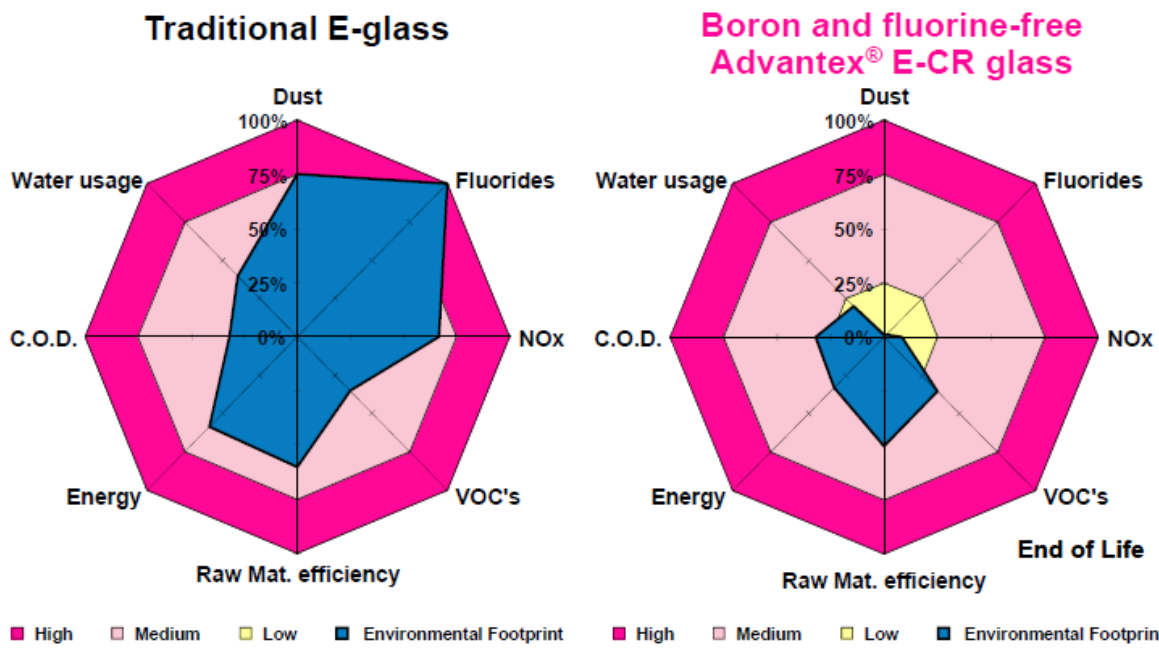


Fig. 156: Spider diagram of traditional E-glass compared to sustainability optimized E-CR glass [P88, p16]

This example shows that although composites are generally much more sustainable than concrete, steel or aluminum, there is still room for improvements, even more improving the efficiency in the production process and thus improving the overall sustainability performance of composites. In the next chapter a small outline on the recycling of composites will be given.

7.6 RECYCLING OF COMPOSITES

Because composites based on thermoplastic matrices can easily be re-melted, they provide better recycling options than the more often used thermoset-based composites. Since composites are made up of fibers and matrix, mechanical recycling is often difficult, because the separation of fibers from the matrix is very difficult and energy-intensive. Thermal recycling is also problematic, because high ash contents are produced after incineration. The most optimal composite would be a composite where the reinforcement and matrix are made up of the same polymer. Melt-spun isotactic polypropylene fibers in a polypropylene matrix is such a composite material, but cannot be used for large-scale structural applications yet. It is expected that thermoplastic-based composites are to pose the greatest potential for recycling, especially considering the developments in bio-degradable polymers. However these materials are so new, that structural applications have not yet been investigated. [B17, p335]

In the past five to ten years several attempts have been made to detailed research on recycling of carbon fiber reinforced polymer composites [P72] [A46]. However, since recycling of these mostly thermoset composites is still not easy, with most of the recycling attempts on CFRP there are difficulties to yield a high retention of mechanical properties [P42, p13] However there are quite a few possibilities for non-critical structural applications of recycled CFRP, it has to be said, though, that these applications still need to be thoroughly investigated. Most of the applications available are sheet molding- and bulk compounds that can successfully be molded into usable CFRP, possibly replacing all current chopped carbon fiber reinforcements. [A46, p2]

8. CODES AND GUIDELINES ON FRP

Fiber reinforced polymers are a building material that originates from other industries than the civil engineering, structural-engineering and bridge-engineering industry. These industries are mainly the aerospace industry, the aviation industry, the naval industry and the wind energy industry. This is also the reason why these industries have introduced codes and guidelines for the use of FRP composites far before the civil engineering industry. In fact, no official international codes do exist at the moment (2012) for FRP materials.

However, since the use of FRP slowly started to grow to significant dimensions in the civil engineering industry in the 1970s it became evident in the 1990s that plastic composite materials were becoming the next large composite building material alongside concrete and timber. Therefore several attempts were made in a number of countries to codify the knowledge on FRP composites. The outcome of three of these attempts will be briefly discussed in this section. It is important to know that neither of these guidelines have the status of an official code; use of these guidelines is not mandatory or obliged by European laws.

First, the European approach of the “European Structural Polymeric Composites Group” will be covered, the “Eurocomp Design Code and Handbook” from 1996. Secondly the Dutch approach from 1999, the “CUR96 Aanbeveling” by the “Civiltechnisch Centrum Uivoering Research en Regelgeving” will be shortly described. Finally, an industry approach from Denmark will be discussed: the “Fiberline Design Manual”, made by the structural FRP profile manufacturer “Fiberline” in 2003.

8.1 EUROCOMP DESIGN CODE AND HANDBOOK

The “Eurocomp Design Code and Handbook” (Eurocomp) is a practical design code for the construction industry, which enables designers to consider the use of a broad range of polymeric composites for structural applications. This code is the product of a three-year research program which started in 1991 in Scandinavia and the United Kingdom and was steered by the consulting engineering and architect firm “Sir William Halcrow and Partners”. [B14, pVII]

The Eurocomp is intended for the use by designers and engineers familiar with design using conventional construction materials such as steel and concrete. The document is based on the available scientific information but has no legal status, although its structure, setup and layout was adapted to the current Eurocodes. The scope of the Eurocomp is limited to glass reinforced polymer materials, components, connections and assemblies but excludes entity structures. The Eurocomp document is officially titled “Structural Design of Polymer Composites” and is divided into three parts: First the Eurocomp Design Code, for which the second part, the Eurocomp Handbook provides a large amount of further background information. Finally, the third part gives technical reports, describing some of the research carried out during the development of the Eurocomp 1996 Design code. [B14, pIX]

8.1.1 EUROCOMP DESIGN CODE

The Eurocomp Design code applies to the structural design of buildings and civil engineering in glass fiber reinforced polymeric composites. However the principles used are expected to be applicable to composites with other types of reinforcements too. It is only concerned with the requirements for resistance,

serviceability and durability of structures. Seismic design of GFRP structures is explicitly not covered. As stated before, the Eurocomp Design code is harmonious with the applicable Eurocodes, thus the actions described in Eurocode 1: Actions on structures can be applied in the Eurocomp Design code as well. [B14, p3]

The Eurocomp Design Code distinguishes between principles and application rules, principle are general statements and definitions for which no alternatives exist. Next to that, requirements and analytical models for which no alternative is permitted are also considered principles. Application rules are generally accepted and recognized rules which follow the principles and satisfy their requirements. [B14, p3-4] In the following a short overview on the topics in the Eurocomp Design code will be given: [B14, p1-240]

- **Chapter 2: Basis of Design:** Fundamental requirements, failure warnings, limit states, actions, material properties, design values for actions.
- **Chapter 3: Materials:** Fibers, resins, cores, foam, honeycombs, gel coats, additives.
- **Chapter 4: Section and member design:** Serviceability and ultimate limit state, members in tension, members in compression, members in flexure, members in shear, stability, combination members, plates, laminate design, laminate stiffness, laminate strength, creep, rupture, fatigue, design for impact, design for explosion, fire design, chemical attack.
- **Chapter 5: Connection design:** joint geometry, mechanical joints, bonded joints, laminated joints, tee joints, molded joints, bonded insert joints, cast in joints, combined joints.
- **Chapter 6: Construction and Workmanship:** manufacture and fabrication, delivery and erection, connections, repair, maintenance, health and safety.
- **Chapter 7: Testing:** compliance testing, testing for design and verification.
- **Chapter 8: Quality control**

According to the number of sub-topics in the design code it becomes clear that the focus of the code is on section and member design of GFRP-elements and -assemblies. In chapter 7 of the design code an interesting remark is made: "Testing shall be carried out where there is insufficient knowledge of the properties of the material." [B14, p225] This means that for all designs with other than glass reinforcements the Eurocomp Design code advises to do testing prior to large-scale application.

8.1.2 EUROCOMP HANDBOOK

The Eurocomp Handbook provides additional information to supplement the Eurocomp Design code. The purpose of the handbook is to make it easier for the user/designer to understand the decisions that have been taken during the development of the Eurocomp documents. It was especially added to the document to cover areas in which there is insufficient data to formulate precise design clauses; in these fields it gives guidance to the user. [B14, p243] The Eurocomp Handbook should be read parallel to the design code, it was not meant as a solitary textbook. Furthermore it only gives additional information where the authors found it necessary. Also, the handbook gives some more information on other reinforcements than glass and provides the reader with some useful backgrounds on reinforcements such as carbon and aramid. [B14, p243-244]

8.1.3 EUROCOMP TEST REPORTS

This section of the Eurocomp document is a mere collection of reports on 5 major tests that were carried out during the Eurocomp research. The particular tests include tests on GFRP panels for traffic bridges, tests on several types of bonded joints, tests on tubular GFRP members in trusses, tests on nominally pinned connections for pultruded frames and testing of a pultruded GFRP pinned base rectangular portal frame. [B14, p547-639]

8.2 CUR96 AND CUR2003-6

The “CUR96 Aanbeveling” (recommendation), in short CUR96, issued by the “Civieltechnisch Centrum Uitvoering Research and Regelgeving (Civil Engineering Centre for the Implementation of Research and Regulation) and is the first Dutch document that tries to give rules on the application of fiber reinforced polymers in the civil engineering industry. Similar to the Eurocomp documents it is divided in two parts, the actual code (CUR96 recommendation) and a CUR 2003-6 Achtergrondrapport (background report). Both documents were produced by a committee which was made up of representatives from the government, the scientific world (e.g. universities) and the industry. [CUR2003-6, p3-4] The CUR documents are not obliged by law, as is the case with the common Eurocodes. However, in the Netherlands for some FRP specific applications, the Dutch infrastructure authority “Rijkswaterstaat” advises to use these documents.

8.2.1 CUR96 RECOMMENDATION

The CUR96 recommendation is only intended for using during the design of GFRP composites structures. Unlike the Eurocomp Design code, the CUR96 does explicitly not cover the design of connections. Furthermore it is focused on material properties, the calculation of strength and stiffness values and the application of appropriate safety factors while designing with GFRP. In the document the future wish of the CUR is expressed, that the recommendation should be extended to more reinforcement materials in the future. Since it is the only Dutch document available it is often used for civil engineering FRP designs, although it has no official code status. [CUR96, p1]

After giving some information on the area of application of this recommendation, which is only suitable for GFRP elements with a minimum reinforcement percentage of 20%, the CUR96 recommendation covers the following important topics: [CUR96, p1-38]

- **Chapter 5: Demands of and for FRP structures:** program of demands, durability
- **Chapter 6: Calculation methods and material properties:** Loads, material factors, safety factors, conversion factors, characteristic material properties,
- **Chapter 7: Materials:** Composition, laminates, resin types, reinforcement types
- Chapter 8: Construction and manufacturing: production methods
- **Chapter 9: Calculations:** Stiffness calculations, line elements, plate elements, stability, beams, strength, fatigue
- **Chapter 10: Inspection and control**

It has to be stated here that the CUR96 recommendation is a much more compact document than the Eurocomp Design guideline, it covers less information on phenomena like creep, impact damage, and foremost no information on connection design.

8.2.2 CUR2003-6 BACKGROUND REPORT

The CUR2003-6 Background report has the same set-up as the Eurocomp Handbook. It acts as a valuable supply of detailed background information for the user of the CUR96 Recommendation. It especially focuses on very informative sections on materials, material properties, and the derivation of the conversion- and material-factors that are used in the recommendations. Next to that it gives a lot of information on the exact procedure to calculate structures under fatigue load. The information on fatigue design was already used in [chapter 2.6.9] on the design of a fiber reinforced polymer structure under fatigue load. [C2003-6, p3-7]

8.3 FIBERLINE DESIGN MANUAL

The Fiberline Design Manual is the most well-known document made by a manufacturer. "It is a tool for architects, engineers and technicians to facilitate the design and construction of well-functioning structures using composite profiles." [B25, p1] It is mentioned in the manual that it is based on the earlier discussed Eurocomp Design Code and Handbook as well as on an earlier Danish code, the [DS456], "Danish Code of Practice for Use of Glass Fiber Reinforced Unsaturated Polyester". [B25, p1]

The Fiberline Design Manual is focused mostly on the design specifications of the available Fiberline profiles. All Fiberline profiles are made using pultrusion and are available in many different shapes and diameters. Because it was produced strictly for Fiberline products, it features only three Fiberline-made matrix materials: P2600 Isophthalic polyester, P3510 Vinyl ester (high temperature resistance) and P4506 Isophthalic polyester (fire retardant). The manual focuses on highly reinforced profiles with an average fiber content of 60% E-glass fiber reinforcement. Because it was made specifically for and by a single manufacturer it can only be used as a guideline on the structural design of composite structures built up of Fiberline structural profiles. [B25, p0.0.6, p0.0.10, p0.0.11]

The first part of Fiberline Design Manual covers the following topics on construction calculations: [B25, 1.1.03-p1.6.117]

- **Chapter 2: Coefficients:** values and definitions, static calculations, deformation limits, material properties, loads, profiles
- **Chapter 3: Profiles used as beams and columns:** tensile strength with examples, compressive strength with examples, flexural strength with examples
- **Chapter 4: Bolted joints:** Calculation of bolted joints, transverse and longitudinal capacity of bolts, tensile capacity of bolts, several example calculations
- **Chapter 5: Glued joints**
- **Chapter 6: Profile tables:** L-profiles, IL-profiles, U-profiles, UL-profiles, Square tube, Pipe profile, T-profile, L-profile, handrails

Especially chapter 6 gives some very informative tabulated data on a large selection of high quality FRP profiles, in this respect the Fiberline Design Manual is unique and gives similar information on FRP profiles as available for steel profiles.

The second part of the Fiberline Design Manual focuses on the construction of planks, pultruded gratings, railings and stairs. [B25, p2.1.03-p2.3.14] Finally some information is given on the fire properties [B25, p4.1.03] on the chemical resistance [B25, p5.1.03] and the environmental and recycling aspects of Fiberline products [B25, p7.1.03] The extract from the manual below gives an idea of the type of information given by the Fiberline Design Manual. [B25, p1.6.81] This kind of tabulated data can be very useful when making (preliminary) designs of FRP structures.

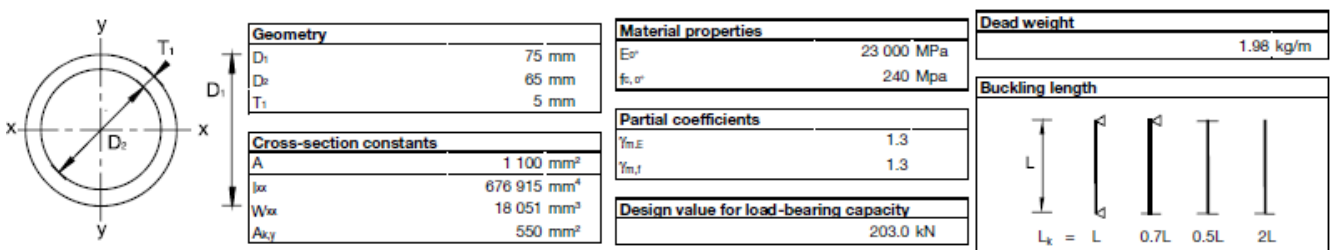


Fig. 157: Example of section properties given in the Fiberline Design Manual [B25, p1.6.81]

9. COSTS OF FIBER REINFORCED POLYMER COMPOSITES

Generally, for bridge design costs can be considered in terms of short-term costs, such as design, construction and installation, and long-term costs such as maintenance, modification, deconstruction and disposal. These groups can be further divided into direct costs, such as raw materials and production, and indirect costs, such as traffic interruption, depreciation, resale value and impact on the environment. [P36, p4]

Fiber reinforced polymer are currently still expensive when compared to conventional construction materials based on initial cost. The most important factor for this high price is the high cost of the base raw materials, usually comprising 40% to 90% of the finished product price. [B16, p1012] Also, often imported products are used; mass production is not yet common for most engineering FRPs and high prices are generally accepted in the aerospace, aviation and marine industries, where most engineering plastics originate from. [P36, p4]

The prices of FRP composites have significantly dropped in the last 20 years. For example, typical FRP stock bridge deck system have become almost 50% cheaper in since 1990, some of them now even approaching the prices of traditional concrete bridge decks. [P16, p18-19] Next to that the developments of the last 10 years led to a totally new approach on cost-estimation of infrastructural projects: the Whole of Life (WOL) approach. Similar to lifecycle costing it includes initial cost, maintenance, operating cost, replacement and refurbishment costs, retirement and disposal costs, and other costs such as taxes, depreciation and management costs. Considering the earlier discussed FRP advantages in durability and sustainability, such an approach shows even more the cost-effectiveness that FRP structures could have. [P36, p5]

In the following the (short-term) costs of two FRP bridges will be considered, as well as the costs of several polymer matrices and the most common fiber reinforcements. Also, different ways of reinforcing will be qualitatively compared. Finally some available FRP bridge deck systems will be discussed cost-wise as well as some stock FRP profiles and sheets.

9.1 FRP BRIDGE COSTING EXAMPLES

In this chapter two examples on cost estimation of fiber reinforced polymer bridges will be given. Considering the scarcity of real-world traffic bridge examples, two pedestrian and cyclist bridges will be described. First a cost-comparison of the “Fiberline pedestrian bridge” in different building materials will be given, the bridge was finally built in all-FRP. Secondly a design study of a FRP alternative to the “London Millennium pedestrian bridge” will be considered.

9.1.1 COST COMPARISON FOR DIFFERENT MATERIAL VARIANTS OF THE FIBERLINE BRIDGE, KOLDING, DK

The “Fiberline pedestrian bridge” in Kolding, Denmark was constructed in 1997. Upon completion the manufacturer/designer of this cable stayed bridge, ‘Fiberline’, published a cost-comparison in which the total costs for the construction of the bridge in glass fiber reinforced polymer were compared to the hypothetical costs of building a bridge with the same specification in steel or concrete. The objective was to demonstrate that FRP bridges can very well be cost-competitive compared to traditional building materials. [A37, p1]

The glass fiber reinforced polyester “Fiberline bridge” in Kolding is used by pedestrians and cyclists and has a total span of 40m. The bridge is cable stayed and the two spans of 27m and 13m are carried by 8 FRP cable stays in total. The deck width is 3,2m over the whole length, and the thickness of the deck varies from 1,2m to 1,5m. The maximum deflection is about L/200, leading to a deflection of 130mm at mid-pint of the long span. The load bearing capacity of the bridge is 5kN/m², and the bridge weighs 12 tons only, making the foundation, assembly and transport simpler and cheaper. The weight of the bridge is only about 50% of a comparable steel bridge. The expected lifetime of the bridge is 50+ years without major maintenance. [A37, p1-2]

Below a table is given in which the actual short-term costs of the built bridge are compared to two design alternatives: One design alternative in typical structural steel and one in reinforced concrete. It can be seen that the GFRP Bridge built is only about 7% more expensive than the traditional material. It has to be said though, that this bridge was made using standard Fiberline stock profiles only, which had a positive influence on the pricing. The long-term costs such as maintenance and impact on the environment have not been considered in this table. It is expected when the long-term costs are also taken into consideration, GFRP will even be more cost-competitive. The table price unit has been converted to € from US-\$ according to the mid-1997 conversion rate. [A37, p2]

Costs in EUR	GFRP	Steel	Concrete
Engineering	52.620	26.310	19.294
Foundation	52.620	65.775	78.930
Materials	105.240	17.540	78.930
Fabrication	52.620	78.930	-
Installation	26.310	52.620	78.930
Surface treatment	8.770	26.310	13.155
Others	26.310	35.080	35.080
Total	324.490	302.565	302.565

Table 43: Comparison of the total costs of GFRP, steel and concrete alternatives for the Fiberline pedestrian bridge in Kolding, Denmark [A37, p2]

9.1.2 DESIGN STUDY OF FRP ALTERNATIVE TO THE MILLENNIUM BRIDGE, LONDON, UK

Being already famous in the bridge engineering world, the “London Millennium bridge” was initially opened in 2000 but soon underwent some drastic redesigning measures that where needed because of excessive vibrations, induced by synchronized pedestrian motion. This design-flaw inspired ‘White Young Green Consulting Ltd.’ to investigate the feasibility of a carbon fiber alternative to the costly “Millennium Bridge”. The original “Millennium Bridge” initially cost € 29,12 million and the redesigning measure (installing added dampers) cost € 8,0 million. The total building sum therefore was substantial: € 37,12 million. [A33, p4-5]

In the feasibility study a carbon fiber alternative for the “Millennium Bridge” was derived, having only one span of 330m, compared to the original 3 spans of 81m, 144m and 108m. The original bridge was made of steel and considered light-weight with a total superstructure weight of 660 tons. The new carbon fiber bridge would have a total superstructure weight of 210 tons and therefore could be lifted into place from

temporary barges in one single piece. The CFRP Bridge would consist of a very flat arch made of a single, stiffened box girder with varying depth from 7m at the supports to 3m at the mid-span. The width of this half-circular cross section varies from 12,5m to 5,9m at mid-span. [A33, p4-5]

Costs in EUR	CFRP alternative	Original Millenium Bridge
Superstructure	13.625.500	n.a.
Abutments	3.206.000	n.a.
Installation and transportation	1.603.000	n.a.
Design and engineering	2.404.500	n.a.
Dampers	1.603.000	8.015.000
Total	22.442.000	37.189.600

Table 44: Cost-comparison of a CFRP alternative to the London Millennium pedestrian bridge. [A33, p5]

The table above shows the preliminary short-term cost estimation of 'White Young Green Consulting Ltd.', in which the costs for the CFRP Bridge are split in superstructure, abutments, installation and transportation, design and engineering and the dampers. The dampers are included because the preliminary eigenvalue analysis showed that the first Eigen frequency was not sufficiently high enough. All original prices have been converted from GB-£ to € according to the mid-2000 conversion rate. [A33, p5]

9.2 COST OF POLYMER MATRICES

The reason for the high prices of some polymer lies in the expensive base raw materials and the research that polymer manufactures have put into the development of more and more optimized resin systems. The real advantage of FRPs is producing at low weight and low processing costs. [B16, p1012]The table below shows the average bulk price of different thermoplastic- and thermoset polymers that are often used in the commodity- and the engineering-plastic industry. Note that the same source also gives some information on the prices that different industries are willing to pay: That is about 4,7 €/kg for the civil engineering industry, 11,5 €/kg for the marine industry and 35 €/kg for the aerospace industry. All prices have been converted from US \$ to € using the mid-2001 conversion rate. [B07, p17]

Polymer	Name	Bulk Price Euro/kg
PE	Polyethylene	1,11
PP	Polypropylene	0,85
PS	Polystyrene	1,34
ABS	Acrylonitrile butadiene styrene	2,05
BPA Epoxy	Bisphenol A Epoxy	3,39
PU	Polyurethane	4,91
Nylon 6	Polycaprolactam	3,39
PAR	Polyarylate	4,68
PBT	Polybutylene terephthalate	2,69
PMMA	Polymethylmethacrylate	2,34
PPO	Polyphenylene Oxide	4,09
Lexan, Makrolar etc.	Polycarbonate	3,33
-	Nylon 66	4,62
-	Polysulfone	11,11
PET	Polyethylene terephthalate	2,51
PVDF	Polyvinylidene fluoride	21,04
SMA	Styrene Maleic Anhydride	3,57
PC/ABS	Polycarbonate ABS blend	4,62
POM	Polyoxymethylene	2,51
PPS	Polyphenylene Sulfide	75,99
LCP	Liquid Crystal polyester	25,72
PEEK	Polyether ketone	81,83
PPSF or PPSU	Polyphenylsulfone	28,06
-	Phenolic	2,05
Rigid PVC	Rigid Polyvinyl chloride	1,02
PEK	Polyehterketone	81,83
PEI	Polyether imide	14,03
PES	Polyester	17,54
PBI	Polybenzimidazole	1636,60
PBO	Polyphenylene bezobisoxazole	257,18
PTFE	Polytetrafluorethylene	56,11
PAI	Polyamide imide	2045,75
PI	Polyimide	1870,40

Table 45: Cost comparison of the bulk price of different polymers; Prices from 2001 [B07, p17]

9.3 COST OF REINFORCEMENT FIBERS

Just as with the polymer matrices, there are also some large differences in price for the different reinforcement types. Fibers like boron which are only used in very small quantities are at a very high price level, which does not yield opportunities for feasible application in civil engineering infrastructure. However, the most common fiber reinforcement, glass fiber has a price level which is very competitive for the use in civil engineering works, such as bridges. For comparison, normal carbon construction steel normally costs about 0,6€/kg to 0,7€/kg. However this number cannot be compared to reinforcement bulk prices because, the composite consists not only of reinforcement, and usually less composite material is needed in weight, compared to steel. [B26, p2.6]

In the following table the prices of common reinforcement per kg are given. It is expected that the prices will further drop, due to recent expansion of FRP materials into new uses and the development of new low-cost production methods. Note that at the time of introduction in the late 1960s carbon fibers had a price in excess of 600€/kg. Since then the prices have been continuously dropping. [WEB: www.netcomposites.com] The prices have been converted from US \$ and GB£ to € using the mid-2000 conversion rate.

Fiber type	Cost [Euro/kg]
Carbon	10-45
E-Glass	1,25-2,5
R-Glass or S-Glass	15-25
Aramid	18-30
Boron	70-500

Table 46: Cost comparison of different reinforcement types [WEB: www.netcomposites.com][B26, p2.6]

Another important factor on the cost of reinforcement is the type of the reinforcement used. For that matter the table below gives a qualitative cost-comparison of different glass reinforcement types. Note that the number 1 denotes the lowest price, in this case most chopped strands. The number 10 denotes the highest price, in this case approached by cloth fabrics and surfacing mats. The price levels are based on the raw bulk prices. [B16, p899]

Reinforcement type	Types	Cost factor
Continuous strand	Continuous yarn, spun roving	1-2,5
Cloth fabrics	Various styles of weave	3,5-6,5
Woven roving fabric	Various styles of weave	2-3,5
Chopped strands	Various lengths from 0,5cm to over 10cm	1-1,5
Reinforcing mats	Chopped strands or continuous strands	1,5-2,5
Surfacing mats	Overlay or monofilament surfacing veils	5,0-6

Table 47: Cost comparison of different reinforcement types for glass fibers, 1=lowest cost and 10=highest cost [B16, p898]

9.4 COSTS OF FRP CONSTRUCTION ELEMENTS

In this chapter the costs of several typical FRP construction elements and composites will be given. Most of the prices given are for GFRP elements, since most available products are still made of this material. First the prices of several different, mostly US-American made, FRP bridge deck systems will be given. Secondly a number of prices of pultruded beams and woven sheeting will be given. Finally two estimates on the price of fully assembled composites will be mentioned.

9.4.1 COST OF DIFFERENT BRIDGE DECK SYSTEMS

Composites have a higher initial cost compared to a conventional concrete deck. The unit cost of FRP materials is often higher than that of conventional materials. Advances in FRP design have brought this cost noticeably down. Installed costs for FRP bridge decks are now slowly approaching the same values as concrete decks. Recently, some component designs have even claimed to be similar in cost to conventional concrete decks. Additionally, added expenses of FRP can be partially offset by other savings such as reduced maintenance and protection of traffic. [P16, p18]

The following table compares the prices of several bridge deck types, available in the USA. Next to the cost, also the depth, the weight and the normalized deflection is given. The prices for these bridge decks can be used for a conservative estimation of the costs for a FRP bridge deck that is to be designed. The prices in the table have been converted from US\$ to € using the mid-2002 conversion rate. [P07, p5]

Bridge Deck Type	Costs [Euro]	Depth [mm]	Weight [kg/m ²]	Normalized Deflection
Hardcore Comp. (Sandwich)	570-1.184	152-710	98-112	L/1.120
KSCI (Sandwich)	700	127-610	76	L/1.300
DuraSpan (Adh. Bond. Pultr.)	700-807	194	90	L/340
Superdeck (Adh. Bond. Pultr.)	807	203	107	L/530
EZSpan (Adh. Bond. Pultr.)	861-1.076	229	98	L/950
Strongwell (Adh. Bond. Pultr.)	700	120-203	112	L/325

Table 48: Comparison of different bridge deck systems in cost, weight, depth and deflection [P07, p5]

9.4.2 COST OF SELECTED FRP PROFILES

The last chapter of the cost-section of this report will give some information on the prices of several glass fiber sheets, GFRP profiles and carbon fiber sheets. The table below gives prices per m² for sheet materials and prices per m for longitudinal members, such as I-profiles. Note for example that the price of a typical, pultruded GFRP I-profile of 550x200x15mm lies at about 500€/m.[P81, p2981]

Element and property	Unit	Cost in Euro
Carbon sheet, 200g/m ²	per m ²	40,00
Carbon sheet, 300g/m ²	per m ²	50,00
Carbon sheet, 400g/m ²	per m ²	58,00
Glass sheet, 90/10 AR	per m ²	25,00
GFRP I-profile, 550x200x15	per m	500,00
GFRP I-profile, 500x200x10	per m	390,00
GFRP I-profile, 450x200x8	per m	310,00

Table 49: Costs of selected CFRP sheets, GFRP sheets and GFRP I-profiles [P81, p2981]

9.4.3 COST ESTIMATES ON FULLY ASSEMBLED COMPOSITES

To conclude this section some estimates found in literature on the costs of assembled FRP materials are given. The first cost estimation is from the "Massachusetts Institute of Technology", 2005: The cost for GFRP composite (pultruded E-glass with vinyl ester matrix) is 7,82 €/kg. (Price converted from US\$ to € using the mid-2005 conversion rate)[T05, p50]

The second estimate comes from the "Swiss Federal Laboratories for Materials Science and Technology" (EMPA), this institution gives the estimate costs for preliminary design of 2-10€/kg for structural composite materials. The price level is of 2009. [P32, p4]

BIBLIOGRAPHY

Note that this list contains all source documents (books, papers, theses, articles and codes) that are explicitly used in this literature study. Next to that, a bigger number of source documents was implicitly used for this literature study. These are not mentioned in this bibliography list, hence the missing documents in this list. For a complete bibliography list please refer to the literature list in the accompanying database on DVD.

Books

- B01** A.H.J. Nijhof (2004); Vezelversterkte Kunststoffen – Mechanica en Ontwerp; Delft University Press
- B07** A.P. Mouritz, A.G. Gibson (2006); Fire Properties of Polymer Composite Materials; Springer
- B11** Industrievereinigung Verstärkte Kunststoffe (Hrsg.) (2009); Handbuch Faserverbundkunststoffe; Vieweg+Teubner
- B12** M.Neitzel, P.Mitschang (2004); Handbuch Verbundwerkstoffe; Carl Hanser
- B14** J.L. Clarke (et al.) (1996); Structural Design of Polymer Composites - Eurocomp Design Code and Handbook; E&FN Spon
- B15** T. Keller (2003); Use of FRP in bridge construction; IABSE
- B16** D.V. Rosato (2004); Reinforced Plastics Handbook; Elsevier
- B17** B. Harris (2003); Fatigue in Composites: Science and Technology of the Fatigue Response of Fibre-Reinforced Plastics; Woodhead Publishing
- B19** L. Tong, A.P. Mouritz, M.K. Bannister (2002); 3D FRP composites; Elsevier
- B21** G.Parke, N.Hewson (2008); ICE Manual of Bridge Engineering; Thomas Telford
- B22** M.H. Kolstein (2008); FRP Structures; Reader; TU Delft
- B23** D.V. Rosato, (2003); Plastics Engineered Product Design, Elsevier
- B25** H.Thorning (et al.) (2003); Fiberline Design Manual; Fiberline A/S
- B26** Department of Defense (2002); Composite Materials Handbook; US Department of Defense Book

Papers

- P07** C.E. Bakis (et al.) (2002); FRP composites for construction – State of the art review; Paper ASCE
- P08** ACI Committee 440 (2002); State of the art report on FRP reinforcement for concrete structures; Paper ACI440R-96
- P10** V.M. Karbhari (et al.) (2003); Durability Gap Analysis for FRP composites in Civil Infrastructure; Paper NIST
- P11** A. Mirmiran, L.C. Bank (et al.) (2003); World Survey of Civil Engineering Programs on FRP Composites for Construction, Paper ASCE
- P12** P. Feng, L. Ye, L. Zhang, W. Li (2004); Experimental Study on Outside Filament Winding Reinforced FRP Bridge Decks; Presentation 4th ICACMBS
- P15** E. Douglas (2005); Background on FRP for Civil Infrastructure; Paper University of Florida
- P16** T.A. Hoffard, L.J. Malvar (2005); FRP Composites in Bridges: A State of the Art Report; Paper NAVFAC
- P18** K. Park (et al.) (2005); Parametric FEA of a GFRP deck-to-girder connection for bridges; Paper KICT
- P19** L.D. Suits, M.L. Ralls (2006); 50 years of interstate structures – Past, Present and Future; Paper TRBoNA E-C104
- P21** W. Alnahhal, A. Aref (2007); Structural Performance of hybrid FRP concrete bridge superstructure systems; Paper Composite Structures 84
- P22** J.M. Skinner (2009); A Critical Analysis of the Aberfeldy Footbridge, Scotland; Proceedings of Bridge Engineering 2 Conference 2009
- P29** M. Hastak (2004); Constructability, Maintainability and Operability of FRP Bridge Deck Panels; Paper Purdue University
- P31** Y. Zhang (et al.) (2006); Vehicle-induced dynamic performance of FRP versus concrete slab; Paper Journal of Bridge Engineering, July/August 2006
- P32** A.Schumacher, A. Herwig (2009); Design of FRP-Profiles and All-FRP Structures; Lecture EMPA
- P36** M.F. Humpreys (2003); The use of polymer composites in construction; Paper Queensland University of Technology
- P39** I.Bennetts, K. Moinuddin (2009); Evaluation of the Impact of Potential Fire Scenarios on Structural Elements of a Cabel-stayed Bridge; Paper Journal of Fire Protection Engineering, Vol. 19, May 2009

- P42** G. Rupprich (2005); Neubau einer Geh- und Radwegbruecke aus GFK; Paper Strassenbauverwaltung Mecklenburg-Vorpommern
- P44** M. Karus (et al.) (2006); Naturfaserverstaerkte Kunststoffe; Paper Fachagentur Nachwachsende Rohstoffe
- P45** E. Bittmann (2006); Das Schwarze Gold des Leichtbaus; Paper Carl Hanser Verlag
- P48** T. Keller (2007); Material-tailored use of FRP in bridge and building construction; Paper Swiss Federal Institute of Technology Lausanne, EPFL
- P49** S. Taj (et al.) (2007); Natural FRP composites; Paper University of Punjab, Lahore, Pakistan
- P58** Y. Chao (2008); Pultruded FRP Composite Profiles for Construction, Paper McGill University, Canada
- P59** T. Keller (2004); FRP Bridge Decks - Status Report and Future Prospects; Paper Swiss Federal Institute of Technology
- P61** J.S. O'Connor, J.M. Hooks (2003); USA's experience using FRP Composite Bridge Decks to extend service life; Paper Federal Highway Administration USA
- P62** R.E. Rodriguez-Ver (et al.) (2011); Fiber Reinforced Polymer Bridge Decks; Paper Purdue University, Indiana
- P72** S. Pimenta, S.T. Pinho (2010); Recycling carbon fibre reinforced polymers for structural applications: Technology review and market outlook; Paper Elsevier Composites
- P77** Y. Bai, T. Keller (2008); Modal parameter identification for a GFRP pedestrian bridge; Paper Elsevier Composites
- P81** P.J.D Mendes (et al.) (2011); Development of a pedestrian bridge with GFRP profiles and fiber reinforced self-compacting concrete deck; Paper Elsevier Composites
- P84** F. Laoutid (et al.) (2008); New prospects in flame retardant polymer materials: From fundamentals to nanocomposites; Paper Elsevier MSaER
- P85** J.A. Sobrino, M.D.G. Pulido (2002); A new glass-fiber reinforced-plastic footbridge; Paper Footbridge 2002
- P86** H. Kolstein (2009); FRP Joints; CT5128 course presentation
- P88** Owens & Corning (2011); Winning with Composites in a World Seeking Sustainable Solutions; Presentation Owens & Corning
- P89** E. Fekka (et al.) (2008); LCA Comparison of Two Aquarium Tank Systems: FRP and Concrete; Paper Kreyssler & Associates
- P90** P.P. Greigger (et al.) (2002); Fire protection of steel bridges; Presentation PPG & Hughes Associates Fire Science
- P91** E. D. Sotelino, M.H. Teng (2002); Strengthening of Deteriorating Decks of Highway Bridges in Indiana Using FRPC; Paper Purdue Unitversiy Indianan
- P92** E. Matta (et al.) (2008); Unbonded CFRP Bar System for External Post-Tensioning; Paper University of Miami
- P93** M.E. Rackliffe, D.W. Jensen (2005); Local and global buckling of ultra-lightweight IsoTruss structures; Paper Brigham Young University, USA
- P97** T. Kashiwagi (2007); Flame Retardant mechanism of the Nanotubes-based Nanocomposites; Paper US NIST

Theses

- T02** A. Carolin (2003); Carbon Fibre Reinforced Polymers for Strengthening of Structural Elements; Doctoral thesis Lulea University of Technology
- T03** H. Nordin (2003); FRP in Civil Engineering, Flexural Strengthening of concrete structures with prestressed near surface mounted CFRP rods; Licentiate thesis, Lulea University of Technology
- T05** C. Tuakta (2005); Use of FRP Composites in Bridge Structures; MSc thesis Massachusetts Institute of Technology
- T06** R.J.A. Kenter (2010); The elevated metro structure in concrete, UHPC and composite; MSc theis Delft University of Technology
- T07** P. B. Potyrala (2011); Use of FRP Composites in Bridge construction - state of the art in hybrid and all composite structures; MSc thesis Universitat Politecnica de Catalunya
- T09** T. van den Driessche (2006); Een tubulair vakwerk als voetgangersbrug; MSc thesis Universiteit van Gent
- T12** K. Vasileios (2009); Strengthening of Steel Bridge by GFRP Plates; MSc thesis TU Delft
- T13** P.K. Majumdar (2008); Strength and Life Prediction of FRP Composite Bridge Deck; Doctoral thesis VirginiaTech

Articles

- A02** P.Bowtell (2003); Webb Bridge, Melbourne; Article Topos Magazine
- A03** Maunsell Structural Plastics (2006); Assessment of the Aberfeldy footbridge; Article
- A06** D. Kendall (2007); Building the future with FRP composites Article ReinforcedPlastics (May 2007)
- A08** J. Knippers (2007); Faserverbundwerkstoffe in Architektur und Bauwesen, Article University of Stuttgart
- A18** Infracore (2011); Infracore Havenbrug; Article FiberCore
- A23** G.Brux (2000); Neuartiger Brandschutz im Stahlbrueckenbau; Artikel Eisenbahningenieur 51, 6/2000

- A25** G. Faller (2008); Fire engineering on the Bridge Pavilion in Zaragoza; Article Sapienza Universita di Roma
- A27** P.Scott (2009); Walking on Waves; Article Ingenia Issue 38, March 2009
- A28** Bentley Systems (2009); Marina Bayfront Pedestrian Bridge; Article
- A30** A. Krijgsman (1999); Een brug te ver – Ontwerp Papendorpse Brug Utrecht – Article Bouwen met Staal 147, maart/april 1999
- A33** D. Kendall (2006); Fiber reinforced polymer composite bridges; Article White Young Green Consulting Ltd., National Composites Network
- A37** Fiberline (2007); The Fiberline Bridge in Kolding; Webarticle
- A38** Martin Marietta Composites (2005); Duraspan and FRP Bridge Solutions and Testing; Product Sheet
- A39** The City of Calgary (2009); Peace Bridge, Calgary's newest bridge across the Bow; Information Brochure
- A40** IDEAS2 Awards (2009); Merit Award T. Evans Wyckoff Memorial Bridge, Seattle; Article IDEAS2 Awards
- A41** Steel Bridge News (2008); Taking Flight, T. Evans Wyckoff Memorial Bridge, Seattle; Article Steel Bridge News
- A42** G.Faller, ARUP (2008); Fire Engineering on Puente Pabellon, EXPO Zaragoza 2008, Presentation Sapienza, Universita di Roma
- A45** Provincie Friesland (2010); Oosterwolde verkeersbrug; Informatiefolder Provincie
- A46** N. Warrior (2011); Recycling Carbon Fiber; Article DTI
- A47** F. O'Brien-Bernini (2011); Composites and sustainability - when green becomes golden; Article Owens & Corning
- A48** Topglass (2011); I Love Composites & Standard profiles; Topglass company brochure

CODES

Fiber reinforced polymers

CUR96	CUR Aanbeveling 96: VVK in Civiele Draagconstructies, 2003
CUR 2003-6	CUR Achtergrondrapport 2003-6; Achtergrondrapport bij CUR Aanbeveling 96
CUR 96+ Draft 2012	Revised CUR Recommendation 96: Update 2012, Draft
B14	J.L. Clarke (et al.) (1996); Structural Design of Polymer Composites - Eurocomp Design Code and Handbook; E&FN Spon
B25	H.Thorning (et al.) (2003); Fiberline Design Manual; Fiberline A/S

Fire safety

NEN-EN 13501-2:2007+A1:2009	Fire Classification of construction products and building elements – Part 2: Classification using data from fire resistance tests, excluding ventilation services
NEN-EN 1991-1-2:2003	Eurocode 1: Actions on structures – Part 1-2: General actions – Actions on structures exposed to fire
NEN-EN 1991-1-2:2003/NB:2007	Dutch National Annex to Eurocode 1: Actions on structures – Part 1-2: General actions – Actions on structures exposed to fire
NEN 4001+C1:2008	Fire protection - Planning of portable and mobile fire extinguishers
NEN-Praktijkgids Brandveiligheid	NEN-Praktijkgids Brandveiligheid; Bouwbesluit, 2006 (in English: Practice Guide Fire Safety in buildings issued by the Dutch normative authority NEN)
NFPA502	US-American National Fire Safety Protection Association; Standard for Road Tunnels, Bridges and Other Limited- Access Highways, 2008
NEN-ISO 23932:2009	Fire Safety Engineering: General Principles
NEN-EN1993-1-2:2005	Eurocode 3 – Design of steel structures – Part 1-2 – General Rules – Structural fire design
NEN-EN1993-1-2:2005/NB:2006	Dutch National Annex to Eurocode 3 – Design of steel structures – Part 1-2 – General Rules – Structural fire design
NEN-EN1994-1-2:2005	Eurocode 4 – Design of composite steel and concrete structures – Part 1-2 – General Rules – Structural fire design
NEN-EN1994-1-2:2005/NB:2007	Dutch National Annex to Eurocode 4 – Design of composite steel and concrete structures – Part 1-2 – General Rules – Structural fire design

Bridge deck layout & road/highway layout

RWS-RONA1986	Richtlijn voor het ontwerpen van niet-autosnelwegen, 1986 (in English: Regulations for the design of non-highways)
RWS-ROA1989	Richtlijn voor het ontwerpen van autosnelwegen, 1989 (in English: Regulations for the design of highways)
RWS-SATO2005	Rijkswaterstaat, Specifieke Aspecten Tunnel Ontwerp, 2005 (in English: specific aspects of tunnel design)
RWS-NOA2007	Nieuwe Ontwerprichtlijn Autosnelwegen, 2007 (in English: New Design Guide for Highways)
NEN-EN1317-2:2010	Road restraint systems – Part 2 – Performance classes, impact test acceptance criteria and test methods for safety barriers

Loads & Deformations/Deflections

NEN-EN 1990: 2002	Eurocode 0: Basis of structural design
NEN-EN 1990:2002/A2	Eurocode 0 - Basis of Structural Design – Annex 2 Application for bridges
NEN-EN 1990+A1+A1/C2:2011	Eurocode 0 - Basis of Structural Design – Correction C1:2004, Annex

	A1:2005, Correction C2: 2010
NEN-EN 1991-1-3:2003	Eurocode 1: Actions on structures – Part1-3: General actions – Snow loads
NEN-EN 1991-1-3:2003/ NB:2007	Dutch National Annex to Eurocode 1: Actions on structures – Part1-3: General actions – Snow loads
NEN-EN 1991-1-4:2005	Eurocode 1: Actions on structures – Part1-4: General actions – Wind actions
NEN-EN 1991-1-4:2005/NB:2007	Dutch National Annex to Eurocode 1: Actions on structures– Part1-4: General actions – Wind actions
NEN-EN 1991-1-5:2011	Eurocode 1: Actions on structures – Part 1-5: General actions – Thermal actions
NEN-EN 1991-1-5:2011/NB:2011	Dutch National Annex to Eurocode 1: Actions on structures – Part 1-5: General actions – Thermal actions
NEN-EN 1991-1-7:2006	Eurocode 1 – Actions on structures – Part 1-7: General actions – Accidental actions
NEN-EN 1991-1-7:2006/NB:	Dutch National Annex to Eurocode 1 – Actions on structures – Part 1-7: General actions – Accidental actions
NEN-EN 1991-2:2003	Eurocode 1: Actions on structures – Part 2: Traffic loads on bridges
NEN-EN 1991-2:2003/NB:2009	Dutch National Annex to Eurocode 1: Actions on structures – Part 2: Traffic loads on bridges
NEN-EN 1991-2:2003	Eurocode 1: Actions on structures – Part 2: Traffic loads on bridges
NEN-EN 1991-2:2003/NB:2009	Dutch National Annex to Eurocode 1: Actions on structures – Part 2: Traffic loads on bridges
AASHTO-LFRD 1998	US-American Association of State Highway and Transportation Officials, AASHTO, LRFD Bridge Design Specifications, 1998
HIVOSS 2008	Human induced vibrations of steel bridges, design of footbridges, guideline, 2008
NEN-EN 1995-2:2005	Eurocode 5 – Design of timber structures – Part 2 - Bridges
NEN-EN 1995-2:2005/NB:2009	Dutch National to Eurocode 5 – Design of timber structures – Part 2 - Bridges

TABLE OF FIGURES

FIG. 1: SELECTION OF MODERN TRUSS BRIDGES: (CLOCKWISE FROM TOP LEFT): WEBB BRIDGE, MELBOURNE, AUSTRALIA; PEACE BRIDGE, CALGARY, CANADA; GREENSIDE PLACE LINK BRIDGE, EDINBURGH, SCOTLAND; LIGHT RAIL VIADUCT, THE HAGUE, THE NETHERLANDS	4
FIG. 2: FIBER REINFORCED POLYMER COMPOSITES MARKET VOLUME FROM 1970 TO 2010. [B12, P6]	10
FIG. 3: MARKET SHARES IN THE FIBER REINFORCED POLYMER COMPOSITE MARKET. (2002) [B12, P7]	11
FIG. 4: DIFFERENT PRODUCTION TECHNIQUES FOR FRP COMPOSITES AND THEIR MARKET SHARES (2002) [B12, P10]	12
FIG. 5: ONE OF THE FIRST KNOWN MAN-MADE COMPOSITE CONSTRUCTION MATERIALS: STRAW-CLAY COMPOSITE	13
FIG. 6: THE 1953 CHEVROLET CORVETTE WITH AN ALL GFRP BODY. [WEB, WWW.CHEVROLET.COM]	14
FIG. 7: THE 70M LONG VISBY SHIP OF THE SWEDISH NAVY. [B12, P4] AND THE AIRBUS A380 WITH EMPHASIS ON THE PARTS MADE OF FRP. [B12, P5]	14
FIG. 8: FIBERLINE FBD300 BRIDGE DECK PROFILE FOR HEAVY LOADS AND NUMEROUS EXAMPLES OF PULTRUDED FRP PROFILES USED IN THE BUILDING INDUSTRY [WEB, WWW.FIBERLINE.DK]	15
FIG. 9: THE ALL-FRP EYECATCHER BUILDING IN BASEL, SWITZERLAND, 1998	16
FIG. 10: NON-METALLIC FRP BUILDING FOR EMC-MEASUREMENTS, BUILT BY FIBERLINE [WEBSITE FIBERLINE] AND AN FRP-DOME ENCLOSSES A TRADITIONAL STEEL SILO. [WEB, WWW.FIBERLINE.DK]	16
FIG. 11: STRUCTURAL SYSTEM OF THE MIYUN BRIDGE IN CHINA, 1982.[B15, P75]	17
FIG. 12: DECK LAYOUT OF THE MIYUN BRIDGE IN CHINA, 1982.[B15, P75]	17
FIG. 13: THE STRUCTURAL SYSTEM OF THE SCOTTISH ABERFELDY FOOTBRIDGE (1992), THE FIRST ALL-FRP PEDESTRIAN BRIDGE [P22, P3]	18
FIG. 14: THE KANSAS STRUCTURAL COMPOSITES HONEYCOMB DECK SYSTEM [WEB: WWW.FHWA.DOT.GOV]	19
FIG. 15: PRINCIPLE OF SHEAR AND FLEXURAL STRENGTHENING USING FRP BONDED SHEETS. [P15, P4]	23
FIG. 16: HIGH PERFORMANCE 3D BRAIDED CFRP ROCKET NOZZLE [B19, P6] AND THE INTERFACE BETWEEN SHORT GLASS FIBERS AND RESIN MATRIX UNDER THE ELECTRON MICROSCOPE [B11, P125]	24
FIG. 17: THE PRODUCTION PROCESS OF GLASS FIBERS AND THE FINAL PRODUCTS [B11, P124].....	27
FIG. 18: SPOOL OF E-GLASS FIBER DIRECT ROVINGS (LEFT) AND ASSEMBLED ROVINGS (RIGHT) [B11, P127].....	29
FIG. 19: TYPICAL GLASS FIBER CHOPPED STRAND MAT [B11, P129].....	30
FIG. 20: TYPICAL GLASS FIBER CONTINUOUS FILAMENT MAT [B11, P129]	30
FIG. 21: WOVEN GLASS FABRIC AS SUPPLIED BY THE MANUFACTURER. [B11, P130].....	31
FIG. 22: GLASS FIBER CUTTINGS [B11, P130]	31
FIG. 23: THE TWO CARBON FIBER PRODUCTION PROCESSES WITH TWO DIFFERENT PRECURSORS.[B11, P140]	32
FIG. 24: TENSILE STRENGTH AND TENSILE MODULUS OF DIFFERENT CARBON FIBER GRADES. [B11, P141]	33
FIG. 25: FEA-DESIGNED CARBON FIBER REINFORCED EPOXY CURVED BEAM [WEB, WWW.ELEMENT6COMPOSITES.COM].....	35
FIG. 26: PULTRUDED CF- REINFORCED SECTIONS [WEB, WWW.ELEMENT6COMPOSITES.COM]	35
FIG. 27: WOVEN CARBON FIBER FABRIC WITHOUT POLYMER MATRIX [WEB, WWW.ELEMENT6COMPOSITES.COM]	35
FIG. 28: RECTANGULAR ARAMID FIBER REINFORCEMENT FOR BRIDGE STAYING CABLES [WEB, WW.TEIJINARAMID.COM]	37
FIG. 29: ARAMID FIBER WOVEN CLOTH WITHOUT POLYMER MATRIX [WEB, WW.TEIJINARAMID.COM]	37
FIG. 30: ARAMID FIBER HONEYCOMB CLOTH USED FOR SANDWICH CONSTRUCTION. [WEB, WWW.FIBERMAXCOMPOSITES.COM].....	37
FIG. 31: COMPARISON OF ULTIMATE TENSILE STRENGTH OF VARIOUS MATERIALS [B16, P59]	42
FIG. 32: THE THREE POLYMER GROUPS, DEFINED BY THEIR CHEMICAL BUILD-UP [B03, P5]	44
FIG. 33: THE A-B-C CURING STAGES OF THERMOSET PLASTICS [WEB, WWW.SUBSTECH.COM]	45
FIG. 34: SEVERAL WEAVE TYPES FOR REINFORCEMENT OF PLASTIC COMPOSITES [B22, P3.6-3.7][B11, P226]	58
FIG. 35: RANDOMLY ORIENTATED CONTINUOUS FILAMENT FABRIC [WEB]	59
FIG. 36: BASIC PRODUCTION PROCESS OF PREPREGS. [B16, P220].....	59
FIG. 37: BASIC SHEET MOLDING COMPOUND PRODUCTION USING ROVINGS AND CHOPPED FIBERS [B16, P224].....	60
FIG. 38: BULK MOLDING COMPOUND PRODUCTION [B16, P241]	61
FIG. 39: HAND LAMINATION PRODUCTION PROCESS [WEB, WWW.OSHA.GOV]	62
FIG. 40: AUTOMATED TAPE LAMINATION PRODUCTION PROCESS [WEB, WWW.OSHA.GOV]	62
FIG. 41: SPRAY UP PRODUCTION PROCESS [B22, P4.4]	63
FIG. 42: FILAMENT WINDING PRODUCTION PROCESS [WEB, WWW.OSHA.GOV]	64
FIG. 43: CENTRIFUGAL CASTING PRODUCTION PROCESS [B22, P4.8]	64
FIG. 44: VACCUM BAG PRODUCTION PROCESS [B22, P4.10]	65
FIG. 45: PRESSURE BAG PRODUCTION PROCESS [B22, P4.11].....	65
FIG. 46: AUTOCLAVE PRODUCTION PROCESS [B22, P4.12]	66
FIG. 47: COLD PRESS PRODUCTION PROCESS [B22, P4.14]	66
FIG. 48: HOT PRESS PRODUCTION PROCESS [B22, P4.16-4.17].....	67
FIG. 49: RESIN INJECTED MOLDING PRODUCTION PROCESS [B22, P4.18].....	67

FIG. 50: INJECTION MOLDING PRODUCTION PROCESS [B22, P4.21]	68
FIG. 51: CONTINUOUS LAMINATION PRODUCTION PROCESS [B22, P4.23]	69
FIG. 52: PULTRUSION PRODUCTION PROCESS [B22, P4.25]	69
FIG. 53: CONTINUOUS FILAMENT WINDING PRODUCTION PROCESS [B11, P358]	70
FIG. 54: STRESS-STRAIN RELATIONSHIPS OF DIFFERENT FIBER REINFORCEMENT MATERIALS [B01, P22]	73
FIG. 55: PLATE ELEMENT WITH FORCES ACTING ON IT [B01, P168]	85
FIG. 56: BENDING STRESS AND STRAIN DIAGRAM FOR A LAMINATE OF FOUR IDENTICAL UNIDIRECTIONAL LAMELLAS [B01, P170]	87
FIG. 57: INFLUENCE OF THE COUPLING BEHAVIOR ON ASYMMETRIC LAMINATES [B01, P191]	91
FIG. 58: INFLUENCE OF THE FIBER DIRECTION ON THE STRENGTH AND STIFFNESS OF LAMINATES (1 OF 2) [B16, P645]	92
FIG. 59: INFLUENCE OF THE FIBER DIRECTION ON THE STRENGTH AND STIFFNESS OF LAMINATES (2 OF 2) [B16, P645]	92
FIG. 60: SCHEMATIZED FATIGUE PROCESS [B17, P4]	97
FIG. 61: LEFT: FATIGUE LIFE FOR INCREASING STRESS AMPLITUDE FOR DIFFERENT GFR COMPOSITES. [B17, P11]	98
FIG. 62: LEFT: STRESS-LOG LIFE CURVES FOR 65% CARBON-, GLASS- AND ARAMID-REINFORCED EPOXY COMPOSITES TESTED AT 45° TO THE MAIN FIBER DIRECTIONS [B17, P27] RIGHT: STRAIN-LOG LIFE CURVES FOR THE SAME CROSS-PLIED COMPOSITES. [B17, P16]	99
FIG. 63: SPLITTING AND KINKING DAMAGE IN KEVLAR-49 FIBERS AFTER FATIGUE CYCLING [B17, P29]	99
FIG. 64: BOLTED FRP CONNECTION FAILURE MODES [P86, P114]	102
FIG. 65: FIBERINE DIMENSION SCHEME FOR BOLTED FRP CONNECTIONS [B25, 1.4.4]	102
FIG. 66: EXAMPLES OF BONDED JOINTS FOR FRP ELEMENTS [B25, 1.5.3]	104
FIG. 67: FAILURE MODES OF DIFFERENT FRP BONDED JOINT TYPES [B14, P175]	104
FIG. 68: STRESS DISTRIBUTION FOR BONDED (LEFT) AND BOLTED (RIGHT) JOINTS UNDER THE SAME CIRCUMSTANCES [P86, P10]	105
FIG. 69: STRESS DISTRIBUTION IN A COMBINED BOLTED-BONDED FRP JOINT [B14, P506]	106
FIG. 70: GENERAL FLOW OF FORCES IN ARCH BRIDGES	107
FIG. 71: GENERAL FLOW OF FORCES IN SUSPENSION BRIDGES	108
FIG. 72: GENERAL FLOW OF FORCES IN CABLE STAYED BRIDGES	109
FIG. 73: GENERAL FLOW OF FORCES IN BEAM BRIDGES	110
FIG. 74: GENERAL FLOW OF FORCES IN TRUSS BRIDGES	110
FIG. 75: DIFFERENT FIBER REINFORCED POLYMER BRIDGE DECK TYPES [T07, P29]	114
FIG. 76: DIFFERENT METHODS TO CONNECT FIBER REINFORCED POLYMER DECK PANELS WITH EACH OTHER [P29, P53-55]	116
FIG. 77: DIFFERENT SOLUTIONS FOR DECK-TO-GIRDER CONNECTION THAT DELIVER COMPOSITE ACTION [P29, P56-59]	117
FIG. 78: FORCE COEFFICIENT FOR TRUSSES WITHOUT END EFFECTS AS A FUNCTION OF THE SOLIDITY FACTOR [NEN-EN 1991-1-4:2005, P71]	120
FIG. 79: END EFFECT FACTOR AS A FUNCTION OF THE SLENDERNESS λ AND THE SOLIDITY RATIO φ [NEN-EN 1991-1-4, FIGURE 7.36, P75]	121
FIG. 80: FATIGUE LOAD MODEL 3 GEOMETRY [EN1991-2:2003, P49, FIG.4.8]	127
FIG. 81: PLACEMENT OF ACCIDENTAL VEHICLE LOADS [EN1991-2:2003, P54]	133
FIG. 82: BRIDGE FIRE IN GERMANY [WEB, WWW.KFV-PINNEBERG.DE]	135
FIG. 83: GROWTH OF A COMPARTMENT FIRE WITH THE DIFFERENT FIRE PHASES [B07, P8]	136
FIG. 84: STANDARD FIRE CURVES [NEN-1991-1-2-2002, P23]	137
FIG. 85: GENERAL FLOWCHART ILLUSTRATING THE FIRE-SAFETY ENGINEERING PROCESS FOR DESIGN, IMPLEMENTATION AND MAINTENANCE [NEN-ISO23932:2009, P4]	139
FIG. 86: TENSILE YIELD STRESS VS. TEMPERATURES FOR PLASTIC, ENGINEERED PLASTICS AND STRUCTURAL STEEL [B23, P407]	143
FIG. 87: SCHEME DEPICTING THE COMPOSITE DECOMPOSITION DURING FIRE [B07, P21]	146
FIG. 88: DIFFERENT DAMAGE ZONES IN A FIRE-DAMAGED LAMINATE [B07, P48]	147
FIG. 89: CHAR YIELD INCREASES THE LIMITING OXYGEN INDEX VALUE [B07, P50]	147
FIG. 90: COMPARISON OF RETAINED MASS AT ELEVATED TEMPERATURE FOR EPOXY AND PHENOLIC COMPOSITES [B07, P38, 40]	150
FIG. 91: LEFT: TYPICAL HEAT RELEASE PROCESS FOR GLASS VINYL ESTER COMPOSITES UNDER CONSTANT HEAT FLUX OF 50 kW/m ² . RIGHT: COMPARISON OF HRR'S OF NORMAL AND HIGH FIRE PERFORMANCE COMPOSITES. [B07, P72-73]	152
FIG. 92: INFLUENCE OF THE LAMINATE THICKNESS ON THE TOTAL HEAT RELEASE [B07, P79]	153
FIG. 93: TIME-TO-IGNITION OF DIFFERENT THERMOSET (LEFT) AND THERMOPLASTIC (RIGHT) RESIN BASED COMPOSITES. [B07, P61,62]	154
FIG. 94: LEFT: COMPARISON OF IGNITION TIMES FOR DIFFERENT REINFORCEMENTS. RIGHT: INFLUENCE OF THICKNESS ON THE IGNITION TIME [B07, P66,67]	154
FIG. 95: LEFT: FLAME SPREAD DISTANCE FOR DIFFERENT POLYMERS OVER TIME. RIGHT: FLAME SPREAD INDEX CORRELATION WITH NORMALIZED PEAK HEAT RELEASE RATE FOR DIFFERENT POLYMERS [B07, P95]	155
FIG. 96: LEFT: LIMITING OXYGEN INDEX FOR DIFFERENT COMPOSITES. RIGHT: TEMPERATURE DEPENDENCE OF LOI FOR TWO COMPOSITES [B07, P92]	156
FIG. 97: LEFT: MAXIMUM SMOKE DENSITY FOR DIFFERENT THERMOPLASTIC/THERMOSET CARBON COMPOSITES. RIGHT: COMPARISON OF SEA's FOR PHENOLIC AND VINYL ESTER GLASS COMPOSITES [B07, P86,87]	157
FIG. 98: CORRELATION BETWEEN HEAT FLUX AND AVERAGE SMOKE DENSITY FOR DIFFERENT THERMOSET POLYMER COMPOSITES [B07, P88]	157
FIG. 99: CORRELATION BETWEEN HRR AND CO YIELD FOR DIFFERENT COMPOSITES [B07, P92]	158

FIG. 100: LEFT: BACK-FACE TEMPERATURE BUILD-UP IN CELLULOSIC FIRE CONDITIONS. RIGHT: COMPARISON OF TIME TO REACH A BACK-FACE TEMPERATURE OF 160°C CORRELATED TO THE MEMBER THICKNESS FOR DIFFERENT COMPOSITES. [B07, P96, 97]	159
FIG. 101: LEFT: YOUNG'S MODULUS OF UD- 60% REINFORCED GLASS POLYESTER PULTRUDED SECTION (INCLUDING ITS COMPONENTS) AND RANDOM SWIRL MAT CORRELATED TO THE TEMPERATURE. RIGHT: YOUNG'S MODULUS OF WOVEN GLASS VINYL ESTER LAMINATE AND ITS PARTS CORRELATED TO THE TEMPERATURE [B07, P183, 185]	160
FIG. 102: LEFT: TENSILE STRENGTH OF DIFFERENT GLASS REINFORCED COMPOSITES AT ELEVATED TEMPERATURES. RIGHT: COMPRESSIVE STRENGTH OF THE SAME GLASS REINFORCED COMPOSITES AT ELEVATED TEMPERATURES [B07, P188, 190].....	161
FIG. 103: FAILURE TIMES OF DIFFERENT COMPOSITES UNDER TENSION AND COMPRESSION [B07, P193, 194].....	162
FIG. 104: FAILURE TIMES UNDER NORMALIZED TENSILE (LEFT) OR COMPRESSIVE (RIGHT) STRESSES OF DIFFERENT RESINS [B07, P195, 196]	162
FIG. 105: RETAINED POST-FIRE FLEXURAL STRENGTH OF DIFFERENT THERMOSET (LEFT) AND THERMOPLASTIC (RIGHT) COMPOSITES [B07, P217, 226]	163
FIG. 106: DEPENDANCE OF THE POST-FIRE FLEXURAL STRENGTH ON HEATING TIME (LEFT) AND HEAT FLUX (RIGHT) [B07, P220]	163
FIG. 107: TWO-LAYER MODEL BY MOURITZ AND MATHYS [B07, P227]	164
FIG. 108: LEFT: EULER BUCKLING STRENGTH AS FUNCTION OF THE SLENDERNESS RATIO FOR VARIOUS TEST SPECIMENS. RIGHT: REDUCTIONS OF THE TENSILE, COMPRESSIVE AND FLEXURAL STRENGTH OF A SLENDER GLASS POLYESTER COMPOSITE BEAM DUE TO A CONSTANT HEAT FLUX OF 50 kW/m ² . [B07, P230]	165
FIG. 109: POST-FIRE FLEXURAL STRENGTH OF A GLASS FIBER VINYL ESTER COMPOSITE PROTECTED AGAINST FIRE BY VARIOUS MEANS. THE TEST SAMPLE WAS EXPOSED TO A HEAT FLUX OF 25 kW/m ² FOR TWENTY MINUTES. [B07, P233]	166
FIG. 110: REDUCTION OF PEAK- (LEFT) AND AVERAGE (RIGHT) HEAT RELEASE DUE TO THE ADDITION OF ATH [B07, P246].....	168
FIG. 111: EFFECT OF 30% ATH FILL ON THE FIRE REACTION PROPERTIES OF A GLASS PHENOLIC COMPOSITE SUBJECTED TO A HEAT FLUX OF 50 kW/m ² [B07, P248]	169
FIG. 112: MECHANISM OF FLAME RESISTANCE IN COMPOSITE FILLED WITH INTUMESCENT FILLER [B07, P254]	170
FIG. 113: COMPARISON OF BACK-FACE TEMPERATURE TIME PROFILES FOR GLASS PHENOLIC COMPOSITES WITH AND WITHOUT INTUMESCENT FILLER [B07, P255].....	171
FIG. 114: COMPARISON OF FIRE REACTION PROPERTIES OF A NON-BROMINATED AND BROMINATED GLASS POLYESTER COMPOSITE [B07, P262]	172
FIG. 115: EFFECT OF FLAME RETARDANT METAL OXIDE FILLERS ON THE FLAME RETARDANT PROPERTIES OF BROMINATED GLASS VINYL ESTER COMPOSITE [B07, P265]	173
FIG. 116: LEFT: VERTICAL BURN TIME FOR A PHOSPHOROUS CARBON EPOXY COMPOSITE. RIGHT: HEAT RELEASE RATES FOR A PHOSPHOROUS CARBON EPOXY COMPOSITE SUBJECTED TO A HEAT FLUX OF 50 kW/m ² . [B07, P268].....	174
FIG. 117: POST-FIRE FLEXURAL STRENGTH OF GLASS POLYESTER COMPOSITES WITH DIFFERENT COATINGS. RIGHT: CORRELATION BETWEEN HEATING TIME AND POST-FIRE FLEXURAL STRENGTH OF PROTECTED AND UN-PROTECTED GLASS POLYESTER COMPOSITE. [B07, P234].....	176
FIG. 118: TWO FIRE REACTION PROPERTIES OF A GLASS VINYL ESTER COMPOSITE WITH AND WITHOUT PHENOLIC SKIN [B07, P275]	177
FIG. 119: EFFECT OF THE GEOPOLYMER COATING THICKNESS ON THE HEAT RELEASE RATE OF A SANDWICH COMPOSITE [B07, P277]	177
FIG. 120: IMPROVEMENT OF TIME-TO-IGNITION (LEFT) AND CHAR DEPTH PROPERTIES OF A GLASS POLYESTER COMPOSITE WITH AND WITHOUT CERAMIC FIBER COATING/BARRIER [B07, P278]	178
FIG. 121: FIRE REACTION PROPERTIES OF CARBON EPOXY COMPOSITE WITH AND WITHOUT ZIRCONIUM OXIDE COATING [B07, P279].....	179
FIG. 122: SEQUENCE OF THE FIRE PROTECTIVE INTUMESCENT COATING REACTION [B07, P281]	179
FIG. 123: INTUMESCENT COATING BEFORE (LEFT, THICKNESS = 0,8 MM) AND AFTER (RIGHT, THICKNESS = 52 MM) FIRE LOADING [B07, P282]	180
FIG. 124: LEFT: BACK-FACE-TEMPERATURE OF AN INTUMESCENT PROTECTED COMPOSITE PANEL. RIGHT: IGNITION TIME OF A GLASS POLYESTER COMPOSITE PROTECTED WITH THIN AND THICK INTUMESCENT COATINGS AT DIFFERENT HEAT FLUXES [B07, P283]	181
FIG. 125: MULTI-WALLED (LEFT) AND SINGLE-WALLED CARBON NANO-TUBES USED IN POLYMER NANO-COMPOSITES [P84, P19].....	182
FIG. 126: IMPRESSIONS OF THE SINGAPORE MARINA BAY FRONT PEDESTRIAN BRIDGE [WEB, WWW.MARINABAY.SG].....	190
FIG. 127: IMPRESSIONS OF THE SINGAPORE HENDERSON WAVES BRIDGE [A27].....	191
FIG. 128: IMPRESSIONS OF THE LIGHTRAIL VIADUCT, BEATRIXKWARTIER, THE HAGUE [WEB, WWW.ZWARTS.JANSMA.NL].....	192
FIG. 129: IMPRESSIONS OF THE PEACE BRIDGE IN CALGARY, CANADA [WEB, WWW.CALGARY.CA].....	193
FIG. 130: IMPRESSIONS OF THE GREENSIDE PLACE LINK BRIDGE, EDINBURGH [T09][WEB, EN.STRUCTURAE.DE]	194
FIG. 131: IMPRESSIONS OF THE DESIGN OF THE PAPENDORPSE BRUG, Utrecht BY ABT [A30]	195
FIG. 132: IMPRESSIONS OF THE ROCH-SUR-YON PEDESTRIAN BRIDGE, FRANCE [WEB: WWW.COMPLEXITYS.COM].....	196
FIG. 133: IMPRESSION OF THE LUTON GALAXY LINK BRIDGE BY AKT UK [WEB, WWW.AKT-UK.COM]	197
FIG. 134: IMPRESSION OF THE T. EVANS WYCKOFF MEMORIAL BRIDGE, SEATTLE [WEB, WWW.MUSEUMOFFLIGHT.COM]	197
FIG. 135: IMPRESSION OF THE HARTHILL FOOTBRIDGE IN GLASGOW, SCOTLAND [WEB, WWW.HAPPYPONTIST.BLOGSPOT.COM]	198
FIG. 136: IMPRESSION OF THE WEBB BRIDGE IN MELBOURNE, AUSTRALIA [A02]	198
FIG. 137: TWO VIEWS OF THE ABERFELDY FOOTBRIDGE OVER THE RIVER TAY IN SCOTLAND [P22, P1]	199
FIG. 138: LEFT: MAUNSELL STRUCTURAL PLASTICS, ACCS MODULAR SYSTEM USED FOR THE ABERFELDY FOOTBRIDGE. RIGHT: BUILD-UP OF THE ABERFELDY BRIDGE-DECK. [P22, P3]	200
FIG. 139: LLEIDA FOOTBRIDGE NEAR LLEIDA, SPAIN [P85, P2]	201

FIG. 140: STRUCTURAL SYSTEM OF THE LLEIDA FOOTBRIDGE IN SPAIN. [P85, P2]	202
FIG. 141: OOSTERWOLDE HEAVY TRAFFIC LIFT BRIDGE [A45] [WEB: WWW.FIBERCORE-EUROPE.COM].....	203
FIG. 142: FIBERCORE HARBOURBRIDE ROTTERDAM. [A18, P2]	204
FIG. 143: OLD AND NEW LOAD-BEARING SYSTEM OF THE HAFENSTRASSENUNTERFUEHRUNG, FRANKFURT AM MAIN, GERMANY [A23, P1].....	205
FIG. 144: APPLICATION OF THE INTUSMESCENT COATING (LEFT) AND THE FINISHED, COATED AND POINTED PRODUCT (RIGHT) [A23, P2].....	206
FIG. 145: ARTIST IMPRESSION OF THE BRIDGE PAVILLON AT THE EXPO 2008 IN ZARAGOZA, SPAIN [A42, P1].....	207
FIG. 146: MAIN STRUCTURAL SYSTEM OF THE BRIDGE PAVILLON [A42, P7]	207
FIG. 147: ARRANGEMENT OF PODS IN THE BRIDGE PAVILLON [A42, P16]	208
FIG. 148: TWO DIFFERENT FIRE SCENARIOS (A AND B) FOR CABLE-STAYED BRIDGES [P39, P4].....	209
FIG. 149: TEMPERATURE EFFECTS OF THE FIRE SCENARIOS ON THE BRIDGE CABLE SUPPORTS [P39, P22]	210
FIG. 150: GEOMETRY OF TYPICAL 8-NODE IsoTRUSS BUILDUP. LEFT: CROSS-SECTION. RIGHT: SIDE-VIEW [P93, P2].....	211
FIG. 151: FORCE DIAGRAM OF AN IsoTRUSS UNDER BENDING LOAD [WEB: WWW.ALATUSPOLES.COM]	212
FIG. 152: CLOSE-UP OF THE CARBON EPOXY COMPOSITE IsoTRUSS STRUCTURE OF THE DELTA 7 ASCEND ROAD BIKE [WEB: WWW.DELTA7BIKES.COM]	212
FIG. 153: GENERAL VIEW OF THE 7 IsoTRUSS ELEMENTS USED IN THE FRAME OF THE DELTA 7 ARANTIX MOUNTAINBIKE FRAME [WEB: WWW.DELTA7BIKES.COM]	213
FIG. 154: BALANCE OF PEOPLE, PLANET AND PROSPERITY IN THE SUSTAINABILITY CHART [A47, P1]	218
FIG. 155: SPIDER DIAGRAM COMPARING A COMPOSITE FISH TANK TO A CONCRETE FISH TANK [P89, P22]	219
FIG. 156: SPIDER DIAGRAM OF TRADITIONAL E-GLASS COMPARED TO SUSTAINIBILITY OPTIMIZED E-CR GLASS [P88, P16]	220
FIG. 157: EXAMPLE OF SECTION PROPERTIES GIVEN IN THE FIBERLINE DESIGN MANUAL [B25, P1.6.81]	226

TABLE OF TABLES

TABLE 1: CHEMICAL COMPOSITION OF DIFFERENT GRADES OF E-, R-, A-, C-, AND EC- GLASS FIBERS [B11, p1123][B15, p114]	28
TABLE 2: COMPARISON BETWEEN E-, R-, A-, C-, AND EC- GLASS FIBERS [B11, p132]	28
TABLE 3: MECHANICAL PROPERTIES OF THREE DIFFERENT GFRP PRODUCTS [B16, p49].....	29
TABLE 4: MECHANICAL PROPERTIES OF DIFFERENT TYPES OF CARBON FIBER TOWS. [B16, p70]	34
TABLE 5: COMPARISON BETWEEN THREE TYPES OF CARBON FIBER/EPOXY PRODUCTS [WWW.MATWEB.COM] [B16, p78]	34
TABLE 6: MECHANICAL PROPERTIES OF FOUR TYPES OF ARAMID FIBERS [B16, p135]	36
TABLE 7: COMPARISON BETWEEN TWO ARAMID FIBER REINFORCED EPOXY COMPOSITES [B16, p137]	36
TABLE 8: OVERVIEW OF MOST NATURAL FIBERS AVAILABLE, DIVIDED IN SUBGROUPS BY ORIGIN.	38
TABLE 9: STRENGTH, STIFFNESS, SHRINKAGE AND HEAT DISTORTION TEMPERATURE COMPARISON OF VARIOUS MINERAL REINFORCEMENTS [B16, p64].....	39
TABLE 10: COMPARATIVE TABLE OF NATURAL, FLORAL FIBERS USED IN THE REINFORCED PLASTICS INDUSTRY [B11, p149].....	40
TABLE 11: COMPARISON BETWEEN NATURAL FIBER REINFORCED PLASTIC PRODUCTS USED IN THE AUTOMOTIVE INDUSTRY [P44, p23]	41
TABLE 12: COMPARISON BETWEEN VIRGIN PLASTIC, REINFORCED PLASTIC AND A PLASTIC WITH ADDED FILLER. [B16, p110]	45
TABLE 13: COMPARISON BETWEEN THE 7 MOST COMMON THERMOSET RESIN TYPES [B16, p135]	47
TABLE 14: MECHANICAL PERFORMANCE OF DIFFERENT GLASS FIBER REINFORCEMENTS OF A POLYESTER THERMOSET MATRIX	49
TABLE 15: COMPARISON BETWEEN LSE VINYL ESTER AND STANDARD VINYL ESTER. [B16, p150]	51
TABLE 16: CRYSTALLINE AND AMORPHOUS THERMOPLASTIC OVERVIEW [B16, p113]	52
TABLE 17: COMPARISON OF THREE HIGH-PERFORMANCE THERMOPLASTICS, WITH AND WITHOUT REINFORCEMENT. [B16, p133].....	55
TABLE 18: COMPARISON BETWEEN VARIOUS BIOLOGICAL RESINS [B11, p105-111]	56
TABLE 19: COMPARISON BETWEEN DIFFERENT FIBER REINFORCED POLYMER PRODUCTION SYSTEMS.	71
TABLE 20: MECHANICAL PROPERTIES OF DIFFERENT REINFORCEMENT FIBER MATERIALS [B01, p21].....	73
TABLE 21: MECHANICAL PROPERTIES OF DIFFERENT THERMOSET MATRICES [B01, p23]	74
TABLE 22: MECHANICAL PROPERTIES OF DIFFERENT COMPOSITES BASED ON EPOXY RESIN WITH A FIBER CONTENT OF 60% [B01, p23]	74
TABLE 23: VALUES FOR THE CONTINGENCY FACTOR ξP [B07, p170] [B01, p92].....	79
TABLE 24: EMPIRICAL VALUES FOR THE PUCK MODEL PARAMETERS $\alpha, \beta, \gamma, \delta$ [B01, p96]	81
TABLE 25: VALUES OF THE PARTIAL MATERIAL FACTOR FOR DIFFERENT FRP PRODUCTION TECHNIQUES [CUR96, TABLE 1, p12]	93
TABLE 26: APPLICATION OF DIFFERENT CONVERSION FACTORS FOR DIFFERENT APPLICATIONS [CUR96, TABLE 2, p13]	94
TABLE 27: COMPARISON OF ADVANTAGES AND DISADVANTAGES OF DIFFERENT FRP JOINT TYPES [B14, p128-129]	101
TABLE 28: IN-DEPTH PROPERTIES OF FRP JOINT TYPES [B14, p128].....	101
TABLE 29: ADVANTAGES AND DISADVANTAGES OF FIBER REINFORCED POLYMER BRIDGE DECKS [P29, p11-12]	113
TABLE 30: COMPARISON BETWEEN DIFFERENT FIBERLINE DECKS [WEB: WWW.FIBERLINE.COM]	115
TABLE 31: PRESCRIBED LOADS FOR LM1 [EN1991-2:2003, p37]	125
TABLE 32: TRAFFIC CATEGORIES FOR FATIGUE LOAD MODELS [EN1991-2:2003, p46, TABLE 4.5]	127
TABLE 33: CHARACTERISTICS OF TYPICAL HUMAN MOVEMENT [B21, p137]	129
TABLE 34: FIRE LOADS DUE TO DIFFERENT ROAD VEHICLES FIRES [NFPA502, p19]	143
TABLE 35: COMPARISON OF PE- AND ARAMID-FIBERS UNDER A HEAT FLUX OF 50 kW/m ² [B07, p46]	152
TABLE 36: EMISSION OF TOXIC GASES OF DIFFERENT FIBER REINFORCED COMPOSITES [B07, p90]	158
TABLE 37: TOXIC GAS EXPOSURE LIMIT [B07, p367].....	158
TABLE 38: FIRE REACTION PROPERTIES OF POLYESTER RESIN WITH AND WITHOUT 2% ZHS FILL [B07, p253]	170
TABLE 39: FIRE PROPERTIES OF DIFFERENT CARBON THERMOSET AND THERMOPLASTIC COMPOSITES COMPARED TO GEOPOLYMER CARBON COMPOSITE [B07, p271]	175
TABLE 40: ENVIRONMENTAL REDUCTION FACTORS OF GFRP ACCORDING TO EUROCOPM [B14, p30].....	217
TABLE 41: ENVIRONMENTAL REDUCTION FACTOR FOR DIFFERENT FRP SYSTEMS AND EXPOSURE CONDITIONS [P32, p22]	217
TABLE 42: TOTAL ENERGY USE OF STEEL, ALUMINUM AND COMPOSITE STRUCTURAL PARTS. [P88, p18-19].....	220
TABLE 43: COMPARISON OF THE TOTAL COSTS OF GFRP, STEEL AND CONCRETE ALTERNATIVES FOR THE FIBERLINE PEDESTRIAN BRIDGE IN KOLDING, DENMARK [A37, p2]	228
TABLE 44: COST-COMPARISON OF A CFRP ALTERNATIVE TO THE LONDON MILLENNIUM PEDESTRIAN BRIDGE. [A33, p5]	229
TABLE 45: COST COMPARISON OF THE BULK PRICE OF DIFFERENT POLYMERS; PRICES FROM 2001 [B07, p17]	230
TABLE 46: COST COMPARISON OF DIFFERENT REINFORCEMENT TYPES [WEB: WWW.NETCOMPOSITES.COM][B26, p2.6]	231
TABLE 47: COST COMPARISON OF DIFFERENT REINFORCEMENT TYPES FOR GLASS FIBERS, 1=LOWEST COST AND 10=HIGHEST COST [B16, p898]	231
TABLE 48: COMPARISON OF DIFFERENT BRIDGE DECK SYSTEMS IN COST, WEIGHT, DEPTH AND DEFLECTION [P07, p5]	232
TABLE 49: COSTS OF SELECTED CFRP SHEETS, GFRP SHEETS AND GFRP I-PROFILES [P81, p2981]	232